Universitat Autònoma de Barcelona

Institut de Neurociències

CREB-dependent transcription in astrocytes: signalling pathways, gene profiles and neuroprotective role in brain injury.

Tesis doctoral

Luis Pardo Fernández

Bellaterra, Septiembre 2015

Instituto de Neurociencias

Departamento de Bioquímica i Biologia Molecular

Unidad de Bioquímica y Biologia Molecular

Facultad de Medicina

CREB-dependent transcription in astrocytes: signalling pathways, gene profiles and neuroprotective role in brain injury.

Memoria del trabajo experimental para optar al grado de doctor, correspondiente al Programa de Doctorado en Neurociencias del Instituto de Neurociencias de la Universidad Autónoma de Barcelona, llevado a cabo por Luis Pardo Fernández bajo la dirección de la Dra. Elena Galea Rodríguez de Velasco y la Dra. Roser Masgrau Juanola, en el Instituto de Neurociencias de la Universidad Autónoma de Barcelona.

Doctorando

Luis Pardo Fernández

Directoras de tesis

Dra. Elena Galea

Dra. Roser Masgrau

In memoriam

María Dolores Álvarez Durán

Abuela, eres la culpable de que haya decidido recorrer el camino de la ciencia. Que estas líneas ayuden a conservar tu recuerdo.

A mis padres y hermanos,

A Meri

INDEX

FIGURE INDEX

Introduction

Material & Methods

Results: Chapter I

TABLE INDEX

Material & Methods

Results. Chapter II

Results. Chapter III

Summary

The study of astrocytes has become highly relevant in the realm of neurosciences since the discovery in the early 90's that those "supportive cells" can respond to synaptic activity. Nowadays, it is accepted that astrocytes have the ability to modulate synaptic transmission through the release of molecules that act at both pre-synaptic and post-synaptic sites, the so-called gliotransmitters. However, there are still many questions to be solved about the role of this glial cell population in brain physiology.

In the present work, we studied a field that has been largely explored in neurons, but that is poorly known in astrocytes: the CREB-dependent transcription. This widely-expressed transcription factor integrates the cellular responses of multiple stimuli, thus regulating numerous physiological and pathological functions. In neurons, CREB is a key player in the mechanisms that underlie synaptic plasticity, which is the molecular basis of memory acquisition, and it is involved in neuroprotective processes triggered by several brain disorders. Given the fact that astrocytes also play a role in synaptic activity and neuroprotection, we ought to know whether those functions are regulated by astrocytic CREB. Thus, we studied the molecular mechanisms of CREB activation in cell cultures upon stimulation with the transmitters ATP and NE and characterized the transcriptional programs triggered by CREB activation through different signalling pathways. Finally, we determine the protective roles of astrocytic CREB in a mouse model of traumatic brain injury.

The main findings of this thesis are: (i) a novel signalling pathway for CREB activation in astrocytes, (ii) the functional association of CREB-dependent transcriptional programs with oxidative metabolism, homeostasis and intercellular communication, and (iii) the neuroprotective roles of astrocytic CREB in a model of traumatic brain injury, through an increase in neuronal survival and axonal regeneration, a decrease in inflammation and a rescue of bioenergetic failure by increasing the mitochondrial metabolic pathways.

Introduction

Introduction

1. Astrocytes: physiology and pathology.

Astrocytes are the most abundant glial cell type in the brain and represent a heterogeneous cell population, playing a key role in brain homeostasis, synaptic plasticity and development. One of the defining features of astrocytes is the expression of glial fibrillary acidic protein (GFAP), an intermediate filament protein that has been commonly used as astrocytic marker. Other common markers are the enzyme glutamine synthetase (GS), the astrocyte glutamate transporters GLAST/EAAT1 and GLT-1/EAAT2 and the Ca^{2+} binding protein S100β. Traditionally, astrocyte visualization with GFAP staining has led to a vision of astrocytes as star-shaped cells, with highly branched processes that ensheath neurons and encapsulate blood vessels. However, the use of alternative methods of staining as intracellular dye filling has promoted a re-evaluation of the astrocytic morphology, being more spongiform than star-shaped (Bushong et al. 2002), which means that astrocytes possess very dense ramifications of fine processes that extend 2-10 μm from the main branches.

The number of astrocytes in total brain relative to neurons has increased with phylogeny and brain complexity, from 0.2 astrocytes for each neuron in *C. elegans* to 1.4 in humans, with variations among brain regions. This predominance of astrocytes in human brain cannot be explained by the differences in glial metabolic support -very similar among higher vertebrates- but rather by the increasing complexity of neural networks (Nedergaard 2003). A comprehensive set of studies carried out by Herculano-Houzel and collaborators has clearly demonstrated that the increase in astrocyte numbers during evolution is not due to an increment in brain size or neuronal density, but to the increase in neuronal size and complexity (Herculano-Houzel 2014). In fact, astrocytes have also become more complex during evolution; human cortical astrocytes have a diameter 2.6 times larger than rodent ones and they present 10 times more primary processes (Oberheim et al. 2009).

1.1 *Anatomical organization:*

The disposition of astrocytes throughout the brain is highly organized and depends mainly on contact spacing. Astrocytes define their own anatomical domain and do not overlap with neighbours, only the most peripheral processes interdigitate, forming an interface of less than 5% of total astrocyte volume. In these interfaces astrocytes exchange information with all the cellular elements included in their domain. Thus, cortical astrocytes enwrap a few neuronal somata and hundreds of dendrites (Halassa et al. 2007), and it has been estimated that a single astrocyte can contact 100000 synapses in the adult rodent hippocampus (Bushong et al. 2002).

Astrocytes are also highly interconnected via GAP junctions, which are mainly formed by connexin 43 (Cx43). This intense coupling has led to the concept of an astroglial syncytium in which cell responses are highly coordinated. Within this syncytium, astrocytes are able to transport charged ions and substrates from the blood vessels to the neurons or to other astrocytes. This coordinated transport between astrocytes requires the propagation of Ca^{2+} signals through GAP junctions and the release of ATP, with subsequent paracellular diffusion and action on neighbouring cells through purinergic receptors. (Parpura et al. 2012)

1.2 *Origins and heterogeneity:*

Gliogenesis generally follows neurogenesis in the developing brain (fig. 1). However, these events partially overlap and their precise temporal relationship at the individual progenitor level remains largely unexplored. To date, five different sources of cortical mature astrocytes have been identified: (i) radial glia (RG) within the ventricular zone, (ii) RG transformation, (iii) glial intermediate progenitors (GP) within the subventricular zone (SVZ), (iv) GPs present in the marginal zone (MZ)/Layer 1 and (v) superficial layer progenitors. At a later stage in embryonic brain development, RG in the ventricular zone gives rise to astrocytes that disperse throughout the ventral forebrain parenchyma. After birth, RG loses its apical processes and directly transforms into cortical astrocytes. RG also generates intermediate

progenitors through asymmetric division within the SVZ. These GPs divide and originate immature proliferative astrocytes that migrate radially out of the germinative zone and disperse through the cortical layers and white matter. When they reach their destination, the immature cells still proliferate and only later fully differentiate into mature astrocytes. GPs present in the Marginal Zone (MZ)/Layer 1 are derived from the ventricular zone and contribute to the generation of superficial cortical astrocytes (Molofsky et al. 2012; Schitine et al. 2015).

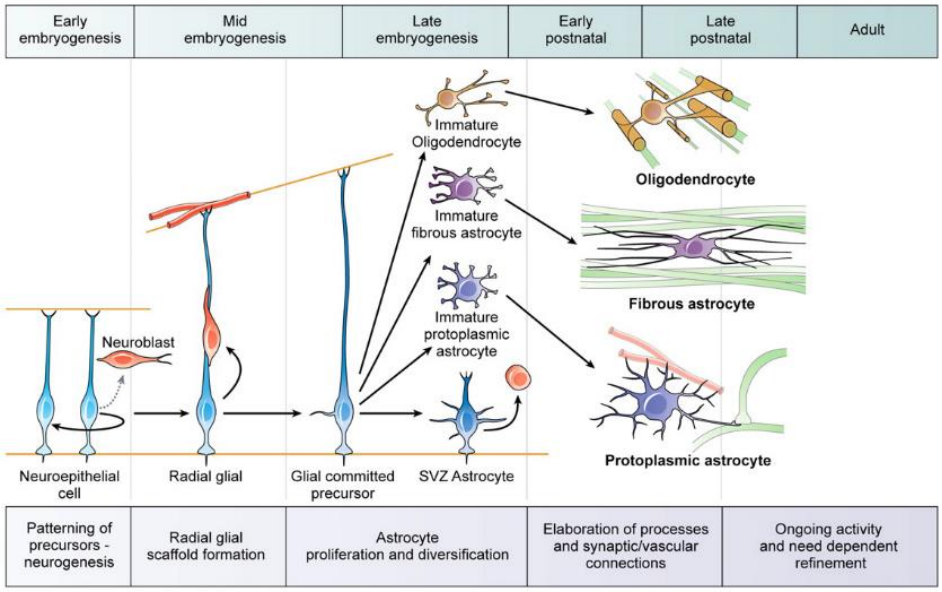

Figure 1. Gliogenesis. During early embryonic stages, multipotent neuroepithelial cells give raise to neuroblasts and subsequently transform into the main astrocyte precursor: radial glia. At the end of neurogenesis, RG functions as a scaffold for newborn migrating neurons. In late embryogenesis, RG transforms into intermediate progenitors that form different astrocyte lineages. During perinatal period, immature astrocytes and oligodendrocytes develop connections and become functional. From (Molofsky et al. 2012).

These differences in lineages result in the heterogeneity of astrocytes. To classify astrocytic populations, a first broad category was stablished, based on location in the white versus gray matter. Thus, protoplasmic astrocytes that populate the gray matter proceed mainly from embryonic radial glia and are characterized by a low expression of GFAP. These astrocytes present

numerous branching processes that envelop synapses and one or two long process that contact with blood vessels. In contrast, fibrous astrocytes from the white matter are generated mainly from neonatal SVZ progenitors and express high levels of GFAP, presenting long and unbranched processes that contact nodes of Ranvier (Wang and Bordey 2008). In addition, there are two types of specialized astrocytes recognized in the central nervous system (CNS): (i) Bergmann glia and (ii) Müller cells. (i) Bergmann glia is found in the cerebellum, with cell bodies in the Purkinje cell layer and processes that extend into the granule cell layer and terminate at the pial surface. (ii) Müller cells are the primary glial cell in the retina and are oriented radially, spanning the photoreceptor layer to the inner retinal surface.

1.3 *Astrocyte functions:*

The initial concept of astrocytes as a supportive element for the maintenance of neurons has dramatically changed in the last quarter of a century, with an increased body of evidence showing active roles of these cells in the transmission and integration of neural information. Astrocytes represent the main cellular element in homeostasis, being responsible for metabolic support, nutrition, control of ion and neurotransmitter environment, and regulation of brain-blood barrier. Besides, astrocytes sense synaptic activity by responding to released neurotransmitters and release gliotransmitters, thus modulating synaptic transmission.

1.3.1 *Developmental functions:*

Neurogenesis

During development, the first astrocyte progenitor (RG) works as neural progenitor for both neurons and astrocytes. During the period of neuronal migration, RG serves as scaffold for newborn neurons, which tangentially migrate along its processes. (Molofsky et al. 2012)

In the adult brain there are two major areas of neurogenesis: the aforementioned SVZ and the sub-granular zone of the hippocampal dentate gyrus (SGZ). A subset of astrocytes in the SVZ express GFAP and Nestin

and display stem cell characteristics. The so called type-B astrocytes divide to self-renew and generate highly proliferating transit-amplifying progenitors which in turn produce neuroblasts. These neuroblasts migrate to the olfactory bulb or to the piriform cortex, and differentiate to interneurons. SVZ astrocyte progenitors can also promote the genesis of oligodendrocytes that populate white matter tracts of corpus callosum and striatum (Wang and Bordey 2008; Gonzalez-Perez and Quiñones-Hinojosa 2012).

Control of neuronal growth and synaptogenesis:

Astrocytes are the major source of extracellular matrix (ECM) proteins and adhesion molecules. Therefore, they can direct neurite outgrowth in development or in response to injury by controlling ECM formation and by releasing adhesion molecules with guidance cues that favour the spread of new forming neurites. Molecules like N-cadherin, laminin, neural cell adhesion molecule (NCAM) or fibronectin act as neurite growing factors, while others like chondroitin sulphate proteoglycans (CSPs) inhibit neurite development and axonal regeneration after injury (Wang and Bordey 2008).

Early post-natal astrocytes actively participate in synaptogenesis by secreting molecules that promote synaptic formation, like neurotrophic factors or the ECM proteins thrombospondins (TSPs). TSPs are expressed in astrocytes during development but are absent in adult brain. Though TSPs are critical for synapse formation, other molecules are needed for the development of mature synapses, since TSP-formed synapses are structurally normal but post-synaptically silent. Recently, two homologous glypicans have been identified as astrocyte-secreted proteins that are sufficient to increase AMPA glutamate receptor levels on synapses, therefore inducing postsynaptic function (Molofsky et al. 2012).

1.3.2 *Neurovascular functions*

Blood Brain Barrier induction and maintenance:

The Blood Brain Barrier (BBB) is a specialized system of brain microvascular endothelial cells surrounded by astrocyte processes (endfeet)

and with pericytes embedded in between. BBB protects the brain from toxic substances in the blood, supplies CNS with nutrients, and filters excess and toxic molecules from the brain to the bloodstream. BBB endothelial cells are characterized by a dense net of tight junctions (zonula occludens) that limits paracellular diffusion of hydrophilic solutes, thus confining the entry across the brain endothelium to transcellular mechanisms involving cellular transporters (Zlokovic 2008).

During post-natal development, astrocytes contribute to the induction of the BBB by releasing factors like angiopoietin-1 (AG-1), glial-derive neurotrophic factor (GDNF) or basic fibroblastic growth factor (FGF). AG-1 participates in BBB differentiation by promoting angiogenesis and enhancing vascular stabilization, and also induces a decrease in endothelial permeability by upregulating the expression of tight junction proteins. Astrocytic growth factors contribute to the formation of membrane transporters (Abbott et al. 2006; Alvarez et al. 2013). In the adult brain, astrocytes control the permeability of the BBB by releasing molecules as ATP, endothelin-1, interleukin 6 (IL-6) or tumour necrosis factor α (TNFα) which promote the opening of the paracellular pathway by increasing the permeability of tight junctions. This allows for the entering of plasma molecules in the CNS and also increases the glucose uptake from the blood flow.

Regulation of cerebral blood flow

Astrocytes regulate the cerebral blood flow (CBF) by matching neuronal activity to vascular tone. Stimulation of astrocytes by synaptic released glutamate leads to intracellular Ca^{2+} increase and wave propagation through endfeet, which results in either vasodilation or vasoconstriction (fig. 2). Glutamate raises Ca^{2+} in astrocytes by acting on metabotropic glutamate receptors (mGluR), which activates phospholipase A2 (PLA2)-arachidonic acid (AA) pathway and thus produces three types of metabolites: prostaglandins (PGs) and epoxieicosatrienoic acid (EET) which dilate vessels, and 20-hydroxyeicosatetraenoic acid (20-HETE) which constricts vessels. A rise of Ca^{2+} in astrocyte endfeet may activate Ca^{2+}-gated K^{+}

channels, which release K^+ and promote vasodilation. Some neurons have been reported to bypass astrocytes and directly contact blood vessels, participating also in the regulation of blood flow. Neurons release PGs and nitric oxide (NO) into the brain capillaries, hence promoting vasodilation (Attwell et al. 2011).

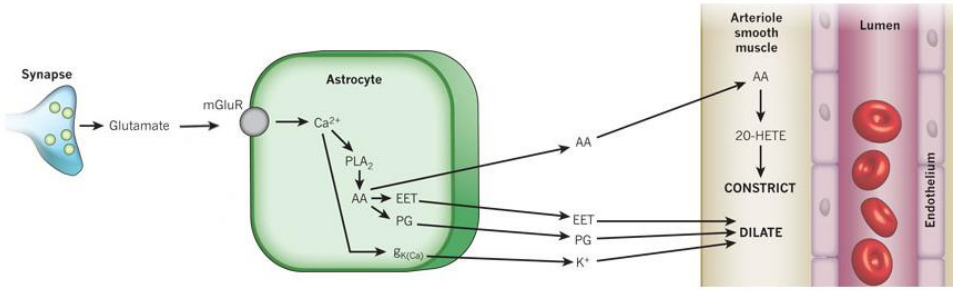

Figure 2. Astrocyte regulation of blood flow. In response to glutamatergic synapses, astrocytic increases of Ca^{2+} can trigger the release either of AA or of PGs, EET and K^+, thus promoting vasoconstriction or vasodilation. Adapted from (Attwell et al. 2011)

Neurovascular coupling:

The ability of astrocytes to regulate BBB permeability and CBF allows for a fine control of nutrient uptake from the blood stream. Astrocytic endfeet have a high expression of the glucose transporter GLUT-1, which allows astrocytes to take up glucose from the blood and make it available to neurons. Glucose uptake is controlled by coordinated local changes in Na^+ and Ca^{2+}, which are due to the glutamate influx through Na^+-glutamate cotransporters, the Na^+/K^+ ATPase pump and the Ca^{2+}-dependent glutamate release. The amount of glutamate uptake by astrocytes depends on its release by synaptic terminals, reflecting synaptic activity. This suggests a coupling between neuronal excitability through glutamate signalling in the synaptic cleft and astrocytic metabolic supply through glucose uptake from the blood stream, as we refer below. (Wang and Bordey 2008).

1.3.3 *Metabolic support*

An overview of brain metabolism gives an oxidative profile to neurons while astrocytes are thought to be mainly glycolytic (Fig. 3). This view is supported by the preferential use of lactate as metabolic substrate by neurons and its requirement for synaptic activity (Magistretti and Pellerin 1999). The mechanism through which the lactate arrives to neurons has been proposed by Pellerin and Magistretti. According to their work, glucose taken up by GLUT1 transporters can be processed in part oxidatively via the tricarboxylic acid cycle pathway (TCA) while the remaining glucose is transformed to lactate and released into the extracellular space via monocarboxilate transporters (MCT1 and MCT4). Lactate released by astrocytes is then transported to neurons via MCT2 and converted into pyruvate for oxidative use in the TCA cycle (Pellerin and Magistretti 1994; Wang and Bordey 2008).

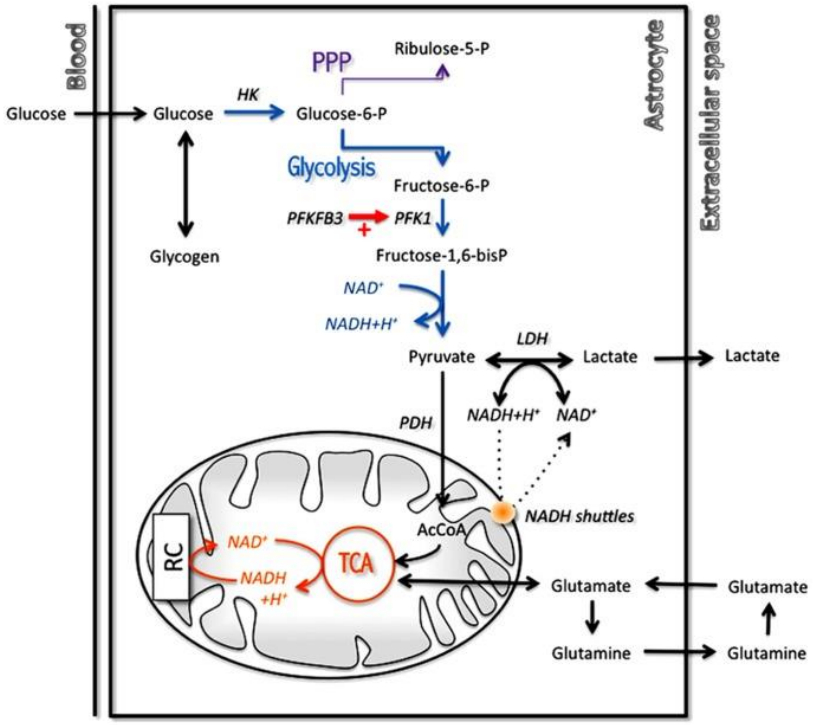

Figure 3. Overview of astrocyte metabolism. Glucose is taken up from the blood stream and can entry in the glycolytic pathway or be stored as glycogen. Part of the glucose processed by glycolysis is transformed to lactate, released to extracellular space and captured by neurons. Glutamate released during synaptic activity is transported to astrocytes. Part of the glutamate

will be transformed to glutamine and then returned to neurons. Glutamate can also be metabolized in the mitochondria to provide energy for glutamine formation and transport. PPP: Pentose phosphate pathway; PFKB3: 6-Bisphosphatase; PFK1: phosphofructokinase 1; LDH: lactate dehydrogenase; PDH: pyruvate dehydrogenase; NAD^+/NADH: nicotinamide adenine dinucleotide; AcCoA: acetyl coenzyme A; RC: respiratory chain. *From* (Bouzier-Sore and Pellerin 2013).

Another metabolic substrate used to provide energy to neurons is glycogen. Part of the glucose taken from the blood by astrocytes is used to synthesize glycogen, via the enzyme glycogen synthase. This glycogen works as a short-term repository for glucose, thus, under hypoglycemic conditions or in periods of increased tissue energy demand, (e.g. in phases of high neuronal activity) astrocytes can metabolize glycogen via the enzyme glycogen phosphorylase. Therefore providing a rapid energy source that bypasses the rate-limiting step in glucose metabolism, i.e. the glucose phosphorylation by hexokinase (HK) enzyme (Brown and Ransom 2007).

1.3.4 *Homeostatic functions:*

Extracellular K^+ buffering:

During neuronal activity, neurotransmission leads to the increment of K^+ in the extracellular space. The accumulation of these ions can result in neuronal depolarization and hyperexcitability. Astrocytes can take up the excess of K^+ mainly via the inwardly rectified K^+ channels (Kir) or by Na^+/K^+ and K^+/Cl^- antiporters. The K^+ is then distributed through the gap junction-coupled astrocytic syncytium and extruded at sites of low concentration of K^+, or directly released into the blood stream by the astrocytic endfeet-capillaries connection (Butt and Kalsi 2006).

Glutamate uptake:

Glutamate is considered the main excitatory neurotransmitter in the CNS and is involved in most of the processes that configure the normal functioning of the CNS as cognition, learning and memory. In addition, glutamate is a potent neurotoxic and high extracellular concentrations of this neurotransmitter can cause excitotoxicity and neuronal death. Thus, removal

of the excess of glutamate from the synaptic cleft is an essential mechanism to ensure the normal functioning of neuronal transmission. Astrocytes express the high affinity glutamate transporters EEAT1 and EEAT2 (also called GLAST and GLT-1) in the membrane of processes that ensheath synapses. Thus, they can uptake the excess of glutamate generated by neurotransmission and prevent overstimulation and excitotoxicity. The expression and the activity of these transporters are controlled by the glutamate released from neuronal presynaptic terminals (Gadea and López-

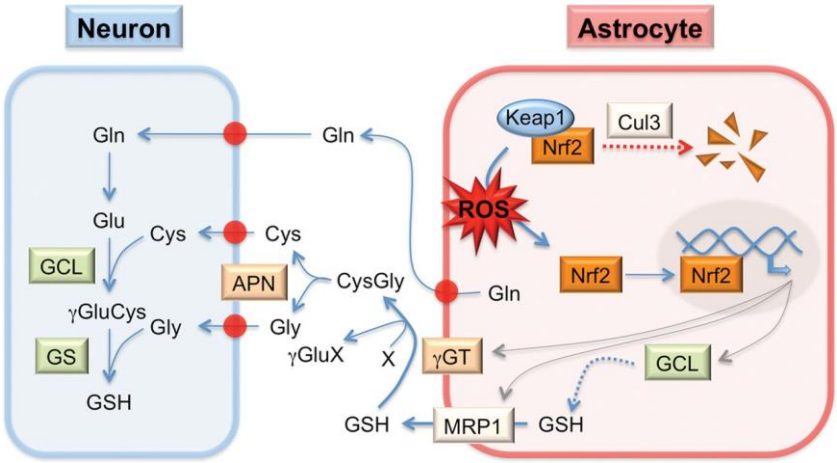

Colomé 2001). Within astrocytes, glutamate is metabolized to glutamine by the action of glutamine synthetase -an enzyme expressed mainly in astrocytes- and then redistributed to neurons for *de novo* synthesis of glutamate. This process of glutamate metabolism requires ATP, which is provided in part by aerobic glycolysis and results in lactate production, thus establishing a coupling between neuronal activity and glucose utilization (Magistretti and Pellerin 1999).

Figure 4. Cooperative biosynthesis of GSH between astrocytes and neurons. Antioxidant enzymes are regulated in astrocytes by the transcription factor Nrf2. In basal conditions, Nrf2 remains inactive in the cytosol by Keap1-mediated sequestration and Cul3-mediated degradation. The increase in ROS promotes the Nrf2-dependent transcription of antioxidant enzymes such as γ-glutamyl transpeptidase (γGT) and glutamate cysteine ligase (GCL) that catalyses GSH formation. GSH is released to the extracellular space through the multidrug resistance protein 1 (MRP1) transporter, cleaved by aminopeptidase N (APN) into Cys and Gly and uptake by neurons.

Glutamine (Gln) is transported from astrocytes and used together with Cys and Gly for *de novo* synthesis of GSH by neurons. Keap1: Kelch-like ECH-associated protein 1; Cul3: cullin 3; Glu: glutamate GS: glutathione synthase. From (Fernandez‐Fernandez et al. 2012).

Extracellular pH regulation

Neuronal activity increases extracellular alkalinisation, which can result in an increase of synaptic potency. Increases in extracellular K^+ during synaptic transmission induce the activation in astrocytes of the electrogenic $Na^+/HCO3^-$ cotransport, which promotes extracellular acidification and stabilizes synaptic strength. Other sources of $HCO3^-$ efflux in response to synaptic activity are the γ-aminobutyric acid A (GABAA) channels, and the Cl^-/HCO_3^- antiporters. Astrocytes possess carbonic anhydrase, an enzyme that participates in pH regulation by catalyse the transformation of CO_2 in $HCO3^-$ and H^+(Simard and Nedergaard 2004).

Brain water homeostasis

Astrocytes control the water transport in the CNS through a concerted action of the water channel aquaporin 4 (AQP4) and the inwardly rectifying potassium channel Kir4.1. These two channels are highly concentrated in astrocytic processes associated to blood vessels and cerebro-spinal fluid (CSF), like astrocytic endfeet and glia limitans. The distroglycan complex provides the molecular scaffolding for their polarized co-localization (Zador et al. 2009).

1.3.5 *Antioxidant functions*

Generation of reactive oxygen species (ROS) as NO or anion superoxide (O^-) during glutamatergic transmission can lead to oxidative damage. Antioxidant molecules such as glutathione peroxidase, catalase or superoxide dismutases (SOD 1/2) are expressed in low levels in neurons. However, astrocytes present high expression of these enzymes, being the main producers of the antioxidant molecule glutathione (GSH) in the brain. During periods of oxidative stress, astrocytes increment the production of GSH, which is released to the extracellular space, cleaved into cysteine (Cys) and glycine (Gly), and taken up by neurons to synthesize *de novo* GSH (fig.

4). Thus, neuronal biosynthesis of GSH depends on the supply of GSH precursors by astrocytes (Fernandez‐Fernandez et al. 2012).

1.3.6 *Signalling functions:*

Astrocyte communication: Calcium waves.

The discovery in the early 90's that astrocytes can respond to extracellular glutamate through fluctuations in intracellular Ca^{2+} ended the idea of astrocytes as passive elements in neurotransmission. Most importantly, their ability to transmit these Ca^{2+} signals to adjacent, non-stimulated astrocytes, provided a model of excitability and long distance communication by the propagation of Ca^{2+} waves between astrocytes (Wang and Bordey 2008). Posterior works have demonstrated that these Ca^{2+} increments in astrocytes are triggered by neuronal activity and promote the release of factors that can, in turn, modulate this neuronal activity, constituting a reciprocal communication network between astrocytes and neurons (Parpura et al. 1994). Nowadays is well reported both *in vitro* and *in vivo* that astrocytes experiment variations in intracellular Ca^{2+} concentrations either spontaneous or due to neuronal activity. These variations can be restricted to microdomains or spread across the entire cell, which points to an integration of small calcium signals from astrocyte processes, mimicking the way the neurons integrate post-synaptic currents. The spread of these intracellular Ca^{2+} increments to adjacent astrocytes have been reported several times *in vitro*, but only recently the use of encoded Ca^{2+} sensors has allowed their observation in intact tissue. Ca^{2+} waves have been observed in astrocyte cultures and acute slices in response to mechanical stimulations, uncaging of intracellular Ca^{2+} or treatment with transporter agonists. *In vivo*, these waves have been reported in retinal Müller cells, Bergmann glia of the cerebellum and in hippocampal astrocytes in response to neuronal activity (Wang and Bordey 2008; Hoogland et al. 2009; Kuga et al. 2011)

The most important signalling pathway leading to intracellular Ca^{2+} increments involves the activation of G-protein-coupled receptors (GPCRs), activation of phospholipase C β (PLCβ), and the production of inositol-

1,4,5-trisphosphate (IP3), which, following IP3 receptor (IP3R) binding, leads to Ca^{2+} release from the endoplasmic reticulum (ER). This increment can be amplified and propagated throughout the cell and is modulated by both positive and negative feedback mechanisms. The positive feedback involves the activation of nearby IP3Rs due to the co-agonistic action of Ca^{2+} on these receptors, the additional generation of IP3 through the Ca^{2+}-dependent activation of PLCβ or PLCδ and the capacitative calcium entry. In contrast, the negative feedback comes from: (i) the buffering power of mitochondria, attenuating the excess of Ca^{2+} levels at IP3R microdomains; (ii) the presence of endogenous low affinity Ca^{2+} buffers (calcium binding proteins) that limits the diffusion of Ca^{2+} ions; (iii) the re-uptake of Ca^{2+} from the ER or (iv) the extracellular efflux through Na^{+}/Ca^{2+}exchangers and the plasma membrane Ca^{2+} pump. Other sources for Ca^{2+} entry that trigger Ca^{2+} responses in astrocytes are purinergic ionotropic receptors, muscarinic acetylcholine receptors and transient receptor potential channels (Scemes and Giaume 2006; Rusakov et al. 2014). In addition, Ca^{2+} release from acidic stores through NAADP also promotes Ca^{2+} responses in astrocytes (Barceló-Torns et al. 2011).

To date, two different mechanisms for cell to cell propagation of Ca^{2+} waves have been proposed. Originally, it was believed that Ca^{2+} or IP3 diffused through gap junction and increased Ca^{2+} levels in neighbouring cells. But the observation of Ca^{2+} propagation in astrocytes lacking physical contact has suggested that an extracellular component might also mediate the signalling. This observation has led to the identification of ATP as the diffusible messenger of Ca^{2+} signalling in astrocytes. The fact that astrocytes express purinergic receptors of the P2Y family and the relation of these receptors with mobilization of Ca^{2+} stores during propagation supported this second model that included ATP release in a regenerative fashion, not ruling out ATP efflux through gap junction open hemichannels. (Nedergaard 2003; Scemes and Giaume 2006).

Modulation of synaptic transmission.

Astrocytes express almost all receptor types for neurotransmitters and neurohormones (fig. 5), being the most important the glutamate and ATP receptors. Ionotropic glutamate receptors (GluRs) expressed in astroglial cells are represented by AMPA and NMDA types while most common metabotropic receptors (mGluRs) are mGluR5 and mGluR3. Purinergic ionotropic receptors functionally expressed by astrocytes include $P2X_{1/5}$ and $P2X_7$ receptors and metabotropic are mainly represented by $P2Y_{1,2,4,6}$ (Verkhratsky et al. 2012).

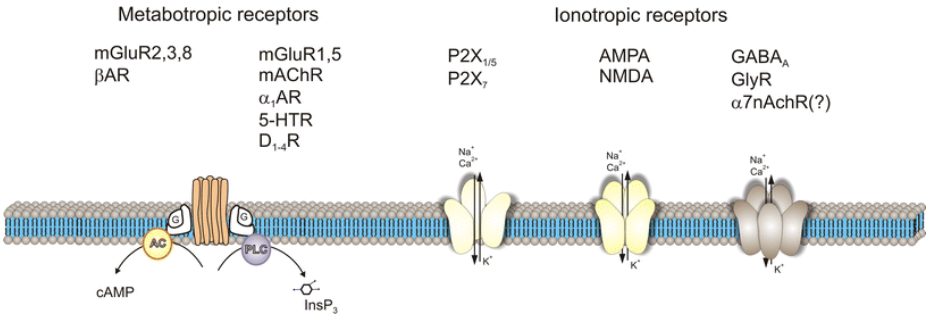

Figure 5. Astrocytic ionotropic and metabotropic receptors. Abbreviations not referred in text: AC adenylyl cyclase, AR adrenaline receptors, DR dopamine receptors, 5-HTR serotonine receptors, mAChR muscarinic acetylcholine receptor, nAChR nicotinic acetylcholine receptor. From (Verkhratsky et al. 2012).

Neurotransmitters released from presynaptic terminals of neurons activate receptors on neighbouring astrocytes, leading to Ca^{2+} increases and, in turn, Ca^{2+} waves propagation. This Ca^{2+} signalling in astrocytes can promote the release of glial derived factors, the so called gliotransmitters, which can signal back to neurons and modulate synaptic transmission in a scale of milliseconds to seconds (fig. 6). This phenomenon was first reported in works with cultured cells that showed an increment of Ca^{2+} in neurons (Nedergaard 1994) or an activation of NMDA neuronal receptors (Parpura et al. 1994) in response to ATP or glutamate released from astrocytes. Moreover, astrocyte Ca^{2+} transients have been shown to induce the appearance of an NMDA receptor-dependent slow inward current in nearby neurons and an increase in the frequency of synaptic currents in the absence of neuronal spiking (Araque et al. 1998).

Astrocyte gliotransmitters are mainly of three classes: amino-acids (glutamate or D-serine), nucleotides (ATP) and peptides (ANP, Bdnf, or TNFα). The release of gliotransmitters responds mainly to Ca^{2+}-regulated exocytosis, although diffusion through membrane channels or transport across membrane proteins has also been reported. Astrocytic Ca^{2+}-dependent exocytosis of glutamate has been shown to induce neuronal slow inward currents (SICs), which are prevented by blocking or downregulation of the SNARE complex (Araque et al. 1998; reviewed in Parpura and Zorec 2010). In general, the release of astrocytic glutamate has been described to target ionotropic and metabotropic receptors in both axonal terminals and dendrites, thereby exerting neuromodulatory activities in several brain regions including hippocampus, thalamus and cortex (Rossi 2015). Gliotransmitters as TNFα and D-serine have been reported to play a role in regulation of long term plasticity at central synapses by increasing surface expression of AMPA receptors in postsynaptic terminals. D-serine is an endogenous co-agonist of NMDA receptors and acts at glutamatergic synapses to support the activity of the receptor thereby enabling NMDAR-mediating synaptic plasticity. ATP can be released from astrocytes upon glutamate stimulation and binds to postsynaptic purinergic receptors thus initiating a signalling cascade (Parpura and Zorec 2010).

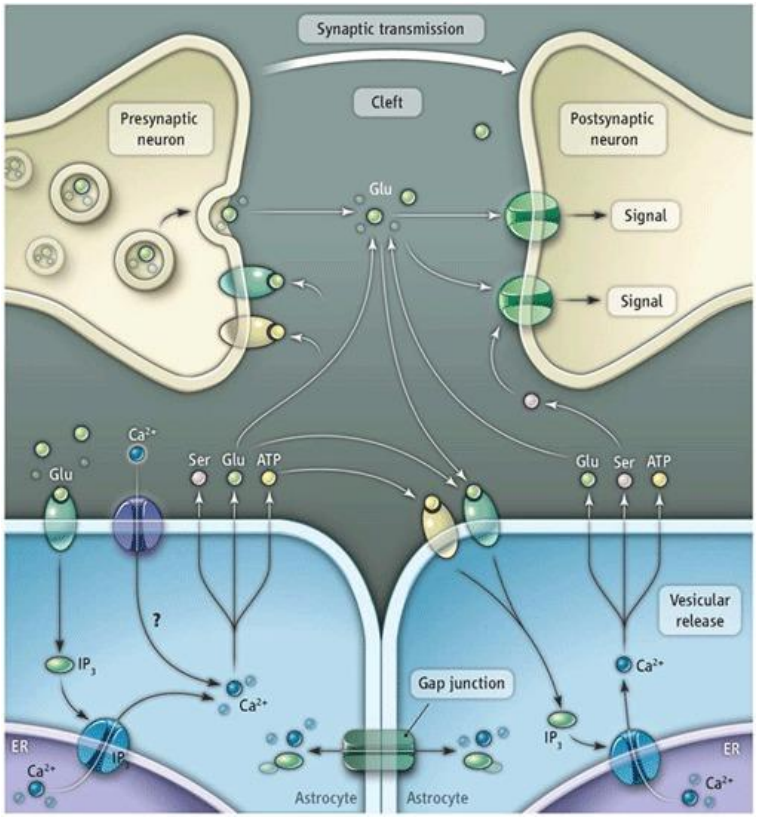

Figure 6. Tripartite synapse. Astrocytes respond to synaptic activity by Ca^{2+} dependent exocytotic release of gliotransmitters such as Glutamate, D-serine or ATP. Gliotransmitters can act at both presynaptic and postsynaptic receptors and modulate synaptic transmission. From (Kirchhoff 2010).

These examples illustrate the fact that most of the known forms of synaptic plasticity are influenced by astrocyte-released gliotransmitters. However, some studies have casted doubts about the ability of astrocyte Ca^{2+}signals to affect synaptic plasticity *in vivo*. Selective increase of Ca^{2+} in astrocytes through the expression and activation of the MAS-related G protein-coupled receptor member A1 (MRGA1) has not evoked glutamate-mediated SICs, nor modulated synaptic plasticity in neurons (Fiacco et al. 2007). Similarly, the use of a knockout mouse of the $IP3R_2$, the main isoform expressed in astrocytes, has reported no effect on short and long-term plasticity in the hippocampus (Agulhon et al. 2010). Conversely, another study with the $IP3R_2$ knockout mice has reported impairment of cholinergic-induced LTP

in the same area (Navarrete et al. 2012). In addition, recent studies using multiphoton microscopy and genetically encoded Ca^{2+} indicators further support the modulation of synaptic plasticity by Ca^{2+}-dependent exocytosis of gliotransmitters. (Lalo et al. 2014; Pankratov and Lalo 2015; Tang et al. 2015). Taken together, arguments favour the role of astrocytes in the regulation of synaptic transmission but further studies will be necessary to elucidate the biological relevance of this astrocytic function.

1.4 *Astrocytes in brain pathology:*

Given the plethora of functions exerted by astrocytes, they are involved in many pathological situations. Astrocytic homeostatic systems exert control over homeostatic imbalances induced by insulting the CNS. The astrogliosis, an evolutionary conserved astrocytic response to a variety of brain lesions, is essential for limiting the area of damage and for the post-insult remodelling and recovery of neural function. However, the astrocytic homeostatic cascades can be deleterious and aggravate damage to the nervous system. Severe insults may compromise astroglial energetics and ion homeostasis, which in turn can trigger glutamate and ATP release increasing neuronal excitotoxicity, release of reactive oxygen species, pro-inflammatory factors and other neurotoxic agents.

The first astrocytopathy discovered was **Alexander disease**, a fatal neurodegenerative disease that mostly affects infants and children and causes developmental delay and changes in physical characteristics. It is consequence of a mutation in the *Gfap* gene affecting not only to astrocytes but also to oligodendrocytes and neurons (Verkhratsky and Parpura 2010).

Epilepsy is one of the most prevalent neurological diseases, affecting about 1% of the population. It is characterized by repetitively occurring seizures, that is, transient disturbances of neuronal function associated with motor behavioural abnormalities and disturbances of consciousness. Epileptic brain tissue is characterized by massive reactive gliosis and focal seizures are associated with astrocyte Ca^{2+}signalling and abnormal glutamate release (Seifert et al. 2006).

During brain **ischemia**, the local impairment of blood flow deprives cells of glucose and O_2, resulting in a depletion of cellular energy stores. In neurons, ATP depletion affects ionic gradients, which causes membrane depolarization and the release of large amounts of glutamate that triggers excitotoxic mechanisms. Astrocytes in the early periods of ischemic damage show a slow decline of ATP and preserve membrane ionic gradients necessary to take up extracellular glutamate, hence protecting neurons from excitotoxicity. However, the loss of ionic gradients during prolonged ischemia leads to astrocytic release of glutamate, thus increasing excitotoxic damage. In addition, abnormal Ca^{2+} signalling and Ca^{2+} waves propagation during ischemia can spread excitotoxic damage through Ca^{2+}-associated release of glutamate (Rossi 2015). Moreover, ionic imbalance during ischemia promotes cell swelling (cytotoxic edema). Likewise, cellular damage results in BBB disruption and blood flow leakage (vasogenic edema). Astrocytic AQP4 contributes to cytotoxic edema formation by facilitating cell water uptake. Conversely, AQP4 decreases vasogenic edema by contributing to the clearance of extracellular fluid accumulated due to BBB leakage (Zador et al. 2009).

Astrocytes in **Alzheimer's disease** (AD) present a degree of astrogliosis that correlates with cognitive decline. Chronic inflammation due to the release of pro-inflammatory factors by astrocytes and microglia during AD contributes to disease pathogenesis. In early stages of AD, atrophic changes in astrocytes may be pathologically relevant as reduced astroglial coverage may lead to synaptic dysfunction and synaptic loss. Thus, astrocyte pathology can represent a mechanism for early cognitive decline in AD and probably in other types of senile dementia (Parpura et al. 2012).

Neuron-astrocyte relations play important roles in **Amyotrophic lateral sclerosis** (ALS) pathology. Prominent astroglial degeneration and atrophy has been found in the animal models of ALS that precedes both neuronal death and the appearance of clinical symptoms. Reduced support of dopaminergic neurones by astroglial cells may contribute to selective cell death in **Parkinson** disease. Astrocytes degeneration has been also observed

in various forms of frontotemporal, thalamic and immunodeficiency virus-1 (HIV-1) associated dementia (Verkhratsky and Parpura 2010).

1.5 *Reactive astrogliosis.*

In response to a pathological situation in the CNS, astrocytes exhibit a series of morphological and functional changes that give rise to the so called astrocyte reactivity or astrogliosis. This is not a unique, well-defined phenomenon but rather consists in a graded, multistage and evolutionary conserved astroglial reaction. Despite being a highly dynamic process, reactive astrogliosis shares some common hallmarks including cellular hypertrophy, hyperplasia, enlargement of cytoplasm and cytoplasmic processes, and increased expression of the filament protein GFAP, which is commonly used as a marker of astrocyte reactivity (fig. 7). In addition to these common changes, gene expression is also altered in astrocyte reactivity in a context-specific manner. Barres and colleagues have compared the transcriptomic profile of isolated astrocytes from mouse brains in two injury models, middle cerebral artery occlusion (MCAO) and LPS-induced global neuroinflammation, and found that at least the 50% of the injury-altered gene expression is specific for each injury type (Zamanian et al. 2012). The severity of the injury also determines the loss of astrocyte individual domains. In the healthy brain as well as in some kinds of mild-to-moderate injuries astrocytes are organized in non-overlapping domains (Bushong et al. 2002; Wilhelmsson et al. 2006), but in response to a severe injury as neurotrauma, this organization is loss and astrocytes close to the lesion present overlapped and intertwined processes. The new organization form compact borders that surround the damage area and isolate from healthy tissue, which is known as glial scar. This structure appears only in severe damage or inflammation after stroke, traumatic brain injury (TBI), or neurodegeneration and is characterized to be formed mainly by newly proliferated astrocytes derived from mature astrocytes in the surroundings of the lesion that re-enter in the cell cycle and proliferate during scar formation (Anderson et al. 2014). Interestingly, recent live imaging observations in the mouse injured cortex have revealed that proliferative astrocytes are mainly

associated to blood vessels and, contrary to what was previously believed, that most astrocytes do not migrate to the injury but stay in their tiled domains (Bardehle et al. 2013).

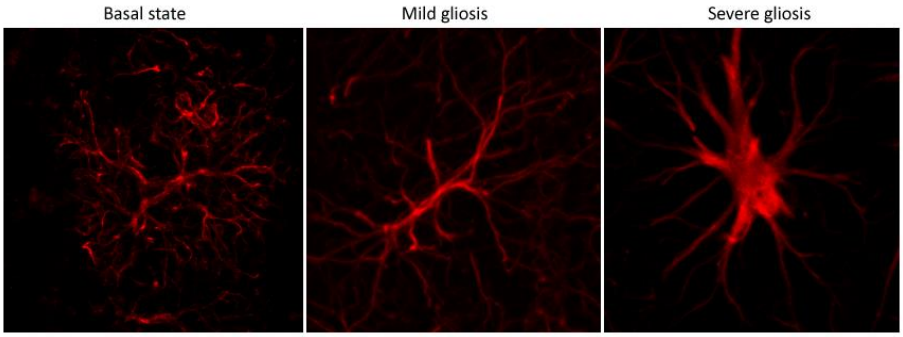

Figure 7. Cortical astrocytes after traumatic brain injury stained for GFAP. Control animal (left), far from the lesion (centre) and close to the lesion (right).

All these changes taking place in astrocytes in response to brain damage are not all-or-none but graded, giving rise to a high number of situations that can be qualified as reactive astrogliosis. To facilitate the characterization of this phenomenon, it has been proposed a model in which astrogliosis is divided in three broad categories depending on the severity of changes, the alterations in astrocyte activity (gain or loss-of-function) and the specific context (Anderson et al. 2014).

- *Mild to moderate reactive astrogliosis:* Features hypertrophy of cell body and processes as well as increase in GFAP expression. Do not present loss of individual domains or proliferation. It is presented in non-contusive trauma, in response to innate immune activation during viral or bacterial infection and in distant areas to some focal CNS lesions. The return to basal state is preserved in most cases.
- *Severe diffuse reactive astrogliosis:* Hypertrophy and GFAP expression are more pronounced and appears some overlap between processes and disperse proliferation. This degree is present in some infections and in areas responding to chronic neurodegeneration or small focal ischemia. Given the changes in gene expression and the tissue

reorganization, the potential for resolution and return to basal degree is reduced.

- *Glial scar formation:* Newly forming astrocytes presented at this stage have lost their organization domains and interact with a variety of cell types in the core of the lesion including fibroblasts, pericytes and other glial cells. This stage is associated with substantive tissue reorganization and structural changes that are essentially permanent and persist even when triggering insults may have resolved.

Astrogliosis has found to be induced by a broad range of mediators, from small molecules such as purines and transmitters to large polypeptide growth factors and cytokines. Such a high diversity of activators results in a wide variety of signalling pathways, promoting an equal amount of functional outputs that modulate astrocyte reactivity. For example, activation of STAT3 signalling pathway promotes astrocyte hypertrophy and upregulation of GFAP while β1-integrin-mediated signalling is related to the acquisition of a mature non-reactive state (Pekny and Pekna 2014).

During brain injury or disease, reactive astrogliosis is commonly triggered by endogenous danger-signals that are typically released by damaged cells. The recognition of such molecules is enabled by the astrocytic expression of specific pattern-recognition receptors, including various members of the Toll-like receptor (TLR) family, and can initiate rapid immune responses in the astrocytes, thus promoting the expression and secretion of several mediators, particularly cytokines and chemokines. To date, it has been reported the ability of astrocytes to produce the cytokines interleukin 1 (IL-1), IL-6, IL- 10, interferon γ (IFNγ), Granulocyte-Macrophage Colony-Stimulating Factor (GM-CSF), Transforming growth factor β (TGFβ) and TNFα; and the chemokines (C– C motif) ligand (CCL) 2 (also known as monocyte chemotactic protein-1, MCP-1), CCL5, CCL20, (C–X–C motif) ligand 10 (CXCL10), CXCL12 (also known as Stromal cell-Derived Factor 1, SDF-1), CXCL1, CXCL2 and CX3CL1. Some of these immune mediators have the potential to activate the neighbouring astrocytes and microglial cells

as well as to attract immune cells from the blood circulation, thus amplifying the local immune responses in the CNS (Rossi 2015).

Astrocyte research has been largely ignored due to a neurocentric view of the brain and only in the last 20 years, since the discovery of astrocyte signalling to neurons (Nedergaard 1994; Parpura et al. 1994), it has increased the attention of researchers. Nowadays, astrocytes are consolidated players in many brain functions and their participation in the processing of neuronal information is already accepted by the scientific community. However, many questions about astrocyte physiology and pathology still remain unanswered. With this thesis, we want to contribute to astrocytic research by studying the role of the transcription factor CREB in these glial cells. CREB is an integrator of multiple stimuli and has been largely studied in neurons, where it mediates important processes such as synaptic plasticity and neuroprotection. Thus, we aim to elucidate if astrocytic CREB also plays a role in such processes.

2. The transcription factor CREB in the CNS: regulation and function.

c-AMP responsive element binding protein (CREB) is a widely expressed transcription factor involved in several biological processes such as ingestion control, cell proliferation, learning and memory or neuroprotection. CREB is a member of a large group of transcription factors, termed the basic leucine zipper domain (bZIP) family, which also includes activation transcription factor-1 (ATF-1) and cAMP-responsive element modulator (CREM). CREB and ATF-1 are ubiquitously expressed while CREM is mainly present in the neuroendocrine system.

Several isoforms of CREB and CREM have been identified by alternative splicing. In the CREB gene, 6 alternative spliced transcripts emerging from the 11 codons have been recognized. The predominant isoforms are CREBΔ (without exons 3, 5, 6) and CREBα (without exons 3, 6), both fully active. Another isoform, CREBβ, has been identified in a knockout mouse lacking CREB exon 2 (Hummler et al. 1994) and it has been reported to

present nearly the same transactivation potential as the predominant isoforms. The other isoforms identified encode truncated CREB peptides either by the insertion of a stop codon in exon 6 (isoforms CREBγ and CREBαγ) or by the lack of functional region coding exons (isoforms CREBΩ and CREBΨ) (Ruppert et al. 1992; Don and Stelzer 2002). In the case of CREM, three main groups appear from alternative splicing. The CREMα group (isoforms α, β, γ) competes with CREB for binding CRE regions and acts as a suppressor of CREB dependent transcription. The CREMτ activator isoforms (τ1, τ2, τ3) are originated from the same promoter as the CREMα group but they are able to induce transcription upon binding to CRE promoter (Don and Stelzer 2002). Other two isoforms produced by alternative intronic promoters are the S-CREM and the Inducible cAMP response element repressor (ICER); the latter is expressed in response to cAMP stimulation and acts as a potent transcriptional repressor, contributing to transcriptional attenuation in tissues as the pituitary gland (Mayr and Montminy 2001). An overview of the CREB family is represented in figure 8.

The primary structure of the CREB family members (fig. 9) reveals a centrally located 60-amino-acid kinase-inducible domain (KID), which contains a PKA phosphorylation site. KID is flanked by hydrophobic glutamine-rich domains, designated Q1 and Q2, which function as constitutive activators in vitro and are known to interact with components of the basal transcriptional complex. A basic region/leucine zipper dimerization domain is located carboxy-terminally in all CREB active isoforms and allows the binding to the regulatory region of the promoter in target genes (Mayr and Montminy 2001; Johannessen et al. 2004).

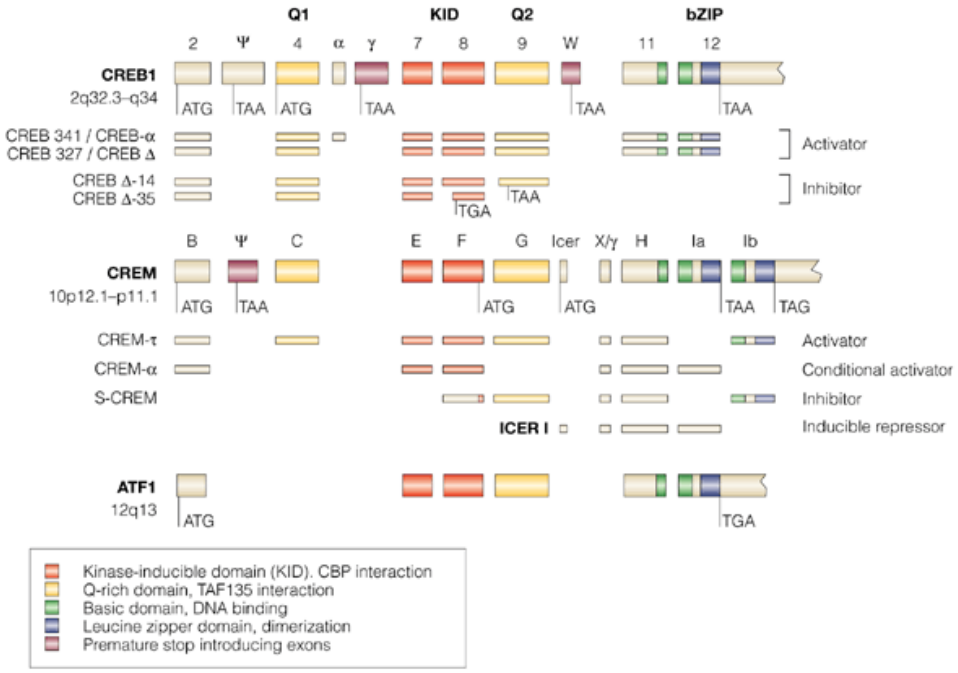

Figure 8. Overview of the mammalian CREB family of transcription factors, showing the alternative splicing variants and the different domains. From (Alberini 2009)

2.1 *Activation of CREB-dependent transcription:*

DNA binding of CREB takes place at the cAMP regulatory element (CRE) sites. This assembly allows CREB dimerization to cooperatively activate the transcription of target genes (Wu et al. 1998). CRE has been originally described as a palindromic sequence of 8 nucleotides (TGACGTCA) (Montminy et al. 1986) but later works have observed that in certain genes this sequence varies to CGTCA (Craig et al. 2001) or TGACG (Impey et al. 2004). These functional CREB binding sites are localized in the promoter proximal regions of about 4000 genes in human genome (Zhang et al. 2005), within 250 base pairs of the transcription start site. As it happens in other promoter proximal elements, CRE sites are most active when placed near a TATA box and become weaker when moved further upstream (Mayr and Montminy 2001). Despite the high number of CREB binding sites, stimulation of CREB-dependent transcription with the adenylyl cyclase

activator forskolin (FSK), which increases cAMP levels, promotes the expression of as few as 100 genes. Moreover, this subset of cAMP inducible genes seems to change between cell types (Zhang et al. 2005). This difference between the number of CREB binding sites and the expressed genes could be explained mainly by four facts: (i),chromatin conformation and methylation state affects CREB binding to target genes (ii) canonical TATA boxes, which are required for cAMP-dependent transcription, are absent in 2/3 of CREB occupied promoters. (iii), the role of CREB regulatory kinases and coactivators that can modulate CREB-DNA binding stabilization and transcriptional activation. (iv), the regulation of CREB phosphorylation state at the KID domain, necessary for the interaction with the coactivators CREB-binding protein (CBP) and p300, which are directly involved in the recruitment of the transcriptional machinery (Lonze and Ginty 2002; Altarejos and Montminy 2011).

The CREB transactivation domain is divided in two regions, KID and Q2 domain, which function cooperatively to promote transcriptional activation in response to stimuli. Q2 domain has been shown to enhance transcription by interacting with the TBP associated factor 4 ($TAF_{II}130$), a component of the basal transcription factor IID (TFIID) (Lonze and Ginty 2002). As opposite to Q2, KID domain needs to be activated to allow binding of CREB coactivators. KID activation depends on phosphorylation and involves mainly serine (Ser) 133 (Gonzalez and Montminy 1989), which is targeted by multiple activity-inducible kinases. These kinases are activated in response to an array of stimuli, like Ca^{2+} and cAMP, and include Ca^{2+}/Calmodulin-dependent kinase II and IV (CaMKII/IV), protein kinase A (PKA), protein kinase C (PKC), mitogen/stress-activated kinase (p38), ribosomal S6 kinase (RSK6) or protein kinase B (AKT) among others (Johannessen et al. 2004; Sakamoto et al. 2011). Other CREB phosphorylation sites have been reported to exert regulatory roles in transactivation depending on the context. Phosphorylation of Ser 142 by Ca^{2+}/CaMKII has been shown to repress CREB transactivation by triggering the dissociation of the CREB dimer, hence inhibiting CBP recruitment. Controversially, the phosphorylation in this Ser 142 is required

for robust CREB-mediated gene expression in the CNS. In a similar way, phosphorylation in the Ser 129 by Glycogen synthase kinase-3β (GSK3β) has been reported to inhibit CREB-binding to DNA, but also to increase its nuclear distribution by acting cooperatively with Ser 133. CREB activation state is also regulated by dephosphorylation in Ser133, which is mediated by Ser/Thr-specific protein phosphatases type1 and 2A (PP1, PP2A) and leads to transcriptional repression (Lonze and Ginty 2002; Johannessen et al.

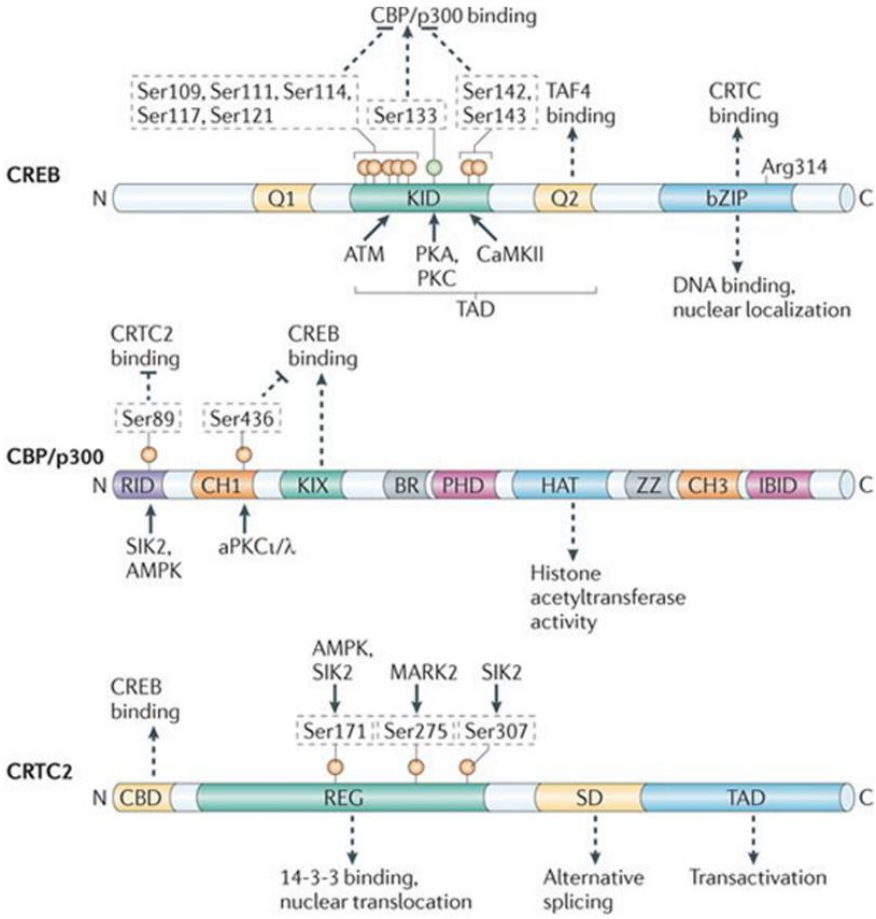

2004; Sakamoto et al. 2011).

Figure 9. Sequence of CREB and its co-activators CPB/p300 and CRTC2 showing the different activation and binding domains and including the phosphorylation sites. From (Altarejos and Montminy 2011)

Phosphorylation of Ser 133 allows CREB binding to kinase-inducible interacting (KIX) domain of the co-activators CBP/p300, which are thought to enhance CREB target gene expression by acetylating nucleosomal histones and recruiting components of the basal transcription complex (Lonze and Ginty 2002). CBP/p300 are two highly homologous proteins that belong to the family of histone acetyl transferases. They function as molecular scaffolds that bring different proteins together to the gene promoters. Their large size (over 2400 aminoacids) and modular organization enable interaction with several proteins at the same time. The following domains can be distinguished in both CBP and p300: (i) three cysteine/histidine-rich regions (CH1 to CH3) that bind zinc and are involved in protein-protein interactions; (ii) an histone acetyltransferase (HAT) domain in the center of the protein; (iii) a bromodomain (BD) that binds acetylated lysines in histones and specific transcription factors; (iv) two transactivation domains located at either end of the protein; and (v) multiple specific interaction domains for different transcription factors, such as the KIX domain that mediates the interaction with CREB phosphorylated at Ser133. CBP/p300 can act as a molecular bridge between DNA-binding transcription factors and components of the basal transcription machinery, such as the TATA-box-binding protein (TBP) and the RNApol II complex. In addition, the HAT activity of CBP/p300 can relax the configuration of the chromatin around the bound DNA sequences by acetylation of histones, thus facilitating transcriptional activation (Valor et al. 2013)

In addition to the transactivation domain, CREB bZIP domain has been reported to participate in transcriptional activation through binding to CREB-regulated transcription coactivators (CRTCs) (Conkright et al. 2003). The CRTCs (formerly called TORCs for transducers of regulated CREB activity) are a family of conserved coactivators (CRTC1/2/3) expressed in most tissues, specifically CRTC2/3 are more abundant in lymphocytes B and T while CRTC1 is highly expressed in the CNS (Conkright et al. 2003; Kovács et al. 2007; Takemori et al. 2007). Structurally, CRTCs share an N-terminal coiled coil domain that associates with the CREB bZIP in a tetrameric form; a central regulatory domain with multiple phosphorylation

sites that regulates activation and nuclear translocation; a splicing domain involved in alternative splicing of certain CREB target genes; and a glutamine-rich C-terminal transactivation domain that interacts with $TAF_{II}130$ (Altarejos and Montminy 2011). This interaction potentiates the binding of CREB with the $TAF_{II}130$ component of TFIID following its recruitment to the promoter and enhances CREB dependent transcription (Conkright et al. 2003; Takemori et al. 2007). The importance of the CREB-CRTC complex formation to induce transcription has been tested by deletion of CRTC2 coiled-coil region (Conkright et al. 2003) or mutation in the CREB-bZIP Arginine 314, binding site of CRTC2 (Screaton et al. 2004). Both approaches resulted in abolition of CREB dependent transcription.

Canonical activation of CRTCs depends on dephosphorylation and nuclear translocation. Under resting conditions, CRTCs are sequestered in the cytoplasm via a phosphorylation dependent interaction with dimeric 14-3-3 proteins. Ca^{2+} and cAMP signals trigger the release from 14-3-3 proteins by activating the CRTC phosphatase Calcineurin (CN) and inhibiting the salt-inducible kinases (SIK) 1-3, respectively. Dephosphorylated CRTC migrates into the nucleus to activate CREB-dependent-transcription (Screaton et al. 2004; Takemori et al. 2007).

2.2 *CREB signalling pathways in the CNS:*

Up to date, more than 300 stimuli have been described as capable to promote the activation of CREB-dependent transcription through different signalling pathways that involve Ser 133 phosphorylation by multiple kinases, as mentioned above. In the CNS, this phosphorylation occurs under a wide variety of circumstances that share the need of an external stimuli to take place, as responses to growth factors during development of the nervous system, depolarization and synaptic activity during normal neuronal function or hypoxia and stress responses in stroke or brain injury. Most of the work in CREB signalling in the CNS has been centered in neurons and little is known about astrocytic CREB signalling, despite the fact that astrocytes also express CREB (Ferrer et al. 1996) and respond to the same variety of stimuli as neurons (Verkhratsky et al. 2012).

The main signalling pathways leading to CREB phosphorylation in the CNS, as reported mostly in neuronal studies, are summarized below and depicted in figure 10.

2.2.1 *cAMP-PKA signalling to CREB:*

Considered the canonical pathway that activates CREB, it was first discover by Goodman and Montminy during the investigation of the cAMP-induced somatostatin transcription (Montminy et al. 1986). The binding of an extracellular ligand to GPCRs promotes the activation of a coupled heterotrimeric (α, β and γ subunit) Gs protein that leads to dissociation of its α subunit from the β-γ complex, stimulating adenylyl cyclase (AC) activity and therefore cAMP production. cAMP interacts with the regulatory subunits of the tetrameric PKA and separates them from the catalytic subunits, thus activating the enzyme and allowing its nuclear translocation to phosphorylate CREB at Ser 133 (Shaywitz and Greenberg 1999).

2.2.2 *Growth factor signalling to CREB:*

Neuronal growth factors, such as neurotrophins, signal trough tyrosine kinases receptors (TrKs) which, upon ligand binding and dimerization, activate different signalling pathways. The mitogen-activated protein kinase (MAPK) pathway starts upon activation by a TrK of the guanine nucleotide exchange factor Sos, via the adaptor complex Grb2/Shc. Sos activates a cascade of subsequent activated kinases (Ras-Raf-MEK) that leads to an intersection point represented by the extracellular signal-regulated kinases (ERK 1/2). ERK 1/2 can either phosphorylate RSK1-3 that translocate to the nucleus and phosphorylate CREB or go to the nucleus to activate mitogen- and stress-activated protein kinases (MSK) 1/2 also leading to CREB phosphorylation (Frödin and Gammeltoft 1999). Other well characterized signalling pathway activated by TrKs is the phosphatidylinositol 3-kinase (PI3K)/Akt pathway, which mediates CREB transcriptional activation in response to serum or insulin-like growth factor 1 (IGF-1) stimulation (Du and Montminy 1998; Leinninger et al. 2004). Upon activation by the receptor, PI3K increases the membrane concentration of

phosphatidylinositol-3, 4, 5-trisphosphate (PIP3), which in turn recruits protein kinase D (PKD) and Akt to the cell membrane. Once activated via PKD phosphorylation, Akt translocate to the nucleus and phosphorylate CREB.

2.2.3 *Ca^{2+} signalling to CREB:*

Kandel and Greenberg first reported that CREB can act as a Ca^{2+} inducible transcription factor (Dash et al. 1991). From this discovery, several Ca^{2+} dependent pathways have been identified to phosphorylate CREB. In neurons, intracellular Ca^{2+} increases are mainly brought about through voltage or ligand-gated cation channels. Thus, Ca^{2+} influx comes via voltage-sensitive Ca^{2+} channels (VSCC) upon membrane depolarization, or through NMDA ionotropic receptors, which function as cation-permeable ion channels and are activated by glutamate binding during glutamatergic synaptic transmission (Lonze and Ginty 2002). However, increase of intracellular Ca^{2+} levels can also take place through the metabotropic glutamate receptors (mGluRs) which are coupled to the activation of PLCβ via protein Gαq/11. PLCβ catalyses the cleavage of phosphatidylinositol-4,5-bisphosphate (PIP2) to ensuing formation of the intracellular second messengers, IP3 and diacylglycerol (DAG). IP3 binds to its receptors (IP3R) in the ER and raises cytosolic Ca^{2+} concentration (Wang and Zhuo 2012). Intracellular Ca^{2+} binds to the protein calmodulin (CaM) to form the Ca^{2+}-CaM complex and activates Ca^{2+}-CaM-dependent kinases (CamKs). This activation can be directly, as it happens in CaMKII, or indirectly through an upstream CaMK kinase as in the case of CaMKIV. Both CamKII and IV have been shown to phosphorylate CREB *in vitro* but the later has been identified as the most important kinase that activates neuronal CREB *in vivo* (Shaywitz and Greenberg 1999; Ho et al. 2000).

Ca^{2+}-CaM complex can also modulate the cAMP-PKA pathway by potentiating the stimulation of Ca^{2+}-sensitive ACs. Besides, Ca^{2+} is involved in the MAPK pathway through the activation of PKC. (Shaywitz and Greenberg 1999; Wang and Zhuo 2012).

2.2.4 *PKC signalling to CREB:*

PKCs are a multigene family of serine/threonine kinases divided in classical (α, β, γ), novel (ε, δ, η, θ) and atypical (ζ, λ/ι) isoforms, which are activated in response to different mediators. Classical PKCs are typically activated by Ca^{2+} and DAG resulting from the cleavage of PIP2 by PLC, which triggers MAPK pathway by PKC direct phosphorylation of Raf, resulting in CREB activation (Wang and Zhuo 2012). In contrast, novel PKCs are Ca^{2+}-independent but DAG dependent while atypical PKCs respond to a set of lipidic second messengers like arachidonic acid, phosphatidylinositol triphosphate or ceramide (Steinberg 2008). Interestingly, many studies of PKC activating CREB in the CNS, including the one presented in this thesis, have not reported the involvement of classical signalling pathway, but rather the direct PKC phosphorylation of ERK 1/2 and/or CREB (Martín et al. 2009; Guo and Feng 2012), thus pointing to the participation of novel and atypical isoforms in CREB phosphorylation.

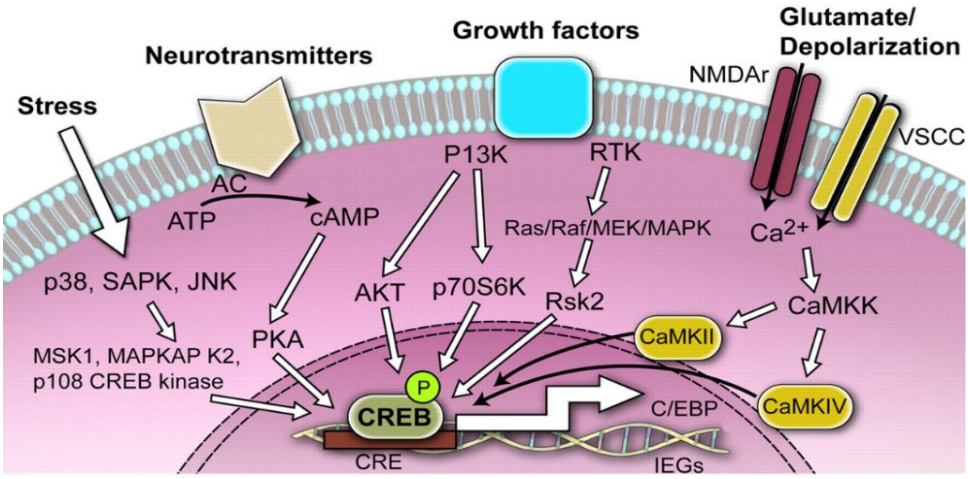

Fig. 10. Signalling pathways leading to activation of CREB-dependent transcription in the brain. CREB has a central role that integrate multiple stimuli. Adapted from (Alberini 2009).

2.2.5 *Stress-induced signalling to CREB:*

In addition to physiological stimuli, CREB can also be phosphorylated in response to harmful or stressful signals, including UV irradiation, hypoxia or inflammatory cytokines. Such signals activate a cascade of MAPKs that leads

to the phosphorylation of SAPK2/p38MAPK. Upon nuclear translocation, p38MAPK activates the downstream kinases MAPKAP K2, MSK1 and MSK2 which are able to phosphorylate CREB (Deak et al. 1998).

2.3 *CREB target genes:*

The list of putative CREB target genes includes genes that control neurotransmission, cell structure, signal transduction, transcription, and metabolism. Despite all these genes share the presence of CREB-binding sites in their promoter regions, their expression does not work as a coordinated switch that relies on CREB phosphorylation. For example, the immediate early gene *c-fos*, one of the first genes identified as CREB-dependent, has a transcriptional activity not correlated with CREB phosphorylation. Even in in the presence of stimuli that produce prolonged phosphorylation of CREB, *c-fos* transcription is still transitory (Lonze and Ginty 2002). The expression patterns of CREB-dependent genes involve regulatory mechanisms that exceed simple CREB activation and are dependent on kinetics, stimulus and cell type, besides other factors (Mayr and Montminy 2001; Johannessen et al. 2004). Thus, neuronal CREB activation in response to neurotransmitters leads to the transcription of genes necessary for synaptic plasticity modulation (Benito and Barco 2010) while the astrocytic CREB response to the same stimuli relies more on homeostatic genes, as shown in the second chapter of this thesis.

In order to identify CREB target genes, reporter-based methods have been used for many years. However, the rapid evolution of high throughput techniques in the last decade has allowed to interrogate vast regions of the genome for CREB binding and CRE-regulated gene expression. The first genome analysis for CREB binding sites was carried out by the Goodman group (Impey et al. 2004) in forskolin-treated PC12 cells. Using a combination of Chromatin immunoprecipitation (ChIP) and serial analysis of gene expression, they identified 6302 CREB-binding regions. These data were tested by microarray analysis finding 1621 genes induced by forskolin treatment, half of which were CREB target genes. Shortly afterwards, Montminy group conducted a genome-wide analysis using microarray and

ChIP on chip techniques, addressed to characterize the expression profile of CREB dependent transcription in different tissues (Zhang et al. 2005). They observed that the differences in expression were not due to CREB promoter occupancy or phosphorylation status but reflected the recruitment of different coactivators to the promoter. More recently, some studies have gained insight into the CREB-dependent gene expression in neurons associated to neuronal activity (Benito et al. 2011), plasticity (Jancic et al. 2009) or long-term memory (Lakhina et al. 2015).

2.4 *CREB functions in CNS physiology and pathology:*

Since the discovery of CREB thirty years ago, much effort has been made to describe its pathways of activation and the multiple CREB associated functions in the brain. However, most of this effort has been concentrated in the study of neuronal CREB, forgetting the roles of glia in CREB related functions.

2.4.1 *CREB in learning, memory and synaptic plasticity*

The first behavioural studies in learning and memory formation demonstrate the requirement of new protein synthesis and gene transcription for these processes. Likewise, long term changes in synaptic plasticity, which are the molecular mechanisms for memory formation, have the same requirements (Kandel 2001). The role of CREB in these processes was first established in a series of works with the mollusc *Aplysia Californica*, in which the long-term facilitation of the gill-withdrawal reflex was associated with CREB-mediated gene expression (Dash et al. 1990). The phylogenetic conservation of these findings was supported by the work with *Drosophila melanogaster*, where the inducible expression either of a CREB activator or a CREB repressor increases or blocks the long-term memory in an olfactory task (Yin et al. 1994; Yin et al. 1995). These findings provide the necessary basis to study the role of CREB in vertebrate synaptic plasticity. First works in rodents were addressed to the manipulation of cAMP-PKA pathway. They showed that mutations in AC and inhibitors of PKA caused deficits in spatial memory and impaired long term potentiation (LTP) in hippocampus (Wu et

al. 1995; Abel et al. 1997). In parallel, robust CREB phosphorylation and CRE-reporter gene expression were detected in hippocampal neurons in response to LTP induction or after memory training tasks (Impey et al. 1998; Davis et al. 2000). These results supported a model in which long term plasticity and memory were strongly dependent of CREB-mediated gene transcription and gave way to the direct manipulation of CREB in rodents. The first studies with CREB α/δ knockout mice, which lacks the two major CREB isoforms, showed deficits in spatial memory, contextual fear conditioning and hippocampal LTP (Bourtchuladze et al. 1994; Kogan et al. 1997). However, results obtained with these mice were not definitive because CREB-dependent transcriptional deficits in this model were compensated by the expression of other CREB isoforms (CREBβ) and CREM. New approaches for inhibiting CREB, either by antisense oligonucleotide infusion or by the expression of dominant negative forms of CREB (KCREB, $CREB^{S133A}$ and ACREB, see Barco and Marie 2011 for review), confirmed the results obtained with CREB α/δ knockout mice. Thus, neuronal CREB inhibition resulted in impairment of fear conditioning memories (Kida et al. 2002), reduced spatial memory (Pittenger et al. 2002) and decreased synaptic plasticity (Jancic et al. 2009). On the other side, gain-of-function approaches as the expression of the constitutively active form of CREB, VP16-CREB, showed a lower threshold for LTP in the Schaffer collateral pathway and enhanced consolidation of context and cued fear memory (Barco et al. 2002; Viosca et al. 2009). Despite the amount of evidence for the involvement of CREB-dependent transcription in learning and memory formation, a comprehensive study using four different strains of CREB-deficient mice reported that the conditional disruption of CREB isoforms have only limited effects on hippocampal-dependent cognitive tasks and no effect on LTP and LTD formation (Balschun et al. 2003). These opposite results could be explained by compensation effects of other transcription factors and suggest that CREB can be sufficient but not necessary to trigger a transcriptional program able to sustain LTP.

CREB coactivator CRTC1 is also involved in synaptic plasticity and memory and its nuclear recruitment seems to be important in the CRE-regulated

transcription underlying modulation of synaptic strength. CRTC1 has been found to promote a transcriptional program in response to coincidental cAMP and Ca^{2+} signals and to be critically involved in the maintenance of the late phase of LTP (Zhou et al. 2006; Kovács et al. 2007).

2.4.2 *CREB in CNS development, neurogenesis and survival*

In vivo studies with mice lacking principal CREB isoforms showed the participation of this transcription factor in neuronal survival and CNS development. These CREB null mice died immediately after birth and showed marked defects in the development of the CNS including a reduction in axon projections in corpus callosum (Rudolph et al. 1998) and degeneration of sensory neurons in dorsal root ganglia (Lonze et al. 2002). However, no increases in neuronal death were observed during embryonic stages. This limited phenotype could be explained by the compensatory role exerted by CREM, which is upregulated in these mice. Supporting this theory, Mantamadiotis and collaborators (Mantamadiotis et al. 2002) showed that the ablation of *Creb1* gene in neurons and glia does not affect neuronal survival during development or post-natally. However, elimination of both *Creb1* and *Crem* genes, results in perinatal lethality and a marked loss of neurons in several regions of the CNS.

The mechanism of CREB promoted cell survival appears to be driven by transcription of pro-survival factors as B-cell lymphoma 2 (Bcl-2) or myeloid cell leukemia 1 (Mcl-1) in response to neurotrophin signalling (Riccio et al. 1999; Arbour et al. 2008). In adult CNS, CREB-dependent transcription continues to be necessary for neuronal survival. For example, when *Creb1* and *Crem* genes are eliminated in adult brain, a progressive degeneration occurs, affecting cortex, hippocampus and striatum (Mantamadiotis et al. 2002). In addition, overexpression of a dominant negative form of CREB ($CREB^{S133A}$) in the cingulate cortex of adult mice, results in cortical neurodegeneration and increased apoptosis (Ao et al. 2006).

As long as the ablation of CREB promotes neuronal death both in perinatal and adult mice, is reasonable to think that its overexpression might have

beneficial effects. However, chronic expression of a constitutively active form of CREB (VP16-CREB) in neurons led to epileptic seizures and marked loss of hippocampal neurons (Lopez de Armentia et al. 2007). Interestingly, cell death resulting from CREB over-activation responds to an excitotoxic mechanism while the lack of CREB leads to an apoptotic death. Moreover, the transcriptional profile of neuronal CREB over-expression showed an increase in stress and inflammatory-related genes, which are likely to contribute to excitotoxic cell loss (Valor et al. 2010).

CREB has also an important role in the regulation of adult neurogenesis. Several studies have reported the presence of phosphorylated CREB (pCREB) in most of the newly generated neurons in the SGZ and in the sub-ventricular zone/olfactory bulb (SVZ/OB) system. This phosphorylation overlaps with the expression of doublecortin (DCX) and is stable upon neuronal maturation, when DCX gives rise to mature granular cell markers as calbindin and CREB phosphorylation becomes transient in response to neuronal activity (Merz et al. 2011).

The CREB coactivator CRTC1 is also implied in neuronal development (S. Li et al. 2009). CRTC1 is highly expressed in the early stages of neural tissue development, correlating with dendrite arborisation, and it has been shown in neuronal cultures that the activation of CRTC1 causes axonal growth while its inhibition decreases dendrite length. The mechanism of CRTC1-dependent dendrite arborisation implies glutamate activation of NMDA receptors and the transcription of the CREB-dependent gene *Bdnf* (Finsterwald et al. 2010).

2.4.3 *CREB in ischemia:*

Cerebral ischemia results in the lack of oxygen and glucose transport to the injured area, which promotes depletion of cellular energy stores and a general failure of homeostatic mechanisms. Decrease in intracellular ATP promotes the dysregulation of ionic gradients through cell membranes and causes a massive efflux of glutamate to the extracellular space. Glutamate binds to ionotropic membrane receptors NMDA/AMPA and promotes

Ca^{2+} influx to the cytosol, which causes the disordered activation of a wide-range of enzymes and leads to excitotoxic cell death. Two main regions can be distinguish in focal ischemia: the ischemic core, with almost impaired blood flow and acute cell death; and the penumbra area, a mild ischemic tissue where cells can survive for hours due to the flow of collateral arteries. Intracellular Ca^{2+} increments in brain ischemia activate several signalling pathways leading to CREB phosphorylation and CREB-dependent transcription of genes such as *Bcl2* and *Bdnf*, which are protective against ischemic-induced neuronal death. This model of CREB activation is supported by several studies and suggests a main role of CREB in neuroprotection (Kitagawa 2007). In vitro ischemic models, such as exposure to glutamate, showed increased CREB phosphorylation after insult and its dependence of NMDA receptor activation and CaMK signalling pathway (Lonze and Ginty 2002; Sakamoto et al. 2011). In addition, neurons exposed to glutamate showed accelerated damage and lower expression of *Bcl2* when treated with CaMK II-IV inhibitors or CREB-decoy oligonucleotides (Mabuchi et al. 2001).

The most extended model of focal cerebral ischemia *in vivo* is the middle cerebral artery occlusion (MCAO). Using this model, Tanaka and collaborators found increased CREB phosphorylation in the penumbra regions surrounding the ischemic core (Tanaka et al. 1999). Similar results were found in a common model of global ischemia, consisting in carotid artery ligation (Walton et al. 1999). In this case CREB phosphorylation appeared increased in the hippocampal dental gyrus (DG) but decreased in *Cornus Amonis 1* (CA1) neurons, which are more vulnerable to ischemic cell death. This findings point to a correlation between the ability of sustain CREB phosphorylation and ischemic resistance. To link these increments in phosphorylation with CREB-driven gene expression, Mabuchi and collaborators used transgenic mice with a CRE-lacZ reporter. After transient global ischemia, they found a subset of hippocampal neurons showing both CREB phosphorylation and CRE-dependent β-galactosidase expression. Furthermore, when performed MCAO in these mice, they observed CRE-

mediated transcription mainly in the surviving neurons of the peripheral area surrounding the ischemic core (Mabuchi et al. 2001).

Treatments for stroke, the leading cause of brain ischemia, are directed to recover cellular function in the penumbra area. To date, treatment strategies have been directed to inhibit glutamate release, antagonize glutamate receptors and abrogate death signalling cascades. However, activation of the Akt/CREB signalling pathway has shown improved outcomes in many models of ischemia by increasing anti-apoptotic and neurotrophic factors (Lai et al. 2014). Accordingly, many drugs that afford protection in ischemic models also induce the activation of this pathway (Carloni et al. 2009; Clarkson et al. 2015).

2.4.4 *CREB in oxidative stress:*

Oxidative stress is caused by the accumulation of ROS formed during mitochondrial respiration due to an insufficient turnover from the antioxidant enzymes as SOD 1/2. ROS cause DNA damage, oxidation of macromolecules and activation of mitochondrial apoptotic pathway. Besides, they trigger many signalling cascades due to inactivation of major cell phosphatases and subsequent phosphorylation of signalling mediators by principal kinases such as MAPK, JNK, ERK or the p38 stress-activated kinase (Korbecki et al. 2013). One of the most studied transcription factors in oxidative stress is the nuclear factor κ B (NFκB), which promotes the transcription of proinflammatory mediators, as IL-1β or TNF-α, and inducible enzymes Cyclooxygenase 2 (COX2) and NO synthase (iNOS). In order to achieve its optimal activity, NFκB must bind to CBP/p300 coactivators through the same region as pCREB and a model has been proposed in which NFκB activity is inhibited by pCREB through competition for limited amounts of CBP/p300 (Parry and Mackman 1997). CREB activation in response to oxidative stress leads to expression of anti-inflammatory factors such as IL-10, so this competitive model could function as a balance between pro and anti-inflammatory mediators in stressful situations (Agarwal et al. 2013).

CREB also functions as a neuroprotective factor in oxidative stress by regulating ROS detoxification. CREB activation in neurons stimulates the expression of antioxidant enzymes, as heme oxigenase 1 or manganese superoxide dismutase, and also the expression of PGC-1α, a key effector of ROS-detoxifying enzyme expression and mitochondrial biogenesis (reviewed in Sakamoto et al. 2011). Moreover, studies in mice expressing the dominant negative form A-CREB showed that the inhibition of CREB-driven transcription leads to increase in seizure-induced ROS production, reduction on PGC-1α and heme oxigenase 1 expression and enhancement of neuronal death (Lee et al. 2009).

2.4.5 *CREB in neurodegeneration:*

The role of CREB in synaptic plasticity and memory formation makes it an ideal candidate to be affected in cognitive disorders and neurodegeneration. Indeed, mouse model lacking *Creb1* and *Crem* genes show striatal degeneration (Mantamadiotis et al. 2002) in a similar pattern to that of Huntington's disease (HD), the first CREB associated disorder. HD is an autosomal dominant heritable disease associated with degeneration of striatal medium spiny neurons and characterized by anemia, chorea and early cognitive impairment. HD is caused by an accumulation of polyglutamine repeats in the N-terminal region of the protein huntingtin (Htt), which causes its nuclear accumulation and the blockade of CREB dependent transcription. Mutant Htt has been shown to interact with CBP and p300 and to reduce their HAT activity, affecting CBP/p300 dependent transcription (Nucifora et al. 2001). In fact, the inhibition of histone deacetylase (HDAC) blocks neuronal degeneration and death in *Drosophila* and mouse HD models (Steffan et al. 2001). Mutant Htt also binds to the promoter of CREB target genes and interferes with CREB-TAF4 association (Cui et al. 2006).

The most prevalent degenerative disorder, Alzheimer's disease (AD), has been also linked to CREB through two of the major molecular mechanisms involved in disease progression: the accumulation of amyloid β (Aβ) peptides and alterations in the presenilin-γ-secretase complex. Effects of Aβ

in hippocampal synaptic plasticity, memory and synapse loss are mediated by CREB (Saura and Valero 2011). Aβ42 accumulation reduces PKA activity and CREB phosphorylation in neuronal cultures and hippocampal slices, which correlates with LTP disruption (Vitolo et al. 2002). Recent works with $APP_{Sw,Ind}$ transgenic mice, a common model of AD, showed that CREB-dependent transcription deficits in AD are prevented by inhibiting Aβ production. Furthermore, the overexpression of CREB coactivators CRTC1/2 rescues CREB transcriptional deficits indicating that the effect of Aβ in the disruption of CREB-dependent transcription is mediated by CRTCs (España et al. 2010). Interestingly, CRTC1 dephosphorylation and nuclear migration are impaired in $APP_{Sw,Ind}$ mice as well as CRTC1-dependent gene expression, which correlates with long-term spatial memory deficits in this model. These deficits can be reduced by overexpression of CRTC1 in the hippocampus (Parra-Damas et al. 2014). Studies that linked presenilin (PS) alterations in AD with CREB dependent transcription were performed mainly with the inducible PS double knockout mouse model (PScDKO). Inactivation of PS in this model results in memory deficits and neurodegeneration that correlates with reduced expression of CREB/CBP related genes (Saura et al. 2004). The PS1 gene has CRE sequences in the promoter and is expressed upon glutamate receptors activation and Bdnf signalling, while impairment of CREB phosphorylation through the dominant negative $CREB^{133A}$ reduces PS1 expression (Mitsuda et al. 2001).

Rubinstein-Taybi syndrome (RTS) is a rare disease characterized by multiple deficits including facial abnormalities and mental retardation. RTS is caused by heterozygous mutation in the CBP gene that leads to a deficit in CBP related transcription and HAT activity. Works with heterozygous CBP deficient mice that expressed a mutant CBP lacking the HAT region ($CBP^{+/-}$) showed a phenotype resembling to RTS while CBP knockout mice died at embryonic stages. $CBP^{+/-}$ mice show cognitive deficits partially due to deficient CREB-dependent transcription and reduced HAT activity but these deficits can be overcome by the administration of phosphodiesterase 4 (PDE4) inhibitors as rolipram, which maintains increased levels of cAMP

and promotes CREB phosphorylation and CREB-dependent transcription (reviewed by Hallam and Bourtchouladze 2006).

Another rare disorder associated with CREB is the Coffin-Lowry syndrome (CLS) which courses with severe mental retardation, physical abnormalities and short stature (Trivier et al. 1996). CLS is caused by a mutation in the *Rsk2* gene resulting in the loss of protein kinase activity, which can directly affect CREB-dependent transcription given that RSK2 phosphorylates CREB through ERK/p38MAPK signalling. RSK2 knockout mice present lower weight and length, disturbed glycogen metabolism and impaired learning and memory (Poirier et al. 2007). These phenotype is associated to an abnormal regulation of MAPK pathway that affects CREB phosphorylation (Schneider et al. 2011). Furthermore, reduced RSK2-mediated CREB phosphorylation correlates positively with cognitive impairment in CLS patients (Harum et al. 2001).

Despite the well-characterized signalling pathways and functional roles of CREB in the CNS physiology and pathology, the neurocentric view has limited the acquired knowledge about this transcription factor to only one cell type. Participation of glial cells in many CREB-regulated processes, such as synaptic plasticity or neuroprotection, claims for a better characterization of CREB in these cell populations. Recent works have reported the beneficial roles of modulating astrocytic CREB in pathological situations such as AD or ischemia (Corbett et al. 2013; Qi et al. 2015) thus supporting the importance of glial CREB in brain pathology. In this thesis, we are trying to elucidate the signalling cascades that lead to CREB activation in astrocytes and to identifying astrocytic CREB-dependent genes both in normal and pathological conditions.

3. Traumatic brain injury.

TBI is one of the major causes of death and severe disability around the world with a 0.5% of incidence. In the severe cases, 39% of the patients die from their injury and 60% have unfavourable outcome. It affects mainly

young adults in the industrialised world, and it is rising in development countries due to the increased use of motor vehicles. Besides car accidents, other causes of TBI are impact falls that affect mainly to elderly people, and blast injuries in the military personnel (Rosenfeld et al. 2012; Roozenbeek et al. 2013).

The principal forms that TBI presents are: focal brain damage due to contact injury types resulting in contusion, laceration, and intracranial haemorrhage, or diffuse brain damage due to acceleration/deceleration injury types resulting in diffuse axonal injury or brain swelling (Werner and Engelhard 2007). Clinically, relevant cases of TBI usually present a combination of both focal and diffuse damage. The outcome from head injury is divided in two substantially different stages: the primary brain injury refers to the unavoidable brain damage that occurs at the moment of impact, resulting in disruption of parenchyma and blood vessels. The secondary brain injury, which occurs from minutes to months after the primary insult, consists in the pathophysiological cascades and the delayed non-mechanical damage that begin immediately after the primary injury. This includes processes like cerebral ischemia, inflammation or metabolic imbalance that, in turn, will lead to neuronal death. Since the first stage of TBI can only be addressed with preventive measures, efforts for TBI treatment have been focused on the secondary brain injury, which offers a therapeutic window to pharmacologically manipulate some of the factors involved (Morganti-Kossmann et al. 2007; Werner and Engelhard 2007).

3.1 *General pathophysiology of TBI*

The first stages of cerebral injury after TBI are characterized by direct tissue damage and impaired regulation of CBF. This reduction of CBF initiates an ischemic cascade that promotes a metabolic switch from aerobic to anaerobic glycolysis and leads to accumulation of lactate. Since the anaerobic metabolism is inadequate to maintain cellular energy states, the ATP-stores deplete and failure of energy-dependent membrane ion pumps occurs. At the same time, tissue damage causes the rupture of the vascular endothelial wall, which allows for uncontrolled ion and protein transfer from the

intravascular to the extracellular brain compartments with ensuring water accumulation and hence formation of vascular edema. The interstitial ion accumulation, together with the failure of membrane ion pumps, increases cellular membrane permeability and leads to water accumulation in the cytoplasm of neurons, astrocytes and microglia, causing a cytotoxic brain edema. The accumulation of glutamate -that leaks out of damaged membranes or is released due to ionic imbalance- in the extracellular space leads to membrane depolarization and hyperexcitabilty. Excess of glutamate binds to NMDA/AMPA receptors, and promotes a massive influx of Ca^{2+} and Na^{+} leading to activation of a number of enzymes that initiate self-digesting intracellular processes. Ca^{2+} activates lipid peroxidases, proteases, and phospholipases which in turn increase the intracellular concentration of free fatty acids and free radicals, causing oxidative damage. Additionally, activation of caspases, translocases, and endonucleases initiates progressive disruption of biological membranes and the nucleosomal DNA fragmentation. Together, these events lead to membrane degradation of vascular and cellular structures and ultimately necrotic or apoptotic cell death. (Werner and Engelhard 2007; Algattas and Huang 2013).

3.2 *Tissue response to TBI: a multicellular event*

The response to a focal injury comprises several cell types (fig. 11) including CNS intrinsic cells –neurons, astrocytes, microglia, oligodendrocytes- and blood-borne derived cells –leukocytes, lymphocytes, thrombocytes-. To examine the action of different cell types we will divide the events that follows the acute brain damage in three phases: acute cell death and inflammation, cell replacement and tissue remodelling.

3.2.1 *Cell death and inflammation:*

After a focal brain damage that cause local acute cell death, second-to-hour scale events take place in the core of the lesion including haemostasis with coagulation cascade, platelet aggregation and clot formation. These rapid events are followed by responses of tissue intrinsic cells, recruitment of inflammatory and immune cells and subacute death of parenchymal cells.

The tissue damage caused by focal injury compromises the BBB and allows infiltration of polymorphonuclear leukocytes (PMN) into the brain parenchyma, which release pro-inflammatory cytokines like IL-1β, IL-6 and TNF-α, cytotoxic proteases and ROS, thus initiating the inflammatory process. This inflammatory environment, caused not only by infiltrating blood-borne cells but also by brain intrinsic cells that release pro-inflammatory factors in response to brain damage, promotes the activation of microglia and astrocytes. Microglial cells immediately migrate to the injury sites and change their morphology and physiology to a monocyte-like, releasing cytokines and chemokines and exerting macrophage functions like scavenging and phagocytosis. In contrast, astrocytes do not migrate to the lesion but become reactive and hypertrophic, releasing also pro-inflammatory factors and in some cases proliferating in the border of damaged tissue. In these early stages after brain injury, the factors released by activated microglia and astrocytes contribute to the secondary damage by increasing the inflammation and excitotoxicity. For example, the chemokines released by microglia and astrocytes promote the expression of adhesion molecules on blood vessels thus allowing leukocyte and lymphocyte extravasation from the periphery to the brain parenchyma and subsequently contributing to inflammatory progression. In the same way, the pro-inflammatory cytokine IL-1β promotes the release of matrix metaloproteinase-9 (MMP-9) in astrocytes, which degrades extracellular matrix and further promotes BBB breakdown, prolonging neuroinflammation (Algattas and Huang 2013; Burda and Sofroniew 2014)

3.2.2 *Cell proliferation and tissue replacement:*

The second phase of response to focal brain injury develops during the first week after primary insult. This phase is characterized by proliferation and local migration of cells that will promote tissue repair and replacement like endothelial and fibroblast progenitors, neural stem cells or proliferative astrocytes. The latter will produce newly forming astrocytes that elongate, surround the damaged tissue and form a glial scar that will isolate the lesion core from the functional tissue, thus restricting the spread of infiltrate

leukocytes. The lesion core accumulates non-neural lineage cells that will collaborate with scar-forming astrocytes to promote tissue repair. The endothelial progenitors are activated by the release of high mobility group protein B1 (HMGB1) from reactive astrocytes and promote vascular remodelling, while the fibroblasts proliferate and secrete ECM proteins such as collagen IV, fibronectin and laminin to form a fibrotic scar that encapsulates infiltrating leukocytes and contribute, together with the glial scar, to isolate the damaged tissue. The glial scar further contributes to the failure of axonal regeneration through the axonal growth-inhibiting property of ECM proteins, like CSPs, produced by reactive astrocytes. This will result in the death of neurons whose axons were transected by the primary injury. During this proliferative phase, neural stem cells in the germinal periventricular areas increase the production of neural progenitors that migrate to the injury sites and stablish in the perimeters of the lesion to participate in tissue remodelling in this areas (Kawano et al. 2012; Burda and Sofroniew 2014).

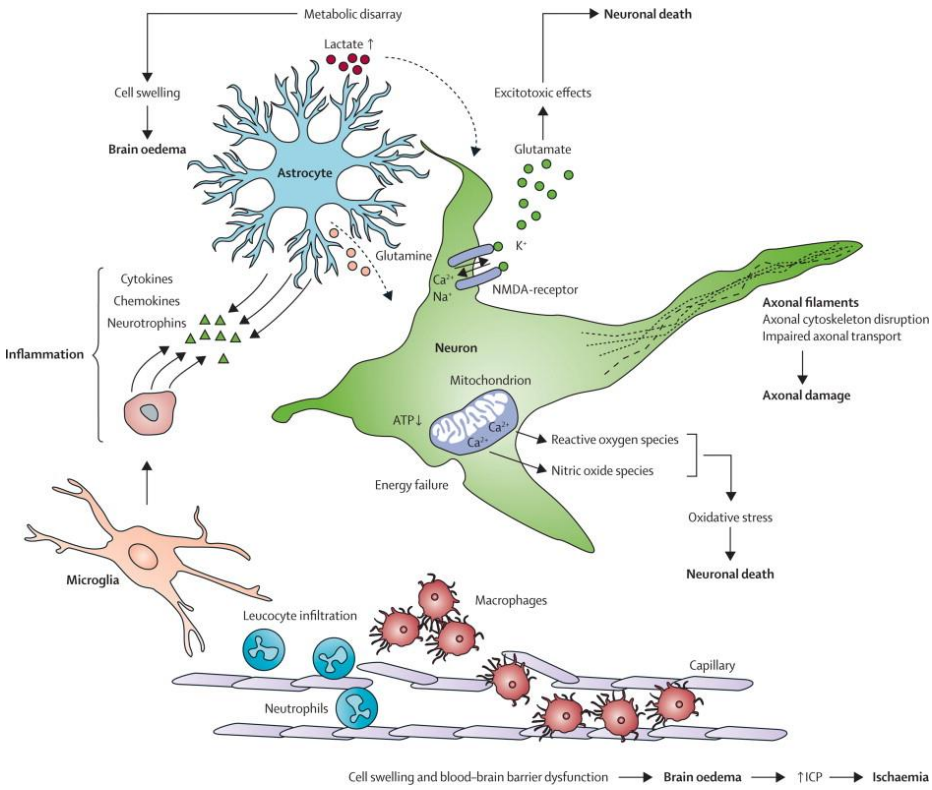

Figure 11. Pathophysiology of TBI. From (Rosenfeld et al. 2012)

3.2.3 *Tissue remodelling:*

The third phase begins a week after the primary insult and comprises events such as BBB repair and glial scar organization, which can last for 2-3 weeks. In this period, damaged tissue is completely isolated and leukocyte infiltration no longer occurs. In the lesion core, tissue remodelling continues for long time and will eventually transform the core into a fibrotic region filled with fibroblasts and ECM proteins. The lesion perimeter will suffer high remodelling at this time. While neurons with transected axons continue to die away from the lesion, new progenitors arrive and formation of new synapses and new potential circuits takes place. Glial activation still continues in the lesion perimeter but gradually disappears in the transition to healthy tissue (Kawano et al. 2012; Burda and Sofroniew 2014).

3.3 ***Animal models of TBI:***

In order to cover the variability often seen in human brain injury, several animal models have been developed to elucidate the biochemical aspects and neurobiological consequences of primary and secondary injury, as well as the patterns of cognitive dysfunction. Commonly used models for simulating human brain injury in animals include the controlled cortical impact model (CCI), the central or lateral fluid percussion injury model (CFP or FPI), the weight drop model, the cryolesion model and the blast injury model (Giralt et al. 2002; Zhang et al. 2014). The CCI model of TBI involves the use of an impact device to deliver a controlled strike to an exposed area of the dural surface. The physical parameters of the strike, such as velocity and depth of impact, are easily controlled in the CCI model and is thus a useful model for detecting the biomechanical consequences of TBI. In the FPI model of TBI, injury is incurred by a pendulum striking a fluid reservoir resulting in a calculated increase of intracranial pressure, which varies as the height and force of strike are altered, leading to deformation of neural tissue. The weight-drop model involves dropping a weight onto an immobilized animal, with injury severity adjusting proportionately with alterations in the mass of the weight. The cryolesion model consists in the application of a dry ice pellet onto the exposed skull, which creates lesions highly reproducible in size and location due to the easy control of the pellet diameter. In blast models of TBI, the effects of blast waves from an explosion are emanated at varying locations and carried through shock tubes or open exposure to an immobilized animal. The blast model provides an accurate representation of TBI incurred by explosive devices (Xiong et al. 2013; Zhang et al. 2014).

In this thesis we used the cryolesion as a model for TBI (Giralt et al. 2002) due to its high reproducibility and technical simplicity as craniotomy is not required. This method reproduces many characteristics of human focal brain injury as vasogenic edema, brain swelling or inflammation.

3.4 *Pharmacological treatments for TBI:*

Clinical intervention is critical to improve the outcomes of TBI. Removal of haematomas and reduction of intracranial pressure have proved to

ameliorate the evolution of TBI patients and induced hypothermia is also a promising treatment that has showed many beneficial effects in animal models of TBI, though its benefits for patients are still controversial. In addition, some drugs addressed to avoid the effects of secondary damage following TBI have proven its efficacy in animal models and are now tested in clinical trials. Treatment with statins, inhibitors of cholesterol biosynthesis, suppresses inflammation, rescues neurons from excitotoxic effects and reduces apoptosis. A study in rats showed improve in spatial learning, reduced neuronal loss and increased neurogenesis in the DG after treatment with atorvastatin and simvastatin (Lu et al. 2007). In addition, simvastatin has found to inhibit IL-1β and to reduce microglial activation and astrogliosis (Li et al. 2009). Treatment with progesterone has also proved to be neuroprotective in animal models through inhibition of glutamate toxicity, cell death and inflammation (Schumacher et al. 2007). Cyclosporine-A, an immunosuppressive drug, diminishes oxidative stress and attenuates axonal failure and disconnection (Mbye et al. 2009). One of the most promised drugs against TBI is erythropoietin, an endogenous hormone that stimulates haemopoiesis and has neuroprotective and neuroregenerative effects through reduction of apoptosis, inflammation, oxidative stress, and excitotoxicity. This hormone decreases lesion volume and brain accumulation of leucocytes while promotes angiogenesis and neurogenesis and improves motor and cognitive function. Erythropoietin crosses the blood–brain barrier and binds to receptors on most brain cells. The brain is susceptible to erythropoietin treatment because its receptor is upregulated after injury or hypoxia. Erythropoietin has a long half-life and maintains its effectiveness with delayed administration; however, risk of thrombotic events is increased with this drug (Sirén et al. 2009).

3.5 *Beneficial and detrimental roles of astrocytes following focal TBI:*

The impact of astrocyte gliosis on the pathogenesis of focal brain injury has been largely studied but is still under controversy. The old conception from Ramon y Cajal promoted a negative view of reactive astrogliosis *per se* based mainly in the inhibition of axonal regeneration by the glial scar formation

(Clarke 1992). This detrimental view of astrocytic response to brain injury has been supported by studies addressing the inhibitory properties of glial scar such as the production of CSPs, pro-apoptotic factors or pro-inflammatory cytokines (Sofroniew 2009). However, the work of Sofroniew and colleagues using a transgenic model to completely ablate reactive and dividing astrocytes, challenged the classical view and showed that astrogliosis is an essential process that exerts protective and beneficial functions in response to brain injury. They produced transgenic mice expressing HSV-thymidine kinase under the control of the GFAP promoter, and ablated dividing astrocytes by the administration of ganciclovir. When exposed to brain injury, the ablation of reactive astrocytes in these mice results in an increase of neurodegeneration and inflammation, failure of BBB restoration, and prolonging leukocyte infiltration (Bush et al. 1999; Faulkner et al. 2004).

Many studies have addressed both positive and negative roles of astrogliosis in tissue and function recovery after brain injury without arriving to a clear conclusion. So far, the amount of collected evidence points to the importance of timing and type of injury in determining the beneficial or detrimental functions of reactive astrocytes. Below we summarize the most relevant.

In response to a focal damage in the CNS, astrocytes close to the injured area present hypertrophic and interdigitate processes that surround the damaged region and form a glial scar that isolate the healthy tissue. This barrier limits the spread of inflammatory cells or infectious agents into healthy CNS parenchyma and contribute to the restoration of Blood-Brain-Barrier integrity (Sofroniew 2009). In addition to the works of Sofroniew group referred above, Pekny and collaborators developed a mutant mouse lacking astrocyte intermediate filaments GFAP and Vimentin (Vim) (Pekny et al. 1999). They showed reduced reactive gliosis and scar formation as well as an increased loss of neuronal synapses after neurotrauma, thus supporting the protective roles of astrogliosis.

Astrogliosis protects tissue from the secondary degeneration that takes place hours to days after primary injury. During secondary damage, neuronal death

occurs in the surrounds of the injured area because of the increment in glutamate toxicity, oxidative stress and limited metabolic supplies (Algattas and Huang 2013). Astrocytes are involved in the uptake of glutamate via glutamate transporter GLT-1 and GLAST but, in the injured brain, levels of glutamate transporters in astrocytes are decreased (van Landeghem et al. 2006). In agreement, the upregulation of GLT-1 has shown to be protective against neuronal loss following injury (Ouyang et al. 2007). Astrocytes are also a source of antioxidants as SOD1/2/3 or glutathione which expression is increased in brain injury (Goss et al. 1997; Fernandez‐Fernandez et al. 2012). Regarding metabolism, astrocytes, the main source of metabolic fuel to neurons, upregulate their oxidative metabolism after brain injury to provide energy to dying neurons (Bartnik-Olson et al. 2010). Reactive astrocytes also enhance neuronal survival after secondary damage by the secretion of grow factors like GDNF or VEGF, which stimulates the formation of new blood vessels and promotes synaptogenesis (Pekny and Pekna 2014).

Reactive astrocytes and glial scar formation play essential roles in the regulation of the CNS inflammation after TBI. In response to different stimuli, reactive astrocytes can make many different kinds of molecules with either pro- or anti-inflammatory potential and reactive astrocytes can exert both pro- and anti-inflammatory effects on microglia, a key player in brain injury. This duality in astrocyte inflammatory responses to focal brain injury is a hallmark of neuroinflammation and is reflected in the actions of cytokines, the molecules that initiate and regulate the process (Morganti-Kossmann et al. 2007). IL-1 has been extensively characterized as a promoter of neuroinflammation and neurotoxicity but also induces the release of nerve growth factor (NGF) in astrocytes (Lu et al. 2005). In a similar way, TNFα has largely view as a pure pro-inflammatory factor that promotes recruitment of leukocytes from the peripheral circulation, release of proteolytic enzymes leading to degradation of the BBB, inhibition of neuronal regeneration and increase of brain edema. However, ablation of TNFα in a transgenic mouse model led to post-traumatic deficits in memory and motor function and increased mortality (Scherbel et al. 1999). IL-6 is

one of the cytokines that better illustrates the dual role of these molecules in neuroinflammation. IL-6 plays a major role in the acute phase of inflammation by influencing chemotaxis and promoting reactive astrogliosis (Romano et al. 1997). On the other hand, IL-6 also acts as an anti-inflammatory and neuroprotective molecule by inhibition of TNFα, stimulation of NGF production, defence against glutamate-mediated toxicity and oxidative stress, and promotion of revascularisation (Swartz et al. 2001). This apparent paradox can be explained by a model in which astrocytes exert different actions at different times after insult and in different locations related to the damaged area. For example, astrocytes can release pro-inflammatory mediators in the early stages following insult and in the injured areas, whereas they release anti-inflammatory molecules at later times and in the border between damaged and healthy tissue (Sofroniew and Vinters 2010).

The main detrimental effect of reactive astrogliosis and glial scar formation is the inhibition of axonal growth and regeneration (Sofroniew 2009). This inhibitory effect has been tested in many experimental models and one of the principal implicated molecules are the CSPs, whose production is increased after trauma (Properzi et al. 2003). Ephrin-A5, expressed by astrocytes and upregulated after injury, is other molecule that limits functional recovery after injury by blocking axonal sprouting (Overman et al. 2012). The inhibition of these two molecules is associated with improved axonal regeneration after injury. In the same way, attenuation of reactive astrogliosis either by ablation of reactive astrocytes or by downregulation of GFAP and Vim results in increased post-traumatic axonal regeneration. (Bush et al. 1999; Pekny et al. 1999).

Brain edema is an important outcome of focal brain injury. The formation of cerebral edema results in increase of tissue water content and brain swelling that can lead to an increment in cranial pressure, reduced blood flow and neuronal death. The astrocyte water channel AQP4 plays a role in formation of cytotoxic edema by increasing water uptake in astrocyte endfeet and promoting astrocyte swelling. The ablation of AQP4 in

astrocytes leads to reduction in brain edema and improved survival after ischemic stroke or acute water intoxication model. In spite of this results AQP4 has also been seen as responsible for the reabsorption of extracellular edema fluid thus helping in the resolution of vasogenic edema (Shields et al. 2011)

3.6 *Regulation of the transcription factor CREB in TBI*:

Several studies have reported alterations of CREB phosphorylation and dependent transcription in TBI but the changes observed did not follow the same direction. Early works with neuronal CREB in TBI found increased pCREB levels 5 minutes after injury that drops to basal at 30 minutes (Dash et al. 1995). On the other hand Atkins and collaborators (Atkins et al. 2009) found decreased CREB activation 2 to 12 weeks after hippocampal TBI. These findings suggest that, during the different stages of TBI, levels of CREB activation pass from a high increase immediately after primary insult to a recovery of normal levels minutes to hours after injury. Finally, levels drop and remain low weeks after, which points to a role of CREB in cognitive deficits observed in clinical patients months to years after TBI.

Attempts to treat the secondary damage in TBI also involve CREB activation. For instance, pharmacologically inhibition of PDE4 with rolipram (Titus et al. 2013) rescued chronic cognitive deficits observed in an hippocampal model of TBI. The activation of Glucagon-like peptide-1 (GLP-1) receptor with GLP-1 analogue liraglutide led to CREB phosphorylation in a PKA dependent manner and has been shown to ameliorate neuropathology in a cold lesion model of TBI (Dellavalle et al. 2014). Also numerous treatments that increase cognitive performance in TBI models implied the use of antioxidants as flavonoids or estrogens, which activate CREB through mGluRs and TrKs receptors.

3.7 *Targeting astrocytes in focal brain injury:*

Giving the central role that astrocytes play in brain injury, they constitute an ideal target to develop therapeutic strategies for the treatment of this condition. Some efforts have been performed in this field. For instance,

antioxidant therapy using metallothionein-1, a protein strongly expressed by astrocytes after injury, decreases oxidative stress and proapoptotic signalling, thus enhancing neuronal survival following brain injury (Leung et al. 2010). Similarly, overexpression of SODs improves behavioral outcomes, decreases brain edema and confers neuroprotection. Another antioxidant enzyme widely expressed by astrocytes, glutathione peroxidase, has been shown to reduce neuronal damage and modulate recovery in the injured brain, clearly demonstrating the importance of astrocytes for neuronal survival (reviewed in Barreto et al. 2011). However, given the multicellular nature of TBI, treatments directed to address the profound alterations suffered by the different implied cells are more like to success. In this direction, we propose the activation of astrocytic CREB as a novel multi-modal treatment for TBI. The ability of CREB to control several cell functions together with the central role of astrocytes in brain injury make it a valuable candidate to address the multifactorial events that take place during TBI progression. In this thesis, we show how the constitutive activation of CREB in astrocytes exerts protective roles in a TBI model ranging from the decrease in inflammation and leukocyte infiltration to the metabolic rescue and axonal regeneration.

REFERENCES

Abbott NJ, Rönnbäck L, Hansson E. 2006. Astrocyte-endothelial interactions at the blood-brain barrier. Nat. Rev. Neurosci. 7:41–53.

Abel T, Nguyen P V., Barad M, Deuel TAS, Kandel ER, Bourtchouladze R. 1997. Genetic demonstration of a role for PKA in the late phase of LTP and in hippocampus-based long-term memory. Cell 88:615–626.

Agarwal D, Dange RB, Raizada MK, Francis J. 2013. Angiotensin II causes imbalance between pro- and anti-inflammatory cytokines by modulating GSK-3?? in neuronal culture. Br. J. Pharmacol. 169:860–874.

Agulhon C, Fiacco TA, McCarthy KD. 2010. Hippocampal short- and long-term plasticity are not modulated by astrocyte Ca2+ signaling. Science 327:1250–1254.

Alberini CM. 2009. Transcription Factors in Long-Term Memory and Synaptic Plasticity. New York:121–145.

Algattas H, Huang JH. 2013. Traumatic Brain Injury pathophysiology and treatments: Early, intermediate, and late phases post-injury. Int. J. Mol. Sci. 15:309–341.

Altarejos JY, Montminy M. 2011. CREB and the CRTC co-activators: sensors for hormonal and Metabolic Signals. Nat. Publ. Gr. 12:141–151.

Alvarez JI, Katayama T, Prat A. 2013. Glial influence on the blood brain barrier. Glia 61:1939–1958.

Anderson M a., Ao Y, Sofroniew M V. 2014. Heterogeneity of reactive astrocytes. Neurosci. Lett. 565:23–29.

Ao H, Ko SW, Zhuo M. 2006. CREB activity maintains the survival of cingulate cortical pyramidal neurons in the adult mouse brain. Mol. Pain 2:15.

Araque A, Sanzgiri RP, Parpura V, Haydon PG. 1998. Calcium elevation in astrocytes causes an NMDA receptor-dependent increase in the frequency of miniature synaptic currents in cultured hippocampal neurons. J. Neurosci. 18:6822–6829.

Arbour N, Vanderluit JL, Le Grand JN, Jahani-Asl A, Ruzhynsky V a, Cheung ECC, Kelly M a, MacKenzie AE, Park DS, Opferman JT, et al. 2008. Mcl-1 is a key regulator of apoptosis during CNS development and after DNA damage. J. Neurosci. 28:6068–6078.

Atkins CM, Falo MC, Alonso OF, Bramlett HM, Dietrich WD. 2009. Deficits in ERK and CREB activation in the hippocampus after traumatic brain injury. Neurosci. Lett. 459:52–56.

Attwell D, Buchan AAM, Charpak S, Lauritzen M, MacVicar BAB, Newman EEA. 2011. Glian and neuronal control of brain blood flow. Nature 468:232–243.

Balschun D, Wolfer DP, Gass P, Mantamadiotis T, Welzl H, Schütz G, Frey JU, Lipp H-P. 2003. Does cAMP response element-binding protein have a pivotal role in hippocampal synaptic plasticity and hippocampus-dependent memory? J. Neurosci. 23:6304–6314.

Barceló-Torns M, Lewis AM, Gubern A, Barneda D, Bloor-Young D, Picatoste F, Churchill GC, Claro E, Masgrau R. 2011. NAADP mediates ATP-induced Ca2+ signals in astrocytes. FEBS Lett. 585:2300–2306.

Barco A, Alarcon JM, Kandel ER. 2002. Expression of constitutively active CREB protein facilitates the late phase of long-term potentiation by enhancing synaptic capture. Cell 108:689–703.

Barco A, Marie H. 2011. Genetic approaches to investigate the role of CREB in neuronal plasticity and memory. Mol. Neurobiol. 44:330–349.

Bardehle S, Krüger M, Buggenthin F, Schwausch J, Ninkovic J, Clevers H, Snippert HJ, Theis FJ, Meyer-Luehmann M, Bechmann I, et al. 2013. Live imaging of astrocyte responses to acute injury reveals selective juxtavascular proliferation. Nat. Neurosci. 16:580–6.

Barreto GE, Gonzalez J, Torres Y, Morales L. 2011. Astrocytic-neuronal crosstalk: Implications for neuroprotection from brain injury. Neurosci. Res. 71:107–113.

Bartnik-Olson BL, Oyoyo U, Hovda DA, Sutton RL. 2010. Astrocyte oxidative metabolism and metabolite trafficking after fluid percussion brain injury in adult rats. J. Neurotrauma 27:2191–2202.

Benito E, Barco A. 2010. CREB's control of intrinsic and synaptic plasticity: implications for CREB-dependent memory models. Trends Neurosci. 33:230–240.

Benito E, Valor LM, Jimenez-Minchan M, Huber W, Barco A. 2011. cAMP Response Element-Binding Protein Is a Primary Hub of Activity-Driven Neuronal Gene Expression. J. Neurosci. 31:18237–18250.

Bourtchuladze R, Frenguelli B, Blendy J, Cioffi D, Schutz G, Silva AJ. 1994. Deficient long-term memory in mice with a targeted mutation of the cAMP-responsive element-binding protein. Cell 79:59–68.

Bouzier-Sore A-K, Pellerin L. 2013. Unraveling the complex metabolic nature of astrocytes. Front. Cell. Neurosci. 7:179.

Brown AM, Ransom BR. 2007. Astrocyte glycogen and brain energy metabolism. Glia 55:1263–1271.

Burda JE, Sofroniew M V. 2014. Reactive gliosis and the multicellular response to CNS damage and disease. Neuron 81:229–248.

Bush TG, Puvanachandra N, Horner CH, Polito A, Ostenfeld T, Svendsen CN, Mucke L, Johnson MH, Sofroniew M V. 1999. Leukocyte infiltration, neuronal degeneration, and neurite outgrowth after ablation of scar-forming, reactive astrocytes in adult transgenic mice. Neuron 23:297–308.

Bushong E a, Martone ME, Jones YZ, Ellisman MH. 2002. Protoplasmic astrocytes in CA1 stratum radiatum occupy separate anatomical domains. J. Neurosci. 22:183–192.

Butt AM, Kalsi A. 2006. Inwardly rectifying potassium channels (Kir) in central nervous system glia: A special role for Kir4.1 in glial functions. J. Cell. Mol. Med. 10:33–44.

Carloni S, Girelli S, Buonocore G, Longini M, Balduini W. 2009. Simvastatin acutely reduces ischemic brain damage in the immature rat via Akt and CREB activation. Exp. Neurol. 220:82–89.

Clarke E. 1992. Cajal's Degeneration and regeneration of the nervous system. Med. Hist. 36:465.

Clarkson AN, Parker K, Nilsson M, Walker FR, Gowing EK. 2015. Combined ampakine and BDNF treatments enhance poststroke functional recovery in aged mice via AKT-CREB signaling. J Cereb Blood Flow Metab 35:1272–1279.

Conkright MD, Canettieri G, Screaton R, Guzman E, Miraglia L, Hogenesch JB, Montminy M, Jolla L. 2003. TORCs : Transducers of Regulated CREB Activity The Salk Institute for Biological Studies. 12:413–423.

Corbett GT, Roy A, Pahan K. 2013. Sodium phenylbutyrate enhances astrocytic neurotrophin synthesis via protein kinase C (PKC)-mediated activation of cAMP-response element-binding protein (CREB): implications for Alzheimer disease therapy. J. Biol. Chem. 288:8299–312.

Craig JC, Schumacher M a., Mansoor SE, Farrens DL, Brennan RG, Goodman RH. 2001. Consensus and Variant cAMP-regulated Enhancers Have Distinct CREB-binding Properties. J. Biol. Chem. 276:11719–11728.

Cui L, Jeong H, Borovecki F, Parkhurst CN, Tanese N, Krainc D. 2006. Transcriptional Repression of PGC-1α by Mutant Huntingtin Leads to Mitochondrial Dysfunction and Neurodegeneration. Cell 127:59–69.

Dash PK, Hochner B, Kandel ER. 1990. Injection of the cAMP-responsive element into the nucleus of Aplysia sensory neurons blocks long-term facilitation. Nature 345:718–721.

Dash PK, Karl K a, Colicos M a, Prywes R, Kandel ER. 1991. cAMP response element-binding protein is activated by Ca2+/calmodulin- as well as cAMP-dependent protein kinase. Proc. Natl. Acad. Sci. U. S. A. 88:5061–5065.

Dash PK, Moore a N, Dixon CE. 1995. Spatial memory deficits, increased phosphorylation of the transcription factor CREB, and induction of the AP-1 complex following experimental brain injury. J. Neurosci. 15:2030–2039.

Davis S, Vanhoutte P, Pages C, Caboche J, Laroche S. 2000. The MAPK/ERK cascade targets both Elk-1 and cAMP response element-binding protein to control long-term potentiation-dependent gene expression in the dentate gyrus in vivo. J. Neurosci. 20:4563–4572.

Deak M, Clifton AD, Lucocq JM, Alessi DR. 1998. Mitogen- and stress-activated protein kinase-1 (MSK1) is directly activated by MAPK and SAPK2/p38, and may mediate activation of CREB. EMBO J. 17:4426–4441.

Dellavalle B, Hempel C, Johansen FF, Anders J, Kurtzhals L. 2014. GLP-1 improves neuropathology after murine cold lesion brain trauma. Ann. Clin. Transl. Neurol. 1:721–732.

Don J, Stelzer G. 2002. The expanding family of CREB / CREM transcription factors that are involved with spermatogenesis. Science. 187:115– 124.

Du K, Montminy M. 1998. Communication CREB Is a Regulatory Target for the Protein Kinase Akt / PKB *. J. Biol. Chem. 273:32377–32379.

España J, Valero J, Miñano-Molina AJ, Masgrau R, Martín E, Guardia-Laguarta C, Lleó A, Giménez-Llort L, Rodríguez-Alvarez J, Saura CA. 2010. beta-Amyloid disrupts activity-dependent gene transcription required for memory through the CREB coactivator CRTC1. J. Neurosci. 30:9402–9410.

Faulkner JR, Herrmann JE, Woo MJ, Tansey KE, Doan NB, Sofroniew M V. 2004. Reactive astrocytes protect tissue and preserve function after spinal cord injury. J. Neurosci. 24:2143–2155.

Fernandez-Fernandez S, Almeida A, Bolaños JP. 2012. Antioxidant and bioenergetic coupling between neurons and astrocytes. Biochem. J. 443:3–11.

Ferrer I, Blanco R, Rivera R, Carmona M, Ballabriga J, Olivé M, Planas AM. 1996. CREB-1 and CREB-2 immunoreactivity in the rat brain. Brain Res. 712:159–164.

Fiacco TA, Agulhon C, Taves SR, Petravicz J, Casper KB, Dong X, Chen J, McCarthy KD. 2007. Selective Stimulation of Astrocyte Calcium In Situ Does Not Affect Neuronal Excitatory Synaptic Activity. Neuron 54:611–626.

Finsterwald C, Fiumelli H, Cardinaux JR, Martin JL. 2010. Regulation of dendritic development by BDNF requires activation of CRTC1 by glutamate. J. Biol. Chem. 285:28587–28595.

Frödin M, Gammeltoft S. 1999. Role and regulation of 90 kDa ribosomal S6 kinase (RSK) in signal transduction. Mol. Cell. Endocrinol. 151:65–77.

Gadea A, López-Colomé a. M. 2001. Glial transporters for glutamate, glycine, and GABA: II. GABA transporters. J. Neurosci. Res. 63:461–468.

Giralt M, Penkowa M, Lago N, Molinero A, Hidalgo J. 2002. Metallothionein-1+2 protect the CNS after a focal brain injury. Exp. Neurol. 173:114–128.

Gonzalez GA, Montminy MR. 1989. Cyclic AMP stimulates somatostatin gene transcription by phosphorylation of CREB at serine 133. Cell 59:675–680.

Gonzalez-Perez O, Quiñones-Hinojosa A. 2012. Role of astrocytes as neural stem cells in the adult brain. Genes Dev. 29:997–1003.

Goss JR, Taffe KM, Kochanek PM, DeKosky ST. 1997. The antioxidant enzymes glutathione peroxidase and catalase increase following traumatic brain injury in the rat. Exp Neurol 146:291–294.

Guo Y, Feng P. 2012. OX2R activation induces PKC-mediated ERK and CREB phosphorylation. Exp. Cell Res. 318:2004–2013.

Halassa MM, Fellin T, Takano H, Dong J-H, Haydon PG. 2007. Synaptic islands defined by the territory of a single astrocyte. J. Neurosci. 27:6473–6477.

Hallam TM, Bourtchouladze R. 2006. Rubinstein-Taybi syndrome: Molecular findings and therapeutic approaches to improve cognitive dysfunction. Cell. Mol. Life Sci. 63:1725–1735.

Harum KH, Alemi L, Johnston M V. 2001. Cognitive impairment in Coffin-Lowry syndrome correlates with reduced RSK2 activation. Neurology 56:207–214.

Herculano-Houzel S. 2014. The glia/neuron ratio: How it varies uniformly across brain structures and species and what that means for brain physiology and evolution. Glia 62:1377–1391.

Ho N, Liauw J a, Blaeser F, Wei F, Hanissian S, Muglia LM, Wozniak DF, Nardi a, Arvin KL, Holtzman DM, et al. 2000. Impaired synaptic plasticity and cAMP response element-binding protein activation in Ca2+/calmodulin-dependent protein kinase type IV/Gr-deficient mice. J Neurosci 20:6459–6472.

Hoogland TM, Kuhn B, Göbel W, Huang W, Nakai J, Helmchen F, Flint J, Wang SS-H. 2009. Radially expanding transglial calcium waves in the intact cerebellum. Proc. Natl. Acad. Sci. U. S. A. 106:3496–3501.

Hummler E, Cole TJ, Blendy J a, Ganss R, Aguzzi a, Schmid W, Beermann F, Schütz G. 1994. Targeted mutation of the CREB gene: compensation within the CREB/ATF family of transcription factors. Proc. Natl. Acad. Sci. U. S. A. 91:5647–5651.

Impey S, McCorkle SR, Cha-Molstad H, Dwyer JM, Yochum GS, Boss JM, McWeeney S, Dunn JJ, Mandel G, Goodman RH. 2004. Defining the CREB regulon: A genome-wide analysis of transcription factor regulatory regions. Cell 119:1041–1054.

Impey S, Smith DM, Obrietan K, Donahue R, Wade C, Storm DR. 1998. Stimulation of cAMP response element (CRE)-mediated transcription during contextual learning. Nat. Neurosci. 1:595–601.

Jancic D, Lopez de Armentia M, Valor LM, Olivares R, Barco A. 2009. Inhibition of cAMP response element-binding protein reduces neuronal excitability and plasticity, and triggers neurodegeneration. Cereb. Cortex 19:2535–47.

Johannessen M, Delghandi MP, Moens U. 2004. What turns CREB on? Cell. Signal. 16:1211–27.

Kandel ER. 2001. The molecular biology of memory storage: A dialogue between gene and synapses. Science. 294:1030–1038.

Kawano H, Kimura-Kuroda J, Komuta Y, Yoshioka N, Li HP, Kawamura K, Li Y, Raisman G. 2012. Role of the lesion scar in the response to damage and repair of the central nervous system. Cell Tissue Res. 349:169–180.

Kida S, Josselyn SA, de Ortiz SP, Kogan JH, Chevere I, Masushige S, Silva AJ. 2002. CREB required for the stability of new and reactivated fear memories. Nat. Neurosci. 5:348–355.

Kirchhoff F. 2010. Questionable Calcium. Science. 327:1212–1213.

Kitagawa K. 2007. CREB and cAMP response element-mediated gene expression in the ischemic brain. FEBS J. 274:3210–3217.

Kogan JH, Frankland PW, Blendy JA, Coblentz J, Marowitz Z, Schütz G, Silva AJ. 1997. Spaced training induces normal long-term memory in CREB mutant mice. Curr. Biol. 7:1–11.

Korbecki J, Baranowska-Bosiacka I, Gutowska I, Chlubek D. 2013. The effect of reactive oxygen species on the synthesis of prostanoids from arachidonic acid. J. Physiol. Pharmacol. 64:409–421.

Kovács K a, Steullet P, Steinmann M, Do KQ, Magistretti PJ, Halfon O, Cardinaux J-R. 2007. TORC1 is a calcium- and cAMP-sensitive coincidence detector involved in hippocampal long-term synaptic plasticity. Proc. Natl. Acad. Sci. U. S. A. 104:4700–4705.

Kuga N, Sasaki T, Takahara Y, Matsuki N, Ikegaya Y. 2011. Large-scale calcium waves traveling through astrocytic networks in vivo. J. Neurosci. 31:2607–2614.

Lai TW, Zhang S, Wang YT. 2014. Excitotoxicity and stroke: Identifying novel targets for neuroprotection. Prog. Neurobiol. 115:157–188.

Lakhina V, Arey RN, Kaletsky R, Kauffman A, Stein G, Keyes W, Xu D, Murphy CT. 2015. Genome-wide Functional Analysis of CREB/Long-Term Memory-Dependent Transcription Reveals Distinct Basal and Memory Gene Expression Programs. Neuron 85:330–345.

Lalo U, Palygin O, Rasooli-Nejad S, Andrew J, Haydon PG, Pankratov Y. 2014. Exocytosis of ATP From Astrocytes Modulates Phasic and Tonic Inhibition in the Neocortex. Bacci A, editor. PLoS Biol. 12 (4):e1001857.

Van Landeghem FKH, Weiss T, Oehmichen M, von Deimling A. 2006. Decreased expression of glutamate transporters in astrocytes after human traumatic brain injury. J. Neurotrauma 23:1518–1528.

Lee B, Cao R, Choi Y, Cho H, Rhee AD, Cyrus K, Hoyt KR, Obrietan K. 2009. NIH Public Access. 108:1251–1265.

Leinninger GM, Backus C, Uhler MD, Lentz SI, Feldman EL. 2004. Phosphatidylinositol 3-kinase and Akt effectors mediate insulin-like growth factor-I neuroprotection in dorsal root ganglia neurons. FASEB J. 18:1544–1546.

Leung YKJ, Pankhurst M, Dunlop SA, Ray S, Dittmann J, Eaton ED, Palumaa P, Sillard R, Chuah MI, West AK, et al. 2010. Metallothionein induces a regenerative reactive astrocyte phenotype via JAK/STAT and RhoA signalling pathways. Exp. Neurol. 221:98–106.

Li B, Mahmood A, Lu D, Wu H, Xiong Y, Qu C, Chopp M. 2009. Simvastatin attenuates microglial cells and astrocyte activation and decreases interleukin-1B level after traumatic brain injury. Neurosurgery 65:179–185.

Li S, Zhang C, Takemori H, Zhou Y, Xiong Z-Q. 2009. TORC1 regulates activity-dependent CREB-target gene transcription and dendritic growth of developing cortical neurons. J. Neurosci. 29:2334–2343.

Lonze BE, Ginty DD. 2002. Function and Regulation of CREB Family Transcription Factors in the Nervous System CREB and its close relatives are now widely accepted. Neuron 35:605–623.

Lonze BE, Riccio A, Cohen S, Ginty DD. 2002. Apoptosis, axonal growth defects, and degeneration of peripheral neurons in mice lacking CREB. Neuron 34:371–385.

Lopez de Armentia M, Jancic D, Olivares R, Alarcon JM, Kandel ER, Barco A. 2007. cAMP response element-binding protein-mediated gene expression increases the intrinsic excitability of CA1 pyramidal neurons. J. Neurosci. 27:13909–13918.

Lu D, Qu C, Goussev A, Jiang H, Lu C, Schallert T, Mahmood A, Chen J, Li Y, Chopp M. 2007. Statins increase neurogenesis in the dentate gyrus, reduce delayed neuronal death in the hippocampal CA3 region, and improve spatial learning in rat after traumatic brain injury. J. Neurotrauma 24:1132–1146.

Lu K-T, Wang Y-W, Yang J-T, Yang Y-L, Chen H-I. 2005. Effect of interleukin-1 on traumatic brain injury-induced damage to hippocampal neurons. J. Neurotrauma 22:885–895.

Mabuchi T, Kitagawa K, Kuwabara K, Takasawa K, Ohtsuki T, Xia Z, Storm D, Yanagihara T, Hori M, Matsumoto M. 2001. Phosphorylation of cAMP response element-binding protein in hippocampal neurons as a protective response after exposure to glutamate in vitro and ischemia in vivo. J. Neurosci. 21:9204–9213.

Magistretti PJ, Pellerin L. 1999. Astrocytes Couple Synaptic Activity to Glucose Utilization in the Brain. News Physiol. Sci. 14:177–182.

Mantamadiotis T, Lemberger T, Bleckmann SC, Kern H, Kretz O, Martin Villalba A, Tronche F, Kellendonk C, Gau D, Kapfhammer J, et al. 2002. Disruption of CREB function in brain leads to neurodegeneration. Nat. Genet. 31:47–54.

Martín F, Laorden ML, Milanés MV. 2009. Morphine withdrawal regulates phosphorylation of cAMP response element binding protein (CREB) through PKC in the nucleus tractus solitarius-A2 catecholaminergic neurons. J. Neurochem. 110:1422–1432.

Mayr B, Montminy M. 2001. Transcriptional regulation by the phosphorylation-dependent factor CREB. Nat. Rev. Mol. Cell Biol. 2:599–609.

Mbye LHAN, Singh IN, Carrico KM, Saatman KE, Hall ED. 2009. Comparative neuroprotective effects of cyclosporin A and NIM811, a nonimmunosuppressive cyclosporin A analog, following traumatic brain injury. J. Cereb. Blood Flow Metab. 29:87–97.

Merz K, Herold S, Lie DC. 2011. CREB in adult neurogenesis - master and partner in the development of adult-born neurons? Eur. J. Neurosci. 33:1078–1086.

Mitsuda N, Ohkubo N, Tamatani M, Lee YD, Taniguchi M, Namikawa K, Kiyama H, Yamaguchi A, Sato N, Sakata K, et al. 2001. Activated cAMP-response element-binding protein regulates neuronal expression of presenilin-1. J. Biol. Chem. 276:9688–9698.

Molofsky A V, Krencik R, Krenick R, Ullian EM, Ullian E, Tsai H, Deneen B, Richardson WD, Barres B a, Rowitch DH. 2012. Astrocytes and disease: a neurodevelopmental perspective. Genes Dev. 26:891–907.

Montminy MR, Sevarino KA, Wagnertt JA, Mandel G, Goodman RH. 1986. Identification of a cyclic-AMP-responsive element within the rat somatostatin gene. Proc. Natl. Acad. Sci. U. S. A. 83:6682–6686.

Morganti-Kossmann MC, Satgunaseelan L, Bye N, Kossmann T. 2007. Modulation of immune response by head injury. Injury 38:1392–1400.

Navarrete M, Perea G, de Sevilla DF, Gómez-Gonzalo M, Núñez A, Martín ED, Araque A. 2012. Astrocytes Mediate In Vivo Cholinergic-Induced Synaptic Plasticity. Scheiffele P, editor. PLoS Biol. 10 (2):e1001259.

Nedergaard M. 1994. Direct signaling from astrocytes to neurons in cultures of mammalian brain cells. Science 263:1768–1771.

Nedergaard M. 2003. New roles for astrocytes: Redefining the functional architecture of the brain. Trends Neurosci. 26:523–530.

Nucifora FC, Sasaki M, Peters MF, Huang H, Cooper JK, Yamada M, Takahashi H, Tsuji S, Troncoso J, Dawson VL, et al. 2001. Interference by huntingtin and atrophin-1 with cbp-mediated transcription leading to cellular toxicity. Science 291:2423–2428.

Oberheim NA, Takano T, Han X, He W, Lin JHC, Wang F, Xu Q, Wyatt JD, Pilcher W, Ojemann JG, et al. 2009. Uniquely hominid features of adult human astrocytes. J. Neurosci. 29:3276–3287.

Ouyang Y-B, Voloboueva LA, Xu L-J, Giffard RG. 2007. Selective dysfunction of hippocampal CA1 astrocytes contributes to delayed neuronal damage after transient forebrain ischemia. J. Neurosci. 27:4253–4260.

Overman JJ, Clarkson a. N, Wanner IB, Overman WT, Eckstein I, Maguire JL, Dinov ID, Toga a. W, Carmichael ST. 2012. PNAS Plus: A role for ephrin-A5 in axonal sprouting, recovery, and activity-dependent plasticity after stroke. Proc. Natl. Acad. Sci. 109:E2230–E2239.

Pankratov Y, Lalo U. 2015. Role for astroglial α1-adrenoreceptors in gliotransmission and control of synaptic plasticity in the neocortex. Front. Cell. Neurosci. 9:230.

Parpura V, Basarsky TA, Liu F, Jeftinija K, Jeftinija S, Haydon PG. 1994. Glutamate-mediated astrocyte-neuron signalling. Nature 369:744–747.

Parpura V, Heneka MT, Montana V, Oliet SHR, Schousboe A, Haydon PG, Stout RF, Spray DC, Reichenbach A, Pannicke T, et al. 2012. Glial cells in (patho)physiology. J. Neurochem. 121:4–27.

Parpura V, Zorec R. 2010. Gliotransmission: Exocytotic release from astrocytes. Brain Res. Rev. 63:83–92.

Parra-Damas A, Valero J, Chen M, España J, Martín E, Ferrer I, Rodríguez-Alvarez J, Saura C a. 2014. Crtc1 activates a transcriptional program deregulated at early Alzheimer's disease-related stages. J. Neurosci. 34:5776–5787.

Parry GC, Mackman N. 1997. Role of cyclic AMP response element-binding protein in cyclic AMP inhibition of NF-kappaB-mediated transcription. J. Immunol. 159:5450–5456.

Pekny M, Johansson CB, Eliasson C, Stakeberg J, Wallén A, Perlmann T, Lendahl U, Betsholtz C, Berthold CH, Frisén J. 1999. Abnormal reaction to central nervous system injury in mice lacking glial fibrillary acidic protein and vimentin. J. Cell Biol. 145:503–514.

Pekny M, Pekna M. 2014. Astrocyte Reactivity and Reactive Astrogliosis: Costs and Benefits. Physiol. Rev. 94:1077–1098.

Pellerin L, Magistretti PJ. 1994. Glutamate uptake into astrocytes stimulates aerobic glycolysis: a mechanism coupling neuronal activity to glucose utilization. Proc. Natl. Acad. Sci. U. S. A. 91:10625–10629.

Pittenger C, Huang YY, Paletzki RF, Bourtchouladze R, Scanlin H, Vronskaya S, Kandel ER. 2002. Reversible Inhibition of CREB/ATF Transcription Factors in Region CA1 of the Dorsal Hippocampus Disrupts Hippocampus-Dependent Spatial Memory. Neuron 34:447–462.

Poirier R, Jacquot S, Vaillend C, Soutthiphong AA, Libbey M, Davis S, Laroche S, Hanauer A, Welzl H, Lipp H-P, et al. 2007. Deletion of the Coffin–Lowry Syndrome Gene Rsk2 in Mice is Associated With Impaired Spatial Learning and Reduced Control of Exploratory Behavior. Behav. Genet. 37:31–50.

Properzi F, Asher RA, Fawcett JW. 2003. Chondroitin sulphate proteoglycans in the central nervous system: changes and synthesis after injury. Biochem. Soc. Trans. 31:335–336.

Qi Y, Li Y, Cui S-C, Zhao J-J, Liu X-Y, Ji C-X, Sun F-Y, Xu P, Chen X-H. 2015. Splicing factor NSSR1 reduces neuronal injury after mouse transient global cerebral ischemia. Glia 63:826–845.

Riccio A, Ahn S, Davenport CM, Blendy JA, Ginty DD. 1999. Mediation by a CREB family transcription factor of NGF-dependent survival of sympathetic neurons. Science 286:2358–2361.

Romano M, Sironi M, Toniatti C, Polentarutti N, Fruscella P, Ghezzi P, Faggioni R, Luini W, Van Hinsbergh V, Sozzani S, et al. 1997. Role of IL-6 and its soluble receptor in induction of chemokines and leukocyte recruitment. Immunity 6:315–325.

Roozenbeek B, Maas AIR, Menon DK. 2013. Changing patterns in the epidemiology of traumatic brain injury. Nat. Rev. Neurol. 9:231–6.

Rosenfeld J V, Maas AI, Bragge P, Morganti-kossmann MC, Manley GT, Gruen RL. 2012. Early management of severe traumatic brain injury. Lancet 380:1088–98.

Rossi D. 2015. Progress in Neurobiology Astrocyte physiopathology : At the crossroads of intercellular networking , inflammation and cell death. Prog. Neurobiol. 130:86–120.

Rudolph D, Tafuri A, Gass P, Hämmerling GJ, Arnold B, Schütz G. 1998. Impaired fetal T cell development and perinatal lethality in mice lacking the cAMP response element binding protein. Proc. Natl. Acad. Sci. U. S. A. 95:4481–4486.

Ruppert S, Cole TJ, Boshart M, Schmid E, Schütz G. 1992. Multiple mRNA isoforms of the transcription activator protein CREB: generation by alternative splicing and specific expression in primary spermatocytes. EMBO J. 11:1503–1512.

Rusakov D a., Bard L, Stewart MG, Henneberger C. 2014. Diversity of astroglial functions alludes to subcellular specialisation. Trends Neurosci. 37:228–242.

Sakamoto K, Karelina K, Obrietan K. 2011. CREB: A multifaceted regulator of neuronal plasticity and protection. J. Neurochem. 116:1–9.

Saura C a., Valero J. 2011. The role of CREB signaling in Alzheimer's disease and other cognitive disorders. Rev. Neurosci. 22:153–169.

Saura CA, Choi SY, Beglopoulos V, Malkani S, Zhang D, Rao BSS, Chattarji S, Kelleher RJ, Kandel ER, Duff K, et al. 2004. Loss of presenilin function causes impairments of memory and synaptic plasticity followed by age-dependent neurodegeneration. Neuron 42:23–36.

Scemes E, Giaume C. 2006. Astrocyte calcium waves: What they are and what they do. Glia 54:716-25.

Screaton R a, Conkright MD, Katoh Y, Best JL, Canettieri G, Jeffries S, Guzman E, Niessen S, Yates JR, Takemori H, et al. 2004. The CREB coactivator TORC2 functions as a calcium- and cAMP-sensitive coincidence detector. Cell 119:61–74.

Scherbel U, Raghupathi R, Nakamura M, Saatman KE, Trojanowski JQ, Neugebauer E, Marino MW, McIntosh TK. 1999. Differential acute and chronic responses of tumor necrosis factor-deficient mice to experimental brain injury. Proc. Natl. Acad. Sci. U. S. A. 96:8721–8726.

Schitine C, Nogaroli L, Costa MR. 2015. Astrocyte heterogeneity in the brain : from development to disease. Front. Cell. Neurosci. 9:76.

Schneider A, Mehmood T, Pannetier S, Hanauer A. 2011. Altered ERK/MAPK signaling in the hippocampus of the mrsk2-KO mouse model of Coffin-Lowry syndrome. J. Neurochem. 119:447–459.

Schumacher M, Guennoun R, Ghoumari A, Massaad C, Robert F, El-Etr M, Akwa Y, Rajkowski K, Baulieu EE. 2007. Novel perspectives for progesterone in hormone replacement therapy, with special reference to the nervous system. Endocr. Rev. 28:387–439.

Seifert G, Schilling K, Steinhäuser C. 2006. Astrocyte dysfunction in neurological disorders: a molecular perspective. Nat. Rev. Neurosci. 7:194–206.

Shaywitz AJ, Greenberg ME. 1999. CREB: A stimulus-induced transcription factor activated by a diversearray of extracellular signals. Annu. Rev. Biochem. 68:821–861.

Shields J, Kimbler DE, Radwan W, Yanasak N, Sukumari-Ramesh S, Dhandapani KM. 2011. Therapeutic targeting of astrocytes after traumatic brain injury. Transl. Stroke Res. 2:633–42.

Simard M, Nedergaard M. 2004. The neurobiology of glia in the context of water and ion homeostasis. Neuroscience 129:877–896.

Sirén AL, Faßhauer T, Bartels C, Ehrenreich H. 2009. Therapeutic Potential of Erythropoietin and its Structural or Functional Variants in the Nervous System. Neurotherapeutics 6:108–127.

Sofroniew M V. 2009. Molecular dissection of reactive astrogliosis and glial scar formation. Trends Neurosci. 32:638–647.

Sofroniew M V., Vinters H V. 2010. Astrocytes: Biology and pathology. Acta Neuropathol. 119:7–35.

Steffan JS, Bodai L, Pallos J, Poelman M, McCampbell A, Apostol BL, Kazantsev A, Schmidt E, Zhu YZ, Greenwald M, et al. 2001. Histone deacetylase inhibitors arrest polyglutamine-dependent neurodegeneration in Drosophila. Nature 413:739–743.

Steinberg SF. 2008. Structural basis of protein kinase C isoform function. Physiol. Rev. 88:1341–1378.

Swartz KR, Liu F, Sewell D, Schochet T, Campbell I, Sandor M, Fabry Z. 2001. Interleukin-6 promotes post-traumatic healing in the central nervous system. Brain Res. 896:86–95.

Takemori H, Kajimura J, Okamoto M. 2007. TORC-SIK cascade regulates CREB activity through the basic leucine zipper domain. FEBS J. 274:3202–3209.

Tanaka K, Nogawa S, Nagata E, Suzuki S, Dembo T, Kosakai A, Fukuuchi Y. 1999. Temporal profile of CREB phosphorylation after focal ischemia in rat brain. Neuroreport 10:2245–2250.

Tang W, Szokol K, Jensen V, Enger R, Trivedi C a, Hvalby Ø, Helm PJ, Looger LL, Sprengel XR, Nagelhus E a. 2015. Stimulation-Evoked Ca 2 ع Signals in Astrocytic Processes at Hippocampal CA3 – CA1 Synapses of Adult Mice Are Modulated by Glutamate and ATP. J neurosc 35:3016–3021.

Titus DJ, Sakurai A, Kang Y, Furones C, Jergova S, Santos R, Sick TJ, Atkins CM. 2013. Phosphodiesterase inhibition rescues chronic cognitive deficits induced by traumatic brain injury. Ann. Intern. Med. 158:5216–5226.

Trivier E, De Cesare D, Jacquot S, Pannetier S, Zackai E, Young I, Mandel JL, Sassone-Corsi P, Hanauer A. 1996. Mutations in the kinase Rsk-2 associated with Coffin-Lowry syndrome. Nature 384:567–570.

Valor LM, Jancic D, Lujan R, Barco A. 2010. Ultrastructural and transcriptional profiling of neuropathological misregulation of CREB function. Cell Death Differ. 17:1636–44.

Valor LM, Viosca J, Lopez-Atalaya JP, Barco A. 2013. Lysine acetyltransferases CBP and p300 as therapeutic targets in cognitive and neurodegenerative disorders. Curr. Pharm. Des. 19:5051–64.

Verkhratsky A, Parpura V. 2010. Recent advances in (patho)physiology of astroglia. Acta Pharmacol. Sin. 31:1044–1054.

Verkhratsky A, Rodríguez JJ, Parpura V. 2012. Neurotransmitters and integration in neuronal-astroglial networks. Neurochem. Res. 37:2326–2338.

Viosca J, Lopez de Armentia M, Jancic D, Barco A. 2009. Enhanced CREB-dependent gene expression increases the excitability of neurons in the basal amygdala and primes the consolidation of contextual and cued fear memory. Learn. Mem. 16:193–197.

Vitolo O V, Sant'Angelo A, Costanzo V, Battaglia F, Arancio O, Shelanski M. 2002. Amyloid beta -peptide inhibition of the PKA/CREB pathway and long-term potentiation:

reversibility by drugs that enhance cAMP signaling. Proc. Natl. Acad. Sci. U. S. A. 99:13217–13221.

Walton M, Connor B, Lawlor P, Young D, Sirimanne E, Gluckman P, Cole G, Dragunow M. 1999. Neuronal death and survival in two models of hypoxic-ischemic brain damage. Brain Res. Brain Res. Rev. 29:137–168.

Wang DD, Bordey A. 2008. The astrocyte odyssey. Prog. Neurobiol. 86:342–367.

Wang H, Zhuo M. 2012. Group I metabotropic glutamate receptor-mediated gene transcription and implications for synaptic plasticity and diseases. Front. Pharmacol. 3 NOV:1–8.

Werner C, Engelhard K. 2007. Pathophysiology of traumatic brain injury. Br. J. Anaesth. 99:4–9.

Wilhelmsson U, Bushong EA, Price DL, Smarr BL, Phung V, Terada M, Ellisman MH, Pekny M. 2006. Redefining the concept of reactive astrocytes as cells that remain within their unique domains upon reaction to injury. Proc. Natl. Acad. Sci. U. S. A. 103:17513–17518.

Wu X, Spiro C, Owen WG, McMurray CT. 1998. cAMP response element-binding protein monomers cooperatively assemble to form dimers on DNA. J. Biol. Chem. 273:20820–20827.

Wu ZL, Thomas SA, Villacres EC, Xia Z, Simmons ML, Chavkin C, Palmiter RD, Storm DR. 1995. Altered behavior and long-term potentiation in type I adenylyl cyclase mutant mice. Proc. Natl. Acad. Sci. U. S. A. 92:220–224.

Xiong Y, Mahmood A, Chopp M. 2013. Animal models of traumatic brain injury. Nat. Rev. Neurosci. 14:128–142.

Yin JC, Del Vecchio M, Zhou H, Tully T. 1995. CREB as a memory modulator: induced expression of a dCREB2 activator isoform enhances long-term memory in Drosophila. Cell 81:107–115.

Yin JCP, Wallach JS, Del Vecchio M, Wilder EL, Zhou H, Quinn WG, Tully T. 1994. Induction of a dominant negative CREB transgene specifically blocks long- term memory in Drosophila. Cell 79:49–58.

Zador Z, Stiver S, Wang V, Manley GT. 2009. Role of Aquaporin-4 in Cerebral Edema and Stroke. Handbook of Experimental Pharmacology (190):159-170

Zamanian JL, Xu L, Foo LC, Nouri N, Zhou L, Giffard RG, Barres BA. 2012. Genomic Analysis of Reactive Astrogliosis. J. Neurosci. 32:6391–6410.

Zhang X, Odom DT, Koo S-H, Conkright MD, Canettieri G, Best J, Chen H, Jenner R, Herbolsheimer E, Jacobsen E, et al. 2005. Genome-wide analysis of cAMP-response element binding protein occupancy, phosphorylation, and target gene activation in human tissues. Proc. Natl. Acad. Sci. U. S. A. 102:4459–4464.

Zhang YP, Cai J, Shields LBE, Liu N, Xu XM, Shields CB. 2014. Traumatic Brain Injury Using Mouse Models. Transl. Stroke Res. 5:454-471.

Zhou Y, Wu H, Li S, Chen Q, Cheng XW, Zheng J, Takemori H, Xiong ZQ. 2006. Requirement of TORC1 for late-phase long-term potentiation in the hippocampus. PLoS One 1(1): e16.

Zlokovic B V. 2008. The Blood-Brain Barrier in Health and Chronic Neurodegenerative Disorders. Neuron 57:178–201.

Objectives

Objectives

- To determine the signalling pathways that activate CREB in astrocytes upon stimulation of ATP and NE.

- To characterize the transcriptional programs induced in astrocytes upon CREB activation by FSK, NE or the overexpression of a constitutive form of CREB (VP16-CREB).

- To generate a transgenic mouse with targeted expression of VP16-CREB in astrocytes.

- To test the protective roles of astrocytic CREB in a model of acute brain injury by using VP16-CREB mice.

Materials & Methods

Materials and Methods.

Materials

DMEM, ATP, NE, glutamate, forskolin (FSK), phentolamine, propanolol, the inhibitor of PKA (myr-PKA), ampicillin, trypsin, DNAse, phosphatase inhibitor coktail 2, Nonidet P-40, Tween-20, Triton-X-100, isopropanol, diaminobenzidine, toluidine blue solution, DPX and all the chemicals used to prepare buffers (including PB, PBS,TBS, Krebs Ringer, KH, lysis buffer A/B/Ripa, electrophoresis and transference buffers, stripping buffer, Tris-EDTA buffer) and the luminol/coumaric reagent (ECL) were purchased from Sigma. The calcium chelator BAPTA, the analogue of cAMP (RpAMPc) and inhibitors of the P2X receptor (iso-PPADS), ERK (U0126), PKC (Go6976, GF109203X), CaMKII (KN-93), PKG (KT-5823), PI3K (LY- 294002), adenosine receptor (8-pst) and calcinaurin inhibitor (CSA) were from Tocris. Diacylglicerol analogue (Dic8) was from Avanti. Penicillin, streptomycin, soybean trypsin inhibitor and normal goat serum were from Gibco. FBS was from Chambrex and the Bradford reagent was from Biorad. The Ca^{2+} dye fura-2/AM was purchased from Molecular Probes. The plasmids pCRE-Luc, pHSV-TK-Ren and Gl3-Null were from Stratagene. Plasmid m133-CREB was kindly provided by Dr. Naranjo from the Centro nacional de Biotecnología (Madrid) and DN-CRTC1/2 were provided by Dr. Cardinaux from th Brain and Mind Institute (Lausanne) Adenoviruses Ad2/5-CMV-VP16-CREB and Ad2/5-CMV-NULL were synthesized in the CEBATEG. Fugene 6, protease inhibitors (C0mplete, tablets), polyvinyl difluoride membranes for protein transference were from Roche. Passive Lysis Buffer and Dual-Luciferase reporter assay system were from Promega. Turbo DNA-free™ kit was from Ambion. DH5α competent bacteria, LB medium, the Qubit™ kit, *SuperScript™ II* reverse transcriptase, Oligo(dt) primers, random hexamers, dNTP, DTT, RNAseOut, DNA ladder, Taq DNA polymerase and reaction buffer, $MgCl_2$, the Power SYBR Green PCR Master Mix, the Taqman Universal Master Mix, the Horseradish-linked or Alexa fluor secondary antibodies and DAPI were purchased from life technologies. QAFilter Plasmid Maxi Kit was from

Qiagen and RNAeasy spin kit from Capsumlab. Fluoromount-G was from Southern biotech. Peroxidase-streptavidin and lectin conjugated with FITC were from Vector Labs. Rest of the products and equipment are indicated in the text.

Methods

1. Cell culture and treatments

1.1 *Primary rat astrocyte cultures:*

Astrocyte cultures were prepared from cortices from 1day-old Sprague-Dawley rats as previously described (Servitja et al. 2003). In detail, rats were decapitated and brains immediately dissected out under a binocular microscope in a laminar flow hood. After meninges and blood vessels were removed, the cortices were minced with a scalpel and tissue was incubated for 10 min at 37ºC in Ca^{2+}-free Krebs Ringer buffer (120 mM NaCl, 4.8 mm KCl, 1.2 mM KH2PO4, NaHCO3 25 mM, Glucose 14.3 mM; 0.15 g of bovine serum albumin in 1L H_2O) containing 0.025% trypsin. Cells were then mechanically triturated through a glass pipette and filtered through a 40-μm nylon mesh in the presence of 0.52 mg mL^{-1} soybean trypsin inhibitor and 170 IU mL^{-1} DNase (Sigma-Aldrich). After centrifugation (500 xg), cells were resuspended in 90% DMEM, 10% FBS, 20 U mL^{-1} penicillin, and 20 μg mL^{-1} streptomycin. An aliquot of this resuspension was stained by Trypan Blue exclusion, counted in a Neubauer chamber, and then cells were seeded at a density of 3 x 10^5 cells mL^{-1} and maintained in an incubator at 37ºC with an humidified atmosphere of 90% air-10% CO_2. Cells were plated in different types of culture dishes according to the type of test. For subcellular fractionation, cells were seeded on 100 mm plates (Nunc), for total RNA/protein extraction or immunocytochemistry on 35 mm plates (Corning), for luciferase assays on 48 well plates (Falcon) and for Ca^{2+} imaging onto 25 mm glass coverslips placed on 35 mm plates. The culture medium was changed after 2 h to avoid the growth of neurons and other brain cells, and then every 7 days. Cells were immediately used when cultures reached confluency (12-14 DIV) in order to minimize contamination by

microglia that rapidly proliferates when the astrocyte monolayer attains confluency (Agullo et al. 1998).

1.2 *Cell Line:*

Human embryonic kidney (HEK293) cells were cultured in DMEM containing 10% FBS, 20 U mL^{-1} penicillin, and 20 μg mL^{-1} streptomycin. Cells were maintained at 37ºC with an humidified atmosphere of 95% air-5% CO_2 and cell pasages were performed once a week by tripsinization. For luciferase assays, cells were seeded in 48-well plates.

1.3 *Cellular treatments*

Treatments with ligands ATP (3/100 μM), FSK (1 μM), NE (0.5/10 μM) and glutamate (100 μM) were performed in confluent cultures at the appropriate times by direct addition to the culture medium. Inhibitors Iso-PPADS (100 μM), 8-PST (10 μM), propanolol (10 μM), phentolamine (10 μM), Rp-cAMP (20 μM), myr-PKA peptide (1 μM), GF109203X (2-25 μM), Go6976 (2 μM), Dic8 (10 μM), KN-93 (10 μM), KT-5823 (10 μM), LY-294002 (3 μM), BAPTA (30 μM), U0126 (10 μM) and CSA (5 μM) were added 30 minutes before. Cell medium was changed 18 h before each treatment to DMEM 1% FBS to avoid cell proliferation and interference with serum proteins during the experiments.

1.4 *Plasmid transfections*

Pre-confluent astrocytes (~ 60% confluency) were transfected with plasmids encoding for: *Firefly* luciferase with 4 copies of CRE promoter (pCRE-Luc); *Renilla* luciferase with timidin kinase promoter from herpes simplex virus (pHSV-TK-Ren); CREB mutated in the canonical phosphorylation site Ser-133 to Ala (pCREB-mSer133) and dominant-negative plasmids for CRTC1 and CRTC2 (pDNCRTC1/2). The transfections were carried out using Fugene 6. For each well in a 48-well plate 2 μL of Fugene 6 were mixed with 0.5 μg of pCRE-Luc, 0.25 μg of pRenilla, and 0.25 μg of the third plasmid (m133-CREB, DN-CRTC1, or DN-CRTC2) in 70 μL of DMEM containing 10% FBS without antibiotics. The mixture was incubated during 30 min at

room temperature to allow for the formation of Fugene-DNA complexes, and was added to the cells for a final volume of 250 μL/well. Two hours later, the Fugene-containing medium was removed and replaced by fresh DMEM containing 10% FBS. Cells were treated 48h after transfection.

1.5 *Viral infections*

Infection with adenoviruses Ad2/5-CMV-VP16-CREB and Ad2/5-CMV-NULL (1-30 MOI) was carried out in pre-confluent cultures (~ 80% confluency) with DMEM 1% FBS without antibiotics. The medium was changed at 3 hours to DMEM 1% FBS with antibiotics and cells were used 18 hours post-infection.

2. Animal model

Transgenic mice expressing VP16-CREB in astrocytes (Gfa2-tTa/TetO-VP16-CREB mice) were generated by crossing the Gfa2-tTA strain (B6.Cg-TgGfa2-tTA110Pop/J) from Jackson laboratories (Lin et al. 2004), with the TetO-VP16-CREB strain (Barco et al. 2002). All the animals have a C57/Bl6 background. Transgene expression is controlled by a tetracycline-responsive promoter and can be prevented by doxycycline administration (TetOff system). However, animals were not treated with doxycycline in our experiments thus allowing continuous expression of VP16-CREB gene. Animals were maintained under standard laboratory conditions (food and water *ad libitum*, 22+/- 2ºC, a 12h dark/light cycle, and 50-60% humidity). All experimental procedures were approved by the Animal Welfare Committee of the Autonomous University of Barcelona and the Generalitat de Catalunya, and were in agreement with the European Union Laws for the protection of experimental animals.

Cryolesions

Five-to-seven month-old mice were cryolesioned under isoflurane anesthesia (IsoFlo, Esteve). Females and males were equally distributed among experimental groups. The skull over the right frontoparietal cortex was exposed, and a focal cryoinjury was carried out on the surface of the brain

by applying a dry ice pellet for 30 s as previously described (Giralt et al. 2002). Animals were allowed to recover under infrared light, returned to the animal room and sacrificed 1-20 days post-lesion (dpl). Buprenorfin (Buprex) was injected i.p. every 12 h for a week.

3. Biochemical methods

3.1 *Total cell lysates*

After appropriate treatments, cells were washed twice in ice-cold PBS to remove the excess of culture medium and lysed by scrapping in cold RIPA buffer (50 mM Tris-HCl, pH 7.4, 150 mM NaCl, 2 mM EDTA, 0.5% Triton X-100, 1% NP-40, 0.1% SDS, 1mM Na3VO4, 50 mM NaF, and 1mM PMSF) supplemented with protease and phosphatase inhibitors. Cell lysates were sonicated during 10 s and stored at -80ºC.

3.2 *Preparation of Cytosolic and Nuclear Extracts*

Following medium removal and PBS washing, cells were scrapped out of the plates in ice-cold PBS, collected by brief centrifugation (500 xg, 4ºC, 30s) and resuspended in buffer A (10 mM Hepes pH 7.9; 1.5 mM $MgCl_2$, 10 mM KCl, 0.5 mM dithiothreitol) with protease and phosphatase inhibitors. After 5 min on ice, Nonidet P-40 was added (final concentration 0.6%) and the cells were vortexed for 10 s. The nuclei were collected by brief centrifugation in a microcentrifuge (500 xg, 4ºC, 30s), and the supernatants kept at -80ºC as cytosolic extracts. The nuclei were washed once with buffer A to prevent contamination of the nuclear fraction with cytosolic proteins and collected again by centrifugation. Nuclear extracts were obtained by incubating nuclei in buffer B (20 mM Hepes buffer, 25% glycerol, 420 mM NaCl, 0.2 mM EDTA), 0.5 mM dithiothreitol, and protease and phosphatase inhibitors) at 4ºC for 30 min with gentle rocking. The suspensions were centrifuged at 15.000 xg for 15 min at 4ºC, and the supernatants stored at -80ºC.

3.3 *Western Blots*

Sample concentration was measured by the Bradford method (Bradford 1976) and equal amounts of protein (15-50 μg depending on cell fraction) were used for electrophoresis (EF). Samples were diluted in loading buffer (62.5 mM Tris HCl pH 6.8, 10% glycerol, 2% SDS, 5% beta-mercaptoethanol, 0.01% bromophenol blue), boiled 5 min at 95 °C and subjected to sodium dodecyl sulphate 8–12% polyacrylamide gel electrophoresis (SDS-PAGE) -EF buffer: 24mM TRIZMA base, 190 mM glycine, 10% SDS in 500 mL H_2O pH 8.5. EF voltage: 80 mV (stacking gel) and 110 mV (running gel)-. After running the samples, proteins were transferred to polyvinyl difluoride membranes previously activated with methanol and balanced in transfer buffer (EF buffer with 20% v/v of methanol) for at least 30 min. The transfer was performed at a constant voltage of 100 mV for 90 min.

Table 1. Antibodies used in this thesis

Antibody	Producer	Host	Dilution	
			Western blot	Immunostaining
CREB	Santa Cruz biotechnology	rabbit	1:750	
pCREB	Cell signalling	rabbit	1:1000	
ERK 1/2	Cell signalling	rabbit	1:750	
pERK 1/2	Cell signalling	rabbit	1:1000	
β-actin	Sigma-Aldrich	mouse	1:100000	
GAPDH	Sigma-Aldrich	mouse	1:10000	
CRTC1	Cell signalling	rabbit	1:1000	1:500
CRTC2	Santa Cruz biotechnology	rabbit	1:250	1:200
VP16	Santa Cruz biotechnology	mouse	1:500	1:150
GFAP	Dako	mouse		1:1000
SMI 312	Covance	mouse		1:1000

The membranes with transferred proteins were blocked for 1 hour in blocking buffer (TBS: 20 mM Tris, 137 mM NaCl, pH 7.6 + 0.1% Tween + 5% skimmed milk) and incubated overnight with the appropriate primary antibody (Table 1) diluted in blocking buffer at 4 °C. After 3 washes of 10 min with TBS-Tween the membrane was incubated for one hour with a peroxidase-conjugated secondary antibody diluted in blocking buffer (Life technologies, 1:10000) at room temperature. The proteins were detected by the luminol/coumaric reagent (ECL1: 5 mL 1 M Tris-HCL pH 8.5, 250 μL 0.5 M Luminol, 250 μL 79.2 mM p-Coumaric acid in 50 mL H2O. ECL2: 5 mL Tris-HCl pH 8.5, 32 μL 8.8 M Hidrogen Peroxide in 50 mL H2O) and visualized by autoradiography on X-ray film (AGFA). Relative band intensity was quantified with ImageJ (National Institutes of Health).

Membranes were occasionally reused after incubating in stripping buffer (2% SDS, 100 mM beta-mercaptoethanol, 50 mM Tris pH 6.8) at 50 °C water bath for 20 min agitation. Then membranes were washed with plenty of TBS-T, blocked again and incubated with the new primary antibody.

4. Molecular biology methods

4.1 *Plasmid DNA purification and amplification*

Bacterial transformation with plasmid DNA was performed by incubating 1μg DNA with 30 μL of DH5α competent bacteria at 4ºC for 15 minutes followed by a thermal shock at 37°C for 40 s and incubation on ice for 10 min . Transformed bacteria were suspended in 800 mL of LB medium (25 g LB in 1L H_2O, pH 7.4) and incubated at 37ºC for 45 minutes with stirring. Part of the bacterial suspension was planted in sterile agar plates with ampicillin (32 g agar in 500 mL LB medium, 100 mg mL^{-1} amp). The plates were incubated at 37ºC overnight and afterwards an individual colony was inoculated in 1 mL of medium LB/amp and grew at 37°C for 6 hours under stirring. Thereafter, 500 μL of the suspension obtained were inoculated in 250 mL of medium LB/amp and grew at 37ºC for 12 h. Bacteria were collected by centrifugation at 3200 g for 30 min at 4ºC and plasmid DNA was extracted with the commercial kit QAFilter Plasmid Maxi Kit, following manufacturer instructions. Purified DNA was diluted in 100 μL of DNAse free water and DNA concentration was measured with the Qubit™ kit.

4.2 *Promoter Assays (luciferase assays)*

The transfection of luciferase reporters (pCREluc and HSV-TK-Ren) was carried out in pre-confluent cells using Fugene 6 as previously described. After appropriate treatments, cells were lysed in 50 μL of Passive Lysis Buffer by 15 min agitation in an orbital shaker and luciferase activity was measured by using the Dual-Luciferase reporter assay system. Briefly, 25 μL of the lysate were incubated with 25 μL of luciferase substrate (LARII) and the resulting luminescence was measured in a 96-well plate with the Synergy HT luminometer (Bio-Tek). Thenceforth, the reaction was stopped with the Stop & Glo reactive –which carries the *Renilla* substrate- and *Renilla*

luminescence was measured to normalize transfection efficiency. Results were expressed as Luc/Ren ratios.

4.3 *Genomic DNA extraction for genotyping*

A piece of mouse tail (2-3 mm) was treated with proteinase K (0.1 mg mL^{-1}, Roche) dissolved in 500 μL of lysis buffer (100 mM Tris HCl, pH 8.5, 5 mM EDTA, 0.2% SDS, 200 mM NaCl) and incubated at 56ºC overnight under stirring to digest proteins. DNA was precipitated with 500 μL of isopropanol, centrifuged at 15000 xg for 10 min, washed with 70% ethanol and precipitated again by centrifugation at 15,000 xg for 10 minutes. The precipitate was suspended in TE buffer (10 mM Tris-HCl, pH 8.5, 1 mM EDTA) and dissolved at 65ºC during 2h. In order to identify mice genotype, DNA was amplified by PCR and run on an agarose gel electrophoresis (see section 4.5).

4.4 *RNA extraction and RT-PCR*

For RNA extraction of mice cortex, animals were sacrificed at 3 dpl by cervical dislocation, the injured hemisphere was excised using a brain matrix (Zyvic instruments) to ensure isolation of equivalent regions in all mice, and the cortex was dissected. The tissue was immediately frozen in N_2 and stored at -80 ºC. In the case of astrocyte cultures, cells were processing immediately after treatments. RNA from cell cultures or brain tissue was isolated using the RNAeasy spin kit according to the manufacturer's instructions in any case. DNA contamination was prevented by treating samples either with DNAse1 (Invitrogen) or with Turbo DNA-free™ kit. The RNA concentration was determined with the NanoDrop 1000 spectrophotometer (Thermo Scientific) and the quality was tested using the Agilent 2100 Bioanalyzer (Agilent Technologies); only samples with RIN>8 were used. Purified RNA was reverse transcribed using *SuperScript™ II* reverse transcriptase (Invitrogen). A reaction mix containing 1 μg RNA, 1 μM of Oligo(dt) primers, 1 μM random hexamers, 0.5 mM dNTP, 0.45 mM DTT, RNAseOut (10 U) and *SuperScript™ II* reverse transcriptase (200 U) was incubated at 25ºC for 10 min, 42ºC for 60 min, and 72ºC for 10 min in a

thermal cycler (Lightcylcer, Roche). cDNA obtained was diluted in 50 μL of Tris-EDTA buffer and stored at -20ºC.

4.5 *Semi-quantitative PCR*

Total genomic DNA (2 μL/sample) or reverse transcribed cDNA (1 μg/sample) were amplified by PCR in a reaction mix containing Taq DNA polymerase (5U), dNTPs (10 μM), $MgCl_2$ (25 μM), reaction buffer (5X) and primers at optimal concentrations for efficient amplification (see table 2). Reactions were carried out in a thermal cycler (Roche) with different configurations depending on the primers. For CRTC1 and CRTC2, samples were incubated at 95ºC for 2 min, subjected to 35 cycles at 95ºC for 1 min, 58ºC for 1 min (annealing), and 2 min at 72ºC (extension), with a 10 min extension at 72ºC after the last cycle. For tta- and tetO- primers samples were incubated at 94ºC for 2 min followed by 35 cycles at 94ºC for 45s, 60ºC for 25seg, and 72ºC for 3min; with a final post-extension at 72ºC for 15min. The expected size of the amplicons was 446 bp for the Crtc1, 691 bp for Crtc2, 480 bp for Tta and 150 bp for TetO. PCR products were separated in a 1.2 % agarose gel electrophoresis stained with syber safe (Invitrogen) (0.84 g agarose in 70 ml TAE buffer: 40mM tris-acetate, 1mM EDTA, pH 8.2) and identified by comparison with a DNA ladder in an UV transiluminator (Gene Genius, Syngene).

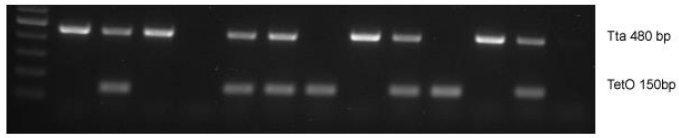

Fig. 1. Genotyping example of a VP16-CREB mice batch. Bitransgenic mice carry both Gfa2-Tta and TetO-VP16 transgenes. Gfa2-Tta mice were used as WT.

4.6 *Quantitative real-time PCR*

Three experimental replicates of each cDNA sample at a 1:10 or 1:100 dilution were amplified in an Applied Biosystems 7500 Fast system using either qPCR standard primers or hydrolysis probes. For cell cultures, a reaction mix containing 5 μL cDNA, primer pairs at optimal concentrations

(Table 2) and 15 μL of the Power SYBR Green PCR Master Mix was used. In the case of mice tissue, the reaction mix consisted in 4 μL cDNA, 16 μL of the Taqman Universal Master Mix , and hydrolysis probes for the genes of interest at appropriate dilutions. Hydrolysis probes were purchased from life technologies except for VP16, which was designed in our laboratory (see table 2).

Table 2. Primers and hydrolysis probes used in this thesis. Commercial *Taqman* probes used for validation of VP16-CREB mice microarray are not showed due to lack of sequence availability.

Gene symbol	Direction	Sequence	Concentration	Technique
Bdnf-IV	Fwd	5'-CTGCCTTGATGTTTACTTTGAC-3'	0.5 μM	qPCR
	Rev	5'-GCAACCGAAGTATGAAATAACC-3'	0.5 μM	qPCR
Gapdh	Fwd	5'-GAAGCTCATTTCCTGGTATGAC-3'	0.3 μM	qPCR
	Rev	5'-TCTCT TGCTCTCAGTATCCT-3'	0.3 μM	qPCR
Crtc1	Fwd	5'-GCGGAAATTTAGC GAGAAGAT-3'	0.5 μM	PCR
	Rev	5'-GCAGGGCAGAGTCA GAGTTGGTC-3'	0.5 μM	PCR
Crtc2	Fwd	5'-TCTTCGTCCACTTCATCTCCTGTC-3'	0.5 μM	PCR
	Rev	5'-GGGCTGCTGCAATCTCCTTAG-3'	0.5 μM	PCR
c-fos	Fwd	5'-AAAGTAGAGCAGCTATCTCCT-3'	0.3 μM	qPCR
	Rev	5'-AGCCATCTTATTCCTTTCCC-3'	0.3 μM	qPCR
Tta	Fwd	5'-CGG CTG TACG CGG ACC CAC TTT-3`	0.5 μM	PCR
	Rev	5'-TCG ACG CCT TAG CCA TTG AGA T-3´	0.5 μM	PCR
TetO	Fwd	5'-AGC TCG TTT AGT GAA CCG TCA GAT-3'	0.5 μM	PCR
	Rev	5'-CCT CGC AGA CAG CGA ATT CTA-3'	0.5 μM	PCR
VP16	Fwd	5'-CTACGGCGCTCTGGATATGG-3'	0.3 μM	qPCR
	Rev	5'-CCAAGGGCATCGGTAAACAT-3'	0.3 μM	qPCR
	Probe	5'-CGACTTCGAGTTTGAGC-3'	0.3 μM	qPCR

The amplification specificity was assessed by melting curve analysis on each sample, and negative controls included non-reverse transcribed RNA, reverse transcribed no-template-control, and a blank for each mix of primer pairs or taqman probes. Data analysis was performed with the comparative Cq method (Pfaffl 2001) using the Cq values and the average value of PCR efficiencies obtained with LinRegPCR software. Gene expression was normalized to *Gapdh* or to the geometric mean of, *18s* and *Tbp,* which were the most stable reference genes across the experimental groups, according to the geNorm algorithm (Vandesompele et al. 2002).

5. Cell biology methods

5.1 *Ca^{2+} imaging*

Experiments were performed as previously described (Barceló-Torns et al. 2011). In detail, cell medium was removed and cells were washed twice with Krebs-Henseleit buffer (KH: 118 mM NaCl, 4.7 mM KCl, 25 mM $NaHCO_3$, 1.2 mM $MgSO_4$, 10 mM Hepes , pH 7.4) suplemented with 10 mM Glucose and 1.2 mM $CaCl_2$. Cultures were loaded with the calcium-sensitive fluorescent dye fura-2 acetoxymethyl ester (fura-2/AM, 2 μM in KH buffer, Molecular Probes), at room temperature for 1 h in the dark. Following incubation, the buffer was removed, and the cells were left in fresh KH for 20 min. Thereafter, glass coverslips with fura-2 loaded cells were placed in the open-bath imaging chamber (Warner) of a TE-2000U inverted epifluorescence microscope equipped with a 403 oil objective (Nikon, Japan). Ligands were added directly in the chamber placed in the microscope except for BAPTA inhibitor, which was added to the cells 30 min before the appropriate stimuli. Cells were excited every 4 s at 340 and 380 nm by a monochromator (Cairns, UK) and fluorescent emission was recorded at 510 nm with a high-sensitivity CCD camera (Hamamatsu Photonics, Japan). Images were collected and analyzed with the MetaFluor image processing software (Universal Imaging, USA). The ratio of 510 nm emission fluorescence at 340 nm excitation to that at 380 nm excitation, F(340/380), was used as an indicator of intracellular calcium concentration in single cells.

5.2 *Immunocytochemistry*

After treatments and removal of culture medium, the cells were fixed for 30 min with 4% paraformaldehyde followed by several washes with PBS and incubated with PBS-Triton X-100 (0.1%) for 15 min to permeabilize cell membranes. Blocking of nonspecific binding was performed with PBS-BSA (1%) and afterwards cells were incubated overnight at 4ºC with primary antibodies (Table 1). The next day, cells were incubated with Alexa fluorescence-labelled secondary antibodies (1:1000), counterstained with the nuclear marker DAPI (1:20000) and mounted with Fluoromount-G (Southern biotech). The staining was visualized in an Eclipse 90i epifluorescence microscope (Nikon).

6. Histological methods

6.1 *Brain sectioning*

Animals were anesthetized with ketamine/xylacine (Imalgene 100 mg/kg; Rompún 16 mg/kg) and sacrificed by cardiac perfusion with 4% paraformaldehyde. After dissection, brains were post-fixed in 4% paraformaldehyde for 24 h. For cryotomy, brains were cryopreserved in 30% sucrose, frozen in cold isopentane, and maintained at -80ºC until sectioning in a Thermo Shandon cryotome to obtain 20 μm sagittal sections. The sections were preserved in anti-freeze solution (40% ethylene glycol, 30% glycerol, 30% phosphate buffer 0.1 M) at -20ºC. For paraffin slices, brains were dehydrated in increasing ethanol concentrations, cleared in xylene and embedded in paraffin. Coronal slices of 5 μm width were obtained using a rotary microtome (Leica RM2135), and collected on Superfrost™ slides.

6.2 *Immunohystochemistry*

Diaminobenzidine (DAB)-based immunohistochemistry was performed in sagittal slices. After several washes in TBS to remove anti-freeze solution, endogenous peroxidase was blocked with 3% H_2O_2 and antigen retrieval was performed by incubation in 10mM sodium citrate (pH 6) for 30 min at 80ºC. Following wash in TBS-Tween (0.5%), slices were blocked with 5% normal goat serum (NGS) solution and incubated overnight with a primary antibodies (see table 1) diluted in NGS 1%. Next day, slices were incubated 1h with secondary antibodies linked to horseradish peroxidase (1:1000), washed with TBS-Tween (0.5%) and incubated again 1h with peroxidase-streptavidin. Thereafter, slices were submerged in DAB solution until precipitate was observed, rinsed with TBS, mounted in Superfrost™ slides and let dry 30 min in a flow hood. Slices were dehydrated in increasing EtOH concentrations following by xylene and mounted with DPX. Images were obtained with an Eclipse 80i brightfield microscope (Nikon).

6.3 *Immunofluorescence*

Sagittal sections were processed as described above for antigen retrieval, blocking and primary antibodies incubation. Secondary antibodies used were Alexa Fluor 488/594 conjugated goat IgGs (1:1000) and nuclear staining was performed by incubation with DAPI (1:20000). Sections were mounted in Superfrost™ slides with Fluoromount G. Images were obtained in a Zeiss LSM700 laser-scanning microscope with the ZEN acquisition software. VP16/GFAP images were acquired in similar regions of the cortex, hippocampus and cerebellum. VP16-positive astrocytes were quantified with the plug-in cell counter from ImageJ. To measure SMI fluorescence, 4 fields of a 40x objective (Plan-Apochromat 40x/1.3 Oil DIC M27) were analysed and a sum projection of three Z-sections (1 μm/section) per image was used. The area of analysis was in the penumbra zone in a square of 320 x 320 μm^2 on the left border of the lesion, or an equivalent region in control animals. Images were analysed for total fluorescence area with ImageJ.

For lectin staining, coronal sections were deparaffinised, washed in TBS containing 1%Triton X-100, incubated for 2 h with *Lycopersicum esculentum* lectin conjugated with FITC, and mounted with Fluoromount-G. Lectin immunofluorescence was quantified with ImageJ. The lesion core was selected, a manual thresholding performed, and the area of fluorescence determined and expressed in mm^2.

6.4 *Cresyl violet staining (Nissl)*

Coronal slices were deparaffinised with xylene and rehydrated with decreasing ethanol concentrations. Sections were immersed in toluidine blue solution for 90 seconds, rinsed in distilled water, dehydrated in ethanol/xilene, and mounted with DPX. Nissl staining was visualized in a brightfield microscope (Nikon Eclipse 80i) and number of neurons was determined by cell counting with ImageJ software. Neurons were counted in the penumbra area extending 400 μm from the border of the lesion core in both ipsilateral and contralateral hemispheres and normalized per area.

7. Microarray analysis

7.1 *DNA microarray*

DNA arrays were carried out by Bioarray® (Alicante, Spain) using SurePrint G3 Rat Gene Expression 8x60K (Agilent, Santa Clara, California, USA). These microarrays include 39,430 Entrez Gene RNAs and 16,251 lincRNAs. RNA was extracted from cell cultures as described previously. The concentration was determined with the NanoDrop 1000 spectrophotometer (Thermo Scientific), and the RNA quality with Tape Station, using the R6K ScreenTape kit (Agilent). The samples were amplified, labeled for Cy5 or Cy3 using the Low Input Quick Amp Labeling kit (Agilent), and hybridized in the SurePrint G3 Microarray slides according to the manufacturer's protocol. For astrocyte cultures, three samples of each condition (CT, FSK, NE, Null, VP16-CREB) were analysed. Two independent designs for the treated and the infected samples were performed and each sample was hybridized three times and balanced with respect to the use of Cy3 and Cy5 in the samples (Fig. 2a). For mice cortex, 5 to 6 samples for each condition (WT, T, WTC, TC) were analysed. We used a loop design in which each sample was hybridized four times, and balanced with respect to the use of Cy3 and Cy5 in the samples (Fig. 2b). The microarray slides were scanned using the Agilent microarray scanner (G2565CA), and the resulting images were extracted with Agilent Feature Extraction Software (version 10.7).

a

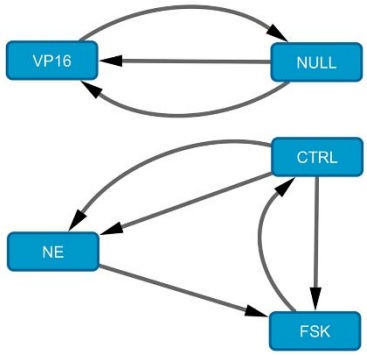

7.2 *Transcriptome analysis*

Pre-processing of raw data and statistical analyses were performed using Bioconductor packages in R programming environment.

Background correction was performed using the "normexp" method (offset = 10) implemented in the LIMMA package to adjust local median (M) background estimates. Background-corrected intensity data were normalized using the loess method to remove the bias within each array and A-values quantile normalization (Aquantile) was used to remove the bias between arrays. Two-color arrays were analysed independently. To have equal

variances in both arrays, we used Intraspot Correlation to re-scale the M and A-values for each gene. Normalized data were adjusted to a linear model in LIMMA to determine the target genes differentially expressed between the experimental groups. P-values were computed with empirical Bayes moderated t-statistics at the level of 0.05 to calculate differential gene expression in the paired comparisons FSK-CT, NE-CT, VP16-Null, for astrocyte culture samples and WTC-WT, TC-T, T-WT, TC-WTC for mice cortex. The results of the VP16-CREB mice array were deposited in NCBI's Gene Expression Omnibus, and are accessible through GSE68187 (http://www.ncbi.nlm.nih.gov/geo/ query/acc.cgi?acc=GSE68187).

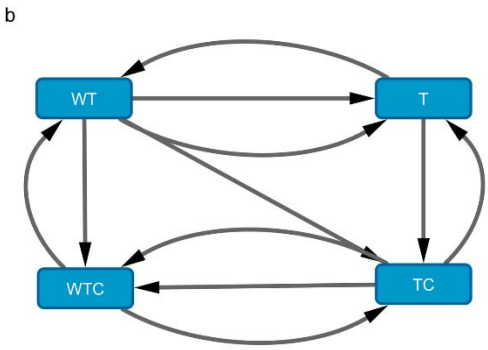

Fig. 2. Designs for astrocyte cultures (a) and VP16-CREB mice (b) microarrays. Arrowheads indicate Cy5 hybridization and arrow tails Cy3 hybridization.

7.3 *Functional enrichment analysis (astrocyte cultures)*

Functional association of differentially expressed genes to GO terms was performed with the Gene Set Enrichment Analysis (GSEA) (www.broadinstitute.org/gsea/index.jsp) (Subramanian et al. 2005). Lists of significantly deregulated genes (adj. $p<0.05$) were pre-ranked by fold change and analysed for enrichment in gene sets representing GO terms of biological process category. Only the enriched sets with a false discovery rate (FDR) <0.25 were computed. Resulting GOs were grouped according to the overlap coefficient, defined as the size of the intersection divided by the smaller of the size of two GOs. Next, a leading edge analysis was carried out in order to identify the genes that most contributed to the enrichment in each GO term.

7.4 *Functional enrichment analysis (VP16-CREB mice)*

For pathway enrichment analyses the resulting lists of differentially expressed genes were annotated by Annbuilder package to obtain Gene

ontology (GO) terms, or by KEGG package and custom software written in Perl and R for pathway annotation. To evaluate which pathways or functional categories were enriched in VP16-CREB mice, we computed the Gene Set Enrichment Analysis (GSEA, "geneSetTest" function) and hypergeometric distribution test (GOHyperG and "phyper" functions). We used $P < 0.0001$ as the cut-off point to determine whether a KEGG pathway was significantly enriched.

7.5 *Meta-analyses (VP16-CREB mice)*

Cell-population analysis. The whole transcriptome represented in the arrays for each pair-wise comparison (WTC-WT, TC-T, T-WT, TC-WTC) was divided into up- and down-regulated genes to take into account the direction of change, and each group was sorted separately according to their adjusted p-value from more to less significant (*p-value* = 1), without considering any threshold. Redundant probesets were removed by selecting only the probeset with the highest average expression to avoid bias due to highly represented genes in the arrays. The resulting lists where then compared to molecular signatures of candidate cells including immune cells in a basal state, activated immune cells, oligodendrocytes, astrocytes, reactive astrocytes, and neurons. The data sets used were: i) GSE10246 for immune cells (B-cells, dendritic lymphoid cells CD8a+, dendritic myeloid cells CD8a-, dendritic plasmacytoid cells B200+, common myeloid progenitor, granulocyte monocyte progenitor, granulocyte mac1+/gr1+, macrophage from bone marrow 0h, 2h, 6h, 24h after LPS, macrophage peripheral 0h, 1h, 7h after LPS/thioglycollate, microglia, mast cell, mast cell with IgE alone and with IgE+ antigen (1h, 6h), megaerythrocyte progenitor, NK-cells, T-cell CD4+, CD8+, foxP3+, thymocyte SP CD4+ and CD8+, thymocyte DP CD4+/CD8+) (Lattin et al. 2008); ii) GSE9566 for neuronal and glial cells in a basal state including astrocyte, astrocytes from gray matter, oligodendrocytes such as oligodendrocyte progenitor cells PDGFRα+ (OPC), post-mitotic oligodendrocytes positive to myelin oligodendrocyte glycoprotein (MOG), or to galactocerebroside (GalC) (Cahoy et al. 2008); iii)

GSE35338 for astrocytes activated by LPS (1 d) or by middle cerebral artery occlusion (MCAO) (1 d, 3d or 7 d) (Zamanian et al. 2012).

The molecular signatures for each cell population were obtained by retrieving the top 500 genes that distinguished each cell type from a cell or tissue of reference. References were "cortex" for "immune cells" (to determine the non-cortical genes from cell infiltration), "neurons isolated from juvenile mice" (>P16) for "glial cells" (to distinguish between neuronal and non-neuronal cells in the cortex), and "basal astrocytes" for "reactive astrocytes" (to determine which astrocytic genes were derived from astrogliosis). Datasets were analyzed using the 'affy' package for normalization with the RMA (Robust MultiArray) method and probe summarization (Gautier et al. 2004), and the LIMMA package for moderated *t* test calculations (Smyth 2005). Next we computed the number of top 500 genes that were present within the entire set of the up and down lists of the experimental group comparisons.

Astrocytic CREB-target genes analysis. To identify of VP16-CREB dependent genes in astrocytes a "cortical astrocyte signature" of 793 genes (adjusted p-value of 0.005) was generated using datasets generated by the TRAP approach (GSE13379). Astrocyte-enriched genes were identified by comparison of the astrocyte transcriptome with oligodendrocyte (mixed, mature) and neuronal profiles (Cck+, Cort+, Pnoc+, and neurons from layers 5a, 5b and 6) using Bioconductor. PSCAN (Zambelli et al. 2009) was used to predict CRE binding sites of the TRANSFAC database in the promoter region (−950/+50) of selected genes. Heat maps and hierarchical clustering were computed with the 'gplots' (CRAN.R-project.org/package=gplots) and 'RColorBrewer' packages (CRAN.R-project.org/package=RColorBrewer).

8. General statistics

Astrocyte culture studies were performed in a minimum of three sample replicates for each experiment. VP16-CREB mice study was carried out in four batches of age-matched 5- to 7-month-old mice. The number of independent cultures or mice used *per* experiment is indicated in the figure legends. Data are presented as the means ± SEM. The statistical analysis was carried out with GraphPad Prism version 6 (Prism software), and SPSS software version 19 (IBM). Data were tested for homogeneity of variances with Levene's test. A logarithmic transformation was carried out in non-homogeneous data to achieve homogeneity (qPCR data for genes *Sdhb, Itgb1, Hspg2, Col1a1, Cxcr2, Ccl2, Ccl5, Nefm*). The statistical tests used for group comparisons were Student's t test or analysis of variance (ANOVA), except for the qPCR data of the *Gfap* gene, which was analyzed with the generalized linear model because variance homogeneity was not achieved. Post-hoc tests used were Newman-Keuls and Bonferroni. The Pearson r index was used for correlation analysis and Chi square for contingency tables. Raw data from Agilent microarrays were analysed as described above and differentially expressed gene lists were compared with Venny software (Oliveros 2007).

REFERENCES

Agullo L, Garcia A, Hidalgo J. 1998. Metallothionein-I+II induction by zinc and copper in primary cultures of rat microglia. Neurochem. Int. 33:237–242.

Barceló-Torns M, Lewis AM, Gubern A, Barneda D, Bloor-Young D, Picatoste F, Churchill GC, Claro E, Masgrau R. 2011. NAADP mediates ATP-induced Ca2+ signals in astrocytes. FEBS Lett. 585:2300–2306.

Barco A, Alarcon JM, Kandel ER. 2002. Expression of constitutively active CREB protein facilitates the late phase of long-term potentiation by enhancing synaptic capture. Cell 108:689–703.

Bradford MM. 1976. A rapid and sensitive method for the quantitation of microgram quantities of protein utilizing the principle of protein-dye binding. Anal. Biochem. 72:248–254.

Cahoy JD, Emery B, Kaushal A, Foo LC, Zamanian JL, Christopherson KS, Xing Y, Lubischer JL, Krieg P a, Krupenko SA, et al. 2008. A transcriptome database for astrocytes, neurons, and oligodendrocytes: a new resource for understanding brain development and function. J. Neurosci. 28:264–78.

Gautier L, Cope L, Bolstad BM, Irizarry RA. 2004. Affy - Analysis of Affymetrix GeneChip data at the probe level. Bioinformatics 20:307–315.

Giralt M, Penkowa M, Lago N, Molinero A, Hidalgo J. 2002. Metallothionein-1+2 protect the CNS after a focal brain injury. Exp. Neurol. 173:114–128.

Lattin JE, Schroder K, Su AI, Walker JR, Zhang J, Wiltshire T, Saijo K, Glass CK, Hume DA, Kellie S, et al. 2008. Expression analysis of G Protein-Coupled Receptors in mouse macrophages. Immunome Res. 4:5.

Lin W, Kemper A, McCarthy KD, Pytel P, Wang J-P, Campbell IL, Utset MF, Popko B. 2004. Interferon-gamma induced medulloblastoma in the developing cerebellum. J. Neurosci. 24:10074–10083.

Oliveros JC. 2007. VENNY. An interactive tool for comparing lists with Venn Diagrams. BioinfoGP of CNB-CSIC:http://bioinfogp.cnnb.csic.es/tools/venny/index.ht.

Pfaffl MW. 2001. A new mathematical model for relative quantification in real-time RT-PCR. Nucleic Acids Res. 29:2003–2007.

Servitja JM, Masgrau R, Pardo R, Sarri E, Von Eichel-Streiber C, Gutkind JS, Picatoste F. 2003. Metabotropic glutamate receptors activate phospholipase D in astrocytes through a protein kinase C-dependent and Rho-independent pathway. Neuropharmacology 44:171–180.

Smyth GK. 2005. Limma: linear models fro microarray data. In: Bioinformatics and Computational Biology Solutions using R and Bioconductor. p. 397–420.

Subramanian A, Subramanian A, Tamayo P, Tamayo P, Mootha VK, Mootha VK, Mukherjee S, Mukherjee S, Ebert BL, Ebert BL, et al. 2005. Gene set enrichment analysis: a knowledge-based approach for interpreting genome-wide expression profiles. Proc. Natl. Acad. Sci. U. S. A. 102:15545–50.

Vandesompele J, De Preter K, Pattyn F, Poppe B, Van Roy N, De Paepe A, Speleman F. 2002. Accurate normalization of real-time quantitative RT-PCR data by geometric averaging of multiple internal control genes. Genome Biol. 3:0034.1–0034.7.

Zamanian JL, Xu L, Foo LC, Nouri N, Zhou L, Giffard RG, Barres BA. 2012. Genomic Analysis of Reactive Astrogliosis. J. Neurosci. 32:6391–6410.

Zambelli F, Pesole G, Pavesi G. 2009. Pscan: Finding over-represented transcription factor binding site motifs in sequences from co-regulated or co-expressed genes. Nucleic Acids Res. 37:247–252.

Results I

ATP and Noradrenaline Activate CREB in Astrocytes via Non canonical Ca^{2+} and Cyclic AMP Independent Pathways

Published in GLIA, April 2012

GLIA

ATP and Noradrenaline Activate CREB in Astrocytes via Non canonical Ca^{2+} and Cyclic AMP Independent Pathways

PAULINA CARRIBA,[1] LUIS PARDO,[1,2] ARNALDO PARRA-DAMAS,[1,2,3] MATHIEU P. LICHTENSTEIN,[1,2] CARLOS A. SAURA,[1,2,3] AURORA PUJOL,[4,5,6] ROSER MASGRAU,[1,2] AND ELENA GALEA[1,2,4]*

1 Institut de Neurociències, Universitat Autònoma de Barcelona, Spain 2 Departament de Bioquımica i Biologia Molecular, Universitat Autònoma de Barcelona, Spain 3 Centro de Investigacion Biomedica en Red de Enfermedades Neurodegenerativas (CIBERNED), Spain 4 Catalonian Institution for Advanced Studies (ICREA), Spain 5 Centre de Genètica Mèdica i Molecular, Institut d'Investigacio Biomèdica de Bellvitge (IDIBELL), Hospitalet de Llobregat, Barcelona, Spain 6 Centro de Investigacion Biomédica en Red de Enfermedades Raras (CIBERER), Spain

KEY WORDS
BAPTA; bdnf; calcineurin; CRTC; protein kinase C

Additional Supporting Information may be found in the online version of this article.

Paulina Carriba and Luis Pardo contributed equally to this work.
Paulina Carriba is currently at Institut de Recerca Hospital Vall d'Hebron, Barcelona, Spain
Grant sponsor: MICINN, Spain; Grant numbers: BFU2007-63031/BFI and BFU2010-21281/BFI.
Correspondence to: Elena Galea, Institut de Neurociències, Edifici M, Universitat Autònoma de Barcelona, Bellaterra, 08193 Barcelona, Spain.
E-mail: galea.inc@gmail.com
Received 9 December 2011; Accepted 20 April 2012
DOI 10.1002/glia.22352
Published online 16 May 2012 in Wiley Online Library (wileyonlinelibrary.com).

ABSTRACT

In neurons, it is well established that CREB contributes to learning and memory by orchestrating the translation of experience into the activity-dependent (i.e., driven by neurotransmitters) transcription of plasticity-related genes. The activity-dependent CREB-triggered transcription requires the concerted action of cyclic AMP/protein kinase A and Ca^{2+}/calcineurin via the CREB-regulated transcription co-activator (CRTC). It is not known, however, whether a comparable molecular sequence occurs in astrocytes, despite the unquestionable contribution of these cells to brain plasticity. Here we sought to determine whether and how ATP and noradrenaline cause CREB-dependent transcription in rat cortical astrocyte cultures. Both transmitters induced CREB phosphorylation (Western Blots), CREB-dependent transcription (CRE-luciferase reporter assays), and the transcription of Bdnf, a canonical regulator of synaptic plasticity (quantitative RT-PCR). We indentified a Ca^{2+} and diacylglycerol-independent protein kinase C at the uppermost position of the cascade leading to CREB-dependent transcription. Notably, CREB-dependent transcription was partially dependent on ERK1/2 and CRTC, but independent of cyclic AMP/protein kinase A or Ca^{2+}/calcineurin. We conclude that ATP and noradrenaline activate CREB-dependent transcription in cortical astrocytes via an atypical protein kinase C. It is of relevance that the signaling involved be starkly different to the one described in neurons since there is no convergence of Ca^{2+} and cyclic AMP-dependent pathways on CRTC, which, moreover, exerts a modulatory rather than a central role. Our data thus point to the existence of an alternative, non-neuronal, glia-based role of CREB in plasticity.

INTRODUCTION

It is widely accepted that the transcription factor CREB (cyclic AMP-response element-binding protein) couples synaptic activity to the long-term changes in synaptic plasticity that underlie learning and memory (Benito et al., 2010; Sakamoto et al, 2011). Traditionally, neurons have been at the center stage of the association of CREB and memory. Thus, the signal transduction leading to CREB activation, the ensuing gene expression, and the functional consequences have been actively examined in neuronal cultures (Li et al., 2009), or in brains with transgenic (Barco et al., 2005) or viral (Han et al., 2009) manipulation of CREB activity in neurons. Altogether, the accumulated evidence supports a model whereby, upon the NMDA-mediated neuronal depolarization, the joint increases of intracellular Ca^{2+} and cyclic AMP (cAMP) synergistically activate CRTC (CREB-regulated transcription co-activator, formerly called TORC) via protein kinases, namely Ca^{2+}/calmodulin kinases (CaMK), protein kinase A (PKA), and MAPK (Altarejos et al., 2011; Benito et al., 2010; Kovacs et al., 2007). CRTC in turn promotes CREB-dependent transcription by facilitating the association of CREB with components of the basal transcription complex (Conkright et al., 2003).

Microarray analyses and technologies based on chromatin immunoprecipitation (ChIP) for genome-wide gene mapping have been used to identify activity-driven CREB-regulated genes allegedly in neurons. Analyzed materials have included: (1) whole brains from animals subjected to behavioral stimuli (Leil et al., 2002); (2) PC12 neuronal cell lines stimulated with growth factors or second messenger activators (Impey et al., 2004); (3) brain slices processed after an episode of long-term potentiation (LTP) (Park et al., 2006; Ryan et al., 2010); and (4) brains with neuronally targeted loss or gain of CREB function (Benito et al., 2010), which have informed about CREB targets while avoiding possible biases introduced by experimental stimulations that may fall short in mimicking reality. This collective endeavor has led to the identification of hundreds of CREB-regulated candidate genes including *Bdnf, c-fos*, *Jun*, *Arc*, and members of the

CREB family, which contribute to presynaptic or postsynaptic structural or functional remodeling thereby increasing synaptic strength. Of note, genes regulated by LTP tend to cluster around CREB-interacting segments on chromosomes, thus facilitating the coordinated expression of functionally related genes during the molecular adjustments caused by external stimuli (Park et al., 2006; Ryan et al., 2010).While the literature documents well the importance of CREB in learning and memory, the notion has to be dispelled that CREB-related events are exclusively neuronal and spare astrocytes. First, astrocytes are an integral part of the synapse (Araque et al., 1999), and essential for the generation of LTP (Suzuki et al., 2011), or the consolidation of long-term memory as recently shown in a model of inhibitory avoidance in rats (Suzuki et al., 2011). Second, some of the models used to establish a link between CREB and memory—e.g. CREB knockout mice, mice over-expressing a dominant-negative CREB, or infusion of CREB-antisense oligonucleotides—do not discriminate the cellular source of the observed deficits in plasticity and learning (Bourtchuladze et al., 1994; Guzowski et al., 1997; Kida et al., 2002; Kogan et al., 1997; Pittenger et al., 2002). Likewise, note that whole tissues from tetanized brains, and not dissected neurons, were the starting material that led to the important, aforementioned discovery of CREB-dependent, LTP-regulated gene clusters.

It is therefore necessary to establish the role of astrocytic CREB in plasticity. The analysis of CREB-driven transcription is indeed not foreign to astrocytes, stemming from the notion that intracellular Ca^{2+} transients, the landmark feature of astrocyte excitability, may couple external stimuli to selected programs of gene expression as in neurons. Two studies have thus analyzed the relationship of Ca^{2+} and CREB activation in astrocytes, with conflicting results. One study has shown increased *Bdnf* expression induced by ATP via Ca^{2+}/CaMK/CREB in the astrocytoma RCG-12 (Takasaki et al., 2008). By contrast, a second study in mouse primary cortical astrocytes showed no activation of CREB-dependent transcription by ATP, despite the robust increase in intracellular Ca^{2+} caused by the gliotransmitter (Murray et al., 2009). Here we sought to determine whether the dual Ca^{2+}/cAMP-dependent stimulation of CREB described in neurons operates also in

astrocytes. As upstream inducers we tested Ca^{2+}-elevating transmitters including ATP, as in the previous studies, as well as glutamate and noradrenaline (NE). The latter is a potent stimulator of cAMP/dependent pathways in addition to inducing elevation of intracellular Ca^{2+}. To assess the capacity of CREB to trigger transcription we used CRE-directed luciferase reporter assays in combination with analysis of *Bdnf* expression by qPCR, which was intended as the ultimate demonstration that the activated CREB caused transcription of real genes. We found that ATP and NE, but not glutamate, activated CREB-dependent transcription and induced *Bdnf* mRNA upregulation. An atypical Ca^{2+}-independent PKC was identified as the uppermost regulator leading to CREB activation by ATP and NE. CRTC was involved too, as in neurons, but it was not activated by the convergence of Ca^{2+}/calcineurin and PKA. We conclude that ATP and NE cause CREB-dependent transcription in astrocytes using unique, glia-specific signaling pathways. These findings provide molecular grounds to posit that CREB-driven long-lasting changes in astrocyte plasticity may play a role in learning and memory.

RESULTS

NE and ATP But Not Glutamate Caused CREB-dependent Transcription in Astrocytes

We first compared the capacity of several transmitters to induce CREB-dependent transcription by using a CRE-containing luciferase reporter assay. Forskolin (1 μM) was used as a positive control of robust cAMP-dependent CREB activation (Murray et al., 2008). ATP and NE caused activation of CREB-dependent transcription, the EC50 of ATP being 3.8 ± 0.4 μM (media ± SEM, n = 3), and that of NE 0.99 ± 0.2 μM (media ± SEM of n = 3). At concentrations causing maximal responses, the extent of CREB activation caused by ATP (100 μM) and NE (10 μM) was similar to that forskolin, while glutamate (100 μM) had a modest, statistically insignificant effect (Fig. 1A). We hence proceeded only with ATP and NE to gain further insight into signaling pathways. The effect of NE was partially reversed by

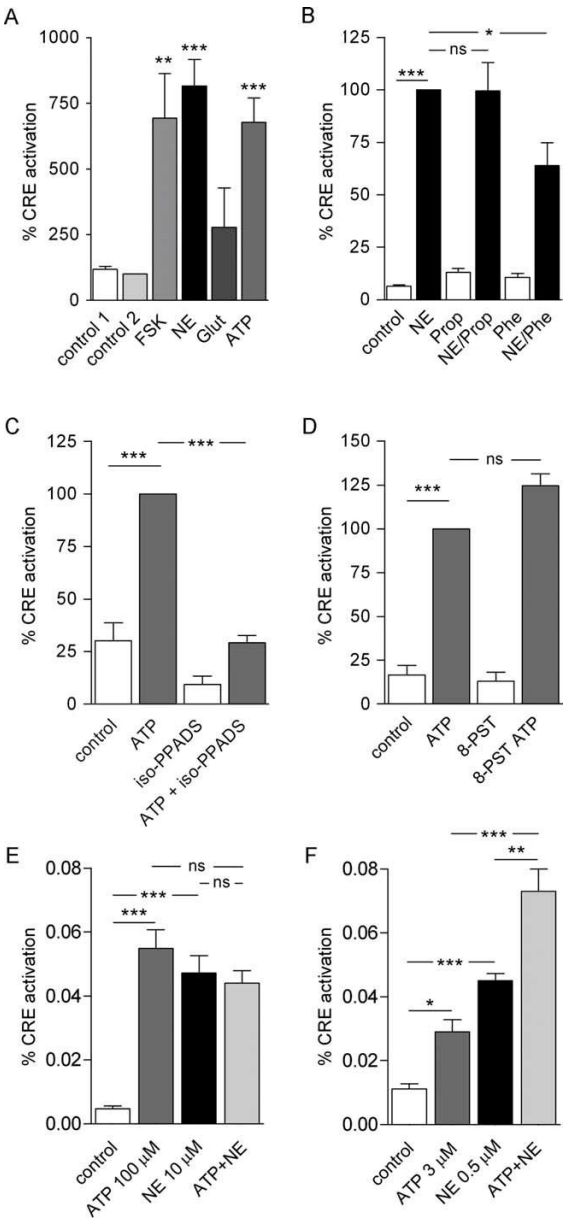

phentolamine (10 µM), while propanolol (10 µM) had no effect, indicating the involvement

Fig. 1. CREB dependent transcription in astrocytes as measured by luciferase assays. (A) Comparison of the activation of CREB by ATP, NE, glutamate (GLU) and forskolin (FSK) as a positive control; (B) effect of noradrenergic receptor inhibitors propanolol (β inhibitor) and phentolamine (α inhibitor) on the effect of NE; (C) effect of the P2X receptor antagonist iso-PPADS on the activation by ATP; (D) effect of the adenosine receptor inhibitor 8-PST on the effect of ATP; E and F show the interplay between ATP and NE. (E) Effect of stimulating P2X receptors when maximal CREB activation was achieved with NE; and (F) Effect of simultaneous incubation with submaximal doses of ATP (3 µM) and NE (0.5 µM). In A–D, astrocytes were incubated with 1 µM FSK, 100 µM ATP, 10 µM NE or 100 µM GLU for 6 h and processed for CRE-luciferase assays. Iso-PPADS (100 µM), 8-PST (10 µM), propanolol (10 µM), and phentolamine (10 µM) were administered 30 min before the transmitters. Control 1 were cells transfected with Luc and renilla plasmids but not treated with any transmitter, and Control 2 nontransfected cells but treated with NE. Data are the means +/- SEM of 5 (A), 3 (B), 4 (C), 5 (D) and 3 (E) independent determinations in independently obtained cultures. In A, E, and F the actual values from the luciferase assays are represented, while in the rest of the figures the data are presented as the percentage of values in ATP-treated or NE-treated cells. (*) $P < 0.05$, (**) $P < 0.01$, (***) $P < 0.001$, one-way ANOVA analysis followed by the Newman-Keuls test. NE and ATP, but not GLU, stimulated CREB activation to a similar extent than FSK. See EC50s in the text. The effect of ATP was dependent on P2X receptors and independent of adenosine, while the effect of

NE was partially dependent on α receptors. The joint effect of the transmitters was additive rather than synergistic.

of α but not β noradrenergic receptors (Fig. 1B). The effect of ATP in turn was blocked by 100 μM iso-PPADS (Fig. 1C), an inhibitor of P2X receptors, indicating dependence on P2X receptors, and was not altered by 35 μM 8-PST, a general inhibitor of adenosine receptors, indicating that the activation of CREB by ATP was independent of adenosine (Fig. 1D). This result was of relevance to unmistakably ascribe CREB activation to ATP because the nucleotide degrades naturally into adenosine (Cunha et al., 1992; Franco et al., 1986), which can induce cAMP-dependent CREB activation (Socodato et al., 2011).

The simultaneous stimulation of P2X and α noradrenergic receptors using maximal concentrations of the transmitters did not increase CREB stimulation with respect to the individual responses, indicating saturation (Fig. 1E). In addition, when used at submaximal concentrations close to their respective EC50 (3 μM for ATP and 0.5 μM for NE), the joint effect of the transmitters was additive (Fig. 1F). Taken together, this evidence supports that the transmitters acted at the same cells and on the same pathway, to be characterized as follows. In neurons, CREB phosphorylation does not appear to be sufficient to activate CREB-dependent transcription (Kovacs et al., 2007). Rather, the complete CREB activation requires CRTC which, in turn, is the convergence point of two signaling pathways mediated by cAMP/PKA and Ca^{2+}/ calcineurin, respectively. To determine whether a similar scenario existed in astrocytes, we systematically explored the role of PKA, Ca^{2+}/calcineurin, CREB phosphorylation, and CRTC1/2 in the activation of CREB-dependent transcription elicited by the transmitters. Below are the results.

CREB-Dependent Transcription Depended on Atypical PKC But Not on Ca^{2+} and PKA

The implication of PKA was examined by using its specific inhibitors, Rp-cAMP (20 μM) and a myr-PKA peptide (1 μM). None of them caused a statistically significant change of the CREB-dependent transcription elicited

by ATP or NE (Fig. 2A,B). As a positive control, myr-PKA was tested in the

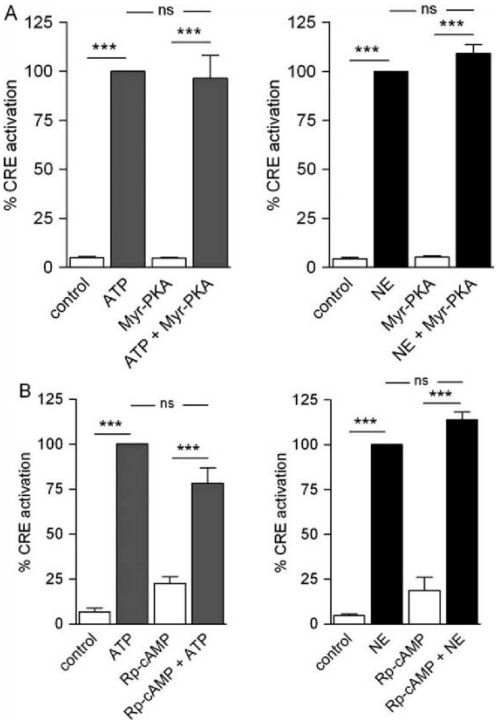

Fig. 2. CREB-dependent transcription did not depend on cAMP/ PKA. Effect of PKA inhibitors myr-PKA (A) and Rp-cAMP (B) on CREB activation measured by luciferase assays. Rp-cAMP (20 μM) or myr-PKA peptide (1 μM) were added 30 min before the transmitters. Data are the means +/- SEM of n = 3–5 independent determinations in independent cultures. (***) P < 0.001, (ns) nonsignificant, one-way ANOVA followed by the Newman–Keuls test.

HEK293 cell line, wherein cAMP/PKA-dependent activation of CREB-dependent pathway has been described (Hirota et al., 2000; Katoh et al., 2006). In experiments carried out simultaneously, the inhibitor inhibited, in a statistical significant manner, the forskolin-mediated activation of CREB-dependent transcription in HEK293 , while it had no effect on the NE-elicited one in primary astrocytes (Supp. Info. Fig. 1). Taken together, the data indicated that CREB activation in astrocytes was largely independent of cAMP/PKA-dependent pathways.

PKC is a widespread stimulator of CREB-dependent transcription (Nguyen et al., 2009; Roberson et al., 1999). PKC encompasses over 10 isozymes divided into three subfamilies according to their second messenger requirements: classical (a, b, g), novel (d, e, h, u), and atypical (z, i). Classical PKCs are activated by Ca^{2+} and diacylglycerol, novel PKCs require diacylglycerol but not Ca^{2+}, whereas atypical PKCs neither require Ca^{2+} nor

diacylglycerol for activation. GF109203X can be used to discriminate among PKCs since at 25 μM the drug inhibits all PKCs, whereas at 2 μM inhibits novel and classical isozymes, and at 0.2 μM only classical PKCs. In luciferase assays, only 25 μM CHF109203X completely inhibited the effect of ATP and NE (Fig. 3A), identifying by exclusion an atypical PKC as the isozyme accounting for CREB activation. Accordingly, the PKC α/β inhibitor Go6976 had no effect (Fig. 3A). Moreover, the diacylglycerol analog Dic 8 (40 μM) neither stimulated CREB activation per se nor it amplified the effect of NE or ATP (Fig. 3B), thus granting further support to the participation of a diacylglycerol-independent, atypical PKC. In addition, inhibitors of protein kinase M (10 μM ZIP), protein kinase G (10 μM KT5823), Akt/PI3K (3 μM LY-294002), or CaMKs (10 μM KN-93) had no effect on the transmitter-elicited CREB-dependent transcription, thus ruling out the implication of these kinases.

Because atypical PCKs do not depend on Ca^{2+}, the data obtained so far ruled out the participation of this second messenger in CREB-dependent transcription in astrocytes. To seek further proof of this conclusion, we examined by quantitative RT-PCR the effect of the Ca^{2+} chelator BAPTA on the expression of the mRNA encoding for the transcript IV of *Bdnf*, which has been shown to directly depend on CREB in rat neurons and astrocytes (Tao et al., 1998). We chose this approach instead of testing BAPTA in luciferase assays for two reasons. One, because BAPTA inhibits the activity of GL3-based luciferase-reporting vectors, thus disqualifying the use of this technique to assess the Ca^{2+} dependence of a given promoter. Moreover, in our hands, while BAPTA inhibits luciferase activity at both 10 and 30 μM (data not shown), on the magnitude of the Ca^{2+} increases when used at 10 μM, BAPTA had no significant effect (Fig. 4A). Incidentally, the inhibitory effect of BAPTA on GL3-based vectors casts doubts on the conclusions drawn from numerous studies reporting Ca^{2+} dependency of CREB activation using these assays. Second, the analysis of gene expression lends credence to the functional relevance of CREB activation assessed by luciferase assays. We found that both ATP and NE increased *Bdnf* (Exon IV) mRNA expression in astrocytes, the effect of NE being much greater

(Fig. 4B, left panel). The upregulation induced by both ATP and NE was completely inhibited by GF109203X (Fig. 4B, right), but was not reduced by BAPTA at 30 μM (Fig. 4B, right), a dose that abrogated increases in intracellular Ca^{2+} (Fig. 4A). It is worth noting that BAPTA appeared to have a stimulatory effect on the ATP-elicited CREB activation, that is, BAPTA per se did not affect the contents of bdnf IV mRNA, but the reduction of intracellular Ca^{2+} increased the expression of bdnf IV mRNA induced by ATP but not by NE. Overall, the data suggests that the activation of CREB by the two transmitters was not triggered by Ca^{2+}.

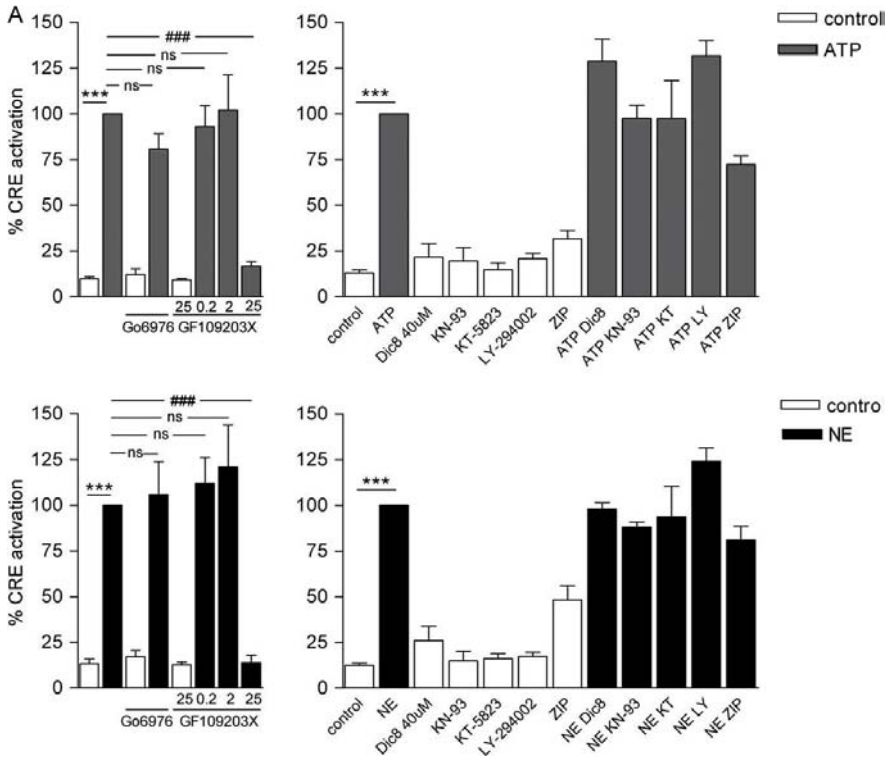

Fig. 3. CREB-dependent transcription depended on atypical PKC. (A) Effect of two PKC inhibitors: the general PKC inhibitor GF109203X, tested at increasing doses to discriminate among PKC subfamilies, and the PKCα/β inhibitor Go6976, and (B) Effect of Dic8 (diacylglycerol analog), 10 μM KN-93 (CaMK inhibitor), 10 μM KT-5823 (protein kinase G inhibitor), 3 μM LY- 294002 (Akt inhibitor). Astrocytes were incubated with 100 μM ATP or 10 μM NE and processed after 6 h for luciferase reporter assays. Dic 8 and kinase inhibitors were added 30 min before the transmitters. Data are the means +/- SEM of n = 3–5 independent determinations in independent cultures. (***) P < 0.001, one-way ANOVA followed by the Newman–Keuls test. The PKC inhibitor completely inhibited the activation of CREB.

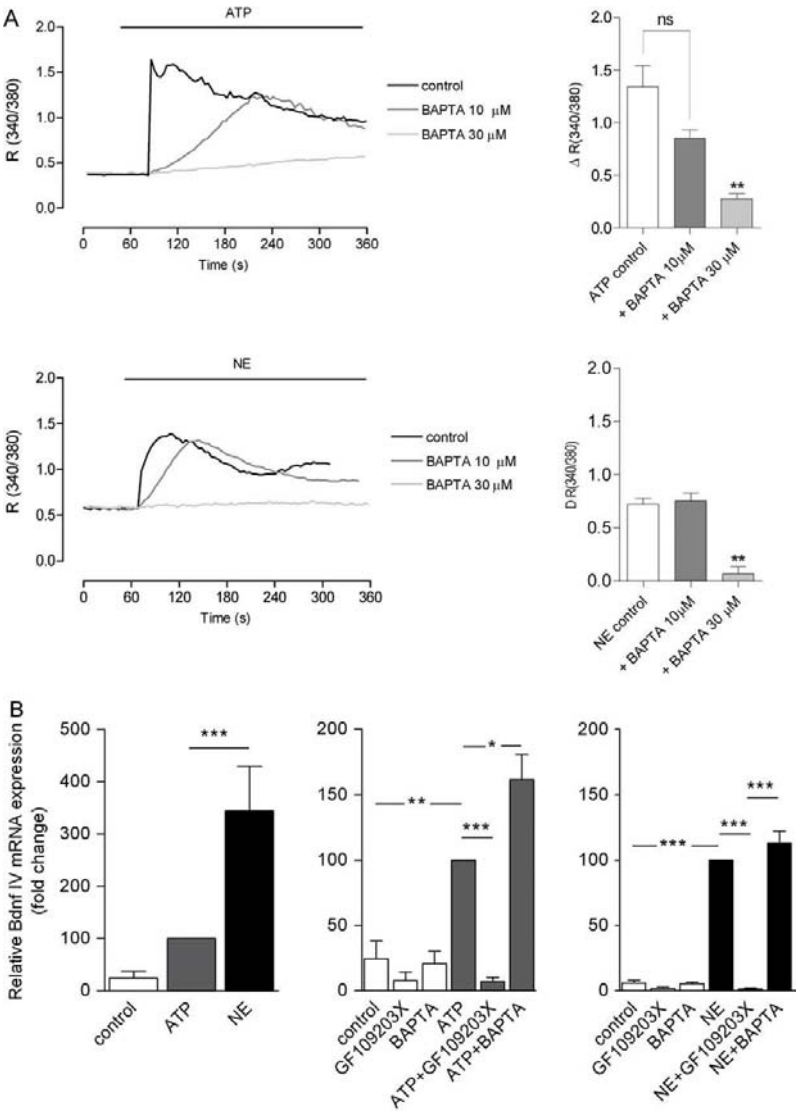

Fig. 4. CREB-dependent transcription is independent of calcium. (A) Effect of 10 and 30 µM BAPTA on Ca^{2+} transients induced by ATP or NE. Left panel, representative traces; right panel, quantitation of intracellular Ca^{2+} increases. The data are the means +/- SEM of three independent determinations. In each experiment, 20 cells were analyzed. (B) Expression of BDNF IV mRNA measured by RT-PCR. The graph to the left shows a comparison between NE and ATP, while the graphs to the right show the effects of 30 µM BAPTA and 25 µM GF109203X on the upregulation of bdnf by ATP or NE. Data are the means +/- SEM of n = 3 independent determinations in independent cultures. In all experiments, astrocytes were incubated with 100 µM ATP or 10 µM NE. BAPTA-AM or the PKC inhibitor were added 30 min before the transmitters. (*) $P < 0.05$, (**) $P < 0.05$, (***) $P < 0.001$, one-way ANOVA followed by the Newman–Keuls test. When used at 30 µM, BAPTA completely obliterated the increase in intracellular calcium but had no effect

CREB-Dependent Transcription Depended on the Phosphorylation of CREB and ERK

The role of CREB phosphorylation on ATP and NE-elicited CREB-dependent transcription was examined by determining: (1) whether NE and ATP caused CREB phosphorylation, analyzed by Western blots; and (2) the effect on CRE-assays of m133-CREB, which prevents CREB phosphorylation.

Both ATP and NE induced the transient phosphorylation of CREB (Fig. 5A). The effect of ATP was statistically significant within 2.5–15 min, peaked at 5 min and returned to basal values at 20 min. The phosphorylation induced by NE was more delayed but sustained overtime. Thus, it was maximal within 5 min and lasted up to 30 min, returning to basal values at 60 min.

The transfection of m133-CREB completely inhibited CREB-dependent transcription as assessed in luciferase assays (Fig. 5B). Taken together, these data indicate that CREB phosphorylation was essential for CREB-dependent transcription to occur. Because ERK 1/2 often acts as mediators of PKC (Ueda et al., 1996) we examined: (1) whether NE and ATP induced ERK phosphorylation by Western blots, and (2) if the ERK inhibitor U0126 inhibited CREB-dependent transcription. U0126 inhibits ERK1/2 by inhibiting the kinase activity of MEK1/2, which is upstream ERK1/2. We found that both ATP and NE phosphorylated ERK (Fig. 5A) transiently. The phosphorylation caused by ATP was only significantly different than nonstimulated controls at 2.5–5 min. The phosphorylation caused by NE was more robust and sustained, spanning 5–15 min. U0126 (10 μM) inhibited CREB-dependent transcription by 50% (Fig. 5C). Overall, the data indicated that ERK1/2 contributed partially to the ATP and NE-elicited CREB activation. Recapitulating, our results thus far indicated that two factors, PKC and pCREB, were essential for the activation of CREB-dependent transcription, suggesting that PKC accounted directly or indirectly for CREB phosphorylation. We put this idea to the test by examining the effect of GF109203X on pCREB. We found that the PKC

inhibitor completely abrogated the phosphorylation of CREB caused by NE and ATP (Fig. 6A). Thus, PKC appeared to be upstream CREB.

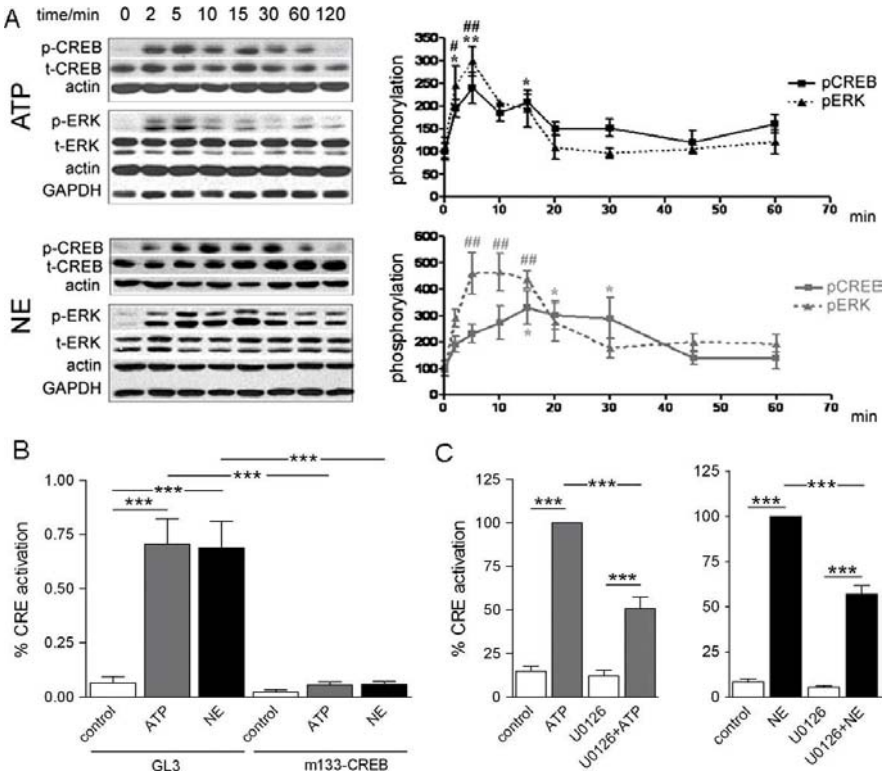

Fig. 5. CREB-dependent transcription depended on the phosphorylation of ERK and CREB. (A) Western blot analyses of ERK and CREB phosphorylation overtime; (B) Effect of m133-CREB on CREB activation measured by luciferase assays; (C) Effect of the ERK inhibitor U0126 (10 μM) on CREB-dependent transcription measured by luciferase assays. Astrocytes were incubated with 100 μM ATP or 10 μM NE, and processed after 6 h for luciferase assays (C, D), or 5–60 min for Western blots (A). plasmids GL3 (control) and m133-CREB were transfected as described in Methods. The control for U0126 was DMSO. In A, data are the means +/- SEM of n = 3–5 independent determinations in independent cultures; (*) P < 0.05, (**) P < 0.01 for pCREB, and (#) P < 0.05, (##) P < 0.01 for pERK respect to time 0 (nontreated cells). In B, C data are the means +/- SEM of n 5 3–5 independent determinations in independent cultures, (***) P < 0.001. In all cases data were analyzed by one-way ANOVA followed by Newman–Keuls test.

We next asked if ERK1/2 contributed to the PKC-mediated phosphorylation of CREB. We reasoned that, if this were the case, PKC should be upstream ERK1/2, and ERK1/2 upstream CREB; that is, GF109203X should diminish ERK1/2 phosphorylation, and U0126 diminish CREB phosphorylation. Indeed, the PKC inhibitor completely abolished the increase in pERK1/2 caused by the transmitters (Fig. 6C), thus confirming that atypical PKC regulated ERK1/2. U0126, as expected,

inhibited ERK1/2 phosphorylation completely (Fig. 6D). However, U0126 did not inhibit CREB phosphorylation when the inducer was NE, and inhibited it partially when the inducer was ATP (Fig. 6B). This indicated that, particularly for NE, ERK1/2 had to activate CREB-dependent transcription by a mechanism independent of CREB phosphorylation. For the sake of clarity a schematic is provided in Fig. 9.

CREB-Dependent Transcription Partially depended on CRTCs

CRTCs have not been described in astrocytes before. We detected CRTC1 and CRTC2 in the cortical astrocytes by nonquantitative PCR (Fig. 7A). We sought to establish their role by assessing: (1) the effect of DNCRTC1 and DNCRTC2, previously shown to block CRTC function (Kovacs et al., 2007), on luciferase reported CREB activation, and (2) whether ATP and NE caused the activation of the cofactors, which we examined by Western blots and immunocytochemistry. The blockade of CRTC1 or 2 with the respective DN constructs caused the partial inhibition of CREB-dependent transcription for both transmitters (Fig. 7B). However, CREB activation was not affected by cyclosporine A (CsA, Fig. 7B), an inhibitor of the phosphatase PP2B/calcineurin, which is the best characterized stimulator of CRTC. Because calcineurin is Ca^{2+}-dependent, the data provided further support to the conclusion that there is no role for Ca^{2+} in CREB-dependent transcription in astrocytes. The Western blot analyses showed that, upon NE and ATP administration, CRTC1 decreased in the cytosol but increased in the nuclear fraction (Fig. 7C), indicating that the transmitters had caused the translocation of the factor to the nucleus. This was confirmed by immunocytochemistry (Fig. 7D). In control cells, CRTC1 and 2 appeared distributed all over the cells, while the administration of ATP and NE caused the stark concentration of the transcription factors in the nuclei (Fig. 7D, photographs). The quantification of nuclei positive for CRTC1 or CRTC2 indicated that the migration to the nuclei happened between 30 min to 2 h, and that the activation was more pronounced for NE than for ATP (Fig. 7D, graphs).

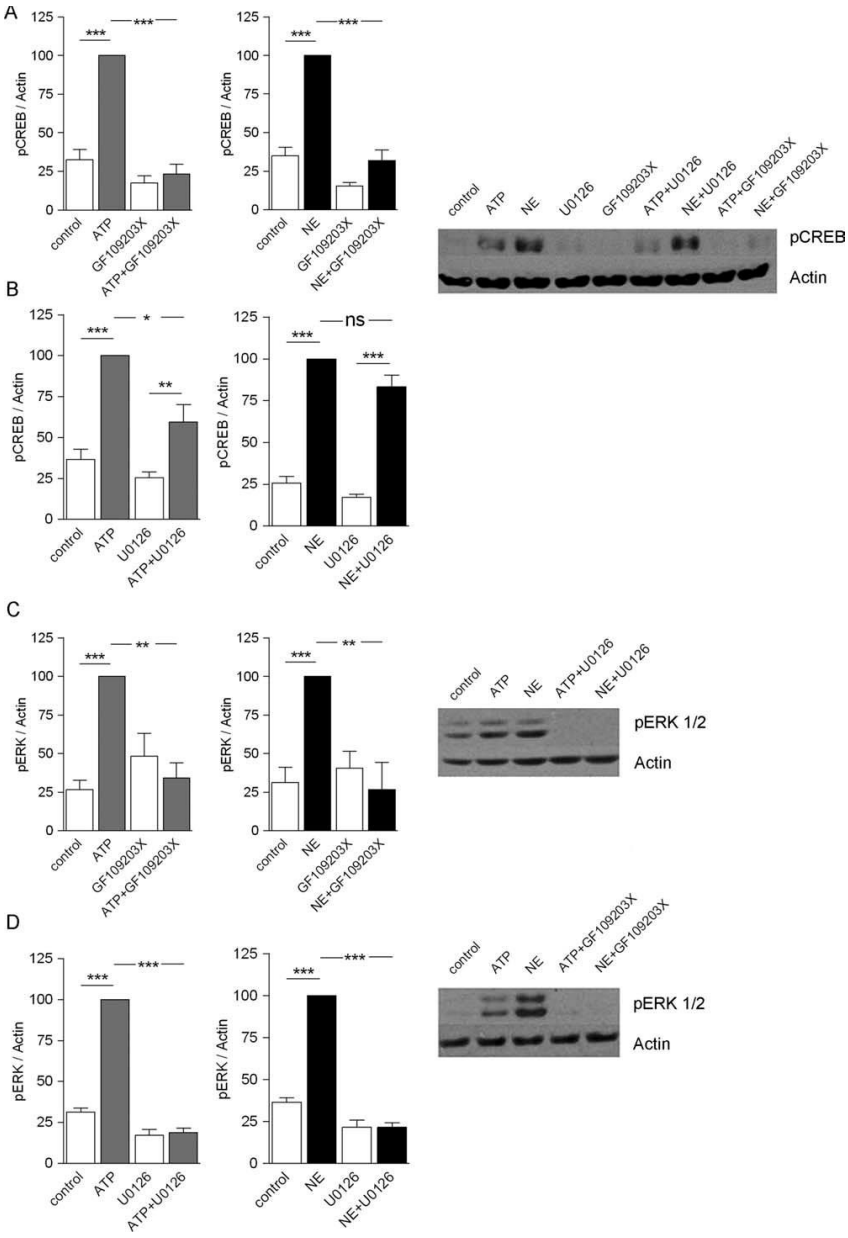

Fig. 6. Atypical PKC was upstream ERK and CREB phosphorylation. (A, C) Effect of the PKC inhibitor GF109203X on pCREB (A) and pERK (C) contents; (B, D) Effect of the ERK inhibitor U0126 on pCREB (B), and pERK (D) contents. Astrocytes were incubated with 100 μM ATP or 10 μM NE, and processed after 5 min for Western blots analyses of pERK and pCREB. PKC or ERK inhibitors (25 μM GF109203X and 10 μM U0126) were added 30 min before the transmitters. Values are the means +/- SEM of n = 3–5 independent determinations in independent cultures. (*) $P < 0.05$, (**) $P < 0.01$, (***) $P < 0.001$, one-way ANOVA followed by the Newman–Keuls test. GF109203X completely abolished the phosphorylation of ERK and CREB, while ERK partially abolished the ATP-elicited CREB phosphorylation but had no effect on the NE-elicited one.

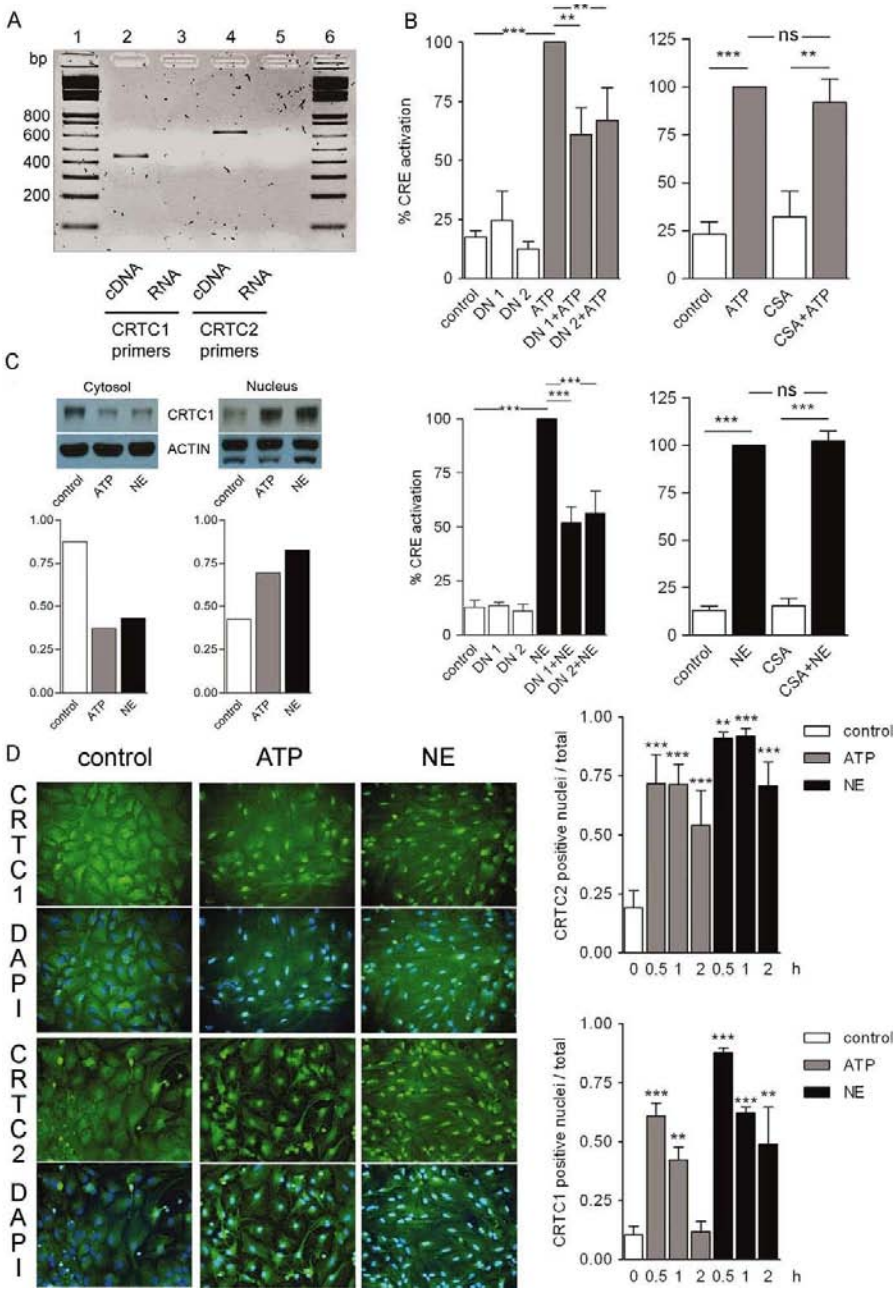

Fig. 7. CRTC1 and 2 partially contributed to CREB-dependent transcription. (A) Detection of CRTC1/2 in astrocytes by PCR; (B) DNCRTC1 and DNCRTC2 partially blocked CREB activation in luciferase assays, but cyclosporine A (CsA) had no effect; (C) Western blots of CRTC1 and densitometries showing that ATP and NE promoted the translocation of the factor from the cytosol to the nucleus; representative of n = 3 independent determinations; (D) Immunocytochemical analysis showing that ATP and NE promoted the translocation of CRTC to

the nuclei. Images are representative, the counts of CRTC1or CRTC2-positive nuclei being shown to the right. Astrocytes were incubated with 100 μM ATP or 10 μM NE, and processed after 6 h for luciferase assays (B), 15 min for Western blots of CRTC1 in cytosol or nuclei, or after 0.5–2 h for immunocytochemical detection of CRTC1 and CRTC2. Values are the means of 5 (B) or 3 (D) independent determinations; (**) $P < 0.01$, (***) $P < 0.001$, one-way ANOVA followed by the Newman–Keuls test.

We next asked whether a PKC/ERK axis regulated CRTC because: (i) PKC was the step detected at the uppermost position of the signaling pathways leading to CREB-dependent transcription; therefore, PKC should be upstream CRTC, too; (ii) ERK activation was completely dependent on PKC; and (iii) according to data reported in Fig. 6, a pathway linking ERK and CREB-dependent transcription appeared to exist, independent of pCREB, particularly for NE. We thus tested the effect of the PKC and ERK inhibitors on CRTC1 activation by NE, as measured by the decrease in the cytosol contents of the cofactor in Western blots (Fig. 8). The most prominent change caused by GF109203X or U0196 was the appearance of a CRTC1 band of a faster electrophoretic mobility, both when the inhibitors were administered alone or with NE (Fig.8, top gels). Because the presence of a phosphate group retards the electrophoretic mobility, we speculate that the different mobility of CRTC forms may be due to different phosphorylation states, the faster band corresponding to nonphosphorylated CRTC and the top band to a phosphorylated one. When considering total CRTC1 (that is, the slow and the fast bands together) we observed that GF109203X and U0196 partially reversed the decrease of CRTC caused by NE (Fig. 8A), thus confirming that PKC/ERK mediated the activation of CRTC by NE. The measurement of fast-to-slow CRTC ratios revealed relative increases of the allegedly nonphosphorylated CRTC in the presence of the PKC and ERK1/2 inhibitors (Fig. 8B). This, in turn, suggests that the NE-elicited activation of CRTC may involve the phosphorylation of the cofactor via PKC/ERK.

DISCUSSION

CREB is essential for the long-term changes in gene expression that mediate neuronal plasticity and memory processing. Here, we have described a novel mechanism of CREB activation by transmitters leading to CREB-dependent transcription in astrocytes (see Fig. 9). The new mechanism is activated by both NE and ATP, involves an atypical PKC independent of Ca^{2+} or cAMP, and leads to the expression of *Bdnf*, a type of immediate early gene (IEG) that causes functional and structural remodeling of the synapses. By contrast,

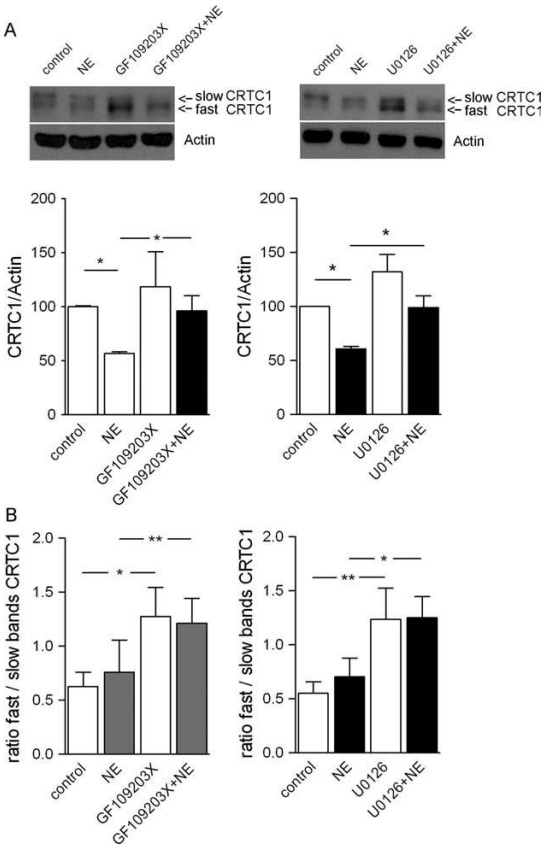

Fig. 8. PKC/ERK are upstream CRTC1. Effect of U0126 and GF109203X on CRTC1 activation by NE presented as the total CRTC1 (A) or the ratio between fast and slow CRTC1 bands (B) measured in cytosols by Western blots. Astrocytes were incubated with 10 µM NE and processed 15 min thereafter. GF109203X (25 µM) or U0126 (10 µM) were added 30 min before the transmitters. The blots on top show that both kinase inhibitors induced the appearance of a CRTC1 of increased electrophoretic mobility, perhaps representing non phosphorylated CRTC1. Data are the means +/- SEM of n = 5 independent determinations in independent cultures. (*) $P < 0.05$, (**) $P < 0.01$, ANOVA followed by the Newman–Keuls test.

glutamate, one of the principal transmitters acting both at neurons and astrocytes, failed to activate CREB-dependent transcription significantly. The fast removal of glutamate by astrocytic transporters may undermine actions of the transmitter on its receptors. Whatever the reason, our data highlights the important notion that the regulation of CREB-dependent transcription in astrocytes may be transmitter-specific. Below we elaborate

further on the three major differences between CREB activation in neurons and astrocytes concerning PKC, CRTC, and Ca^{2+}.

PKC isoforms, whether classical, novel, or atypical, consist of a N-terminal regulatory domain and a C-terminal catalytic domain tethered by a hinge (Sampson et al., 2006). The regulatory domain contains binding sites for second messengers and an auto-inhibitory pseudosubstrate sequence, which blocks the active site of the catalytic domain. Second messengers stimulate PKCs by inducing a conformational change that releases the autoinhibition. Here we report that an atypical PKC accounts for the NE and ATP-elicited CREB activation in astrocytes, as supported by: (i) the lack of effect of Ca^{2+} and diacylglycerol, and (ii) the inhibitory effect of GF109203X only at the highest dose; and (iii) the lack of effect of Go6976, specific inhibitor of classical PKCs. In agreement, glutamate, previously shown to stimulate diacylglycerol-dependent PKCs (a, b, d, e) in astrocytes (Servitja et al., 2003), do not appear involved in CREB activation.

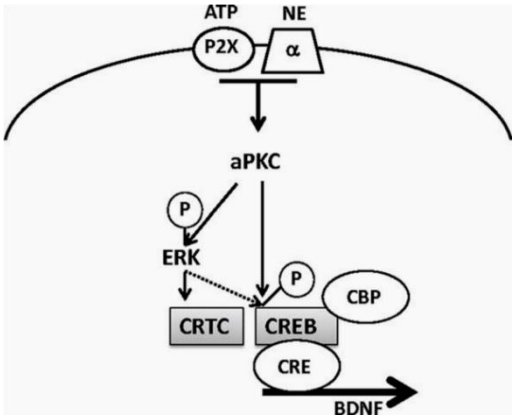

Fig. 9. Schematic representation of the signaling pathways leading to the CREB-dependent transcription induced by ATP and NE in astrocytes. Both transmitters would activate CREB via an atypical Ca^{2+} independent PKC (aPKC), which in turn would activate CREB by inducing, on the one hand, CREB phosphorylation and, on the other hand, CRTC activation via ERK. Pathways elicited by NE and ATP would be similar except that ERK would partially contribute to the phosphorylation of CREB by ATP (dashed line).

Ceramide (Muller et al., 1995), protein/protein interactions (Moscat et al., 2009), nitroalkene derivatives (Guo et al., 2011), or the phosphorylation state of PKC (Mayanglambam et al., 2011) have been reported to regulate atypical PKCs. The identity of the atypical PKC and its mechanism of activation upon P2X and α-adrenergic receptor stimulation remain to be determined.

Although the key role of an atypical PKC in CREB activation detected in astrocytes has no parallel in neurons, coincidentally, PKM, a type of PKCζ lacking the regulatory domain and therefore constitutively active, is necessary for the maintenance of late-phase LTP and long-term spatial and associative memories (Sacktor et al., 1993). It is unlikely that the regulatory function ascribed to PKC in the present study be due to PKM because: (i) PKM acts by reconfiguring postsynaptic AMPAR trafficking, this effect being independent of CREB (Sacktor, 2011), (ii) the PKC inhibitor GF109203X acts by interfering with the ATP binding to the regulatory domain that is missing from PKM, and (iii) the PKM inhibitor ZIP (Pastalkova et al., 2006) had no effect on our CREB transcriptional assays.

The family of cofactors CRTCs is involved in diverse physiological processes including energy homeostasis, cancer, endoplasmic reticulum stress, and LTP (Altarejos et al., 2011; Kovacs et al., 2007; Zhou et al., 2006). In cultured neurons, CRTC1 is essential for the activation of CREB-dependent transcription, to the extent that this does not proceed despite a robust CREB phosphorylation in serine 133 when the cofactor is inhibited (Kovacs et al., 2007). Importantly, the neuronal CRTC requires co-stimulation by Ca^{2+}- and cAMP-dependent signaling—the former triggered by NMDA-dependent depolarization and the latter initiated by catecholamines or growth factors. CRTC is activated in this scenario by dephosphorylation as a result of the inhibition of the kinase SIK via cAMP/PKA, and the activation of the phosphatase calcineurin via Ca^{2+}/CaM. By contrast, CREB phosphorylation in astrocytes appears necessary and sufficient for CREB-dependent transcription induced by ATP and NE, whereas CRTC rather plays a modulatory role, its activation neither depending on calcineurin nor requiring dual stimulation.

Our data supports that PKC stimulates CRTC by changing its phosphorylation state via ERK, as suggested by the enhanced electrophoretic mobility of CRTC—indicative of loss of a phosphate group—in the presence of the ERK or PKC inhibitors. Importantly, precedents exist of CRTC activation independent of the canonical calcineurin-elicited dephosphorylation, for example via a direct

phosphorylation by MEKK1 (Siu et al., 2008). Note that both ERK and CRTC contribute only partially to CREB-dependent transcription, as documented in CREB transcriptional assays, further suggesting a link between the kinase and the cofactor.

We conclude that Ca^{2+} did not mediate the ATP and NE-elicited CREB activation because: (i) the master regulator, PKC, is a Ca^{2+} independent isoform; (ii) the calcium chelator BAPTA had no effect on the upregulation of *Bdnf* mRNA; and (iii) CRTC activation was independent of Ca^{2+}/calcineurin. We did observe that the quenching of intracellular Ca^{2+} with BAPTA potentiated the upregulation of *Bdnf* by ATP. This observation suggests the existence of a yet to be characterized Ca^{2+}-mediated negative feedback acting on the signaling pathway triggered by ATP that leads to *Bdnf* upregulation. Our results are in any event at variance with a previous study showing complete inhibition by BAPTA of the ATP-elicited upregulation of *Bdnf* mRNA in an astrocytoma cell line (Takasaki et al., 2008). The study also reports no role for ERK and a partial role for CaMK, according to results with pharmacological inhibitors. The differences with our study might be attributed to the use of different astrocyte models. Our study also differs from another study describing no activation of CREB-dependent trascription by ATP (1–100 μM) in mouse primary cultures (Murray et al., 2009). According to the authors, the absence of CaMKIV linking Ca^{2+} to CREB as in neurons accounts for the failure. Perhaps the disagreement in this case can be attributed to a species difference (rat vs. mouse).

Little knowledge exists about the role of astrocytes in learning, memory, and cognition. Astrocytes are anatomically and functionally part of the synapse (Araque, 1999; Witche et al., 2007), and LTP modifies the topographic relations between neurons and glia (Wenzel et al., 1991). Indeed, astrocytes appear indispensable for the maintenance of LTP (Henneberger et al., 2010; Suzuki et al., 2011). By what mechanisms may astrocytes control neurotransmission?: (1) by changes in expression of the EphA4/ephrin-A3 system, which controls the distance between astrocyte processes and neurons (Filosa et al., 2009); (2) by taking up glutamate via specific transporters thereby controlling the time that the transmitter lingers in the

synaptic cleft; (3) by releasing neurotransmitters including glutamate itself (Perea et al., 2007), D-serine (Henneberger et al., 2010), or lactate (Suzuki et al., 2011); and (4) by responding to transmitters. A matching set of transmitter receptors exist in both astrocytes and neurons (Koles et al., 2011), revealing the close communication existing between the two cell types. Note that throughout the text we use the term transmitter instead of glio- or neuro-transmitter to reflect the dual cellular origin of molecules embodying cell-to-cell transmission in the brain.

Given their key stance at the synapse, astrocytes may not only control synaptic activity but be shaped by it. We thus reason that experience-triggered, activity-dependent, CREB-driven gene transcription may occur in astrocytes. In this study we have shown that two transmitters can activate CREB-dependent transcription in cortical astrocytes. Future research ought to address the following outstanding questions ranging from the molecular underpinnings to behavioral repercussions of astrocyte-based plasticity. First, in addition to *Bdnf* the complete profiling is necessary of CREB-activated genes in astrocytes. Attention should be focused, for example, on genes regulating glutamate uptake or release and Ca^{2+} transients, for the fact that CREB activation does not require Ca^{2+} does not preclude that, conversely, Ca^{2+} responses are regulated by CREB-dependent genes. Second, what is the effect of these genes on synaptic strength? Third, do astrocytes and neurons hold specialized functions in types, or stages, of memory formation? As noted, CREB requires in neurons co-activation by depolarization-induced Ca^{2+} signaling and cAMP-linked signaling. It has been argued that the detection of coincident signals is the basis for storing associative memories (Kovacs et al., 2007). By contrast, CREB in astrocytes does not appear to be a convergence point of signals acting synergistically when activated by NE and ATP. Rather, the CREB-activating cascade features divergence of signals from the master regulator PKC. Molecular divergence is a biological strategy to amplify signals. Whether in memory formation this process may be necessary, remains to be clarified. Overall, the upcoming development of cellular and animal models where manipulation

of CREB activity be specifically targeted to astrocytes, presumably by transgenic or viral approaches, will facilitate progress toward the clarification of these questions.

ACKNOWLEDGMENTS

The authors express their gratitude to J.M. Naranjo (Centro Nacional de Biotecnologıa, Madrid, Spain) for providing m133-CREB, to Cristina Gutierrez for expert assistance with astrocyte cultures, to J.R. Cardinaux (Brain and Mind Institute, Lausanne, Switzerland) for providing DN-CRTC1 and DN-CRTC2. Support for this study was provided by grants BFU2010-21281/BFI and BFU2007-63031/BFI from the Ministry of Education and Science (Spain) to EG.

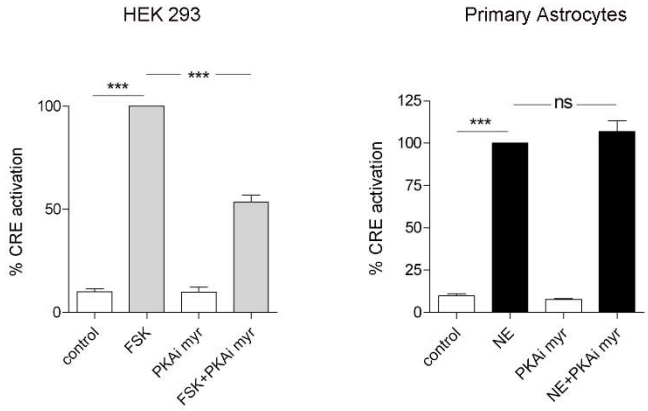

Supporting Information Figure 1. Validation of the PKA inhibitor myr-PKA. The drug was tested simultaneously on CREB-dependent transcription, measured by luciferase assays, in HEK293 cells and astrocytes, respectively stimulated with 5 µM forskolin or 10 µM NE. The myr-PKA peptide (1 µM) was added 30 min before the activators. Data are the means ± SD of n=4 determinations,

representative of n=2 independent cultures; (***) p<0.001, (ns) non-significant, one-way ANOVA followed by the Newman-Keuls test

REFERENCES

Abraham WC, Williams JM. 2003. Properties and mechanisms of LTP maintenance. Neuroscientist 9:463–474.

Agullo L, Garcia A, Hidalgo J. 1998. Metallothionein-I1II induction by zinc and copper in primary cultures of rat microglia. Neurochem Int 33:237–242.

Altarejos JY, Montminy M. 2011. CREB and the CRTC coactivators: Sensors for hormonal and metabolic signals. Nat Rev Mol Cell Biol 12:141–151.

Araque A, Sanzgiri RP, Parpura V, Haydon PG. 1999. Astrocyte-induced modulation of synaptic transmission. Can J Physiol Pharmacol 77:699–706.

Barcelo-Torns M, Lewis AM, Gubern A, Barneda D, Bloor-Young D, Picatoste F, Churchill GC, Claro E, Masgrau R. 2011. NAADP mediates ATP-induced Ca2+ signals in astrocytes. FEBS Lett 585:2300–2306.

Barco A, Patterson SL, Alarcon JM, Gromova P, Mata-Roig M, Morozov A, Kandel ER. 2005. Gene expression profiling of facilitated L-LTP in VP16-CREB mice reveals that BDNF is critical for the maintenance of LTP and its synaptic capture. Neuron 48:123–137.

Benito E, Barco A. 2010. CREB's control of intrinsic and synaptic plasticity: Implications for CREB-dependent memory models. Trends Neurosci 33:230–240.

Bourtchuladze R, Frenguelli B, Blendy J, Cioffi D, Schutz G, Silva AJ. 1994. Deficient long-term memory in mice with a targeted mutation of the camp-responsive element-binding protein. Cell 79:59–68.

Caruso C, Carniglia L, Durand D, Gonzalez PV, Scimonelli TN, Lasaga M. 2012. Melanocortin 4 receptor activation induces brain-derived neurotrophic factor expression in rat astrocytes through cyclic. Mol Cell Endocrinol 348:47–54.

Conkright MD, Canettieri G, Screaton R, Guzman E, Miraglia L, Hogenesch JB, Montminy M. 2003. Torcs: Transducers of regulated CREB activity. Mol Cell 12:413–423.

Cunha RA, Sebastiao AM, Ribeiro JA. 1992. Ecto-5^0-nucleotidase is associated with cholinergic nerve terminals in the hippocampus but not in the cerebral cortex of the rat. J Neurochem 59:657–666.

Espana J, Valero J, Minano-Molina AJ, Masgrau R, Martin E, GuardiaLaguarta C, Lleo A, Gimenez-Llort L, Rodriguez-Alvarez J, Saura CA. 2010. Beta-amyloid disrupts activity-

dependent gene transcription required for memory through the CREB coactivator CRTC1. J Neurosci 30:9402–9410.

Filosa A, Paixao S, Honsek SD, Carmona MA, Becker L, Feddersen B, Gaitanos L, Rudhard Y, Schoepfer R, Klopstock T, Kullander K, Rose CR, Pasquale EB, Klein R. 2009. Neuron-glia communication via Epha4/Ephrin-A3 modulates LTP through glial glutamate transport. Nat Neurosci 12:1285–1292.

Franco R, Canela EI, Bozal J. 1986. Heterogeneous localization of some purine enzymes in subcellular fractions of rat brain and cerebellum. Neurochem Res 11:423–435.

Guo CJ, Schopfer FJ, Gonzales L, Wang P, Freeman BA, Gow AJ. 2011. Atypical Pkczeta transduces electrophilic fatty acid signaling in pulmonary epithelial cells. Nitric Oxide 25:366–372.

Guzowski JF, Mcgaugh JL. 1997. Antisense oligodeoxynucleotide-mediated disruption of hippocampal camp response element binding protein levels impairs consolidation of memory for water maze training. Proc Natl Acad Sci USA 94:2693–2698.

Han JH, Kushner SA, Yiu AP, Hsiang HL, Buch T, Waisman A, Bontempi B, Neve RL, Frankland PW, Josselyn SA. 2009. Selective erasure of a fear memory. Science 323:1492–1496.

Henneberger C, Papouin T, Oliet SH, Rusakov DA. 2010. Long-term potentiation depends on release of D-serine from astrocytes. Nature 463:232–236.

Hirota K, Matsui M, Murata M, Takashima Y, Cheng FS, Itoh T, Fukuda K, Junji Y. 2000. Nucleoredoxin, glutaredoxin, and thioredoxin differentially regulate NF-Kb, AP-1, and CREB activation in HEK293 cells. Biochem Biophys Res Commun 274:177–182.

Impey S, Mccorkle SR, Cha-Molstad H, Dwyer JM, Yochum GS, Boss JM, Mcweeney S, Dunn JJ, Mandel G, Goodman RH. 2004. Defining the CREB regulon: A genome-wide analysis of transcription factor regulatory regions. Cell 119:1041–1054.

Katoh Y, Takemori H, Lin Xz, Tamura M, Muraoka M, Satoh T, Tsuchiya Y, Min L, Doi J, Miyauchi A, Witters LA, Nakamura H, Okamoto M. 2006. Silencing the constitutive active transcription factor CREB by the LKB1-SIK signaling cascade. FEBS J 273:2730–2748.

Kida S, Josselyn SA, Pena De OS, Kogan JH, Chevere I, Masushige S, Silva AJ. 2002. CREB required for the stability of new and reactivated fear memories. Nat Neurosci 5:348–355.

Kogan JH, Frankland PW, Blendy JA, Coblentz J, Marowitz Z, Schutz G, Silva AJ. 1997. Spaced training induces normal long-term memory in CREB mutant mice. Curr Biol 7:1–11.

Koles L, Leichsenring A, Rubini P, Illes P. 2011. P2 receptor signaling in neurons and glial cells of the central nervous system. Adv Pharmacol 61:441–493.

Komiya T, Coxon A, Park Y, Chen WD, Zajac-Kaye M, Meltzer P, Karpova T, Kaye FJ. 2010. Enhanced activity of the CREB co-activator Crtc1 in LKB1 null lung cancer. Oncogene 29:1672–1680.

Kovacs KA, Steullet P, Steinmann M, Do KQ, Magistretti PJ, Halfon O, Cardinaux JR. 2007. TORC1 is a calcium- and camp-sensitive coincidence detector involved in hippocampal long-term synaptic plasticity. Proc Natl Acad Sci USA 104:4700–4705.

Leil TA, Ossadtchi A, Cortes JS, Leahy RM, Smith DJ. 2002. Finding new candidate genes for learning and memory. J Neurosci Res 68:127–137.

Li S, Zhang C, Takemori H, Zhou Y, Xiong ZQ. 2009. TORC1 regulates activity-dependent CREB-target gene transcription and dendritic growth of developing cortical neurons. J Neurosci 29:2334–2343.

Mayanglambam A, Bhavanasi D, Vijayan KV, Kunapuli SP. 2011. Differential dephosphorylation of the protein kinase C-Zeta (Pkczeta) in an integrin alphaiibbeta3-dependent manner in platelets. Biochem Pharmacol 82:505–513.

Moscat J, Az-Meco MT, Wooten MW. 2009. Of the atypical Pkcs, Par-4 And P62: Recent understandings of the biology and pathology of a PB1-dominated complex. Cell Death Differ 16:1426–1437.

Muller G, Ayoub M, Storz P, Rennecke J, Fabbro D, Pfizenmaier K. 1995. PKC Zeta is a molecular switch in signal transduction of TNFalpha, bifunctionally regulated by ceramide and arachidonic acid. EMBO J 14:1961–1969.

Murray AJ, Shewan DA. 2008. Epac mediates cyclic AMP-dependent axon growth, guidance and regeneration. Mol Cell Neurosci 38: 578–588.

Murray PD, Kingsbury TJ, Krueger BK. 2009. Failure of Ca2+-activated, CREB-dependent transcription in astrocytes. Glia 57:828–834.

Nguyen TV, Yao M, Pike CJ. 2009. Dihydrotestosterone activates CREB signaling in cultured hippocampal neurons. Brain Res 1298:1–12.

Park CS, Gong R, Stuart J, Tang SJ. 2006. Molecular network and chromosomal clustering of genes involved in synaptic plasticity in the hippocampus. J Biol Chem 281:30195–30211.

Pastalkova E, Serrano P, Pinkhasova D, Wallace E, Fenton AA, Sacktor TC. 2006. Storage of spatial information by the maintenance mechanism of LTP. Science 313:1141–1144.

Perea G, Araque A. 2007. Astrocytes potentiate transmitter release at single hippocampal synapses. Science 317:1083–1086.

Pittenger C, Huang YY, Paletzki RF, Bourtchouladze R, Scanlin H, Vronskaya S, Kandel ER. 2002. Reversible inhibition of CREB/ATF transcription factors in region CA1 of the dorsal hippocampus disrupts hippocampus-dependent spatial memory. Neuron 34:447–462.

Roberson ED, English JD, Adams JP, Selcher JC, Kondratick C, Sweatt JD. 1999. The mitogen-activated protein kinase cascade couples PKA and PKC to camp response element binding protein phosphorylation in area CA1 of hippocampus. J Neurosci 19:4337–4348.

Ryan BK, Vollmayr B, Klyubin I, Gass P, Rowan MJ. 2010. Persistent inhibition of hippocampal long-term potentiation in vivo by learned helplessness stress. Hippocampus 20:758–767.

Sacktor TC. 2011. How does Pkmzeta maintain long-term memory? Nat Rev Neurosci 12:9–15.

Sacktor TC, Osten P, Valsamis H, Jiang X, Naik MU, Sublette E. 1993. Persistent activation of the zeta isoform of protein kinase C in the maintenance of long-term potentiation. Proc Natl Acad Sci USA 90:8342–8346.

Sakamoto K, Karelina K, Obrietan K. 2011. CREB: A multifaceted regulator of neuronal plasticity and protection. J Neurochem 116:1–9.

Sampson SR, Cooper DR. 2006. Specific protein kinase C isoforms as transducers and modulators of insulin signaling. Mol Genet Metab 89:32–47.

Screaton RA, Conkright MD, Katoh Y, Best JL, Canettieri G, Jeffries S, Guzman E, Niessen S, Yates JR III, Takemori H, Okamoto M, Montminy M. 2004. The CREB coactivator TORC2 functions as a calciumand camp-sensitive coincidence detector. Cell 119:61–74.

Siu YT, Ching YP, Jin DY. 2008. Activation of TORC1 transcriptional coactivator through MEKK1-induced phosphorylation. Mol Biol Cell 19:4750–4761.

Servitja JM, Masgrau R, Pardo R, Sarri E, Von Eichel-Streiber C, Gutkind JS, Picatoste F. 2003. Metabotropic glutamate receptors activate phospholipase D in astrocytes through a protein kinase C-dependent and Rho-independent pathway. Neuropharmacology 44:171–180.

Socodato R, Brito R, Calaza KC, Paes-De-Carvalho R. 2011. Developmental regulation of neuronal survival by adenosine in the in vitro and in vivo avian retina depends on a shift of signaling pathways leading to CREB phosphorylation or dephosphorylation. J Neurochem 116:227–239.

Suzuki A, Stern SA, Bozdagi O, Huntley GW, Walker RH, Magistretti PJ, Alberini CM. 2011. Astrocyte-neuron lactate transport is required for long-term memory formation. Cell 144:810–823.

Takasaki I, Takarada S, Tatsumi S, Azegami A, Yasuda M, Fukuchi M, Tabuchi A, Kondo T, Tabuchi Y, Tsuda M. 2008. Extracellular adenosine 5'-triphosphate elicits the expression of brain-derived neurotrophic factor exon IV mRNA in rat astrocytes. Glia 56:1369–1379.

Tao X, Finkbeiner S, Arnold DB, Shaywitz AJ, Greenberg ME. 1998. Ca2+ influx regulates BDNF transcription by a CREB family transcription factor-dependent mechanism. Neuron 20:709–726.

Ueda Y, Hirai S, Osada S, Suzuki A, Mizuno K, Ohno S. 1996. Protein kinase C activates the MEK-ERK pathway in a manner independent of Ras and dependent on Raf. J Biol Chem 271:23512–23519.

Wenzel J, Lammert G, Meyer U, Krug M. 1991. The influence of longterm potentiation on the spatial relationship between astrocyte processes and potentiated synapses in the dentate gyrus neuropil of rat brain. Brain Res 560:122–131.

Witcher MR, Kirov SA, Harris KM. 2007. Plasticity of perisynaptic astroglia during synaptogenesis in the mature rat hippocampus. Glia 55:13–23.

Zhang W, Linden DJ. 2003. The other side of the Engram: Experiencedriven changes in neuronal intrinsic excitability. Nat Rev Neurosci 4:885–900.

Zhou Y, Wu H, Li S, Chen Q, Cheng XW, Zheng J, Takemori H, Xiong ZQ. 2006. Requirement of TORC1 for late-phase long-term potentiation in the hippocampus. Plos One 1:E16

Results II

Genome-wide characterization of CREB-dependent transcriptional programs in astrocytes

In preparation

Genome-wide characterization of CREB-dependent transcriptional programs in astrocytes.

Luis Pardo[1], Luis Miguel Valor[2], Abel Eraso[1], Roser Masgrau[1], Elena Galea[1, 3]

1. Institut de Neurociències and Unitat de Bioquímica, Facultat de Medicina, Universitat Autònoma de Barcelona, Bellaterra, 08193 Barcelona, Spain. 2 Instituto de Neurociencias de Alicante, Universidad Miguel Hernández/Consejo Superior de Investigaciones Científicas, Sant Joan d'Alacant, 03550 Alicante, Spain. 3 Institució Catalana de Recerca i Estudis Avançats (ICREA), Barcelona, Spain

Abstract:

CREB is a transcription factor that integrates a wide variety of stimuli and promotes transcriptional programs underlying many physiological processes, such as synaptic plasticity or cell survival. To date, most of the studies that associate CREB-dependent genes with these processes have been performed in neurons, despite the fact that astrocytes are also key players in several CREB putative functions. In this study, we intended to gain insight into the transcriptional programs promoted in astrocytes upon activation of CREB-dependent transcription through different stimuli. To this end, we treated primary astrocytic cultures with the adenylate cyclase activator forskolin (FSK), the gliotransmitter norepinephrine (NE) and expressing the constitutively active form of CREB, VP16-CREB. Afterwards, we performed a transcriptome analysis and studied the profiles of distinct CREB activation by functional enrichment of differentially expressed genes in Gene Ontology (GO) terms. In addition, we took advantage of the publicly available databases of CREB-binding sites to extract CREB-target candidates and we associated those genes with the enriched GO terms. Thus defining a core set of markers responsible for the observed changes in the transcriptome. Our results showed few differences between FSK and NE stimulated astrocytes and a strong transcriptomic deregulation after VP16-CREB overexpression, which encompasses the observed changes in the former treatments. Functional enrichment suggested a positive regulation of

signalling and transcriptional activity as well as an increase in oxidative metabolism. At the same time, CREB seems to participate in mechanisms directed to modulate synaptic activity and astrocyte-neuron communications such as Ca^{2+} and K^{+} homeostasis, or neuropeptide release. In addition, downregulated genes showed a decrease in cytoskeleton organization and cell cycle arrest, thus agreeing with the loss of stress fibers and the decrease in proliferation rate observed in cultured astrocytes after CREB activation. Finally, we identified a small group of transcription factors, known to be expressed as immediate early genes after CREB-dependent transcriptional activation, which could be responsible for the observed changes in the transcriptome.

Introduction:

The cAMP responsive element binding protein (CREB) is a widely distributed transcription factor of the bZIP family that regulates many physiological functions as cell development and survival, differentiation, metabolism, or synaptic plasticity (Mayr and Montminy 2001). CREB activation involves phosphorylation in the Ser133, binding to cAMP responsive element (CRE) motifs in the promoter of target genes and recruitment of coactivators, such as CBP or CRTCs, to form the CREB transcriptional complex and induce the expression of downstream genes (Altarejos and Montminy 2011). Since the discovery of CREB in 1986, many studies have been undertaken to identify CREB target genes in different cell types, aiming to characterize the distinct phenotypes underlying CREB activation. First genome-wide studies of CREB target genes were performed by the groups of Montminy and Goodman (Impey et al. 2004; Zhang et al. 2005), who used chromatin immunoprecipitation–based approaches to identify thousands of genes with CREB binding sites. However, the presence of CRE motifs does not guarantee CREB occupation nor gene transcription since CREB target gene selection suffers great variations depending on the context and cell type (Cha-Molstad et al. 2004). In fact, only a small subset of CREB-target genes identified in

Montminy and Goodman analyses was upregulated after a treatment of HEK293 or PC12 cells with forskolin (FSK), pointing to a partial role of cAMP activation in the induction of CREB-dependent transcription. Subsequent genome-wide analyses were directed to elucidate the roles of neuronal CREB in plasticity, learning and memory, first discovered in the mollusc *Aplysia Californica* by Kandel and collaborators (Dash et al. 1990). Thus, activated CREB-target genes were identified after an episode of long-term potentiation (LTP) (Chang et al. 2006), induced upon memory conditioning (Lakhina et al. 2015) or deregulated in Alzheimer's disease (Satoh et al. 2009; Parra-Damas et al. 2014). Other approaches for the identification of memory-related CREB-dependent genes involved the use of gain or loss-of-function models (Barco and Marie 2011). For example, a study with mice overexpressing a constitutively active form of CREB - VP16-CREB-, which was generated by binding the transactivation domain of the herpes simplex virus (HSV) to the N-terminal region of CREB, identified a small subset of 4 genes related to long-term-potentiation facilitation (Barco et al. 2005). However, no studies have addressed the transcriptional profile induced by CREB activation in astrocytes, despite the fact that these cells are also key players in synaptic modulation (Araque 2008; Navarrete et al. 2012). To date, few astrocytic genes are known to be CREB targets, involving mainly neurotrophins and glutamate transporters (Carriba et al. 2012; Corbett et al. 2013; Karki et al. 2013), thus making it necessary a more profound analysis to understand the roles of CREB in the regulation of astrocytic functions.

In this study, we have characterized the CREB transcriptional profile in rat astrocyte cultures under different stimulations, aiming to generate a signature of CREB astrocytic genes. In order to address the differences in CREB transcriptional programs depending on the activation context, we have used three distinct stimuli to activate CREB-dependent transcription: the well-known adenylate cyclase activator FSK, which phosphorylates CREB via cAMP-PKA pathway; the neurotransmitter NE, which activates CREB transcription in astrocytes via PKC (Carriba et al. 2012) and the constitutively active form of CREB, VP16-CREB (Barco et al. 2002).

Our study is divided in three stages. First, characterization of the global changes in the transcriptome by performing a functional analysis, associating deregulated genes with gene ontology terms (GOs). Second, identification of potential CREB-target genes by comparison with publicly available databases of CREB binding sites (Zhang et al. 2005). Third, association of those CREB-target gene candidates to the GOs upregulated in the functional analysis.

Results:

VP16-CREB promotes CREB-dependent transcription in astrocytes:

We have previously shown the induction of CREB-dependent transcription in astrocytes by FSK and NE (Carriba et al. 2012). Here we characterized the virally-mediated expression of VP16-CREB and functional consequences thereof. Astrocytes infected with Ad2/5-CMV-VP16-CREB efficiently transduced VP16-CREB at 18 hours post-infection, as deduced by the robust expression of VP16 mRNA and protein detected with Western blotting, immunocytochemistry and qPCR (Fig. 1a, b, d). The Western blots showed a MOI-dependent expression of a band of 65 kD, the molecular weight of the fusion protein VP16-CREB (Fig 1b). That VP16-CREB activates CREB-dependent transcription was confirmed with luciferase assays, which showed CRE-based activation comparable to that induced by 6 hours treatment of FSK or NE (Fig.1c), and with qPCR, which showed a 10-15-fold upregulation of the *c-fos* gene (Fig. 1d). Infection with the Null adenovirus, which carries an empty vector, did not result in expression of VP16 or activation of CREB-dependent transcription. Altogether, these analyses support the use of VP16-CREB as a tool to induce CREB-dependent transcription in astrocyte cultures. The viruses were used at 5 MOI for transcriptome analysis.

Transcriptomic profile upon activation of CREB-dependent transcription in astrocytes:

We characterized the transcriptional programs induced by CREB through a transcriptome analysis with the Agilent rat *SurePrint G3* microarray in astrocyte cultures subjected to the aforementioned treatments. A first

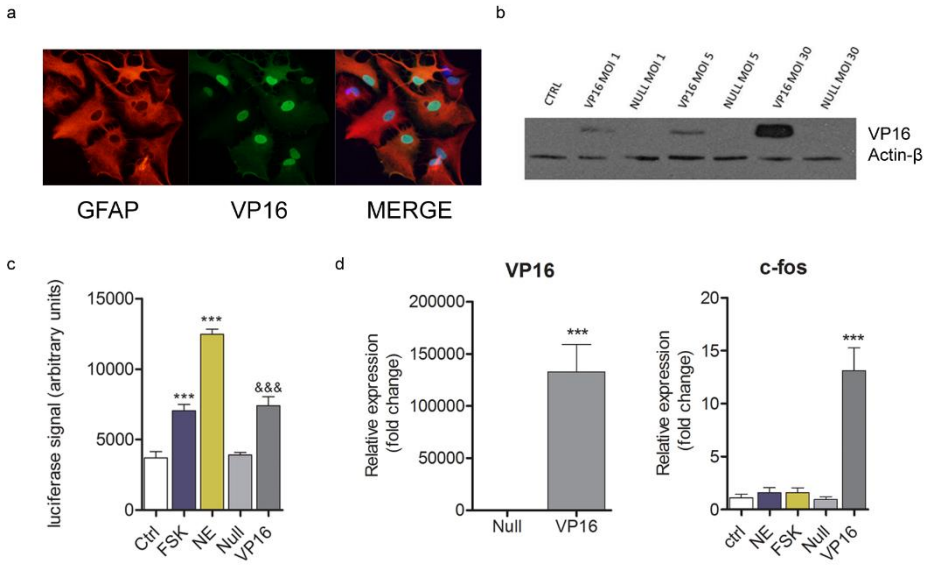

analysis of differentially expressed genes showed an equal distribution in FSK and NE conditions between up and downregulated genes, while in the case of VP16-CREB there was a slight tendency to upregulation. In addition, upregulated genes in VP16-CREB reached larger fold changes than in the other two

Figure 1. Functional characterization of VP16-CREB over-expression. Astrocytes were incubated with Ad2/5-CMV-VP16-CREB or Ad2/5-CMV (Null) at MOIs within 1-30, and processed for western blots, immunocytochemistry, CRE-luciferase assays or qPCR. a) Localization of the VP16-CREB transgene in the nucleus, as shown with VP16-CREB immunodetection after viral infection with a MOI 5. b) Expression of VP16-CREB is MOI-dependent, as assessed with Western blots using anti-VP16 or anti-actin antibodies—the latter to control for equal protein load. c) VP16-CREB stimulates CRE-dependent transcription in luciferase-reporter assays (MOI 5). Forskolin (FSK, 1 µM) and noradrenaline (NE, 10 µM)—well characterized stimulators of CREB-dependent transcription—were assayed in parallel as positive controls using 6-hour incubations. d) The qPCR shows robust expression of VP16 and *c-fos*—a canonical CREB-dependent gene—in Ad2/5-CMV-VP16-CREB infected astrocytes at a MOI of 5. Western blot, immunofluorescence and luciferase are representative of 3 independent assays, whereas qPCR represent the mean ± SEM of 3 independent experiments. Data were analyzed by Student's T-test or one-way ANOVA followed by Bonferroni. (**) $p<0.01$; (***) $p<0.001$.

conditions (fig. 2a). Moreover, FSK and NE stimulation showed a high similarity -Pearson's correlation = 0.87 (Fig 2c) - while the profile of VP16-

CREB was markedly different from the other two -Pearson's correlation = 0.18 vs FSK, 0.21 vs NE-. After removal of repeated probes and selection by adjusted p-value <0.05 the number of differentially expressed genes was 3279 for FSK-stimulated astrocytes -1642 UP/1636 DOWN- and 2667 for NE treatment -1276 UP/1393 DOWN-, relative to untreated controls. The infection with VP16-CREB adenoviruses showed the amount of 9885 differentially expressed genes- 5276 UP/4609 DOWN- compared to Null adenovirus infection. Such differences between the three conditions were reflected in their expression profiles (Fig. 2b) and in the overlap of differentially expressed genes among groups observed in Venn diagrams (Fig. 2d). Thus, FSK and NE shared 2079 differentially expressed genes and more than 80% of genes deregulated in either condition were included in the VP16-CREB profile. This indicates that the changes promoted in the transcriptome upon activation of CREB by FSK and NE are comprised in the VP16-CREB induced transcription.

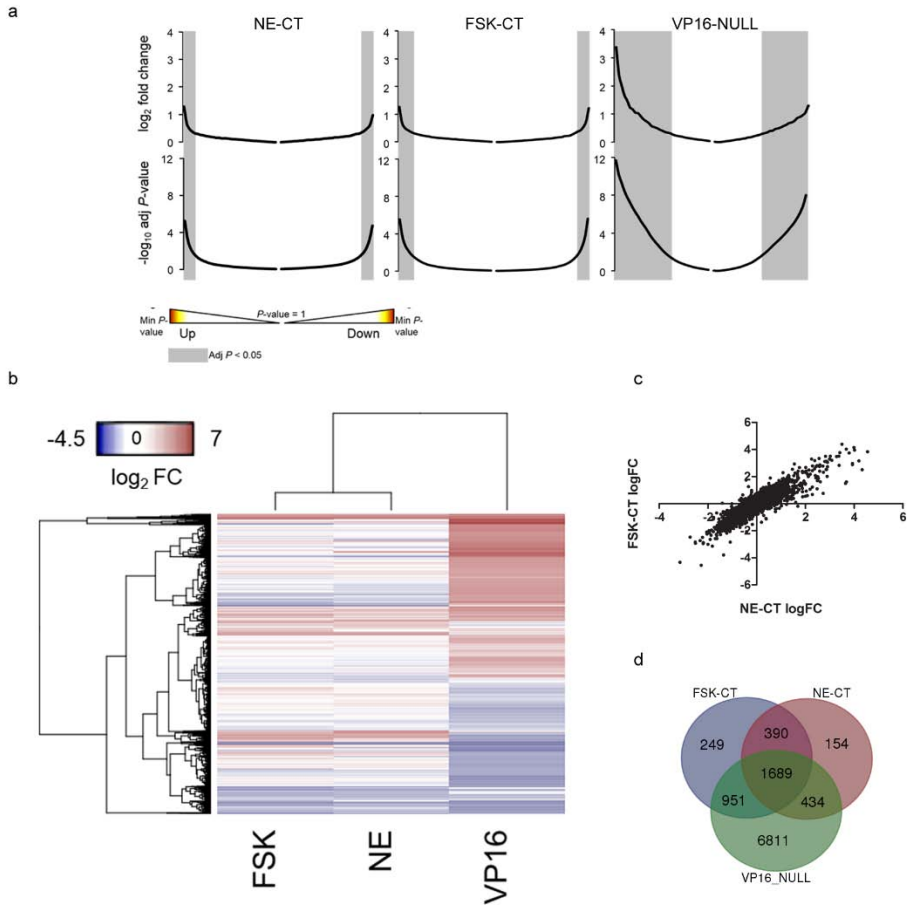

Figure 2. Transcriptomic profile of astrocyte cultures after CREB activation. a) Distribution of differentially expressed genes in paired comparisons FSK-CT, NE-CT and VP16-Null according to logFC and p-value b) Heatmap of differentially expressed genes in the three conditions, filtered by p-value>0.05. Data represent the log_2FC and is clustered by Euclidean distance; c) Correlation of log FC values between FSK and NE conditions d) Venn diagram showing the number of genes in the intersection between different gene lists.

Functional enrichment analysis

In order to interpret microarray results and gain insight into the functional changes produced in astrocytes upon CREB activation, we performed a GSEA analysis to associate the differentially expressed genes into GOs and generated categories of grouped GOs according to their overlap coefficient (see methods). GSEA analysis gives more weight to the top and bottom

genes in a ranked list in order to build enrichment sets, which means that the most deregulated genes will be primarily responsible for the observed GO profile. In the case of FSK and NE, GO enrichment was very similar, however, upon selection of the most significant GOs by setting FDR to 0.25, FSK showed a predominance of downregulated terms while NE profile was more balanced (fig 3 a, b; supplementary table 1, 2). This could be explained because the highest deregulated genes (logFC>1) in either condition showed an opposite distribution than the entire gene lists -NE: 238 UP/ 171 DOWN and FSK: 260 UP/294 DOWN-. In addition, GO profiles suggested that the top upregulated genes after NE treatment were more clustered -according to GO annotation- while in the case of FSK the highest relation appeared between the top downregulated genes. In VP16-CREB overexpression, the vast majority of significant GOs were upregulated, agreeing with the predominance and the highest FCs reached by the upregulated genes. Below we analyse together GO enrichment in FSK and NE, addressing their differences, and then we move to VP16-CREB.

The most significative GOs upregulated in NE were comprised in the categories homeostasis, amine metabolism and signal transduction through GPCRs. There was also an important expression of neuropeptides included in the GOs "behaviour" and "reproduction", and a number of chemokines

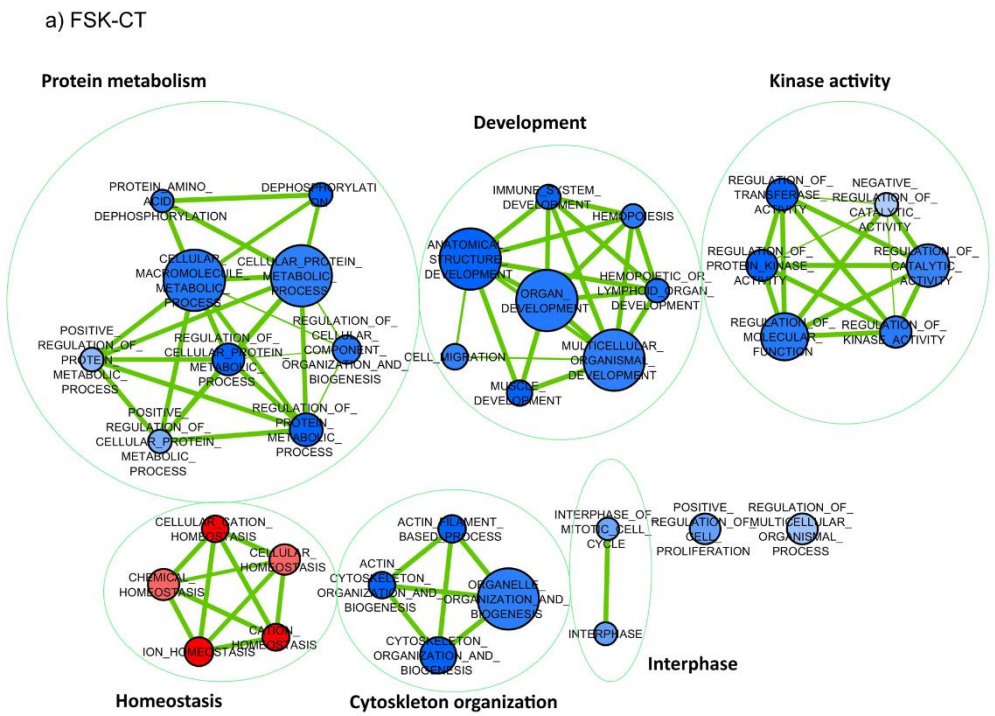

and receptors in the GOs "response to chemical stimulus" and "inflammatory response". In FSK condition, most of the aforementioned GOs appeared enriched, although only the homeostasis-related GOs were significant for a FDR<0.25. On the other hand, downregulated genes were clustered in GOs related to cytoskeleton organization, protein metabolism, regulation of kinase activity and development. In this case, both NE and FSK shared most of the GOs but changes in FSK were more pronounced (Fig 3 a,b).

Figure 3. Functional enrichment of genes deregulated after CREB activation. Ranked lists of differentially expressed genes (p<0.05, ranked by logFC) were subjected to a GSEA and matched to GO terms (biological process). Significantly enriched GOs (FDR<0.25) were depicted with the Cytoscape plugin "enrichment map" and grouped according to the overlap coefficient (terms

with OVL<0.5 were considered linked, thickness of the edges represent OVL, the thicker, the smaller). Upregulated GOs are showing in red and downregulated in blue. Colour gradient reflect FDR (the darker, the smaller) and size of the nodes represent number of enriched genes in the GO (the larger, the higher). Categories that encompass linked GOs were manually curated and are showing for clarity. a) FSK-CT; b) NE-CT.

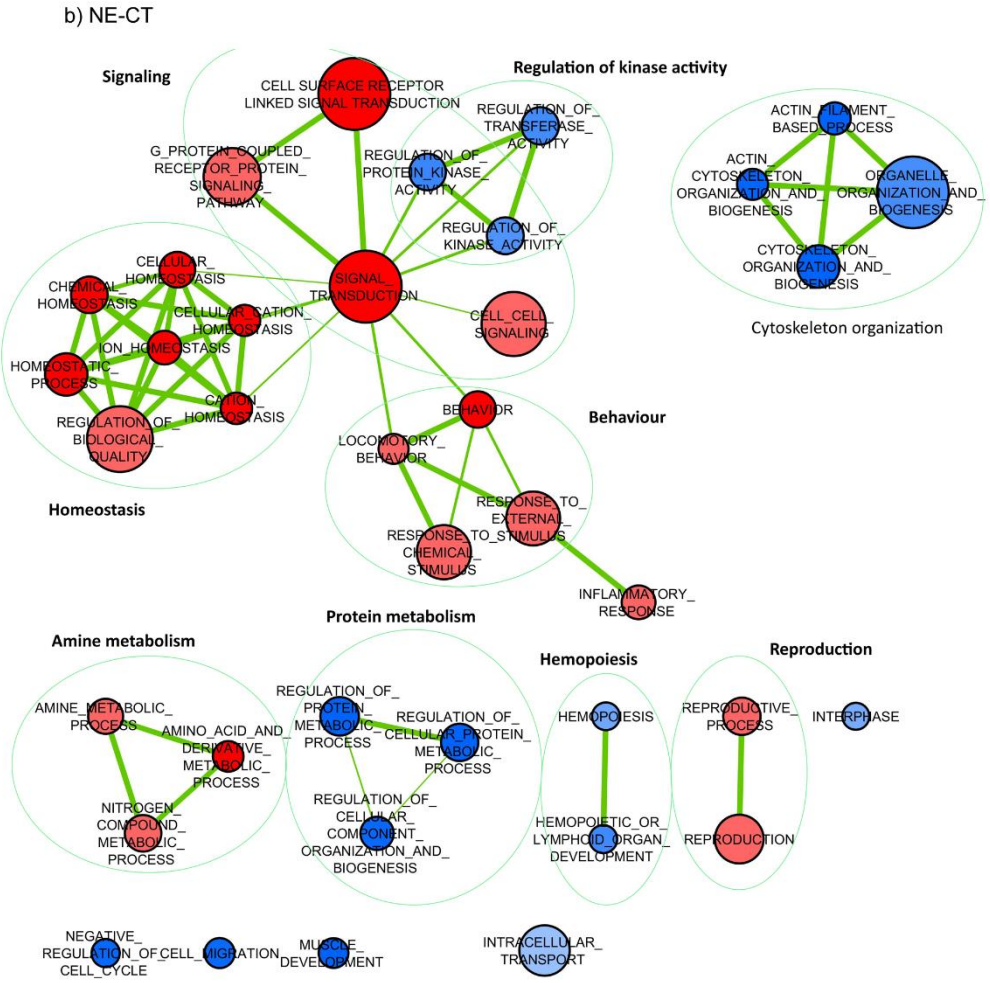

In order to understand the functional changes underlying GOs, we performed a leading edge analysis to identify genes that contribute most to the enrichment in each term. The homeostasis category revealed a diverse group of genes, most prominent among which are Ca^{2+}-related genes such as the calcitonins *Calca* and *Calcb*, the Ca^{2+} channel *Trpv4*, the Ca^{2+}-transporting ATPase (*Atp2c1*) or the neuropeptide prokineticin2 (*Prok2*).

The latter was one of the most upregulated genes in both FSK and NE conditions and it has been shown to increase cytosolic Ca^{2+} levels in astrocytes through activation of PLC (Koyama et al. 2006). Within GOs grouped in the amine metabolism category, we found genes related to glutamate metabolism, as glutaminase 2 (*Gls2*), which catalyses the conversion of glutamine to glutamate, and glutamate decarboxylase (*Gad1*), which catalyses the conversion of glutamate to GABA. Both enzymes have been shown to be expressed by astrocytes *in vivo* and they have been related to ammonia detoxification -*Gls2*- (Cardona et al. 2015) and regulation of microglial activation -*Gad1*- (Lee et al. 2011). Moreover, a role of these enzymes in oxidative metabolism has also been proposed because they increase the pool of glutamate and GABA, which can be oxidized in the TCA in periods of high energetic demand (Behar and Rothman 2001; Lovatt et al. 2007; Cardona et al. 2015).

The signal transduction category contained the largest group of deregulated genes associated to GOs. Many genes encoded GPCRs as the endothelin receptor (*Ednra, Ednrb*), or the prostaglandin receptor α2 (*Ptgfr*), and tyrosine kinases receptors as the family of high affinity nerve growth factor receptors (*Nrtk1/2/3*). The MAPK pathway was also represented in this category with genes encoding proteins from different levels throughout the pathway like *Gem, Rasd1, Map3k6, Mapk6/10 or Sik1*. Finally, the transcription factor cAMP responsive element modulator (*Crem*) appears between the most upregulated genes, indicating a strong regulation of CREB-dependent transcription. We also need to mention the large group of upregulated genes that encoded neuropeptides such as tachykinin1 (*Tac1*), corticotropin (*Crhbp*) or urocortin (*Ucn*) and the representative number of inflammatory genes like the chemokines *Ccl2* and *Ccl7* or the chemokine receptor *Ccr5*.

Among downregulated categories, cytoskeleton organization comprised many genes encoded filament proteins like actin and myosin (*Acta1, Myh9/10/11*) but also proteins that control cytoskeleton dynamics as Rho-GTPases (*Rnd1*, *Cdc42*) or the kinase *Pak1*. The joint decrease of such cytoskeletal genes could underlie the depolymerisation of actomyosin stress

fibers observed in astrocytes upon stimulation with FSK or NE (Perez et al. 2005; Vardjan et al. 2014). Related to cytoskeletal proteins, but enclosed in the development category, we found several extracellular matrix genes as integrins (*Itgb1*) laminins (*Lamc1*) and thrombospondins (*Thbs1*). In addition, many growth factors were included in this category such as fibroblastic growth factor (*Fgf18*) or colony stimulation factor (*Csf1*); and regulatory factors of the G1/S cell cycle phases like cyclin D (*Ccnd1*) and Cyclin-dependent kinase 6 (*Cdk6*), which also appeared in the kinase activity category. Together, downregulated genes in these categories pointed to a switch from a proliferative profile to a more differentiated state of astrocytes. Besides, the protein metabolism category encompassed many phosphatases from the family of dual protein phosphatases (*Dusp5/6/8*) and protein tyrosine phosphatases (*Ptpn9/13*), which could contribute to the high signalling activity observed in the upregulated GOs.

Despite the high overlap between FSK and NE, which is reflected in the GO profiles, several deregulated genes are characteristic for each condition. In NE, the most prominent among the upregulated genes -according to FC and functional relation- encoded for neuropeptide receptors as melanin (*Mchr1*) or prostaglandin (*Ptgfr*), regulators of thyrotropin (*Trh, Dio3*), inflammatory receptors (*Trem1/3)* and chemokines (*Ccl2, Ccl6, Ccr5*). In FSK condition appeared many genes related to cAMP-PKA pathway inhibition such as phosphodiesterases (*Pde3b, Pd9a*) or the CaMKII inhibitor (*Camk2n1*), but also inflammatory mediators as chemokines (*Cxcl2*), interleukines (*Il1b*) and transcription factors (*Cebpb*).

The functional analysis of VP16-CREB transcriptome revealed an intense activity directed to the generation of new proteins, which was reflected in the high number of genes clustered in the categories of signalling, transcription, translation and protein processing (fig. 3 c; supplementary table 3). The high expression of signalling receptors -mainly GPCRs- together with genes encoding proteins of the MAPK pathway and early transcription factors -*Fos, Myc, JunB*-, suggested a positive feedback of CREB-dependent transcription, which is supported by the upregulation of

the very *Creb1* gene (logFC 5.28) upon VP16-CREB overexpression. Regarding genes related to the transcriptional and translational machinery,

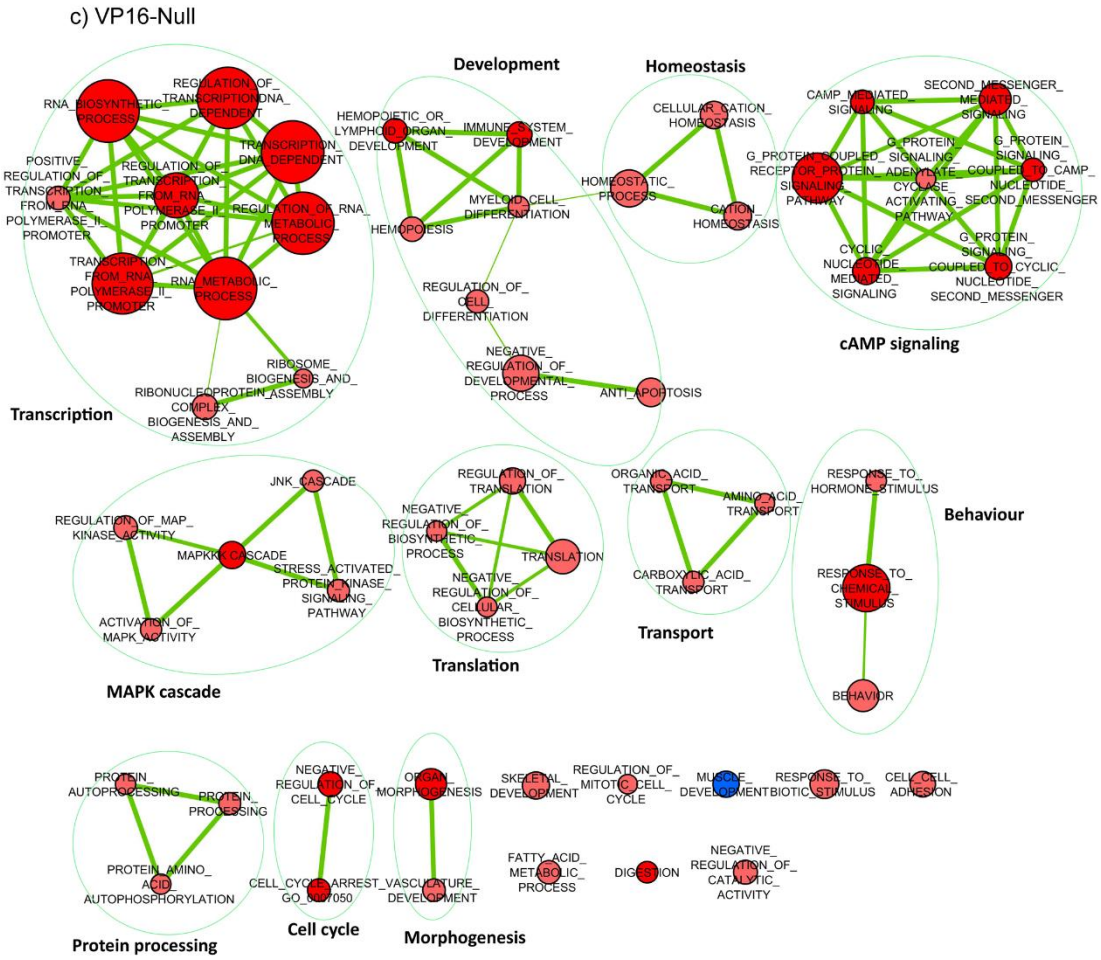

we found helicases (*Dhx8/38*), RNA metil-transferases (*Rnmt*), splicing factors (*Sf1/a3*), translation initiation factors (*Eif1/2/3*), ribosomal proteins (*Mrps7, Rps6kb2*) and tRNA ligases (*Yars, Mars, Wars, Aars*). In addition, the upregulated expression of multiple chaperones (*Hspa1a/1l/2, Dnajb1/2/4*) agreed with the high level of protein generation.

Figure 4. Functional enrichment of genes deregulated after VP16-CREB overexpression. Significantly enriched GOs (FDR<0.25) were depicted with the Cytoscape pluguin "enrichment map" and grouped according to the overlap coefficient (terms with OVL<0.5 were considered linked, thickness of the edges represent OVL, the thicker, the smaller). Upregulated GOs are showing in red and downregulated in blue. Colour gradient reflect FDR (the darker, the smaller) and size of the nodes represent number of enriched genes in the GO (the larger, the higher). Categories that encompass linked GOs were manually curated and are showing for clarity.

Besides this strong activity of protein synthesis, we found an increase in oxidative metabolism, especially related to fatty acids. Thus, upregulation of enzymes like Acyl-CoA thioesterases (*Acot1/2/4*) or palmitoyltransferases (*Cpt1a/b*) pointed to a mobilization of fatty acids, which has been recently reported as an important energy source for brain metabolism (Panov et al. 2014).

Other relevant GOs upregulatd in VP16 are "potassium ion transport" and "carboxylic acid transport" which present many genes related to well-known functions of astrocytes as the voltage gated (*Kcna1/6*) and inwardly rectifying (*Kncj4/5*) K^+ channels or the glutamate (*Slc1a1/4/5*) and monocarboxilate transporters MCT3/4 (*Slc16a8, Slc16a3*) (table 1). In addition, we found an increase in the expression of several claudins (*Cldn3/5/6/7*), which are the major component of tight junctions and key regulators of BBB permeability (Zlokovic 2008).

VP16-CREB overexpression led to continuous activation of CREB-dependent transcription, which caused an increase in stress responses reflected in the upregulation of p38MAPK cascade, stress-related transcription factors (*Nfkb1, Ddit3*), cell cycle inhibitors (*Cdkn1, Gadd45*) or the heat shock protein 70 (*Hsp1a1*). Conversely, many anti-apoptotic factors (*Bcl2, Bfar, Faim3*) and anti-inflammatory genes (*Socs 2/3*) were also found upregulated. This apparent paradox could be explained by the adaptive mechanisms directed to protect the cell under stress conditions. For example, the high expression of *Hsp1a1* (logFC 7.00) could underlie the increase in anti-apoptotic and anti-inflammatory factors (Yenari et al. 2005).

The main common category between VP16-CREB and FSK/NE conditions was related to homeostasis, with the aforementioned *Calcb*, and *Trpv4* genes also found upregulated in V16-CREB. In addition, an important group of

neuropeptides was upregulated in the three conditions being *Tac1*, *Prok2* and *Crhbp* the most expressed. Among downregulated genes, only the GO "muscle development" appeared significative in VP16-CREB. Interestingly, some genes enclosed in this GO were shared with FSK/NE conditions, namely cytoskeletal components, as *Act1a* or *Myh11*, and ECM genes as collagen (*Col5a3*) keratin (*Krt19*) or sarcoglycans (*Sgca/b/c*).

Table 1. Solute-carrier-family transporters and K^+ channels upregulated after CREB activation.

SLC transporters			
Type	Gene	LogFC	Condition
Monocarboxilate transporters	*Slc16a3*	5,26	NE, FSK, VP16
	Slc16a10	1,83	VP16
	Slc6a17	2,51	NE, FSK
	Slc16a11	1,69	VP16
	Slc16a8	1,67	NE, FSK, VP16
	Slc16a6	1,54	NE, FSK, VP16
Glutamate transporters	*Slc1a5*	1,87	VP16
	Slc1a1	1,75	VP16
	Slc1a4	0,90	VP16
Glucose transporters	*Slc2a3*	2,01	VP16
	Slc2a4	2,09	VP16
	Slc2a13	1,26	NE, FSK
GABA transporters	*Slc32a1*	7,11	VP16

K^+ channels			
Type	gene	logFC	condition
Inward rectifiers	*Kcnj9*	1,817635763	VP16
	Kcnj4	1,45142444	VP16
Voltage-gated	*Kcnh1*	1,886816358	NE, FSK
	Kcna7	3,753948562	VP16
	Kcng2	3,477599011	VP16
	Kcns1	2,831435193	VP16
	Kcnh6	2,396829111	VP16
	Kcnc1	2,081120995	VP16
	Kcna1	1,259302661	VP16

Taken together, the changes in the astrocyte transcriptome resulting from the activation of CREB-dependent transcription pointed to a high alteration in signalling and transcriptional activity, the regulation of Ca^{2+} and K^{+} homeostasis and the increase in oxidative metabolism mainly through aminoacids and fatty acids mobilization. The high expression of neuropeptides could underlie an intense intercellular communication. In addition, astrocyte "stellation" produced after FSK/NE stimulation should be a consequence of the observed decrease in cytoskeleton components and the cell cycle arrest.

Identification of CREB target genes

Differentially expressed genes found after CREB-dependent transcriptional activation can be categorized according to the regulatory mechanisms that induce their expression. Upregulated genes should comprise two large groups: (i) directly regulated by CREB, i. e., genes whose expression is induced by CREB binding to their promoters; (ii) indirectly regulated by CREB, i. e., genes regulated by the first group, notably by transcription factors. Downregulated genes should respond to many factors such as CREB transcriptional repression by heterodimerization; recruitment of inhibitory co-activators –as histone deacetylases- or compensatory mechanisms triggered after sustained transcriptional activity (Euskirchen et al. 2004).

In order to extract the CREB-dependent genes responsible for the observed changes in the transcriptome, we took advantage of the CREB database (Zhang et al. 2005), which annotates genes with conserved CRE sequences proximal to the promoters. We decided to compare our lists of upregulated genes with the entire database in order to identify CREB binding sites, reasoning that, given the function of CREB as a transcriptional activator, most genes directly regulated by CREB should be among the upregulated lists. This comparison showed 734 common genes in FSK treatment, 596 in NE and 2291 in VP16-CREB. Next, we matched these lists of CREB target candidates with the leading edge genes of the upregulated GOs, thus obtaining a broad genetic signature of the transcriptional programs elicited

by CREB activation. FSK and NE reached 11 and 77 common genes respectively while in the case of VP16 288 genes were shared. CREB candidates appeared in all upregulated GOs for the three conditions (see tables 2, 3, 4) and highly overlapped leading edge genes, accordingly with the wide range of functions covered by this transcription factor.

Not many CREB-target genes were common for FSK, NE and VP16-CREB given the few GOs significantly upregulated in the former condition. The most relevant were the Ca^{2+} related genes *Calcb* and *Trpv4* and the neuropeptides *Prok2* and *Tac1*. In addition, NE and VP16-CREB shared several related genes as *Crhbp* or the calcitonin receptor *Calcr*, but also genes for other representative functions like the kinases *Rasd1* and *Map3k6* or the transcription factor *Crem*. Intriguingly, a CREB-target candidate among the most expressed in NE condition was not included in VP16-CREB list, namely the small GTPase *Gem*, involved in cytoskeleton organization (Wen et al. 2013; Chevalier et al. 2014). Finally, most representative candidates in the VP16 group were transcription factors as *Fos, Myc, Junb, Cebp, Rela, Nfkb, Pparg, Foxc2, Mafb, Hsf4 or Atf4*, probably responsible for much of the observed changes in the transcriptome. Other relevant CREB candidates were the adhesion molecules claudins (*Cldn3/4*), the GPCRs α2 and β3 adrenergic (*adra2a/c, Adrb3*), the dopaminergic D4 receptor (*Ddr4*) and the somatostatin receptor 1 (*Sstr1*), and a relevant number of genes encoding for proteins of the Mapk pathway, the transcriptional/translational machinery and for protein processing.

In conclusion, global changes in gene expression after CREB-dependent transcriptional activation in astrocytes appear to be driven by a small group of CREB target genes, mainly represented by immediate transcription factors. However, other functional changes seem to be directly regulated by CREB as GPCRs signalling, Ca^{2+} homeostasis and neuropeptide expression, which comprise principal ways of signal transduction and communication between astrocytes.

Table 2. CREB-target genes in FSK vs CT associated to enriched GO terms.

Category	Leading edge-CREB genes	Top genes logFC
HOMEOSTASIS	*Calca, Calcb, Slc40A1, Stc1, Atp2C1, Ccl7, Trpv4, Prok2, Ccl2, Tac1*	*Prok:* 2.51 *Stc1:*2.39

Table 3. CREB-target genes in NE vs CT associated to enriched GO terms.

Category	Leading edge-CREB genes	Top CREB genes logFC
HOMEOSTASIS	*Abca1, Calca, Calcb, Apoa2, Stc1, Cacna1C, Atp2C1, Ccl7, Trpv4, Prok2, Ccl2, Tac1, Ccr5,*	*Calcb* : 3,68 *Prok2* : 2,87 Tac1: 2,08 Stc1: 2,58
BEHAVIOR	*Ccl7, Prok2, Ccl2, Cdh13, Ccr5, Scg2, Cmklr1,*	*Prok2* : 2,87
REPRODUCTION	*Crhbp, Ptgfr, Hist1H1T, Prok2, Ccl2, Hspa2, Tac1, Bmpr1B*	*Crhbp* : 2,48
AMINE METABOLISM	*Slc7A5, Gad1, Dio2, Chst1, Uap1, Cdo1, Sncaip,*	*Dio2:* 3,68
RESPONSE TO CHEMICAL STIMULUS	*Apoa2, Stc1, Calcr, Ccl7, Prok2, Ccl2, Cdh13, Ccr5, Scg2, Cmklr1*	*Stc1:* 2,58 *Prok2:* 2,87
INFLAMMATORY RESPONSE	*Tnfaip6, Adora3, Ptx3, Ccr5, Cdo1, Scg2, Nfatc4,*	*Adora3:* 1,94
REGULATION OF BIOLOGICAL QUALITY	*Calca, Dyrk3, Calcb, Stc1, Plat, Cacna1C, Atp2C1, Ccl7, Prok2, Ccl2, Tac1, Ccr5, Abca1, F12, Apoa2, Sncaip, Trpv4, Aldh9A1*	*Tac1:* 2,08 *Prok2:* 2,870 *Calcb:* 3,68 *Stc1:* 2,58
SIGNAL TRANSDUCTION	*Ret, Ucn, Ecm1, Vipr2, Tnfaip6, Cited2, Dgka, Trh, Trem1, Rgs4, Crhbp, Rgs2, Ednrb, Alcam, Adamts1, Adora3, Prok2, Ccr5, Map3K6, Vav3, Gem, Cort, Cdh13, Scg2, Tlr2, Ptgfr, Calca, Calcb, Igsf6, Crem, Stc1, Gna14, Rasd1, Calcr, Ccl7, P2Ry1, Ccl2, Otx2, Cd14, Mapk6, Abca1, Ntrk2, Ntrk3, Ecel1, Apoc3, Cck, Gcg, Baiap2, Mapk10, Nr4A1, Nr4A3, Rit2, Artn, Trpv4, Pnoc, Nmu, Pde7B, Fcgr2B, Shc3, Nlk*	*Cck:* 3,928066508 *Calcb:* 3,687798589, *Prok2:* 2,870888574 *Gem:* 2,822395374, *Stc1:* 2,588015462 *Crem:* 2,582731965, *Pnoc:* 2,490583775 *Crhbp:* 2,482787358, *Trh:* 2,037853626 *Ednrb:* 1,991021166, *Adora3:* 1,94071405

Table 4. CREB-target genes in VP16 vs Null associated to enriched GO terms.

GO term	*Leading edge CREB genes*	*Top 50 CREB gens logFC*
DIGESTION	*Cckbr, Galr2, Acsl1, Galr1, Nmu, Apoa4, Sstr1, Sstr2, Ldlr, Ppargc1A*	*Sstr1: 6,33155170748291* *Nmu: 3,50518854060527* *Apoa4: 3,31588942346694*
G PROTEIN COUPLED RECEPTOR SIGNALLING	*Ucn, Grp, Gipr, Chrm4, Ptger2, Adrb1, Ltb4R, Gpr176, C5, Calcr, Rasd1, Tbxa2R, Galr2, Grm6, P2Ry2, Ccrl2, Qrfpr, Drd4, Ghsr, Sphk1, Ecel1, Gpr75, Apoc3, Gpr4, Gpr50, Sstr1, Adra2C, Sstr2, Adra2A, Cort, Tbl3, Adrb3, Cckbr, Gnas, Ang, Gprc5C, Gpr19, Ptger4, Lpar3, Gpr3, Adcy7, Tshr, Gabbr2, Galr1, Cdh13,*	*Cort: 3,94614701681369* *Adra2a: 3,70625421318438* *Chrm4: 3,36611643928098* *Gpr4: 3,24228699004704* *P2ry2: 3,18333258638761* *Adra2c: 3,14317237258233* *Grp: 3,12511759518953* *Adrb3: 7,06690093815397* *Sstr1: 6,33155170748291* *Sphk1: 5,30145422642719* *Drd4: 4,70717048709384* *Calcr: 4,48987375658947* *Rasd1: 4,16646378585761*
NEGATIVE REGULATION OF CELL CYCLE	*Ppp1R15A, Hexim1, Cdkn1C, Btg3, Foxc1, Ppp1R13B, Cdkn1B, Gadd45A, Bmp7, Tbrg4, Ppm1G, Uhmk1, Rassf1, Stk11, Bmp2, Myc, Sesn1, Plagl1, Mfn2, Inha*	*Foxc1: 3,71702103773472* *Inha: 3,63191385451982* *Myc: 3,13724480021369*
DEVELOPMENT	*Hrk, Ldb1, Npr1, Notch4, Alox12, Triap1, Psen1, Aatf, Prkcz, Rela, Socs2, Socs3, Mapk8, Bag4, Bcl2L10, Bag1, Prok2, Nphp3, Mcl1, Srgn, Hspa9, Iqcb1, Ahsg, Sphk1, Bnip3, Bfar, Mif, Hipk3, Tbx3, Nfkb1, Vegfa, Gclc, Mafb, Gdnf, Akt1S1, Cdh13, Birc6, Ciapin1, Inha, Cryab, Hspa1B, Bcl2L2, Tpt1, Tbx1, Kirrel3,*	*Sphk1: 5,30145422642719* *Mafb: 4,79329057413319* *Tbx1: 4,42023233486614* *Mmp9: 3,79619662367681* *Inha: 3,63191385451982* *Pparg: 3,44441341813836*
MAPKKK CASCADE	*Shc1, Gps2, Crkl, C5, Mapk8, Prok2, Nrtn, Map3K6, Map4K5, Map3K2, Dusp4, Map3K3, Dusp2, Daxx, Gadd45B, Adra2C, Dusp9, Adra2A, Mapk8Ip1, Adrb3, Taok3, Mapkapk2, Madd, Ren, Map3K13, Map3K11, Trib3, Hipk3*	*Adrb3: 7,06690093815397* *Dusp9: 5,07605210820427* *Map3k6: 4,17842153864158* *Adra2a: 3,70625421318438* *Nrtn: 3,56476952885242* *Gadd45b: 3,33643008977942* *Adra2c: 3,14317237258233*
ORGAN MORPHOGENESIS	*Foxc1, Foxc2, Npr1, Notch4, Cebpg, Htt, Rorb, Comp, Hey2, Prok2, Dgcr6, Pitx2, Tbx1, Tle1, Sphk1, Ptch1, Glmn, Aplp1, Lsr, Prox1, Tbx3, Vegfa, Runx1, Lhx1, Ncl, Cdh13, Ang,*	*Sphk1: 5,30145422642719* *Foxc25,28954236509808* *Comp: 5,14343706378451* *Tbx1: 4,42023233486614* *Lhx1: 3,89886226149247* *Foxc1: 3,71702103773472* *Dgcr6: 3,05098481015267*
PROTEIN PROCESSING	*Map3K3, Ptch1, Eif2Ak3, Lmtk2, Psen1, Ppp2R5C, Uhmk1, Aph1A, Mex3B, Aph1B, Taok3, Scg5, Cdk12, Map3K13, Map3K11, Taf1*	
RESPONSE TO CHEMICAL STIMULUS	*Foxc2, Srxn1, Gipr, Hspa4L, Adipor2, Ndrg1, Cxcl2, Cygb, Rela, Herpud1, Dnajb2, Duox1, Dnajb1, C5, Prdx5, Calcr, Dnajb4, Ccrl2, Prok2, Duox2, Ghsr, Eif2B4, Hspa1L, Plaur, Apoa4, Sstr1, Hspa2, Tor1B, Sstr2, Fosl1, Cdh13, Pparg, Ang, Dgkk, Atf6, Hspa1B, Abcg2, Map2K1, Htt, Adcy8, Crhbp, Cckbr, Galr2, Crh, Hprt1, Tulp4, Rbm14, Gclc, Lats2, Gata3, Eif2B1,*	*Sstr1: 6,33155170748291* *Foxc2: 5,28954236509808* *Calcr: 4,48987375658947* *Hspa1l: 4,38429526391667* *Pparg: 3,44441341813836* *Apoa4: 3,31588942346694* *Fosl1: 3,28190264183572* *Crhbp: 3,10655840961567* *Cygb: 3,08404044171222*

NEGATIVE REGULATION OF CATALYTIC ACTIVITY	*Hexim1, Gabbr2, Dusp2, Dnajb6, Galr1, Gps2, Trib3, Dusp9, Gla, Adra2A, Hipk3,*	*Dusp9: 5,07605210820427* *Adra2a: 3,70625421318438*
REGULATION OF MITOTIC CELL CYCLE	*Btg3, Foxc1, Sphk1, Sik1*	*Foxc1: 3,71702103773472* *Sphk1: 5,30145422642719*
CARBOXYLIC ACID TRANSPORT	*Slc7A5, Slc1A1, Slc3A1, Slc16A8, Slc16A10, Slc1A5, Slc16A3, Slc25A22*	*Slc16a3: 5,26098830446775*
RESPONSE TO BIOTIC STIMULUS	*Hspa1L, Bnip3, Hspa4L, Eif2Ak3, Hspa2, Tor1B, Herpud1, Fosl1, Dnajb2, Isg20, Dnajb1, Dnajb4, Irf7,*	*Hspa1l: 4,38429526391667* *Fosl1: 3,28190264183572*
TRANSLATION	*Hbs1L, Asmt, Ebi3, Cebpg, Gla, Mrpl10, Mrpl41, Paip2B, Igf2Bp2, Eif3A, Eif2B1, Abcf1, Yars, Eif5A, Ghsr, Eif2B4, Wars, Eif1Ax, Mars2, Glmn, Eif2Ak3, Samd4A, Eif2Ak4, Mrps7, Eif1, Sigirr, Eif3I, Rps6Kb2, Eif3J, Etf1, Ltb, Inha, Eif3C, Metap1, Aars,*	*Inha: 3,63191385451982*
TRANSCRIPTION	*Ccnk, Dbr1, Ccnt1, Ccnh, Maml1, Gfi1, Gtf2B, Ppan, Jmjd1C, Ubp1, Prdm1, Rorb, Yy1, Fbl, Kat5, Sox18, Myc, Trim27, Pitx2, Junb, Ccrn4L, Abt1, Map2K3, Daxx, Scaf11, Cd3Eap, Sars, Gtf2F1, Gtf2F2, Hic1, Cdc40, Runx1, Ddit3, Nhp2, Erf, Srsf2, Gemin5, Preb, Atf6, Atf4, Sf1, Slbp, Rnaseh2A, Dhx8, Max, Notch4, Crem, Nolc1, Gata3, Foxo3, Gata2, Htatsf1, Taf5L, Neurod2, Dhx38, Nkx2-5, Ppargc1A, Ppargc1B, Hexim1, Yars, Tfap2C, Nop14, Smarca5, Scrt1, Nfkb1, Fosl2, Nfkb2, Srpk1, Fosl1, Isg20, Bmp2, Sp2, Fev, Fubp1, Maff, Ints5, Ints6, Aars, Cited1, Ldb1, Ell, Foxe1, Aff4, Bicd1, Chd1, Pqbp1, Mecp2, Sufu, Klf10, Tgif1, Zhx2, Rbm14, Klf13, Wars, Zhx3, Dis3, Mars2, Nsun2, Ddx54, Msl3, Fos, Tfb2M, Utf1, Pax1, Elf1, Prpf18, Nfx1, Elf4, Myod1, Irf7, Polr1E, Pparg, Ang, Rp9, Pabpc1, Ppard, Cebpb, Sp100, Gtf3C4, Rnmt, Sfswap, Vps4B, Taf9, Srsf1, Cebpg, Cxxc1, Foxk2,*	*Cdx2: 6,07516495739298* *Hsf4: 4,07622627317268* *Crem: 4,0204203349464* *Pou4f2: 3,89096327369052* *Hic1: 3,7411591797682* *Utf1: 3,69666538825456* *Fos: 3,55390731887171* *Sox18: 3,46506379753492* *Pparg: 3,44441341813836* *Fosl1: 3,28190264183572* *Ptf1a: 3,15397549459655* *Myc: 3,13724480021369* *Cited1: 3,12035349178133* *Tfb2m: 3,09453724797587* *Nfil3: 3,07255826482992* *Nkx2-5: 3,06892233928782* *Scrt1: 3,02087601439142*
HOMEOSTASIS	*Dyrk3, Calcb, Ldb1, Npr1, Hfe, Cebpg, Lpar3, Slc2A4, Foxo3, Clcn3, Rdh12, Galr2, P2Ry2, Myc, Prok2, Nphp3, Tac1, Dfnb31, Ppargc1A, Cd55, Bnip3, Slc4A11, Apoa4, Mafb, Cckbr, Trpv4, Ddit3, Fxn*	*Mafb: 4,79329057413319* *Tac1: 4,14116659526825* *Calcb: 3,87803835935731* *Apoa4: 3,31588942346694* *P2ry2: 3,18333258638761* *Myc: 3,13724480021369*
POTASSIUM ION TRANSPORT	*Kcnj4, Kcng2, Kcnj5, Kcnk6, Kcnk7, Kcns1, Kcnc1, Abcc8, Kcnc3, Kcnq1, Kcna1, Kcna6*	
SKELETAL DEVELOPMENT	*Tbx1, Klf10, Srgn, Kl, Gdf11, Msx2, Npr3, Hoxd13, Aebp1, Tbx3, Papss2, Pax1, Dll3, Comp, Sufu, Inha*	*Comp: 5,14343706378451* *Tbx1: 4,42023233486614* *Inha: 3,63191385451982* *Dll3: 3,02897830773686*
FATTY ACID METABOLISM	*Cpt1A, Mif, Cpt1B, Adipor2, Ptgs1, Acot2, Acot1, Hacl1, Acadm, Ppargc1A, Acot4, Ptges, Ppard, Alox12*	
CELL CELL ADHESION	*Cldn5, Cd164, Cldn4, Cldn3, Cd93, Amigo3, Cldn14, Cldn23, Cdh13, Apoa4*	*Cldn3: 4,98158349469111* *Cldn4: 3,35539217579508* *Apoa4: 3,31588942346694*
REGULATION OF GROWTH	*Tspyl2, Cda, Ghsr, Sertad3, Cdkn1B, Sphk1, Ptch1, Bbc3*	*Sphk1: 5,30145422642719*

Discussion

The importance of characterizing CREB-dependent transcription in astrocytes lies on the amount of evidence supporting the role of these cells in the control of synaptic activity (Navarrete et al. 2012; Lalo et al. 2014) and in the well-known participation of neuronal CREB in such process. Thus, with this genome-wide analysis, we aimed to relate transcriptional changes upon CREB activation with astrocytic functions that may affect synaptic activity such as neurotransmitter homeostasis, K^+ clearance or metabolic support.

Activation of CREB-dependent transcription is regulated at three levels: (i) binding to gene promoter; (ii) phosphorylation and (iii) recruitment of co-activators. CREB binding to the promoter of target genes appears to be specific for cell type (Cha-Molstad et al. 2004; Martianov et al. 2010) and it is regulated by chromatin conformation and methylation state (Altarejos and Montminy 2011). CREB phosphorylation is carried out by kinases activated through stimuli-mediated signalling pathways and thus exhibits stimulus-dependence (Naqvi et al. 2014). Finally, co-activators such as CPB or CRTCs are also regulated by phosphorylation and the ability of CREB to recruit them in the promoter of target genes seems to be stimulus-dependent (Altarejos and Montminy 2011). In this study, the use of two external stimuli –NE and FSK- to induce CREB-dependent transcription implies that the aforementioned regulatory mechanisms are present. Therefore, we would expect differences in gene expression based mainly in the different signalling pathways triggered by FSK -PKA/cAMP pathway- and NE –PKC/MAPK pathway (Carriba et al. 2012)-. In addition, we also expect differences regarding the activation of transcription factors other than CREB by both stimuli. Intriguingly, our results show similar transcriptomic profiles in both conditions, differing from previous works in other cell types, in which CREB activation through cAMP and MAPK pathways led to differential gene expression (Ravnskjaer et al. 2007; Naqvi et al. 2014). This suggests that CREB activation in astrocytes promotes a similar transcriptional program regardless of the involved signalling pathway. Taken this into

consideration, the differences between FSK and NE induced gene expression might be attributed in part to the magnitude and time of stimulation for each compound. Thus, both FSK and NE have been shown to stimulate CREB phosphorylation to the same extent (Thonberg et al. 2002) but FSK reaches its maximum activity at 6 hours (Dib et al. 1994) , while NE is progressively degraded in cell cultures, remaining a 75% at 6 hours after addition (Troadec et al. 2001). Besides, the differential downregulation of FSK and NE receptors due to desensitization might also affects the stimulation of both compounds.

In contrast, transcriptional activation by overexpression of VP16-CREB, which binds constitutively to the promoter and is able to induce transcription independently of signalling cascades (Riccio et al. 1999), will be mainly affected by chromatin conformation around CRE sites. Therefore, genes upregulated by VP16-CREB should reflect faithfully the astrocyte population of CREB-target genes, given the fact that chromatin conformation is cell-type specific (Arvey et al. 2012; Dekker 2014). In addition, the strong transactivation domain of the HSV promotes a high rate of VP16-CREB expression and hence a continuous activation of CREB-dependent transcription, as it is confirmed by the expression levels of *Fos* (fig. 1d). With this in mind, a comprehensive analysis of the differentially expressed genes in our three experimental conditions should provide an accurate vision of the functional roles of astrocytic CREB.

We used the GSEA analysis to extract functional information from gene expression because it takes into account the magnitude of changes in each gene, opposite to other methods based in over-representation, which only consider the number of genes to assign a significance value of enrichment (Khatri et al. 2012). Our results show a high increase in genes related to newly protein formation, indicating not only the CREB activation of protein machinery buy also a positive feedback in CREB transcriptional activation that increases signal transduction activators, RNA processing enzymes and ribosomal proteins. Interestingly, the signalling mediators in our three studied conditions belong predominantly to the MAPK pathway, thus agree

with our previous results (Carriba et al. 2012) that presented this cascade as an important pathway for CREB activation in astrocytes.

The upregulation of genes related to glutamate, GABA and fatty acid mobilization, which can provide energetic substrates for the TCA cycle, points to an increase in oxidative metabolism after CREB activation. Astrocytes have been traditionally view as glycolytic cells, which metabolize glucose to provide lactate for neuronal metabolism. However, this dogma is starting to be overwhelmed with findings that suggest a more complex astrocyte metabolism, with the utilization of neuron-released transmitters –like glutamate or GABA- as metabolic substrates for oxidation (Patel et al. 2005; Hertz et al. 2007) and the importance of fatty acid metabolism as responsible for the 20% of total brain energy (Panov et al. 2014). In addition, glutamate has been proposed as a source for lactate formation (Dienel and McKenna 2014), participating together with glucose in neuronal metabolic supply. According to this and taking into account the upregulation of lactate transporters after CREB activation (table 1), we hypothesize a regulatory role of CREB in astrocyte metabolism and lactate export to neurons.

Astrocyte communicate with neurons at the synapses by responding to neurotransmitters with increases in Ca^{2+} signals and by releasing gliotransmitters –as ATP or neuropeptides- which modulate synaptic activity (Rossi 2015). The results of this analysis might point to an alteration in Ca^{2+} signalling in astrocytes. For example, the Ca^{2+} channel *Trpv4* (logFC 1.94 in VP16-CREB) has been shown to participate in the initiation of Ca^{2+} waves in response to neuronal activity, as well as in the modulation of synaptic activity by triggering the release of gliotransmitters (Shibasaki et al. 2014). However, the main proteins implicated in the regulation of Ca^{2+} responses in astrocytes such as type 2 inositol 1, 4, 5 trisphosphate receptors are not altered by FSK/ NE activation of CREB and by VP16-CREB. Thus, functional analysis of Ca^{2+} homeostasis are needed in order to associate CREB-dependent transcription to Ca^{2+} signalling in astrocytes. In addition, K^+ buffering, which is necessary to remove the excess of K^+ generated by

synaptic activity and thus represent another level of synaptic modulation (Butt and Kalsi 2006), appears to be regulated by CREB since high number of K^+ channels are upregulated after CREB activation (table 1).

On the other side, downregulated genes upon CREB activation reflect the morphological changes observed in cultured astrocytes. Thus, cell cycle arrest and cytoskeleton reorganization promote the transformation from a highly-proliferative fibroblastic-type to a differentiate state that resembles a mature reactive astrocyte. This semblance has promoted several attempts to create a model of reactive astrogliosis *in vitro* through differentiation induced by different factors such as TGF-β or ATP. However, the resulting phenotypes did not reflect the complexity of *in vivo* reactive astrocytes (Wandosell et al. 1993; Wu and Schwartz 1998) and actual efforts are directed to the work with 3D cultures that seem to mimic *in vivo* astrocyte features (Puschmann et al. 2014; Maclean et al. 2015).

Finally, CREB target genes responsible for the global changes in astrocyte transcriptome appear distributed through all the enriched categories, supporting the role of CREB in multiple astrocytic functions. However, the most represented genes enclose transcription factors as the immediate early genes (IEGs) *Fos, Junb* or *Myc*, suggesting that changes elicited by CREB-dependent transcription in astrocytes are developed in various transcriptional waves, as it happens in neurons (Greenberg et al. 1992). In fact, our results regarding CREB-target gene candidates show coincidences with neuronal reported CREB genes as the aforementioned IEGs, therefore, a comparison with other studies which have characterized the transcriptomic profile upon CREB activation in neurons (Benito et al. 2011; Lakhina et al. 2015) would elucidate the differences between both cell types. In addition, validation of array data would be necessary in order to support the conclusions reached from differential gene expression. In this direction, qPCR experiments should be performed on key genes from the enriched functional categories and chromatin immunoprecipitation assays should be carried out in order to assess the occupancy of CREB in selected gene candidates.

In conclusion, while neuronal CREB is responsible for the synaptic modulations that underlie learning and memory processes, we posit that the activation of CREB-dependent transcription in astrocytes triggers mechanisms directed to modulate synaptic activity -such as Ca^{2+} homeostasis, K^{+} buffering and the release of neuropeptides- and increases oxidative metabolism and lactate export, thus playing a role in neuronal metabolic support. Further experiments directed to elucidate if synaptic activity is able to promote CREB-dependent transcription in astrocytes should help to depict the role of CREB as a central regulator in the astrocytic modulation of synaptic transmission.

Supplementary tables 1, 2, 3. Enriched GO terms for the three conditions showing normalized p-value and FDR. Leading edge genes are showing for each group of GOs.

GO term (UP)	NOM p-val	FDR q-val	Leading edge genes
CATION HOMEOSTASIS	0.0	**0.014065838**	
CELLULAR CATION HOMEOSTASIS	0.0	0.01713272	*Abca1, Calca, Calcb, Slc40A1, Stc1, Slc4A11, Lpar2,*
ION HOMEOSTASIS	0.0	0.05979695	*Cartpt, Atp2C1, Ednra, Ccl7, Trpv4, Prok2, Ccl2,*
CELLULAR HOMEOSTASIS	0.01002004	0.13519394	*Tac1, Cd24, Nphp3,*
CHEMICAL HOMEOSTASIS	0.009025271	0.14632013	
GO term (DOWN)			
MUSCLE DEVELOPMENT	0.0	**0.004935886**	*Cyr61, Cdc42Ep5, Cdc42Ep2, Cdc42Ep1, Fbn2, Cap2,*
HEMOPOIESIS	0.002008032	0.018789047	*Wnt7A, Krt18, Fgf18, Csf1, Nab2, Fhl3, Rnd1, Ctgf,*
HEMOPOIETIC OR LYMPHOID ORGAN DEVELOPMENT	0.012096774	0.02729869	*Csrp3, Sgcd, Enc1, Trim3, Nrtn, Mbnl1, Lmo4,*
IMMUNE SYSTEM DEVELOPMENT	0.006423983	0.03333894	*Igfbp3, Ifrd1, Emp1, Sox11, Runx1, Cd2Ap, Acta1,*
CELL MIGRATION	0.017857144	0.13035719	*Adora2A, Myh9, Angptl4, Vamp5, Vcl, Hbegf, Hdac5,*
ANATOMICAL STRUCTURE DEVELOPMENT	0.0	0.13468315	*Tagln, Gypc, Twist1, Tnfrsf11B, Pthlh, Gyltl1B, Ankh,*
ORGAN DEVELOPMENT	0.013888889	0.18277517	*Tcof1, Flna, Hes1, Slit2, Msx1, Egr2, Crim1, Inhba,*
MULTICELLULAR ORGANISMAL DEVELOPMENT	0.002375297	0.18583901	*Myo16, Bmp4, Ext1, Krt19, Cdk6, Col5A3, Fgfr3,*
			Mef2A, Igf1, Sgce, Smtn, Speg, Utrn, Sgcg, Adra1D,
			Adra1B, Adamts9, Tnfrsf12A, Mmp11, Epha2,
			Thbs1, Gcnt2, Itgb1, Nrp1, Spon2, Clic4, Nrp2,
			Sphk1, Vegfc, Nexn, Lamc1, Egfr, Fez2, Ppap2A,
			Bcar1, Cdk5R1
ACTIN FILAMENT BASED PROCESS	0.0	**0.008304961**	
ACTIN CYTOSKELETON ORGANIZATION AND BIOGENESIS	0.0	0.012851267	*Hdac5, Nexn, Bbc3, Rnd1, Spta1, Lasp1, Pak1,*
CYTOSKELETON ORGANIZATION AND BIOGENESIS	0.0	0.013382859	*Nuak2, Msto1, Nck2, Flna, Myh10, Dffb, Mid1Ip1,*
ORGANELLE ORGANIZATION AND BIOGENESIS	0.0021645022	0.050014906	*Myo9B, Arpc5, Myo7A, Mtss1, Myo1E, Acta1, Krt19,*
			Cxcl12, Cdc42Ep5, Carm1, Cdc42Ep2, Bcl2, Myh9,
			Dbn1, Bcar1, Bcl2L1
REGULATION OF CELLULAR PROTEIN METABOLIC PROCESS	0.0	**0.013175572**	
REGULATION OF PROTEIN METABOLIC PROCESS	0.0	0.014046053	*Ilk, Ptpn21, Lipa, Loxl2, Adamts5, Ccnd2, Ccnd1,*
DEPHOSPHORYLATION	0.0	0.014675258	*Plau, Casp4, Nck2, Adamts9, Parp3, Dusp3, Igfbp3,*
PROTEIN AMINO ACID DEPHOSPHORYLATION	0.0020242915	0.015397613	*Ube2E2, Nrg1, Dusp8, Dusp6, Mmp11, Lats2, Lox,*
REGULATION OF CELLULAR COMPONENT ORGANIZATION AND BIOGENESIS	0.0018939395	0.030445477	*Cdc42Ep5, Cdc42Ep2, Myh9, Erg, Tlr6, Trib1, Eif1B,*
POSITIVE REGULATION OF PROTEIN METABOLIC PROCESS	0.040816326	0.17977226	*Trib2, Prkaa2, Gypc, Adrb2, Fut1, Egfr, Pak1, Nuak2,*
POSITIVE REGULATION OF CELLULAR PROTEIN METABOLIC PROCESS	0.03629032	0.18010876	*Bag2, Fut9, Ptk2B, Stk38L, Ldlr, Csnk1A1, Mid1Ip1,*
CELLULAR MACROMOLECULE METABOLIC PROCESS	0.013129103	0.2327038	*Samd4A, Inhba, Ptpn14, Ptprd, Bmp4, Ext1, Ptpre,*
CELLULAR PROTEIN METABOLIC PROCESS	0.016913319	0.24478796	*Cxcl12, Carm1, Nmt1, Ptpn9, Ptprj, Ptpla, Dusp5,*
			Ptpro, Ptpn13, Ppap2A, Ston1, Nexn, Cdc42Ep1, Slit2
REGULATION OF KINASE ACTIVITY	0.0020449897	**0.022289244**	
REGULATION OF PROTEIN KINASE ACTIVITY	0.0	0.02967508	*Gadd45B, Gadd45A, Adrb1, Cdc6, Adrb2, Dusp8,*
REGULATION OF TRANSFERASE ACTIVITY	0.0	0.033593915	*Egfr, Dusp6, Bbc3, Pak1, Ccnd2, Rgs3, Lats2, Ccnd1,*
REGULATION OF CATALYTIC ACTIVITY	0.01927195	0.185761	*Ppap2A, Nck2, Trib3, Tlr6, Angptl4, Trib1, Trib2,*
NEGATIVE REGULATION OF CATALYTIC ACTIVITY	0.049115915	0.18690541	*Cap2, Bcl2, Flna*
REGULATION OF MOLECULAR FUNCTION	0.01443299	0.19036017	
INTERPHASE	0.03	**0.13039793**	*Lats2, Cdk6, Inhba,*
INTERPHASE OF MITOTIC CELL CYCLE	0.03285421	0.14208221	
REGULATION OF MULTICELLULAR ORGANISMAL PROCESS	0.04496788	**0.18291704**	*Bmp4, Cnn1, Actc1, Kcnb2, Tpm1, Serpine1, Nck2, Scn5A, Inhba, Myl9*
POSITIVE REGULATION OF CELL PROLIFERATION	0.03050109	**0.1835573**	*Fosl1, Edn1, Cdk6, Csf1, Fgf18, Nck2, Pdgfa, Adra1D, Pthlh, Egfr*

FSK-CT

NE-CT (up)

GO terms UP	NOM p-val	FDR q-val	Leading edge genes
CELLULAR CATION HOMEOSTASIS	0.0	**0.0**	
CATION HOMEOSTASIS	0.0	0.0	*Abca1, Calca, Dyrk3, Calcb, C5Ar1, Apoa2, Stc1,*
ION HOMEOSTASIS	0.0	0.0043987823	*Slc4A11, Lpar2, Cartpt, Cacna1C, Atp2C1,*
HOMEOSTATIC PROCESS	0.0	0.011558078	*Mchr1, Ednra, Ccl7, Trpv4, Prok2, Ccl2, Nphp3,*
CHEMICAL HOMEOSTASIS	0.0	0.02716895	*Tac1, Ccr5, Cd24, Cd55*
CELLULAR HOMEOSTASIS	0.0	0.03519026	
BEHAVIOR	0.0	**0.003572844**	*Crhbp, Ccl7, Crh, Prok2, Ccl2, Cdh13, Gcg, Ccr5,*
LOCOMOTORY BEHAVIOR	0.018242123	0.115493186	*Mchr1, Scg2, Cmklr1*
REPRODUCTION	0.00955414	**0.11347163**	*Crhbp, Ptgfr, Spag4, Crh, Hist1H1T, Prok2, Ccl2,*
REPRODUCTIVE PROCESS	0.033980582	0.1673024	*Hsf2Bp, Hspa2, Tac1, Bmpr1B, Wfdc2*
AMINO ACID AND DERIVATIVE METABOLIC PROCESS	0.0048701297	**0.117684476**	*Slc7A5, Gls2, Etnk1, Gad1, Dio2, Chst1, Uap1,*
AMINE METABOLIC PROCESS	0.0075642965	0.12015851	*Cdo1, Sncaip*
NITROGEN COMPOUND METABOLIC PROCESS	0.025356578	0.17114128	
RESPONSE TO CHEMICAL STIMULUS	0.021613833	**0.16741358**	*Srxn1, C5Ar1, Apoa2, Stc1, Ndrg1, Calcr, Ccl7,*
RESPONSE TO EXTERNAL STIMULUS	0.039017342	0.24737479	*Prok2, Ccl2, Cdh13, Ccr5, Cd24, Scg2, Cmklr1*
INFLAMMATORY RESPONSE	0.030303031	**0.16814236**	*Tnfaip6, Adora3, Ptx3, Ccr5, Cdo1, Scg2, Nfatc4*
REGULATION OF BIOLOGICAL QUALITY	0.012162162	**0.1739128**	*Cda, Calca, Dyrk3, Calcb, C5Ar1, Stc1, Lpar2, Plat, Cacna1C, Atp2C1, Mchr1, Ednra, Ccl7, Prok2, Ccl2, Nphp3, Tac1, Ccr5, Cd55, Abca1, F12, Apoa2, Slc4A11, Cartpt, Sncaip, Trpv4, Cd24, Aldh9A1*
CELL SURFACE RECEPTOR LINKED SIGNAL TRANSDUCTION	0.0013020834	**0.13646223**	*Ret, Ucn, Ifitm1, Ecm1, Vipr2, Tnfaip6, Cited2, Dgka, Irs2, Trh, Trem1, Rgs4, Crhbp, Rgs2, Ednra, Ednrb, Alcam, Adamts1, Adora3, Prok2, Qrfpr, Ccr5, Map3K6, Tp63, Vav3, Cartpt, Gem, Clec4A, Cort, Gprc5A, Crh, Cdh13, Sik1, Scg2, Tlr2, Ptgfr, Calca, Calcb, Igsf6, C5Ar1, Crem, Stc1, Lpar2, Mchr1, Gna14, Rasd1, Calcr, Ccl7, Grk5, Penk, P2Ry1, S1Pr1, Ccl2, Sfn, Otx2, Cd14, Mapk6, Ntrk1, Abca1, Ntrk2, Ntrk3, Plk2, Ecel1, Apoc3, Cck, Gcg, Baiap2, Mapk10, Rcan1, Nr4A1, Kitlg, Nr4A3, Rit2, Artn, Trpv4, Pnoc, Nmu, Cd27, Pde7B, Cd24, Fcgr2B, Shc3, Nlk, Pcsk1, Il11, Gad1, Pcdh8, Tfap2C, Aldh9A1, Nptx1, Sncaip*
SIGNAL TRANSDUCTION	0.0011223345	0.1742624	
G PROTEIN COUPLED RECEPTOR PROTEIN SIGNALING PATHWAY	0.027818449	0.2257845	
CELL CELL SIGNALING	0.019099591	0.23500137	
G PROTEIN SIGNALING COUPLED TO CYCLIC NUCLEOTIDE SECOND MESSENGER	0.07191781	0.2408832	

NE-CT (down)

GO terms (DOWN)	NOM p-val	FDR q-val	Leading edge genes
CYTOSKELETON ORGANIZATION AND BIOGENESIS	0.0	**0.014948939**	*Mid1Ip1, Nexn, Myo9B, Arpc5, Mid1, Mtss1, Rnd1, Spta1, Acta1, Lasp1, Pak1, Krt19, Nuak2, Cxcl12, Cdc42Ep5, Cdc42Ep2, Nck2, Flna, Myh9, Myh11, Kif1B, Myh10, Dbn1, Bcar1*
ACTIN FILAMENT BASED PROCESS	0.0	0.024739485	
ACTIN CYTOSKELETON ORGANIZATION AND BIOGENESIS	0.0057142857	0.03212295	
MUSCLE DEVELOPMENT	0.0	**0.036949635**	*Hdac5, Mbnl1, Tagln, Igfbp3, Ifrd1, Fhl3, Bmp4, Acta1, Csrp3, Krt19, Gyltl1B, Sgcd, Col5A3, Speg, Myh11, Utrn, Vamp5*
REGULATION OF PROTEIN METABOLIC PROCESS	0.005602241	**0.08103472**	*Ccnd2, Cxcl12, Ccnd1, Mid1Ip1, Igfbp3, Nck2, Tlr6, Inhba, Egfr*
REGULATION OF CELLULAR PROTEIN METABOLIC PROCESS	0.0053050397	0.11308175	
NEGATIVE REGULATION OF CELL CYCLE	0.007317073	**0.085458346**	*Bmp4, Cdkn2B, Rassf1, Lats2, Pcbp4, Gadd45A, Inhba, Myo16,*
CELL MIGRATION	0.007978723	**0.08702982**	*Hdac5, Nexn, Bbc3, Rnd1, Spta1, Chaf1B, Lasp1, Pak1, Nuak2, Nck2, Flna, Myh11, Kif1B, Myh10, Dffb, Mid1Ip1, Myo9B, Arpc5, Myo7A, Sorbs3, Mid1, Mtss1, Acta1, Krt19, Cxcl12, Cdc42Ep5, Carm1, Bcl2, Cdc42Ep2, Myh9, Dbn1, Bcar1, Ston1, Cdc42Ep1, Nexn, Slit2*
REGULATION OF CELLULAR COMPONENT ORGANIZATION AND BIOGENESIS	0.0075376886	0.087482855	
ORGANELLE ORGANIZATION AND BIOGENESIS	0.0034965035	0.10024252	
REGULATION OF PROTEIN KINASE ACTIVITY	0.019543974	**0.12093302**	*Gadd45B, Gadd45A, Adrb2, Egfr, Pak1, Rgs3, Lats2, Ccnd2, Ccnd1, Ppap2A, Nck2, Trib3, Tlr6*
REGULATION OF KINASE ACTIVITY	0.024922118	0.12954968	
REGULATION OF TRANSFERASE ACTIVITY	0.022012578	0.18824072	
HEMOPOIETIC OR LYMPHOID ORGAN DEVELOPMENT	0.021052632	**0.12460168**	*Cdk6, Csf1, Myh9, Inhba,*
HEMOPOIESIS	0.03307888	0.14885646	
INTERPHASE	0.035128806	0.19059373	*Cdkn2B, Foxn3, Cdc6, Inhba, Tpd52L1, Myo16, Cdc23, Lats2, Cdk6, Cdk4, Timeless, E2F1, Cdk10, Apbb1*
INTERPHASE OF MITOTIC CELL CYCLE	0.075980395	0.22894149	
IMMUNE SYSTEM DEVELOPMENT	0.058666665	**0.21090859**	*Cdk6, Csf1, Myh9, Inhba*
INTRACELLULAR TRANSPORT	0.04373178	**0.23124808**	*Rtp3, Tinagl1, Myo9B, Ltbp2, Adrb2, Trak1, Nudt4, Atxn1, Krt18, Bcl2, Flna, Myh9, Kdelr2, Homer3, Kif1B, Cryab, Kpna3, Myh10, Htatip2, Bcl2L1*

GO terms	NOM p-val	FDR p-val	Leading edge genes
DIGESTION	0.0	**0.0040059304**	*Cckbr, Galr2, Acsl1, Galr1, Nmu, Apoa4, Sstr1, Sstr2, Ldlr, Ppargc1A*
G PROTEIN COUPLED RECEPTOR PROTEINING PATHWAY	0.0	**0.073114395**	*Ucn, Grp, Gipr, Chrm4, Ptger2, Adrb1, Ltb4R, Gpr176, C5, Calcr, Rasd1, Tbxa2R, Galr2, Grm6, P2Ry2, Ccrl2, Qrfpr, Drd4, Ghsr, Sphk1, Ecel1, Gpr75, Apoc3, Gpr4, Gpr50, Sstr1, Adra2C, Sstr2, Adra2A, Cort, Tbl3, Adrb3, Cckbr, Gnas, Ang, Gprc5C, Gpr19, Ptger4, Lpar3, Gpr3, Adcy7, Tshr, Gabbr2, Galr1, Cdh13*
SECOND MESSENGER MEDIATEDING	0.001017294	0.10704527	
G PROTEINING COUPLED TO CYCLIC NUCLEOTIDE SECOND MESSENGER	0.0021008404	0.1183508	
CYCLIC NUCLEOTIDE MEDIATEDING	0.0021141649	0.12066743	
G PROTEINING COUPLED TO CAMP NUCLEOTIDE SECOND MESSENGER	0.0021929825	0.123322636	
CAMP MEDIATED SIGNALLING	0.0033482143	0.1347623	
G PROTEINING ADENYLATE CYCLASE ACTIVATING PATHWAY	0.010152284	0.14473984	
CELL CYCLE ARREST	0.004519774	**0.12219792**	*Ppp1R15A, Hexim1, Cdkn1C, Btg3, Foxc1, Ppp1R13B, Cdkn1B, Gadd45A, Bmp7, Tbrg4, Ppm1G, Uhmk1, Rassf1, Stk11, Bmp2, Myc, Sesn1, Plagl1, Mfn2, Inha*
NEGATIVE REGULATION OF CELL CYCLE	0.003218884	0.14732036	
MYELOID CELL DIFFERENTIATION	0.0062421975	**0.14082494**	*Hrk, Ldb1, Npr1, Notch4, Alox12, Triap1, Psen1, Aatf, Prkcz, Rela, Socs2, Socs3, Mapk8, Bag4, Bcl2L10, Bag1, Prok2, Nphp3, Mcl1, Srgn, Hspa9, Iqcb1, Ahsg, Sphk1, Bnip3, Bfar, Mif, Hipk3, Tbx3, Nfkb1, Vegfa, Gclc, Mafb, Gdnf, Akt1S1, Cdh13, Birc6, Ciapin1, Inha, Cryab, Hspa1B, Bcl2L2, Tpt1, Tbx1, Kirrel3, Tpd52, Dyrk3, Tnfsf13, Cebpg, Foxo3, Mmp9, Runx1, Lck, Ncl, Ang, Sik1, Pparg, Ywhag, Faim3, Api5*
REGULATION OF CELL DIFFERENTIATION	0.011402508	0.15203097	
HEMOPOIETIC OR LYMPHOID ORGAN DEVELOPMENT	0.0045454544	0.15907937	
IMMUNE SYSTEM DEVELOPMENT	0.0033707866	0.16592753	
HEMOPOIESIS	0.029511917	0.20347615	
ANTI APOPTOSIS	0.024691358	0.22613895	
NEGATIVE REGULATION OF DEVELOPMENTAL PROCESS	0.011044176	0.22821549	
ANGIOGENESIS	0.053426247	0.23999564	
MAPKKK CASCADE	0.0031185031	**0.14109088**	*Shc1, Gps2, Crkl, C5, Mapk8, Prok2, Nrtn, Map3K6, Map4K5, Map3K2, Dusp4, Map3K3, Dusp2, Daxx, Gadd45B, Adra2C, Dusp9, Adra2A, Mapk8lp1, Adrb3, Taok3, Mapkapk2, Madd, Ren, Map3K13, Map3K11, Trib3, Hipk3*
JNK CASCADE	0.023463687	0.23027638	
ACTIVATION OF MAPK ACTIVITY	0.026651217	0.23646247	
POSITIVE REGULATION OF MAP KINASE ACTIVITY	0.07101947	0.23854394	
REGULATION OF MAP KINASE ACTIVITY	0.014176663	0.23861583	
STRESS ACTIVATED PROTEIN KINASE PATHWAY	0.037288137	0.24164264	
ORGAN MORPHOGENESIS	0.0	**0.14697216**	*Foxc1, Foxc2, Npr1, Notch4, Cebpg, Htt, Rorb, Comp, Hey2, Prok2, Dgcr6, Pitx2, Tbx1, Tle1, Sphk1, Ptch1, Glmn, Aplp1, Lsr, Prox1, Tbx3, Vegfa, Runx1, Lhx1, Ncl, Cdh13, Ang*
VASCULATURE DEVELOPMENT	0.013605442	0.19045135	
PROTEIN PROCESSING	0.008988764	**0.14925364**	*Map3K3, Ptch1, Eif2Ak3, Lmtk2, Psen1, Ppp2R5C, Uhmk1, Aph1A, Mex3B, Aph1B, Taok3, Scg5, Cdk12, Map3K13, Map3K11,*
PROTEIN AUTOPROCESSING	0.013563502	0.16363926	
PROTEIN AMINO ACID AUTOPHOSPHORYLATION	0.019512195	0.18763559	
RESPONSE TO CHEMICAL STIMULUS	0.0	**0.16279824**	*Foxc2, Srxn1, Gipr, Hspa4L, Adipor2, Ndrg1, Cxcl2, Cygb, Rela, Herpud1, Dnajb2, Duox1, Dnajb1, C5, Prdx5, Calcr, Dnajb4, Ccrl2, Prok2, Duox2, Ghsr, Eif2B4, Hspa1L, Plaur, Apoa4, Sstr1, Hspa2, Tor1B, Sstr2, Fosl1, Cdh13, Pparg, Ang, Dgkk, Atf6, Hspa1B, Abcg2, Map2K1, Htt, Adcy8, Crhbp, Cckbr, Galr2, Crh, Hprt1, Tulp4, Rbm14, Gclc, Lats2, Gata3, Eif2B1*
RESPONSE TO HORMONE STIMULUS	0.040332146	0.2375796	
RESPONSE TO EXTRACELLULAR STIMULUS	0.055621304	0.23003663	
RESPONSE TO NUTRIENT LEVELS	0.050251257	0.2349462	
BEHAVIOR	0.03232534	0.24342304	
NEGATIVE REGULATION OF CATALYTIC ACTIVITY	0.009846827	**0.16481124**	*Hexim1, Gabbr2, Dusp2, Dnajb6, Galr1, Gps2, Trib3, Dusp9, Gla, Adra2A, Hipk3,*
NEGATIVE REGULATION OF TRANSFERASE ACTIVITY	0.06503067	0.235241	
REGULATION OF MITOTIC CELL CYCLE	0.01236094	**0.16799662**	*Btg3, Foxc1, Sphk1, Sik1*
CARBOXYLIC ACID TRANSPORT	0.017381229	**0.16933297**	*Slc7A5, Slc1A1, Slc3A1, Slc16A8, Slc16A10, Slc1A5, Slc16A3, Slc25A22*
ORGANIC ACID TRANSPORT	0.015891032	0.17032318	
AMINO ACID TRANSPORT	0.03452528	0.2391903	
RESPONSE TO BIOTIC STIMULUS	0.007352941	**0.17333063**	*Hspa1L, Bnip3, Hspa4L, Eif2Ak3, Hspa2, Tor1B, Herpud1, Fosl1, Dnajb2, Isg20, Dnajb1, Dnajb4, Irf7, Atf6, Hspa1B, Duox2*

NEGATIVE REGULATION OF CELLULAR BIOSYNTHETIC PROCESS	0.042027194	**0.19876158**	
CYTOKINE BIOSYNTHETIC PROCESS	0.07741117	0.22962262	*Hbs1L, Asmt, Ebi3, Cebpg, Gla, Mrpl10,*
REGULATION OF CYTOKINE BIOSYNTHETIC PROCESS	0.06832298	0.23044181	*Mrpl41, Paip2B, Igf2Bp2, Eif3A, Eif2B1,*
NEGATIVE REGULATION OF BIOSYNTHETIC PROCESS	0.047911547	0.23294853	*Abcf1, Yars, Eif5A, Ghsr, Eif2B4, Wars,*
REGULATION OF TRANSLATION	0.025531914	0.23323952	*Eif1Ax, Mars2, Glmn, Eif2Ak3, Samd4A,*
CYTOKINE METABOLIC PROCESS	0.068043746	0.24048725	*Eif2Ak4, Mrps7, Eif1, Sigirr, Eif3I, Rps6Kb2,*
TRANSLATIONAL INITIATION	0.07398844	0.24504815	*Eif3J, Etf1, Ltb, Inha, Eif3C, Metap1, Aars,*
TRANSLATION	0.01417004	0.24607496	
RRNA METABOLIC PROCESS	0.07870968	**0.22198431**	*Ccnk, Dbr1, Ccnt1, Ccnh, Maml1, Gfi1, Gtf2B, Ppan, Jmjd1C, Ubp1, Prdm1, Rorb,*
REGULATION OF TRANSCRIPTIONDNA DEPENDENT	0.0	0.22550389	*Yy1, Fbl, Kat5, Sox18, Myc, Trim27, Pitx2, Junb, Ccrn4L, Abt1, Map2K3, Daxx, Scaf11,*
POSITIVE REGULATION OF TRANSCRIPTION FROM RNA POLYMERASE II PROMOTER	0.044247787	0.22731736	*Cd3Eap, Sars, Gtf2F1, Gtf2F2, Hic1, Cdc40, Runx1, Ddit3, Nhp2, Erf, Srsf2, Gemin5, Preb, Atf6, Atf4, Sf1, Slbp, Rnaseh2A,*
REGULATION OF RNA METABOLIC PROCESS	0.001	0.2362661	*Dhx8, Max, Notch4, Crem, Nolc1, Gata3, Foxo3, Gata2, Htatsf1, Taf5L, Neurod2,*
RIBONUCLEOPROTEIN COMPLEX BIOGENESIS AND ASSEMBLY	0.013499481	0.23636952	*Dhx38, Nkx2-5, Ppargc1A, Ppargc1B, Hexim1, Yars, Tfap2C, Nop14, Smarca5, Scrt1, Nfkb1, Fosl2, Nfkb2, Srpk1, Fosl1,*
TRANSCRIPTION FROM RNA POLYMERASE II PROMOTER	0.0	0.23658119	*Isg20, Bmp2, Sp2, Fev, Fubp1, Maff, Ints5, Ints6, Aars, Cited1, Ldb1, Ell, Foxe1, Aff4,*
RRNA PROCESSING	0.07125	0.23826896	*Bicd1, Chd1, Pqbp1, Mecp2, Sufu, Klf10, Tgif1, Zhx2, Rbm14, Klf13, Wars, Zhx3, Dis3, Mars2, Nsun2, Ddx54, Msl3, Fos,*
RNA BIOSYNTHETIC PROCESS	0.0	0.2387882	*Tfb2M, Utf1, Pax1, Elf1, Prpf18, Nfx1, Elf4, Myod1, Irf7, Polr1E, Pparg, Ang, Rp9, Pabpc1, Ppard, Cebpb, Sp100, Gtf3C4,*
TRANSCRIPTION DNA DEPENDENT	0.0	0.24150117	*Rnmt, Sfswap, Vps4B, Taf9, Srsf1, Cebpg, Cxxc1, Foxk2, Hoxd13, Rnf4, Hira, Mnt, Nfil3, Creg1, Plagl1, Ubn1, Nrip1, Hsf4,*
REGULATION OF TRANSCRIPTION FROM RNA POLYMERASE II PROMOTER	0.002002002	0.24264829	*Tceb3, E2F3, Polr2G, Polr2I, Exosc3, Cdx2, Nfya, Klf4, Sod2, Meis2, Pou4F2, Tbx3, Apex1, Klf9, Cebpz, Bcor, Ptf1A, Neurog1,*
RIBOSOME BIOGENESIS AND ASSEMBLY	0.046116505	0.2432781	*Hspa1B, Taf2, Ddx20, Paip2B, Eif2B1, Eif5A, Eif2B4, Sf3A2, Eif1Ax, Eif2Ak3, Eif2Ak4, Eif1, Eif3I, Eif3J, Gemin6, Eif3C,*
RNA METABOLIC PROCESS	0.0	0.24880055	*Eif3A, Eif3B, Med13, Sdad1, Exosc7, Nop56, Nop58, Dkc1, Pop4, Rrp9*
HOMEOSTATIC PROCESS	0.010090818	**0.22633311**	*Dyrk3, Calcb, Ldb1, Npr1, Hfe, Cebpg, Lpar3, Slc2A4, Foxo3, Clcn3, Rdh12, Galr2,*
CELLULAR CATION HOMEOSTASIS	0.019169329	0.23111418	*P2Ry2, Myc, Prok2, Nphp3, Tac1, Dfnb31,*
CATION HOMEOSTASIS	0.02208202	0.23914082	*Ppargc1A, Cd55, Bnip3, Slc4A11, Apoa4, Mafb, Cckbr, Trpv4, Ddit3, Fxn*
POTASSIUM ION TRANSPORT	0.057458565	**0.22661947**	*Kcnj4, Kcng2, Kcnj5, Kcnk6, Kcnk7, Kcns1, Kcnc1, Abcc8, Kcnc3, Kcnq1, Kcna1, Kcna6*
SKELETAL DEVELOPMENT	0.02098636	**0.23123316**	*Tbx1, Klf10, Srgn, Kl, Gdf11, Msx2, Npr3, Hoxd13, Aebp1, Tbx3, Papss2, Pax1, Dll3, Comp, Sufu, Inha*
FATTY ACID METABOLIC PROCESS	0.030335862	**0.23430063**	*Cpt1A, Mif, Cpt1B, Adipor2, Ptgs1, Acot2,*
FATTY ACID OXIDATION	0.07607362	0.2289283	*Acot1, Hacl1, Acadm, Ppargc1A, Acot4, Ptges, Ppard, Alox12*
CELL CELL ADHESION	0.02383532	**0.2394498**	*Cldn5, Cd164, Cldn4, Cldn3, Cd93, Amigo3, Cldn14, Cldn23, Cdh13, Apoa4*
REGULATION OF GROWTH	0.07909604	**0.24562493**	*Tspyl2, Cda, Ghsr, Sertad3, Cdkn1B, Sphk1, Ptch1, Bbc3*
GO term (DOWN)			
MUSCLE DEVELOPMENT	0.0	**0.19455878**	*Svil, Tagln, Notch1, Igfbp3, Cby1, Sri, Mapk12, Acta1, Csrp3, Krt19, Sgcd, Gyltl1B, Sgca, Col5A3, Capn3, Speg, Tnni3, Myh11, Vamp5, Myh6, Sgcg, Kcnh1, Myh7*

REFERENCES

Altarejos JY, Montminy M. 2011. CREB and the CRTC co-activators: sensors for hormonal and Metabolic Signals. Nat. Publ. Gr. 12:141–151.

Araque A. 2008. Astrocytes process synaptic information. Neuron Glia Biol. 4:3–10.

Arvey A, Agius P, Noble WS, Leslie C. 2012. Sequence and chromatin determinants of cell-type-specific transcription factor binding. Genome Res. 22:1723–1734.

Barco A, Alarcon JM, Kandel ER. 2002. Expression of constitutively active CREB protein facilitates the late phase of long-term potentiation by enhancing synaptic capture. Cell 108:689–703.

Barco A, Marie H. 2011. Genetic approaches to investigate the role of CREB in neuronal plasticity and memory. Mol. Neurobiol. 44:330–349.

Barco A, Patterson SL, Patterson S, Alarcon JM, Gromova P, Mata-Roig M, Morozov A, Kandel ER. 2005. Gene expression profiling of facilitated L-LTP in VP16-CREB mice reveals that BDNF is critical for the maintenance of LTP and its synaptic capture. Neuron 48:123–37.

Behar KL, Rothman DL. 2001. In vivo nuclear magnetic resonance studies of glutamate-gamma-aminobutyric acid-glutamine cycling in rodent and human cortex: the central role of glutamine. J. Nutr. 131:2498S–504S; discussion 2523S–4S.

Benito E, Valor LM, Jimenez-Minchan M, Huber W, Barco A. 2011. cAMP response element-binding protein is a primary hub of activity-driven neuronal gene expression. J. Neurosci. 31:18237–18250.

Butt AM, Kalsi A. 2006. Inwardly rectifying potassium channels (Kir) in central nervous system glia: A special role for Kir4.1 in glial functions. J. Cell. Mol. Med. 10:33–44.

Cardona C, Sánchez-Mejías E, Dávila JC, Martín-Rufián M, Campos-Sandoval J a, Vitorica J, Alonso FJ, Matés JM, Segura J a, Norenberg MD, et al. 2015. Expression of Gls and Gls2 glutaminase isoforms in astrocytes. Glia:365–382.

Carriba P, Pardo L, Parra-Damas A, Lichtenstein MP, Saura CA, Pujol A, Masgrau R, Galea E. 2012. ATP and noradrenaline activate CREB in astrocytes via noncanonical Ca2+ and cyclic AMP independent pathways. Glia 60:1330–1344.

Corbett GT, Roy A, Pahan K. 2013. Sodium phenylbutyrate enhances astrocytic neurotrophin synthesis via protein kinase C (PKC)-mediated activation of cAMP-response element-binding protein (CREB): implications for Alzheimer disease therapy. J. Biol. Chem. 288:8299–312.

Cha-Molstad H, Keller DM, Yochum GS, Impey S, Goodman RH. 2004. Cell-type-specific binding of the transcription factor CREB to the cAMP-response element. Proc. Natl. Acad. Sci. 101:13572–13577.

Chang SP, Gong R, Stuart J, Tang SJ. 2006. Molecular network and chromosomal clustering of genes involved in synaptic plasticity in the hippocampus. J. Biol. Chem. 281:30195–30211.

Chevalier SA, Turpin J, Cachat A, Afonso P V., Gessain A, Brady JN, Pise-Masison CA, Mahieux R. 2014. Gem-Induced Cytoskeleton Remodeling Increases Cellular Migration of

HTLV-1-Infected Cells, Formation of Infected-to-Target T-Cell Conjugates and Viral Transmission. PLoS Pathog. 10 (2):e1003917.

Dash PK, Hochner B, Kandel ER. 1990. Injection of the cAMP-responsive element into the nucleus of Aplysia sensory neurons blocks long-term facilitation. Nature 345:718–721.

Dekker J. 2014. Two ways to fold the genome during the cell cycle : insights obtained with chromosome conformation capture. Epigenetics Chromatin 7:1–12.

Dib K, el Jamali a, Jacquemin C, Corrèze C. 1994. Cyclic AMP regulation of messenger RNA level of the stimulatory GTP-binding protein Gs alpha. Isoproterenol, forskolin and 8-bromoadenosine 3':5'-cyclic monophosphate increase the level of Gs alpha mRNA in cultured astroglial cells. Eur. J. Biochem. 219:529–537.

Dienel G a., McKenna MC. 2014. A dogma-breaking concept: glutamate oxidation in astrocytes is the source of lactate during aerobic glycolysis in resting subjects. J. Neurochem. 131:395–398.

Euskirchen G, Royce TE, Bertone P, Martone R, Rinn JL, Nelson FK, Sayward F, Luscombe NM, Miller P, Gerstein M, et al. 2004. CREB binds to multiple loci on human chromosome 22. Mol. Cell. Biol. 24:3804–3814.

Greenberg ME, Thompson MA, Sheng M. 1992. Calcium regulation of immediate early gene transcription. In: Journal of Physiology Paris. Vol. 86. p. 99–108.

Hertz L, Peng L, Dienel G a. 2007. Energy metabolism in astrocytes: high rate of oxidative metabolism and spatiotemporal dependence on glycolysis/glycogenolysis. J. Cereb. Blood Flow Metab. 27:219–249.

Impey S, McCorkle SR, Cha-Molstad H, Dwyer JM, Yochum GS, Boss JM, McWeeney S, Dunn JJ, Mandel G, Goodman RH. 2004. Defining the CREB regulon: A genome-wide analysis of transcription factor regulatory regions. Cell 119:1041–1054.

Karki P, Webb A, Smith K, Lee K, Son D-S, Aschner M, Lee E. 2013. cAMP response element-binding protein (CREB) and nuclear factor κB mediate the tamoxifen-induced up-regulation of glutamate transporter 1 (GLT-1) in rat astrocytes. J. Biol. Chem. 288:28975–86.

Khatri P, Sirota M, Butte AJ. 2012. Ten years of pathway analysis: current approaches and outstanding challenges. PLoS Comput. Biol. 8 (2):e1002375.

Koyama Y, Kiyo-oka M, Osakada M, Horiguchi N, Shintani N, Ago Y, Kakuda M, Baba A, Matsuda T. 2006. Expression of prokineticin receptors in mouse cultured astrocytes and involvement in cell proliferation. Brain Res. 1112:65–69.

Lakhina V, Arey RN, Kaletsky R, Kauffman A, Stein G, Keyes W, Xu D, Murphy CT. 2015. Genome-wide Functional Analysis of CREB/Long-Term Memory-Dependent Transcription Reveals Distinct Basal and Memory Gene Expression Programs. Neuron 85:330–345.

Lalo U, Palygin O, Rasooli-Nejad S, Andrew J, Haydon PG, Pankratov Y. 2014. Exocytosis of ATP From Astrocytes Modulates Phasic and Tonic Inhibition in the Neocortex. Bacci A, editor. PLoS Biol. 12 (4):e1001857.

Lee M, Schwab C, Mcgeer PL. 2011. Astrocytes are GABAergic cells that modulate microglial activity. Glia 59:152–165.

Lovatt D, Sonnewald U, Waagepetersen HS, Schousboe A, He W, Lin JH-C, Han X, Takano T, Wang S, Sim FJ, et al. 2007. The transcriptome and metabolic gene signature of protoplasmic astrocytes in the adult murine cortex. J. Neurosci. 27:12255–12266.

Maclean FL, Williams RJ, Horne MK, Nisbet DR. 2015. A Commentary on the Need for 3D-Biologically Relevant In Vitro Environments to Investigate Astrocytes and Their Role in Central Nervous System Inflammation. Neurochem. Res. Special Is:1–4.

Martianov I, Choukrallah M-A, Krebs A, Ye T, Legras S, Rijkers E, Van Ijcken W, Jost B, Sassone-Corsi P, Davidson I. 2010. Cell-specific occupancy of an extended repertoire of CREM and CREB binding loci in male germ cells. BMC Genomics 11:530.

Mayr B, Montminy M. 2001. Transcriptional regulation by the phosphorylation-dependent factor CREB. Nat. Rev. Mol. Cell Biol. 2:599–609.

Naqvi S, Martin KJ, Arthur JSC. 2014. CREB phosphorylation at Ser133 regulates transcription via distinct mechanisms downstream of cAMP and MAPK signalling. Biochem. J. 458:469–79.

Navarrete M, Perea G, de Sevilla DF, Gómez-Gonzalo M, Núñez A, Martín ED, Araque A. 2012. Astrocytes Mediate In Vivo Cholinergic-Induced Synaptic Plasticity. Scheiffele P, editor. PLoS Biol. 10 (2):e1001259.

Panov A, Orynbayeva Z, Vavilin V, Lyakhovich V. 2014. Fatty acids in energy metabolism of the central nervous system. Biomed Res. Int. 2014: 1-22

Parra-Damas A, Valero J, Chen M, España J, Martín E, Ferrer I, Rodríguez-Alvarez J, Saura C a. 2014. Crtc1 activates a transcriptional program deregulated at early Alzheimer's disease-related stages. J. Neurosci. 34:5776–5787.

Patel AB, de Graaf RA, Mason GF, Rothman DL, Shulman RG, Behar KL. 2005. The contribution of GABA to glutamate/glutamine cycling and energy metabolism in the rat cortex in vivo. Proc. Natl. Acad. Sci. U. S. A. 102:5588–5593.

Perez V, Bouschet T, Fernandez C, Bockaert J, Journot L. 2005. Dynamic reorganization of the astrocyte actin cytoskeleton elicited by cAMP and PACAP: A role for phosphatidylinositol 3-kinase inhibition. Eur. J. Neurosci. 21:26–32.

Puschmann TB, Zandén C, Lebkuechner I, Philippot C, De Pablo Y, Liu J, Pekny M. 2014. HB-EGF affects astrocyte morphology, proliferation, differentiation, and the expression of intermediate filament proteins. J. Neurochem. 128:878–889.

Ravnskjaer K, Kester H, Liu Y, Zhang X, Lee D, Yates JR, Montminy M. 2007. Cooperative interactions between CBP and TORC2 confer selectivity to CREB target gene expression. EMBO J. 26:2880–9.

Riccio A, Ahn S, Davenport CM, Blendy JA, Ginty DD. 1999. Mediation by a CREB family transcription factor of NGF-dependent survival of sympathetic neurons. Science 286:2358–2361.

Rossi D. 2015. Progress in Neurobiology Astrocyte physiopathology : At the crossroads of intercellular networking , inflammation and cell death. Prog. Neurobiol. 130:86–120.

Satoh JI, Tabunoki H, Arima K. 2009. Molecular network analysis suggests aberrant CREB-mediated gene regulation in the Alzheimer disease hippocampus. Dis. Markers 27:239–252.

Shibasaki K, Ikenaka K, Tamalu F, Tominaga M, Ishizaki Y. 2014. A novel subtype of astrocytes expressing TRPV4 (Transient Receptor Potential Vanilloid 4) Regulates neuronal excitability via release of gliotransmitters. J. Biol. Chem. 289:14470–14480.

Thonberg H, Fredriksson JM, Nedergaard J, Cannon B. 2002. A novel pathway for adrenergic stimulation of cAMP-response-element-binding protein (CREB) phosphorylation: mediation via alpha1-adrenoceptors and protein kinase C activation. Biochem. J. 364:73–79.

Troadec JD, Marien M, Darios F, Hartmann A, Ruberg M, Colpaert F, Michel PP. 2001. Noradrenaline provides long-term protection to dopaminergic neurons by reducing oxidative stress. J. Neurochem. 79:200–210.

Vardjan N, Kreft M, Zorec R. 2014. Dynamics of β-adrenergic/cAMP signaling and morphological changes in cultured astrocytes. Glia 62:566–579.

Wandosell F, Bovolenta P, Nieto-Sampedro M. 1993. Differences between reactive astrocytes and cultured astrocytes treated with di-butyryl-cyclic AMP. J. Neuropathol. Exp. Neurol. 52:205–215.

Wen H, Cao J, Yu X, Sun B, Ding T, Li M, Li D, Wu H, Long L, Xu G, et al. 2013. Spatiotemporal patterns of Gem expression after rat spinal cord injury. Brain Res. 1516:11–19.

Wu VW, Schwartz JP. 1998. Cell culture models for reactive gliosis: New perspectives. J. Neurosci. Res. 51:675–681.

Yenari MA, Liu J, Zheng Z, Vexler ZS, Lee JE, Giffard RG. 2005. Antiapoptotic and anti-inflammatory mechanisms of heat-shock protein protection. In: Annals of the New York Academy of Sciences. Vol. 1053. p. 74–83.

Zhang X, Odom DT, Koo S-H, Conkright MD, Canettieri G, Best J, Chen H, Jenner R, Herbolsheimer E, Jacobsen E, et al. 2005. Genome-wide analysis of cAMP-response element binding protein occupancy, phosphorylation, and target gene activation in human tissues. Proc. Natl. Acad. Sci. U. S. A. 102:4459–4464.

Zlokovic B V. 2008. The Blood-Brain Barrier in Health and Chronic Neurodegenerative Disorders. Neuron 57:178–201.

Results III

Targeted activation of CREB in reactive astrocytes is neuroprotective in focal acute cortical injury

Submitted to GLIA

Targeted activation of CREB in reactive astrocytes is neuroprotective in focal acute cortical injury

Luis Pardo[1], Agatha Schlüter[2], Luis M. Valor[3], Angel Barco[3], Mercedes Giralt[4], Juan Hidalgo[4], Peilin Jia[5], Zhongming Zhao[5], Mariona Jové[6], Manuel Portero-Otin[6], Montserrat Ruiz[2], Lydia Giménez-Llort[7], Roser Masgrau[1], Aurora Pujol[2,8]and Elena Galea[1,8]

1. Institut de Neurociències and Unitat de Bioquímica, Facultat de Medicina, Universitat Autònoma de Barcelona, Bellaterra, 08193 Barcelona, Spain; luis.pardo82@gmail.com roser.masgrau@uab.cat galea.inc@gmail.com
2. Neurometabolic Diseases Laboratory, Bellvitge Biomedical Research Institute (IDIBELL), L'Hospitalet de Llobregat, 08907 Barcelona, Spain; Center for Biomedical Research on Rare Diseases (CIBERER), ISCIII, Spain; apujol@idibell.cat mruiz@idibell.cat
3. Instituto de Neurociencias de Alicante, Universidad Miguel Hernández/Consejo Superior de Investigaciones Científicas, Sant Joan d'Alacant, 03550 Alicante, Spain; abarco@umh.es lmv@ umh.es
4. Institut de Neurociències and Department of Cellular Biology, Physiology and Immunology, Faculty of Biosciences, Universitat Autònoma, 08193 Barcelona, Spain; juan.hidalgo@uab.es merce.giralt@uab.cat
5. Departments of Biomedical Informatics and Psychiatry, Vanderbilt University School of Medicine, Nashville, TN, USA; peilin.jia@vanderbilt.edu zhongming.zhao@vanderbilt.edu
6. Department of Experimental Medicine, University of Lleida-Biomedical Research Institute of Lleida, 25198 Lleida, Spain; manuel.portero@mex.udl.cat mariona.jove@udl.cat
7. Institut de Neurociènces and Department of Psychiatry and Forensic Medicine, School of Medicine, Universitat Autònoma de Barcelona, 08193 Bellaterra, Spain; lidia.gimenez@uab.cat
8. Institució Catalana de Recerca i Estudis Avançats (ICREA), Barcelona, Spain

Corresponding autor:
Elena Galea
Institut de Neurociències
Universitat Autònoma de Barcelona
Bellaterrra
08193 Barcelona, Spain
Email: galea.inc@gmail.com
Phone: +34 93 586 8143
Fax: +34 93 581 1573

Running title: neuroprotection by astrocytic CREB

Abstract

The clinical challenge in acute injury as in traumatic brain injury (TBI) is to halt the delayed neuronal loss that occurs hours and days after the insult. Here we report that the activation of CREB-dependent transcription in reactive astrocytes prevents secondary injury in cerebral cortex after experimental TBI. The study was performed in a novel bitransgenic mouse in which a constitutively active CREB, VP16-CREB, was targeted to astrocytes with the Tet-Off system. Using histochemistry, qPCR, and gene profiling we found less neuronal death and damage, reduced macrophage infiltration, and rescued expression of mitochondrial pathway genes in bitransgenic mice as compared to wild type littermates. Finally, with meta-analyses using publicly available databases we identified a core set of VP16-CREB candidate target genes that may account for the neuroprotective effect. Enhancing CREB activity in astrocytes thus emerges as a novel avenue in acute brain post-injury therapeutics.

Key words: Astrocytes, CREB, neuroinflammation, neuroprotection, traumatic brain injury

Introduction

It is well established that transcription factor cAMP response element-binding protein (CREB) regulates learning and memory (Barco and Marie, 2011), and that deregulation of CREB-dependent transcription (CDT) may contribute to brain pathologies including addiction (Dong and Nestler 2014), epilepsy (Park et al. 2003), and neurodegeneration (Shimohata et al. 2000; Valor et al. 2010; Parra-Damas et al. 2014). The studies thus far have overwhelmingly focused on the actions of CREB in neurons, where the factor activates the coordinated expression of hundreds of genes controlling activity-dependent synaptic plasticity and neuronal survival (Benito et al. 2011). Henceforth we refer to the activation of CREB-dependent transcriptional programs in neurons as CDTN. By contrast, despite the discovery that several neurotransmitters do trigger CDT in astrocytes (CDTA) (Carriba et al. 2012), the role of this transcriptional program in health and in disease has not been explored. The overarching questions are whether and how astrocytes influence experience-driven memory formation or brain damage *via* CREB, and the differences between CDTN and CDTA.

We sought to determine the effect of stimulating CDTA on the outcome of a focal cortical injury induced by a cryolesion, a model of traumatic brain injury (TBI) (Albert-Weissenberger and Siren 2010). To this end, we have developed a novel bitransgenic mouse using the tetracycline-regulated tTA-TetOff system whereby a constitutively active CREB, VP16-CREB, was targeted to astrocytes by crossing TetO-VP16-CREB and Gfa2-TtA mice. VP16 is a herpes-virus derived strong transcriptional activator that when fused to the DNA binding domain of CREB produces a chimeric protein (Suppl. Fig. 1) that drives transcription from CRE-driven promoters in a constitutive manner (Riccio et al. 1999). VP16-CREB and TetO-VP16-CREB/CaMKII-Tta mice—*CaMKII* being a neuron-specific promoter—have been instrumental in gain-of-function strategies to characterize the impact of CDTN in plasticity and neurodegeneration, and to identify target genes (Barco et al. 2005). *Gfa2* is a widely used construct based on the human promoter of the astrocyte-specific gene encoding for the glial

fibrillary acidic protein (GFAP) (Lee et al. 2008). Thus, VP16-CREB/Gfa2-TtA mice allow us to manipulate CDT in astrocytes decoupling its activation from upstream kinase cascades.

Acute brain injury produced by ischemia and spinal cord injury, as well as by TBI caused by traffic accidents, falls, and blast exposure in the military, affects millions of patients worldwide. Despite a wealth of preclinical studies and clinical trials no satisfactory treatment has yet been discovered for these injuries (for review, Tymianski 2013; Xiong et al. 2013; Silva et al. 2014). The pending challenge is not to stop the brain tissue loss that irremediably occurs soon after the insult, but to arrest secondary damage to prevent further loss of neurons and to aid recovery. Reactive astrogliosis defined by cytoskeleton hypertrophy associated with GFAP upregulation is a standard delayed reaction to brain damage. Although the role of reactive astrocytes is still debated, the inhibition of gliosis is highly detrimental in several experimental models of brain damage including stab injury (Bush et al. 1999), spinal cord injury (Faulkner et al. 2004), and neurodegeneration (Kraft et al. 2013). This evidence strongly suggests that post-injury gliosis helps to withstand insult and improve recovery after brain damage. It follows that the potentiation of astrogliosis-driven genes impinging on secondary protection, repair and regeneration may be a most efficient strategy for therapeutic post-injury intervention.

In the present study, combining genome-wide gene profiling, immunohistochemistry and qPCR-based validations, we found that TetO-VP16-CREB/Gfa2-tTA mice, which show transgene expression conditional to gliosis, are protected against the secondary injury caused in cortex by a cryolesion. With the aid of meta-analyses we narrowed down the search to a short list of VP16-CREB candidate target genes transactivated in reactive astrocytes, and which may account for the observed protection. While therapies targeting CDTN are being pursued in Alzheimer's disease (Parra-Damas et al. 2014), [ClinicalTrials.gov NCT01409564], axon regeneration (Gao et al. 2004; Ma et al. 2014), and stroke (Bell et al. 2013; Lai et al. 2014),

our study paves the way for the development of CDTA-based therapeutics to help treat acute brain injury in a clinically manageable window.

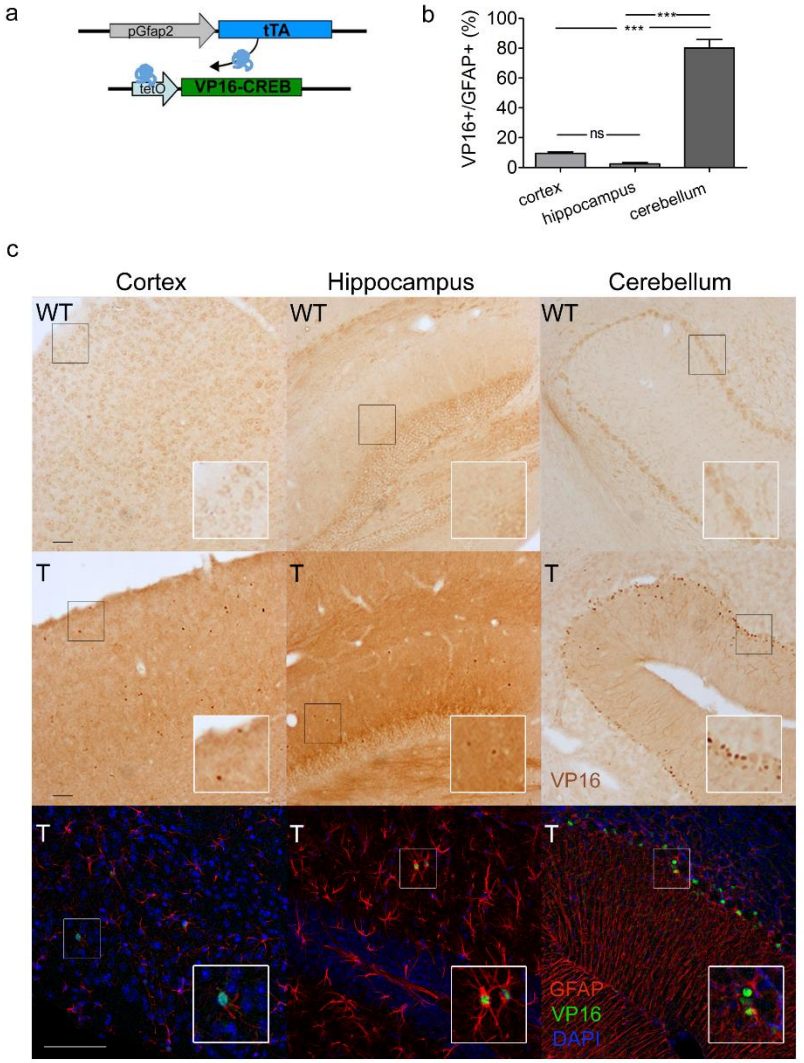

Figure 1. Characterization of the genetic tool in basal conditions. a) Bitransgenic mice were generated by crossing Gfa2-tTA x TetO-VP16-CREB mice. Schematic of the tetracycline-regulated tTA-TetOff system. b) Quantification of the percentage of astrocytes (GFAP-positive cells) expressing VP16-CREB in bitransgenic mice. Data are the means of 3 independent measurements. Images are in Fig. 1c. c) Immunodetection of VP16 in WT and bitransgenic mice (T). First and second rows show DAB-based staining, and the third row confocal images of VP16 (green) GFAP (red) and DAPI (blue) immunodetection. Image processing: the green channel was enhanced to facilitate VP16-CREB visualization, and contrast was equally increased for all images with Adobe Photoshop. Bars are 50 µm.

Results

Region-selective targeted expression of VP16-CREB in astrocytes in basal conditions

First, we characterized by VP16 immunodetection the expression of VP16-CREB in the brain of the newly generated Gfa2-TtA/TetO-VP16-CREB mice (Fig. 1a). The mice show low expression of VP16-CREB across the forebrain—with the exception of a few scattered nuclei in cortex and hippocampus—and high expression in nuclei lining the Purkinje cell layer of the cerebellum (Fig. 1c, first and second rows). The cells expressing VP16-CREB are, in all cases, astrocytes since they co-localize with GFAP (Fig. 1b, and c, last row). While 80% of the Bergmann glial cells present VP16, only 10% of cortical and 2% of hippocampal astrocytes are positive for the antigen (Fig. 1b). This pattern of VP16-CREB distribution with preferential expression in cerebellar radial glia has been repeatedly reported in transgenes driven by *Gfa2* (Corbin et al. 1996; Prado et al. 2013; Almolda et al. 2014) or by other *Gfap*-based promoters (Lioy et al. 2011).

Focal cortical injury drives expression of VP16-CREB in forebrain astrocytes

The regionalized basal expression of *Gfap*-based promoters—for which there is yet no explanation—does not restrict the use of the resulting transgenic mice to the analysis of cerebellar astrocyte genes. On the contrary, because the upregulation of *Gfap* is a hallmark of brain injury, we reasoned that VP16-CREB would be up-regulated in reactive astrocytes in cerebral cortex and that, if this was the case, the novel Gfa2-TtA/TetO-VP16-CREB mice would offer a unique opportunity to examine the therapeutic potential of astrocytic CREB in forebrain injury. The low VP16-CREB expression in basal conditions would, moreover, facilitate the statistical evaluation of the effects of the transgene in experimental injury. To test these ideas, bitransgenic mice and WT littermates were subjected to a cortical cryolesion or spared from it, sacrificed 1-20 dpl, and processed for several analyses as depicted in Fig. 2a.

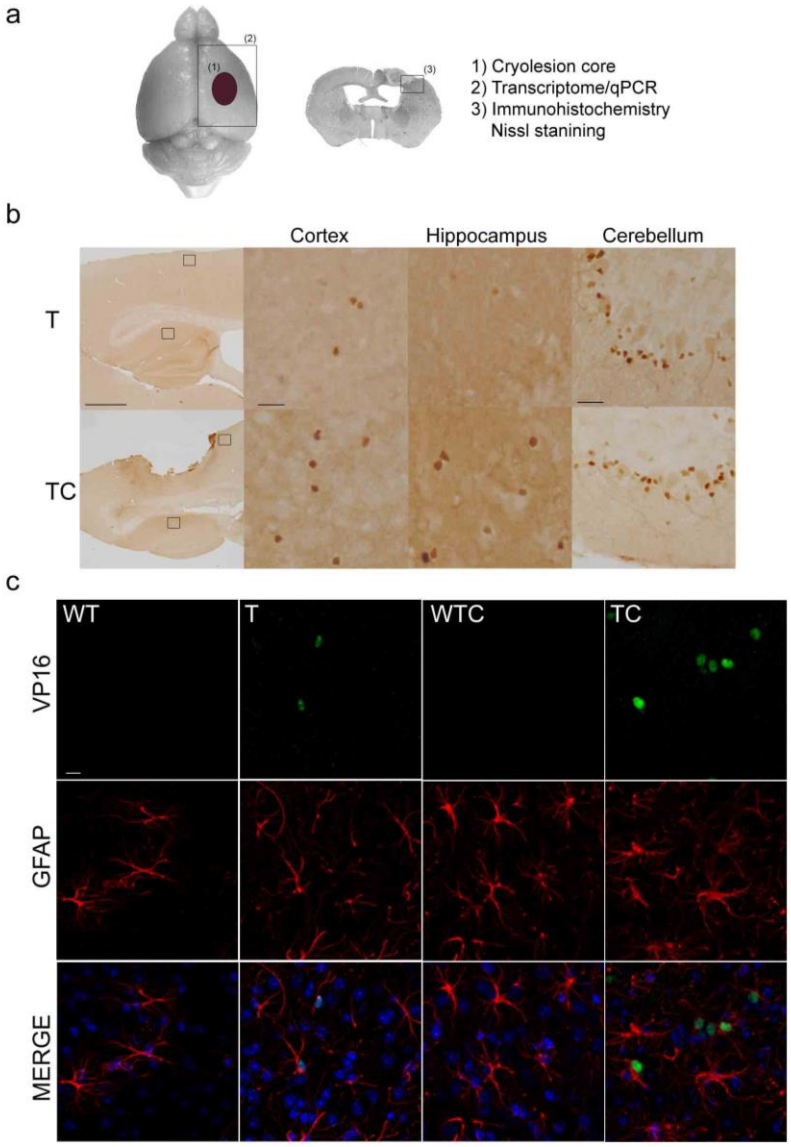

Figure 2. Characterization of the genetic tool after an acute cortical injury. a) Areas analysed and procedures followed after causing a focal cryolesion in the somatosensory cortex. b) DAB-based immunohistochemistry of VP16-CREB showing more nuclei stained in forebrain outside the core of the lesion, but equal expression in cerebellum at 3 dpl. T and TC represent, respectively, bitransgenic mice in basal and injured conditions. Bars are 500 µm for the pictures at a low magnification (first column), and 50 µm for the rest. c) Co-localization of VP16-CREB (green) and GFAP (red) showing that VP16-CREB is still, and only, expressed in astrocyte nuclei after injury. The images are from the cortical area surrounding the core. Bar is 50 µm. d) Quantification of VP16-CREB expression using the materials shown in Fig.1c. The number of astrocytes expressing

VP16-CREB increases 5-fold after the cryolesion. Values are the means ± SEM or n=4 (*) p<0.05; (***) p<0.001, TC *vs* T. Student's T test. e, f) Quantification of VP16-CREB and GFAP expression by qPCR. Cryolesion causes the parallel upregulation of VP16-CREB and GFAP and mRNA expression. VP16 and GFAP mRNA contents were quantified by qPCR 1-3 dpl. Values are the means ± SEM of n=5-6. Symbol utilization: (&&&) control *vs* cryolesion; (*): WT *vs* bitransgenics; and (#): comparison between dpl. *qPCR VP16:* (*) p<0.05; (***) p<0.001. One way ANOVA followed by Bonferroni. *qPCR GFAP:* (&&&) p<0.001 in control *vs* cryolesion, (***) p<0.001 in WT *vs* T; (##) p<0.01 in 1 dpl *vs* 3 dpl; generalized linear model with Wald Chi-square test (see parameters in

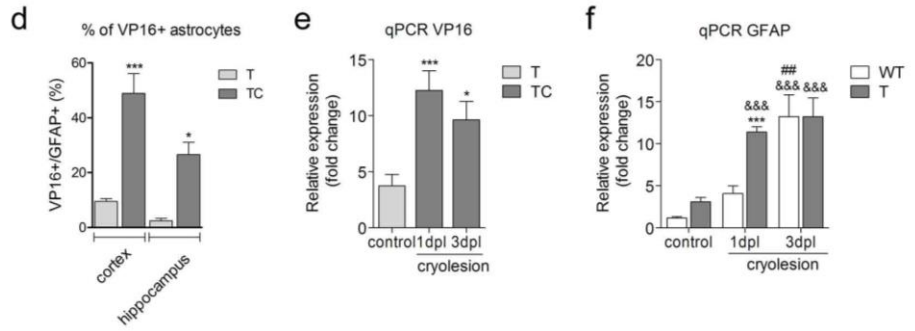

table 1).

Cryolesion is a well-characterized model of acute cortical injury (Penkowa and Moos 1995) that mimics the pathophysiology of TBI, with massive neuronal death after primary injury and increased inflammation, reactive astrogliosis, macrophage infiltration and glial scar formation happening from ours to weeks after insult (Burda and Sofroniew 2014).

VP16-CREB expression did increase after the cortical cryolesion mirroring GFAP as predicted (Fig. 2). First, more nuclei were stained in cortex and hippocampus, but not in cerebellum, as shown by DAB immunostaining (Fig. 2b) and immunofluorescence (Fig. 2c). Quantification of VP16 immunofluorescence showed that 45% of the astrocytes were VP16-positive in cortex, and 25% in hippocampus. These numbers represent 15- and 5-fold increases of VP16 expression over basal in hippocampus and cortex, respectively (Fig. 2d). Second, VP16-CREB mRNA was up-regulated 3-4 fold over basal conditions at 1-3 dpl (Fig. 2e), following the pattern observed for GFAP mRNA. Note that the expression of GFAP was accelerated in bitransgenic mice as compared to WT mice (Fig. 2f),

suggesting that VP16-CREB stimulates *Gfap* expression. Accordingly, note also that GFAP was slightly up-regulated in bitransgenic mice in baseline conditions, as revealed by immunodetection (Fig. 2c, column "T") and PCR (Fig. 2f), although astrocytes lacked the hypertrophy typical of reactive astrocytes post-injury, which is clearly apparent after the cryolesion (compare columns "WTC" and "TC"). Altogether, these results indicate: i) that VP16-CREB is strongly upregulated after the cryolesion, plausibly due to the injury-elicited activation of *Gfa2* as a *Gfap*-based promoter, and ii) that the expression of VP16-CREB in astrocytes promotes an increase in reactive gliosis.

VP16-CREB protects against secondary injury

A necrotic core was visible in injured mice after 3 dpl, and its size decreased 60% by 10 dpl (Fig. 3a, b). The size of the core was not affected by genotype, only by cryolesion ($F = 30.34$, two-way ANOVA, Table 1). Since the core is the result of the immediate cell death that occurs minutes and hours after the insult, the similar core size in WT and bitransgenics indicates that the latter are not protected against *primary* neuronal death, consistent with the low expression of VP16-CREB in basal conditions.

In contrast, the robust up-regulation of VP16-CREB in reactive astrocytes interfered with secondary neuronal damage and death (Fig. 3c-g). Neuronal damage was assessed by the expression of synaptophysin (*Syn*), a marker of synapses, and of intermediate neurofilament (*Nefm*) and SMI, both axonal markers. SMI was assessed with immunohistochemistry, and *Nefm* and *Syn* by qPCR. Neuronal death, in turn, was examined by quantifying neuronal density after Nissl staining.

In WT mice, the cryolesion decreased neuronal density in the injured hemisphere by 50% at 3 dpl, and by 30% at 10 dpl compared to contralateral (Fig. 3c, d). Those values are significantly attenuated in bitransgenic mice (Fig. 3c, d, and $F = 7.104$ for "genotype" in Table 1). The *apparent* increase in neuronal density overtime may be attributed, at least in part, to the

reduction of edema, since the increased cortical thickness detected at 3 dpl was significantly reduced at 10 dpl (Fig. 3d). However, no difference in cortical thickness was detected between WT and bitransgenics (Fig. 3d), thus ruling out that the enhanced neuronal density in the latter was due to differences in edema caused by the transgene. Consistent with the neuronal

death, the expression of S*yn*, *Nefm* (Fig. e), and SMI (Fig. 3f, g) was reduced by 30-50 % in WT mice while this decrease was prevented in bitransgenics (Fig. 3e, f, g) (F = 4.013-12.42 for "genotype", Table 1).

Figure 3. Astrocytic VP16-CREB reduces secondary injury
WT and bitransgenic mice (T) were processed for histochemical or qPCR analysis at 3, 10 and 20

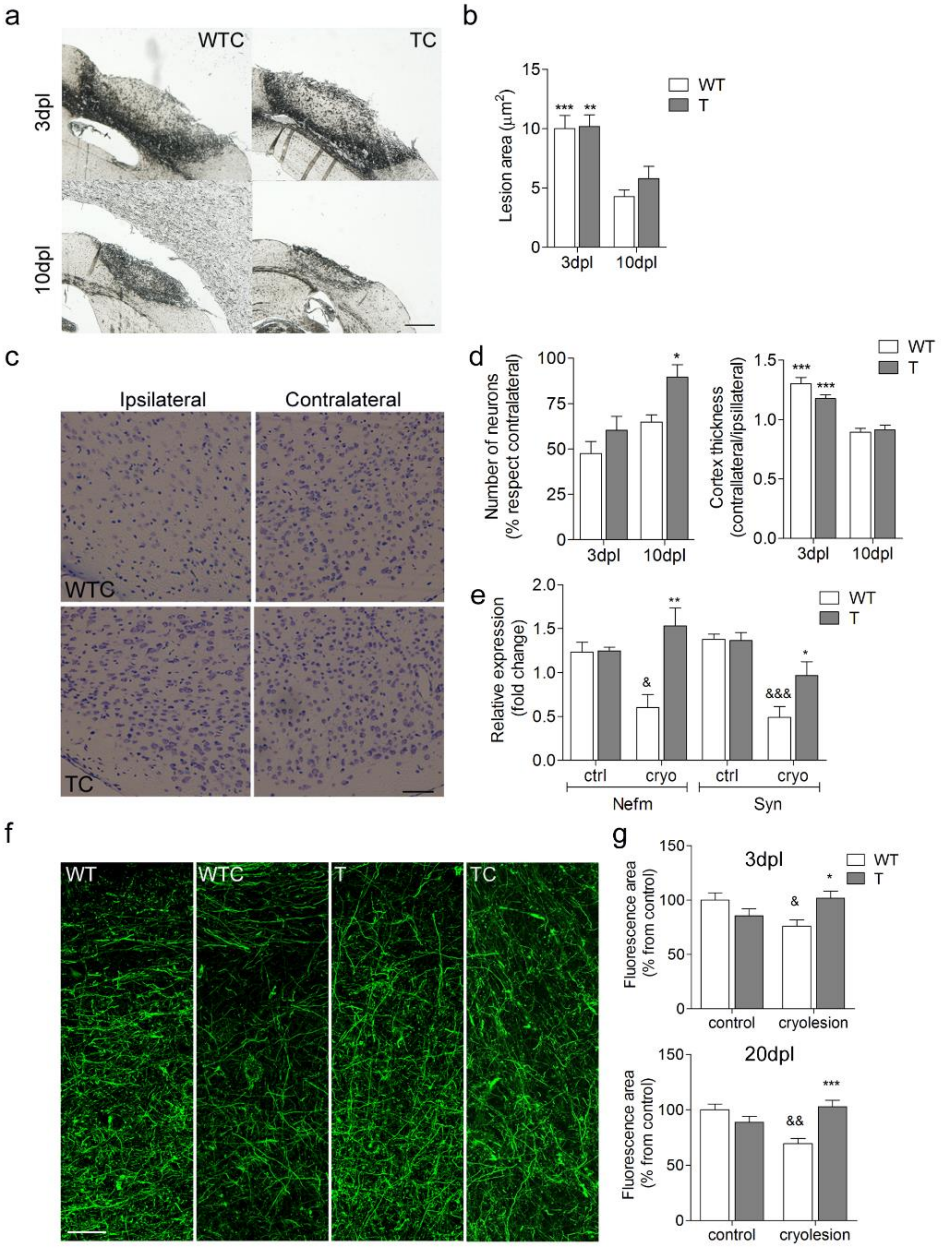

dpl to examine primary injury (core size) and secondary injury, assessed by neuronal density (Nissl staining), neurofilament density (SMI-312 and *Nefm*) and synapse density (*Syn)* in the boundary zone. a, b) Representative lesions at 3 and 10 dpl in paraffin-embedded sections and quantification. Core sizes were greatly reduced at 10 dpl. No difference was observed between WT and bitransgenic mice in core size. Data are the means ± SEM of 6-7 mice. (**) $p<0.01$, (***) $p<0.001$, 3 dpl vs 10 dpl; two-way ANOVA (F-values in Table 1) followed by Bonferroni. Bars are 500 µm. c, d) VP16-CREB increased neuronal survival in the boundary zone. Neurons were identified by Nissl staining and quantified within 400 µM from the edge of the core. Data were normalized with respect to the contralateral site, and they are the means ± SEM of 6 mice per group at 3 dpl, and 5 mice per group at 10 dpl. (*) $p<0.05$; two-way ANOVA (F values in Table 1), followed by Student's T-test. Cortical thickness was measured at the lesion border using the same images. Genotype did not affect cortical thickness. (***) $p<0.001$, 3 dpl *vs* 10 dpl. Bars are 50 µm. e) Quantification of *Syn* and *Nefm* by qPCR at 3 dpl. Data are the means ± SEM of 6-7 mice per group. VP16-CREB completely prevented the loss of neurites, and partially prevented the synaptic depletion caused by the cryolesion. (&) $p<0.05$, (&&&) $p<0.001$, control *vs* cryolesion; (*) $p<0.05$, (**) $p<0.01$, WT *vs* T; two-way ANOVA (F-values in Table 1) followed by Bonferroni. f, g) Quantification of SMI by immunohistochemistry at 3 and 20 dpl. Data are means ± SEM of 6-7 mice per group. VP16-CREB prevents neurite loss. (*) $p<0.05$, (***) $p<0.001$, WT *vs* T; (&) $p<0.05$, (&&) $p<0.01$, control *vs* cryolesion. Two-way ANOVA (F-values in table 1) followed by Bonferroni. The image shows SMI immunofluorescence at 20 dpl. Pictures were taken in comparable areas in all mouse groups. Bars are 50 µm.

In summary, neuroprotection against secondary injury in the boundary zone was documented by 3 independent approaches (Nissl, qPCR and immunodetection) and 4 independent parameters (neuronal death, *Nfem*, *Syn*, SMI) encompassing the morphological triad of neurons, synapses and neurites.

Gene profiling

A transcriptome analysis using Agilent arrays was carried out to gain insight into the actions of astrocytic VP16-CREB. The numbers of differentially expressed genes ($p<0.05$) in the pair-wise comparisons were: WTC/WT: 7852; TC-T: 574; TC/WTC: 3525; T/WT: 0 (Fig. 4a). Several initial information can be drawn from this distribution. First, the absence of differentially expressed genes in the T/WT comparison confirms the low expression of the transgene in basal conditions. Second, as expected, cryolesion causes a dramatic change in the cortical transcriptome affecting thousands of genes. Third, the expression of VP16-CREB in astrocytes limits this change significantly as shown by the decrease (over 10 times) in the number of differentially expressed genes in TC-T (574 versus 7852).

Thus, the neuroprotective effect of VP16-CREB was imprinted in the transcriptome of the damaged zone at 3 dpl.

The KEGG pathways most significantly enriched ($P<0.0001$) in the inter-group comparisons are related to five functions: energy metabolism, tissue remodeling, cell cycle, stress response and chemotaxis/inflammation (Fig. 4b, c and Supplementary Table 1 for the TC/WTC comparison). According to the dominant direction of change (up/down/no change), pathways can be grouped into two patterns. One pattern has pathways down-regulated by the cryolesion in WT but not in bitransgenic mice; i.e., the transgene prevents the decrease caused by the cryolesion, which results in *apparent* gene upregulation in the TC-WTC comparison. These pathways are "Oxidative phosphorylation" (OXPHOS) and "Citrate cycle" (TCA), and they are the most significantly changed in the transcriptome, according to the p-values (Supplementary Table 1). The second pattern has pathways upregulated by the cryolesion in both WT and transgenic mice, but less upregulated in the latter group, which shows as downregulation in the TC/WTC comparison. These pathways represent tissue remodeling, cell cycle, and stress responses including apoptosis and inflammation.

DNA array data require validation with alternative approaches. The decreased neuronal damage and death documented by immunohistochemistry and qPCR in Fig. 3 is consistent with, and hence validates, the downregulation of stress-related pathways, namely the apoptosis observed in the array. In addition, the dual opposite effect of the transgene on inflammation and energy-related pathways was validated with qPCR in a sample of 24 genes differentially expressed in the TC-WTC group with the lowest individual adjusted p-values (Figs. 5, 6). As shown in Table 1, all genes showed a significant effect of "genotype" or "interaction" in two-way ANOVA except *Ccl5*, *Tgbr2* and *Itgb1*, which showed no clear difference in expression between WTC and TC, although for some of them there is a downwards tendency in

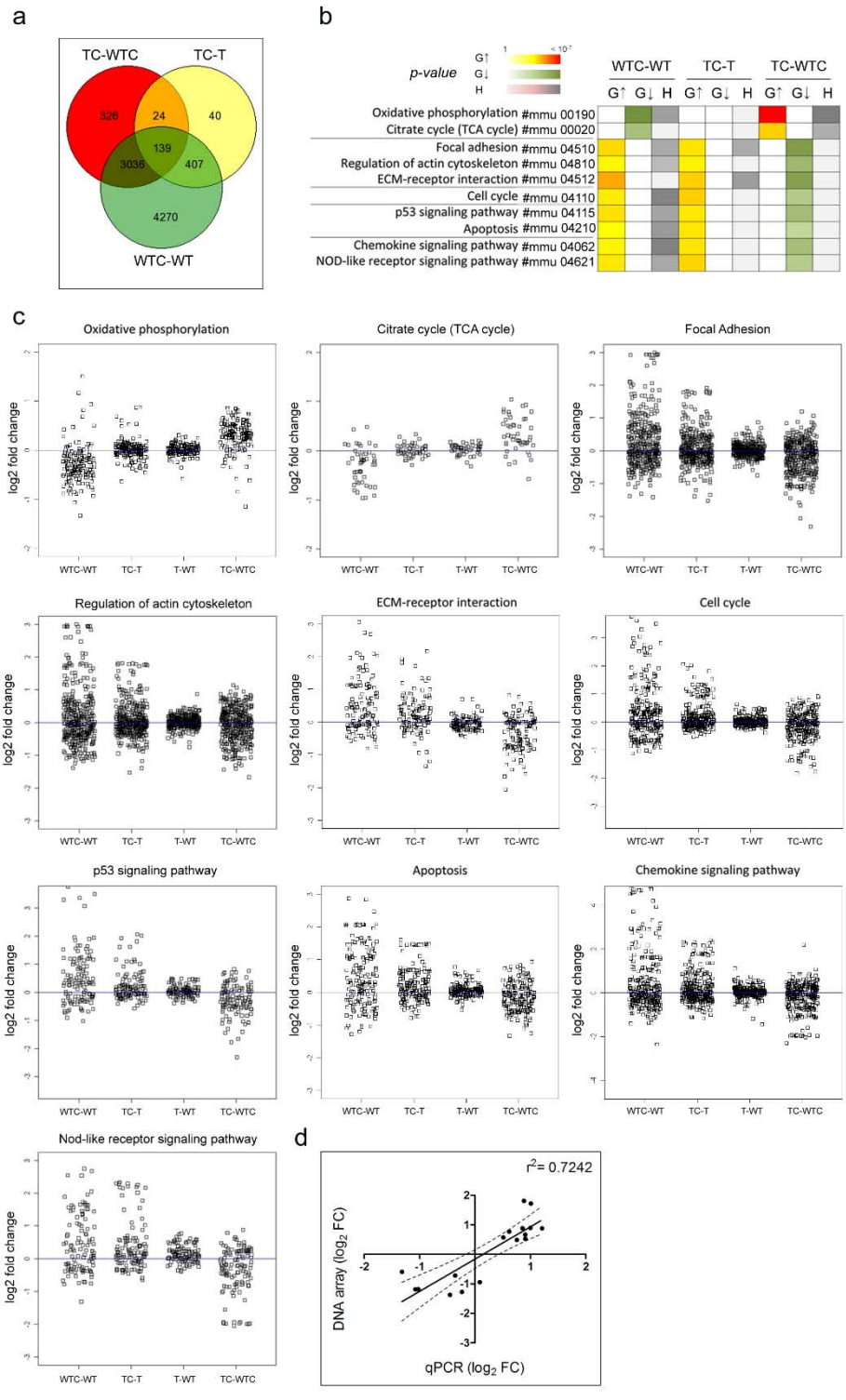
a
TC-WTC
TC-T
WTC-WT
326
24
40
139
3036
407
4270
b
p-value
G↑
G↓
H
WTC-WT
TC-T
TC-WTC
Oxidative phosphorylation #mmu 00190
Citrate cycle (TCA cycle) #mmu 00020
Focal adhesion #mmu 04510
Regulation of actin cytoskeleton #mmu 04810
ECM-receptor interaction #mmu 04512
Cell cycle #mmu 04110
p53 signaling pathway #mmu 04115
Apoptosis #mmu 04210
Chemokine signaling pathway #mmu 04062
NOD-like receptor signaling pathway #mmu 04621
c
Oxidative phosphorylation
Citrate cycle (TCA cycle)
Focal Adhesion
Regulation of actin cytoskeleton
ECM-receptor interaction
Cell cycle
p53 signaling pathway
Apoptosis
Chemokine signaling pathway
Nod-like receptor signaling pathway
log2 fold change
WTC-WT
TC-T
T-WT
TC-WTC
d
r2= 0.7242
DNA array (log2 FC)
qPCR (log2 FC)

TC (Fig. 6a). All genes considered, the extent of change detected by qPCR and transcriptome analysis correlate significantly (Pearson index 0.8510; $p<0.0001$; $R^2=0.7242$, Fig. 4d), strongly supporting the Agilent profiling data.

Figure 4. Transcriptomic signature of bitransgenic mice. a) Venn diagram of differentially expressed genes (P< 0.05) in paired-wise comparisons of experimental groups (WT-WTC, TC-T, WTC-TC) at 3 dpl. The focal injury caused differential expression of 7852 genes in WT and of 574 genes in bitransgenics, suggesting that VP16-CREB reduces the impact of the focal injury on the cortical transcriptome. There were no differentially expressed genes in T-WT. b) Enriched KEGG pathways were identified by two statistic tests: gene set enrichment analysis (GSEA, G), used independently for up-regulated (GSEA up) or down-regulated genes (GSEA down), and hypergeometric distribution function (H) which detects changes but does not inform about their up or down direction. Only pathways statistically significant for at least one test at p <0.0001 in paired comparisons are presented. Color codes differentiate statistical tests: yellow-red for GSEA up, green for GSEA down and gray for hypergeometric. Color gradation refers to p-values. c) Scatter plots of the expression in $\log_2$ of all genes annotated in significantly enriched KEGG pathways. In TC-WTC, note the opposite tendency of "metabolic genes" (apparent upregulation) and the other gene groups (apparent inhibition). d) Correlation between $\log_2$ fold changes detected in selected genes by transcriptome analysis (3 dpl) and qPCR. Pearson correlation index: 0.8510, p<0.0001. Linear regression goodness of fit: $R^2= 0.7242$.

VP16-CREB rescues the down-regulation of mitochondrial pathways

Mitochondria are the site of two of the most important energy generating pathways in mammals, OXPHOS and TCA. In bitransgenic mice, constituents of rescued OXPHOS enzymes include subunits of succinate dehydrogenase, NADH dehydrogenase, ATP synthase, cytochrome C oxidase and ubiquinol cytochrome reductase (Fig. 5a, Supplementary Table 1). Constituents of rescued TCA enzymes are pyruvate dehydrogenase, malate dehydrogenase, succinate-Coenzyme A ligase, isocitrate dehydrogenase and fumarate hydratase (Fig. 5b, Supplementary Table 1). Moreover, perusal of MitoCarta, an inventory of mammalian mitochondrial genes (Pagliarini et al. 2008), revealed that 430 genes encoding for structural and metabolic proteins were significantly deregulated by the cryolesion in the cortex of WT mice (331 down and 99 up), but only 34 in bitransgenic mice (32 up and 2 down) (Fig. 5c). Mitochondria thus appear to be protected in bitransgenic mice. Of note, GO enrichment analysis showed no significant clustering of genes in organelles other than mitochondria (Suppl. Fig. 2).

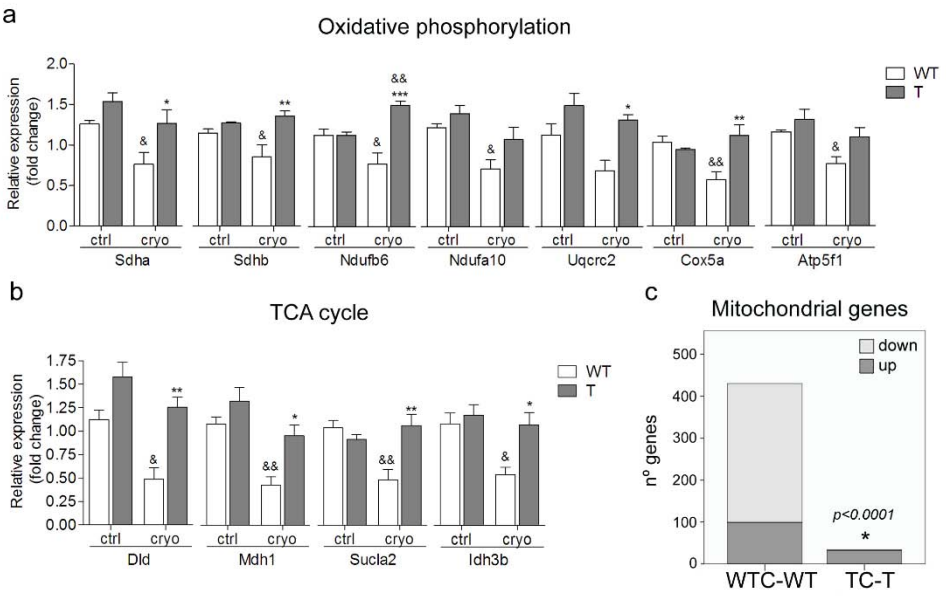

Figure 5. Rescued expression of mitochondrial genes in bitransgenic mice. a, b) Validation by qPCR of genes with lowest adjusted p-values corresponding to tricarboxylic cycle (TCA) and oxidative phosphorylation (OXPHOS). VP16-CREB prevented the down-regulation of genes related to energy metabolism caused by the lesion. Data are means ± SEM of 6-7 mice per group. (*) means WT *vs* T; (&) means control *vs* lesion. (*/&) p<0.05; (**/ &&) p<0.01; (***/ &&&) p<0.001. Two-way ANOVA followed by Bonferroni. Significant effect of "genotype". (F-values in Table 1). Abbreviations: *Dld:* Dihydrolipoamide dehydrogenase*; Mdh1:* Malate dehydrogenase 1, NAD (soluble); *Idh3b:* Isocitrate dehydrogenase 3 (NAD+) beta; *Sucla2:* Succinate-Coenzyme A ligase, ADP-forming, beta subunit; *Sdha*: Succinate dehydrogenase complex, subunit A, flavoprotein (Fp); *Sdhb:* Succinate dehydrogenase complex, subunit B, iron sulfur (Ip); *Ndufb6:*NADH dehydrogenase (ubiquinone) 1 beta subcomplex, 6*; Ndufa10:* NADH dehydrogenase (ubiquinone) 1 alpha subcomplex 10; *Uqcrc2:* Ubiquinol cytochrome c reductase core protein 2; *Cox5a:*Cytochrome c oxidase, subunit Va; *Atp5f1:* ATP synthase, H+ transporting, mitochondrial F0 complex, subunit B1. c) The sharp down-regulation of mitochondrial genes caused by cryolesion in WT mice does not occur in bitransgenics. Number of differentially expressed mitochondrial genes in WTC/WT and TC/T according to the Mitocarta database ($p < 0.05$). Chi-square test indicates significant changes in mitochondrial gene up/down distribution in the WT and bitransgenic. X^2=75.13 with 1 degree of freedom; p< 0.0001.

VP16-CREB abrogates the post-injury inflammatory cascade

Gfa2-TtA/TetO-VP16-CREB mice showed (Supplementary Table 1): i) decreased expression of genes encoding for cytokines like *Tgfb1* and chemokines of the C-X-C and C-C class, namely *Ccl2,* an astrocyte-produced cytokine that plays a key role in leukocyte recruitment in brain disease (Lichtenstein et al. 2012; Kim et al. 2014; Moreno et al. 2014) (Fig. 6a)*;* ii) decreased expression of genes encoding for ECM proteins including collagen, laminin, proteoglycans, fibronectin, and tenascins (Fig. 6b; iii) decreased expression of genes encoding for cell adhesion molecules that mediate inflammatory cell infiltration like integrins and the CD44 antigen and, accordingly, iv) a 50% decrease in microglial activation/macrophage

infiltration assessed by lectin histochemistry (Fig. 6c). Microglia/macrophages thus covered 0.1094 ± 0.007239 mm^2 in WT, and 0.04788 ± 0.01305 mm^2 in TC (means ± SEM; n=5; P value= 0.0019, Student's T-test).

A flaw in transcriptome analysis using whole tissue is that it provides no information about the cellular compartmentalization of the differentially expressed genes, thus complicating the dissection of cause-effect relationships in the pathological cascade. This limitation becomes further complicated when there is a change in cell population contents. Here, we sought to gain insight into the cellular distribution of markers dysregulated by the cryolesion by comparing the transcriptome signatures of the pair-wise comparisons with those of candidate cells. Compared cell types included different types of glia, neurons, reactive astrocytes (activated by LPS or MCAO), and immune cells such as microglia, macrophages, and other leukocytes that may enter the brain after injury (Bush et al. 1999) (Fig. 6d). The rationale was that the cellular distribution of markers in the injured forebrain is dictated by the following scenarios: i) cell infiltration (immune cells in cortex), ii) neuronal loss (imbalance of neurons/glia) and iii) astrocyte activation (insult-dependent gene expression *vs.* basal).

Markers of reactive astrocytes, macrophages and microglia were enriched in WTC/WT mice in the following order: macrophages > microglia > astrocytes MCAO-7d > astrocytes LPS> astrocytes MCAO-1-3d (Fig. 6d).

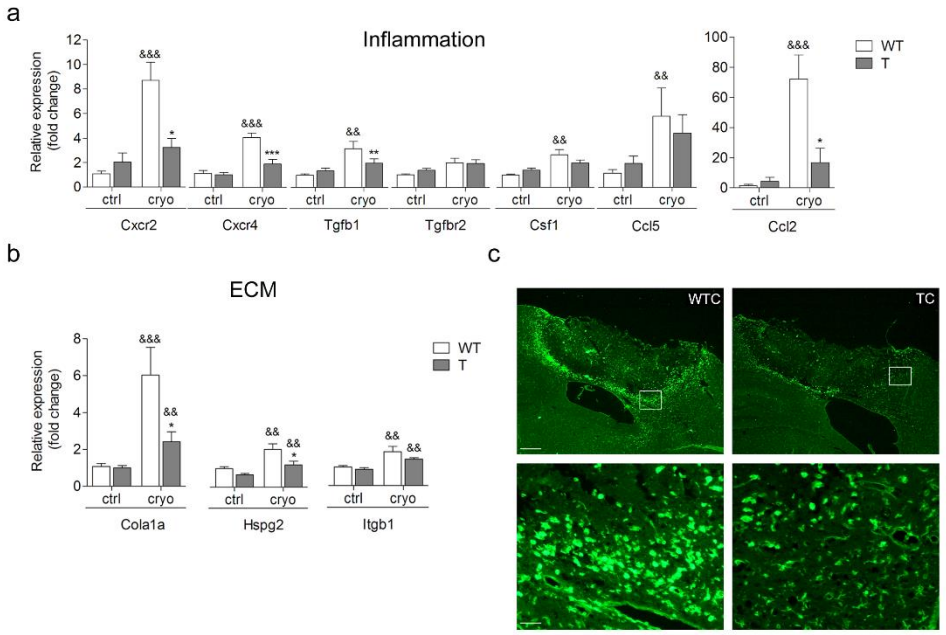

Although the great overlap among inflammatory profiles complicates the identification of the cellular provenance of inflammatory markers, the data point to infiltrated macrophages as a major factor shaping inflammatory gene profile after cryolesion, which is consistent with the histochemical data (Fig. 6c). These markers showed a similar profile in bitransgenic and WT mice, except that changes were less pronounced in bitransgenics (Fig. 6d, e)—again, consistent with the histochemical data. Interestingly, markers of reactive astrocytes showed more enrichment in WTC group than in TC while "resting" astrocytes list was equally enriched in both. In the same way, neuronal markers appear predominantly in bitransgenic mice, both in basal state and upon injury.

Figure 6. Decreased inflammation in bitransgenic mice. a, b) qPCR analysis of genes with the lowest adjusted p-value encoding for inflammation-related and extracellular matrix (ECM) proteins. VP16-CREB generally prevented the upregulation of genes related to inflammation and tissue remodeling. Data are means ± SEM of 6-7 mice per group. (*) means WT *vs* T; (&) means control *vs* lesion. (*/&) p<0.05; (**/ &&) p<0.01; (***/ &&&) p<0.001. Two-way ANOVA followed

by Bonferroni. Significant effect of "genotype" in all genes except for *ccl5*, *csf1*, and *Tgfbr2* (F-values in Table 1). Abbreviations.*Cxcr2:* Chemokine (C-X-C motif) receptor 2; *Cxcr4:* Chemokine (C-X-C motif) receptor 4;*Tgfb1:* Transforming growth factor, beta 1; *Tgfbr2*: Transforming growth factor, beta receptor II; *Csf1*: Colony stimulating factor 1 (macrophage); *Ccl5*: Chemokine (C-C motif) ligand 5; *Ccl2*: Chemokine (C-C motif) ligand 2; *Col1a1*: Collagen, type I, alpha 1; *Hspg2*:

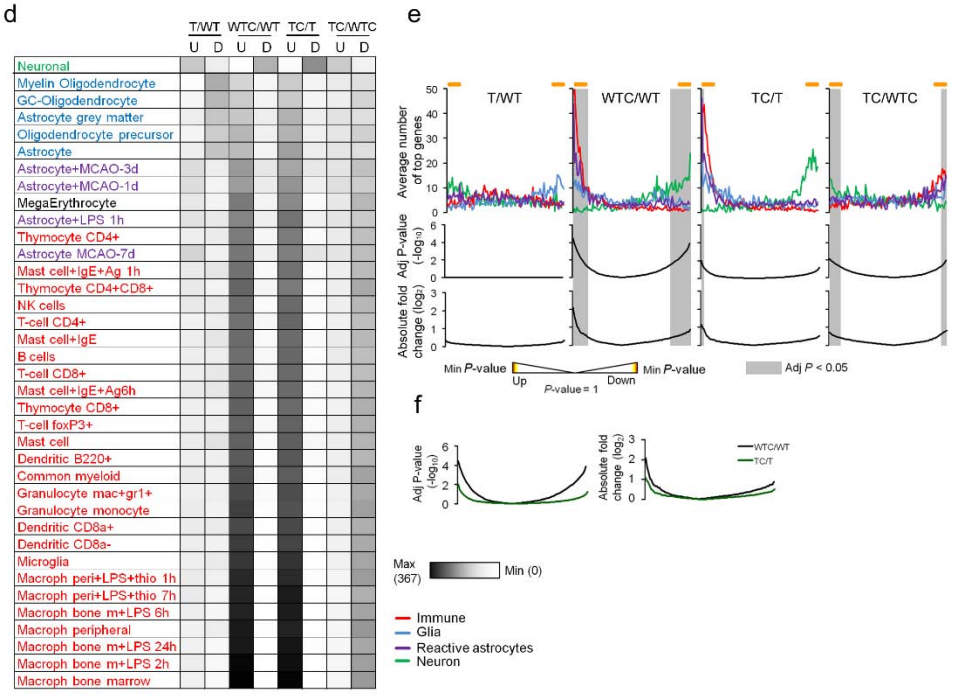

Perlecan (heparan sulfate proteoglycan 2); *Itgb1*; Integrin beta 1 (fibronectin receptor beta). c) Infiltration of lectin-labeled microglia in the core area is reduced in transgenic mice by 50% (see quantification in the text). Bars are 50 µm. d) Cell-population analysis. The Agilent arrays were sorted according to p-values (from more to less significant) and UP or DOWN direction of change in pair-wise comparisons. Each group was compared with cell-population markers of immune, glial and neuronal cells, and activated astrocytes. The table shows the number cell-population markers in the top 2000 genes of UP (U) and DOWN (D) lists. In basal conditions, VP16-CREB caused moderate up-regulation and down-regulation of neuronal and astrocyte markers, respectively. After focal injury, VP16-CREB caused down-regulation of neuronal markers but upregulation of glial, reactive astrocyte and immune markers, indicating a cell population shift that is reflected in the cortical transcriptome. e) Distribution of cell-population markers in the whole array according to fold change, adjusted p-values, and direction of change (UP, left side) and DOWN (right side), summarizing trends observed in d). Gray shades are the region of significance (adjusted p-value< 0.05) of the pair-wise microarray analysis. Orange lines denote the top 2000 genes used in d. f) Adjusted p-value and fold-change for WTC/WT and TC/T superimposed for clarity to show the most relevant conclusion of this analysis: despite a similar marker distribution, the significance and magnitude of change were lower in the transgenic than in the WT mice.

VP16-CREB target genes in astrocytes

Having established that VP16-CREB selectively over-expressed in astrocytes is protective, a fundamental question is the identity of genes activated by VP16-CREB in astrocytes. We approached this question first with further meta-analysis of the astrocyte genes extracted from the pair-wise comparisons. To perform this task, we created a list of genes enriched in astrocytes by statistically comparing databases of astrocytes, neurons and oligodendrocytes. These databases are publicly available, and were generated by Translating Ribosomal Affinity Purification (TRAP), a methodology that identifies mRNAs in the entire cell body in a cell-specific fashion (Heiman et al. 2009).

To identify CREB-dependent genes in astrocytes, we used the PSCAN software to compute the frequency of CRE-motifs in the promoters of astrocyte TRAP genes extracted from the top of the T vs WT pair-wise comparisons regardless of significance of change. Due to the limited number of retrieved markers, we also considered the interaction genotype x lesion in the 2x2 factorial analysis, which shares >74% of genes with the WTC/TC (i.e. "cryolesion") pair-wise comparison.

The number of VP16-CREB candidates, i.e., the astrocyte genes where CRE-sites are significantly over-represented, is shown in Fig. 7a. The complete astrocyte TRAP list, unlike the TRAP neuronal list (Benito et al., 2011), shows no statistically significant enrichment of CREB-dependent genes. By contrast, CRE binding sites are highly enriched in the group of astrocyte genes up-regulated in bitransgenic mice when compared to WT mice, both in basal and injured conditions, although more so in the latter. This is consistent with the robust up-regulation of VP16-CREB post-injury. By contrast, no enrichment of CRE-site containing genes was detected in the astrocyte fraction of down-regulated genes. This observation is important because it confirms the success of the experimental strategy of activating CDTA via the *Gfa2*-driven expression of VP16-CREB. Since VP16-CREB is a strong transcriptional activator, not a repressor, CREB-dependent candidates should be in the up-regulated pool.

The candidate genes fall into two groups shown in a heat map (Fig. 7b). First are the genes showing a net up-regulation in TC. Second are the genes down-regulated in WTC but unchanged in TC, which results in an apparent increase in the TC/WTC comparison.

Note that the general tendency of CREB-dependent genes in WTC is decreased expression. This suggests: i) that *intrinsic* or *natural* CDTA is impaired by cryolesion, and ii) that the over-expression of VP16-CREB in astrocytes restores CDTA, on occasion over basal levels.

We reasoned that in the group "DOWN in WTC and unchanged in TC", the rescue of gene expression in TC mice could be secondary to the general protection elicited by the transgene, while the genes in the group "UP in TC" have a better chance of being the *bonafide* genes up-regulated by VP16-CREB in astrocytes, and accounting for protection. So we focused on the latter set of genes. After validation by qPCR, we produced a short list of genes of true positives according to the criterion that they presented a significant contribution to the variance either from "interaction" and/or from "genotype" factors in a two-way ANOVA test (Fig. 7c, Table 2).

We reasoned that the genes in the short list might be key nodes of the CDTA-regulated protein network. Their functions were thus explored with GeneCards and literature perusal and are exposed below.

Fam181b and *Lactb2* genes do not have known functions, *Dbx2* and *Rfx4* genes are transcription factors involved in development, *Rnft1*, *Fbxo2* and *USP53* are molecules related to ubiquitination, *Kcng4* is a potassium channel, *Ppp1r3c* is a phosphatase that regulates glycogen synthesis, *Aldh1a1* is an alcohol dehydrogenase involved in acetaldehyde metabolism among many other functions and *Gem* is a GTP-binding protein involved in cell migration. This list of VP16-CREB target gene candidates may account for some of the neuroprotective process showing above and will be a valuable resource to enable the full characterization of the CREB-dependent transcriptional program in astrocytes.

Figure 7. Candidates for VP16-CREB target genes in astrocytes The promoters (-950/+50) of astrocytic-specific genes in the top 2000 lists of T/WT, TC/T, WTC/WT, TC/WTC and Interaction (2x2 factorial analysis) were scanned for CRE binding sites using PSCAN software. a) Significant enrichment in the up-regulated genes for basal (T/WT basal), Cryolesion (T/WT lesion) and Interaction (2x2 factorial, T/WT lesion / T/WT basal), but not in the down list or in the full list of astrocyte genes. Rows are different matrices containing variations of CRE motifs. Last row shows the number of astrocytic-specific genes analyzed by PSCAN. b) Hierarchical clustering of astrocytic-specific genes present in Cryolesion and Interaction (top 2000 up-regulated genes). Two subsets were segregated, one with genes down-regulated in WT that appeared normalized in bitransgenics, and another subset with genes specifically up-regulated in the cortex of bitransgenic mice in response to cryolesion. c) qPCR validation of astrocytic VP16-CREB target gene candidates. Data are means ± SEM of 6-7 mice per group. (*) $p<0.05$, (**) $p<0.01$, (***) $p<0.001$ in WT *vs* T. Two-way ANOVA followed by Bonferroni. Only genes with significant effect of "Cryolesion" and/or "Interaction" are shown (Table 3).

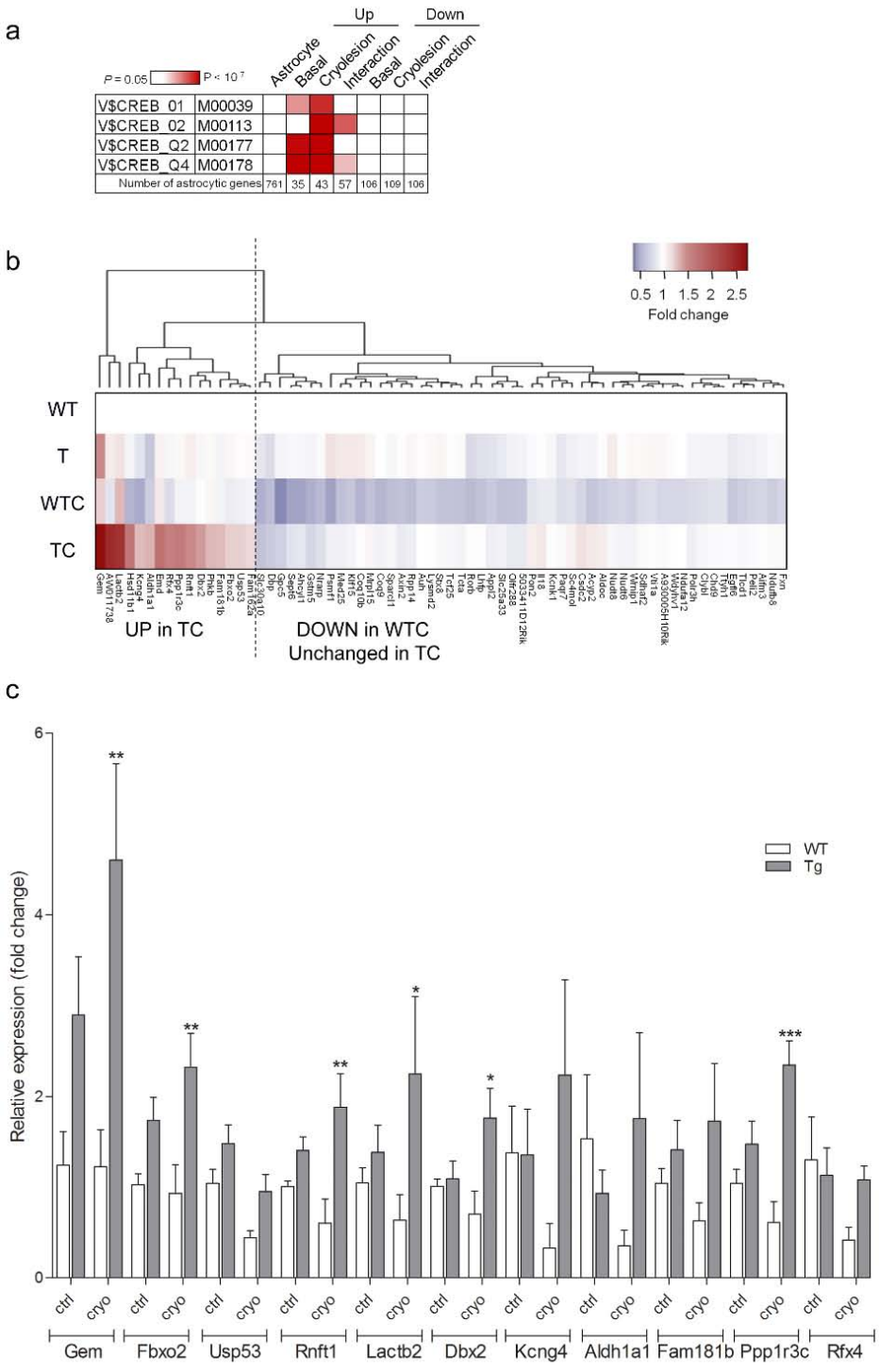
a
Up
Down
Astrocyte
Basal
Cryolesion
Interaction
Basal
Cryolesion
Interaction
P = 0.05
P < 10-7
V$CREB_01 M00039
V$CREB_02 M00113
V$CREB_Q2 M00177
V$CREB_Q4 M00178
Number of astrocytic genes 761 35 43 57 106 109 106
b
0.5 1 1.5 2 2.5
Fold change
WT
T
WTC
TC
UP in TC
DOWN in WTC
Unchanged in TC
c
Relative expression (fold change)
WT
Tg
ctrl
cryo
Gem
Fbxo2
Usp53
Rnft1
Lactb2
Dbx2
Kcng4
Aldh1a1
Fam181b
Ppp1r3c
Rfx4

Discussion

The main finding of this study is the reduction of secondary neuronal damage in an experimental model of acute cortical injury intervening *after* the insult by manipulating astrogliosis through the activation of CREB-dependent transcriptional programs. Astrogliosis was in this approach both a tool and a target, since we used a *Gfap*-based promoter to over-express VP16-CREB, which, in turn, and unexpectedly, increased astrogliosis. That CDT was successfully accomplished in astrocytes was confirmed by the enrichment of CRE-site containing genes in the pool of astrocytic genes differentially expressed in cryolesioned bitransgenic mice. The protection was documented by the decreased neuronal loss, preservation of neurites and synapses, and reduction of leukocyte infiltration, as well as by changes in the transcriptome pointing to reduced cellular stress, reduced apoptosis, and rescue of mitochondrial pathways in the zone surrounding the core of the lesion.

It is worth stressing that protection was achieved with only 45% of the astrocytes expressing VP16-CREB—according to the immunodetection data—supporting the remarkable impact of astrocytes, even when partially manipulated, on the evolution of brain injury.

The finding is of relevance because pharmacological and genetic manipulations of molecular targets before acute injuries occur are of no clinical use. Rather, efficient therapies should be neuroprotective, arresting or diminishing the impact of secondary injury, or neurorestorative, i.e., stimulating neurogenesis, axonal sprouting, synaptogenesis, oligodendrogenesis and angiogenesis, all of which contribute to functional recovery. Below we address in four points how CDTA may afford protection.

First, the effect of CDTA is neuroprotective rather than neurorestorative. Despite the very different etiologies, all brain injuries present a multiphasic evolution of damage that encompasses an acute phase in which neuronal death occurs, followed by delayed pathogenic events that include

bioenergetic collapse, severe inflammatory-cell infiltration, edema, vascular damage, acidosis, oxidative stress, glutamate-mediated excitotoxicity, and over-excitation of neuronal cells followed by spreading depression, all of which exacerbate the primary injury (Kaur et al. 2013; Xiong et al. 2013; Burda and Sofroniew 2014). VP16-CREB has to act during the time window spanning from 1 dpl, when we first detected upregulation of GFAP mRNA, to 3 dpl, when diminished damage in the penumbra zone is already apparent. Of note, VP16-CREB expression in astrocytes potentiates astrogliosis, as judged by GFAP upregulation, thus confirming previous reports that dispel the widespread notion that gliosis is necessarily detrimental in brain injury (Pifarre et al. 2011).

Second, CDTA may act by preventing astrocyte failure, promoting homeostatic function in astrocytes. In order to pinpoint the mechanism of action of CDTA we have to consider what happens to reactive astrocytes in the pathological continuum that develops after brain injury (reviewed by (Burda and Sofroniew 2014). Debated scenarios are: i) loss-of-function; astrocytes may contribute to brain damage by failing to take up the excess of glutamate, water, or potassium, thereby contributing to excitotoxicity, edema and neuronal circuit hyper-excitation; ii) gain-of-toxic function; astrocytes may produce glutamate and cytokines such as ccl2, thereby exacerbating acute excitotoxicity and blood-cell infiltrate-derived damage; or iii) protection; astrocytes may release neuroprotectants like erythropoietin, vascular endothelial growth factor, and glial-derived neurotrophic factor. However, genes encoding for growth factors, glutamate transporters EAAT1 or EAAT2 or aquaporin show negligible expression changes in the transcriptome of bitransgenic mice at 3 dpl, suggesting that the CDTA-mediated protection is not mediated by increased glutamate clearance, edema reduction or release of neuroprotective factors. Rather, based on the VP16-CREB target gene candidates identified by a meta-analysis, our data support a scenario in which activation of CREB-dependent transcription improves, in astrocytes, glycogen metabolism, protein degradation, and potassium clearance, which, in turn, may have beneficial consequences for neurons. In support of this view, it has been shown that the targeted

improvement of mitochondrial and potassium-channel function in astrocytes is protective in experimental ischemia (Sun and Hu 2010; Almeida et al. 2012) and Huntington's disease (Tong et al. 2014). And finally, although the manipulation was not restricted to astrocytes, it has recently been reported that potentiating ubiquitin-mediated clearance of misfolded proteins affords protection in stroke (Liu et al. 2014). All in all, it appears that increasing astrocyte resilience to injury may have global benefits.

Third, CDTA may change the inflammatory profile of astrocytes. The signatures of reactive astrocytes used in our meta-analysis come from a landmark study that put forth the notion of astrocyte heterogeneity among brain diseases by reporting a 50% difference in the transcriptome of astrocytes exposed to LPS, and those exposed to MCAO (Zamanian et al. 2012). The authors concluded that LPS astrocytes are detrimental whereas MCAO astrocytes are protective because the transcriptomes of the former are enriched in genes regulating the initial phase of the classical complement cascade (*C1r*, *C1s*, *C3*, *C4B*, *Serpin1*), which may lead to synaptic pruning (Stephan et al., 2012). On the opposite, MCAO astrocytes present genes encoding for growth factors (*Clcf1*, *Lif*) and anti-inflammatory cytokines (*Il-6* or *Il-10).* In our case*, C3* and *Gfap,* but not *Il10*, *Il6*, *Clcf1* or *Lif,* were differentially upregulated in the TC-WTC comparison, suggesting that the putative molecular signature in VP16-CREB over-expressing astrocytes activated by a cryolesion is a distinct mix of LPS and MCAO astrocytes.

Fourth, although we have not carried the study beyond 20 dpl, and although CDTA appears to target phenomena occurring before 3 dpl rather than repair or regenerative responses, the reduced expression of ECM genes may lead to enhanced neurite outgrowth and aid neuroregeneration in the long term (Burnside and Bradbury 2014). ECM and cell adhesion molecules are the largest class of genes over-expressed in reactive astrocytes after LPS and MCAO (Zamanian et al. 2012), supporting the view that the modification of the extracellular milieu leading to the immune-cell infiltration and lesion confinement by the glia scar is a core property of reactive astrocytes regardless of the insult. It follows that the decrease in ECM and cell-

adhesion pathways detected in Gfa2-TtA/TetO-VP16-CREB mice can be attributed to direct action of the transgene in astrocytes. Also, the increased expression in bitransgenic mice of thrombospondins (*Thbs2),* extracellular glycoproteins typically produced by astrocytes that interact with ECM and enhance synaptogenesis in stroke (Liauw et al. 2008), provides further support for the notion that control of the extracellular milieu by astrocytes may be clinically beneficial.

An important idea derived from this study is that neuroprotection by CDTN and CDTA may rely on different mechanisms. In neurons, a core tenet of the neurosciences is that neuronal plasticity and survival are two sides of the same coin. Neuroprotection is thus acquired by synaptic activity, and lack thereof precedes and contributes to synapse loss and ultimately to neuronal demise (Parra-Damas et al. 2014). Mechanistically, there is a significant overlap and interplay among activity-dependent CREB-dependent genes modulating plasticity and those promoting survival, *Bdnf* being a prototypical example. None of the putative VP16-CREB dependent genes identified by meta-analysis in this study appear among VP16-CREB dependent genes previously identified in neuronal databases (Benito et al. 2011). Although the complete list of CREB target genes in astrocytes is probably largely underrepresented in the short list, the evidence roughly suggests that CREB is protective in neurons by preserving plasticity and promoting survival, while, in astrocytes, CREB impinges on preserving or potentiating homeostatic functions, modifying the inflammatory profile, and influencing ECM in a favorable manner. Our study supports that cell type and context influence CREB actions, thus dispelling the widespread notion that there is a canonical CDT represented in neurons or neuronal cell lines. In line with this thought, we previously reported that the signalling leading to CREB activation in astrocytes is starkly different to the canonical one documented in neurons (Carriba et al. 2012). Here we extend this observation to show that, like in neurons, the activation of CDT in astrocytes is protective—although through different mechanisms— which calls for combined therapies targeting CREB in both cells in unison.

In conclusion, the study reinforces the use of astrocytes as multi-functional therapeutic targets. The genetic manipulation of astrocytic molecules like methyl-CpG-binding protein 2, the potassium channel Kir4, calcineurin-*nfat*, heat-shock protein 70, and superoxide dismutase, is beneficial in animal models of Rett syndrome (Lioy et al. 2011), Huntington's disease (Tong et al. 2014), Alzheimer's disease (Furman et al. 2012), and stroke (Xu et al. 2010; Xu et al. 2011). In general, astrocyte-targeted therapies may exemplify a kind of single manipulation with a strong therapeutic impact due to the key homeostatic functions of astrocytes in the brain (for a fuller development of this idea see (Takano et al. 2009). The global effect of astrocytes may be strengthened further if it implicates a transcription factor like CREB that enables a multi-modal neuroprotective response, thereby mimicking the effects of combination therapy. This asset may be particularly relevant in acute brain injury, in which the failure of translating protective strategies into clinical care has been attributed in part to the multifactorial nature of injury pathogenesis, which is most difficult to recapitulate in animal models and target therapeutically (Xiong et al. 2013).

Funding

This work was supported by Ministerio de Economía y Competitividad, Spain (grant numbers BFU2010-21921 and BFU2012-38844 to E.G.; SAF2011-23272 to J.H.; SAF2011-22506 and Ramón y Cajal contract to L.M.V.; SAF2011-22855 to A.B.; Instituto Carlos III, Spain (grant numbers ISC3 PI10/00283 to P.G. and PI11/01532 to M.P.O.); Autonomous Government of Catalonia AGAUR (grant numbers 2014SGR1430 to A.P. and 2014SGR984 to E.G. and R.M.); Generalitat Valenciana (grant number Prometeo/2012/005 to A.B.); and the Brain & Behavior Research Foundation (NARSAD Independent Investigator Grant to A.B.). The Instituto de Neurociencias de Alicante is a "Centre of Excellence Severo Ochoa", and the CIBER on Rare Diseases (CIBERER) is an initiative of the Institute Carlos III.

Acknowledgements

The authors thank Abel Eraso Pichot of the Institute of Neurosciences at the UAB for critical reading of the manuscript.

Table 1. Two-way ANOVA F values of array validations

	INTERACTION	GENOTYPE	CRYOLESION
Lesion outcome			
Lesion size	0.5422	0.8437	30.34
Nissl counts	0.725	7.104	10.94
SMI area	6.094	5. 254	11.1
Validation of array hits by qPCR			
Atp5f1	0.7993	6.087	9.608
Ccl2	13.89	11.31	27.95
Ccl5	0.8095	0.05936	8.729
Cola1a	6.865	7.531	22.27
Cox5a	14.2	7.248	3.001
Csf1	5.009	0.3472	21.89
Cxcr2	15.57	7.798	29.53
Cxcr4	11.7	13.87	39.02
Dld	1.517	23.65	14.56
GFAP	5.687	12.58	60.87
Hspg2	2.087	11.56	20.7
Idh3b	3.742	7.627	8.222
Itgb1	0.8707	3.486	23.13
Mdh1	1.466	11.04	19.37
Ndufa10	0,7395	5.717	13.54
Ndufb6	19.15	19.39	0.007175
Nefm	6.276	12.42	0.4188
Sdha	0.8474	9.864	9.423
Sdhb	5.975	16.31	1.895
Sucla2	14.77	6.243	5.051
Syn	4.546	4.013	31.27
Tgfb1	5.713	1.713	19.31
Tgfbr2	1.019	0.6023	11.69
Uqcrc2	0.9616	14.22	5.559

Table 2. Two-way ANOVA F values

	INTERACTION	GENOTYPE	CRYOLESION
Gem	1.756	14.99	1.685
Phkb	0.4859	3.577	1.292
Fam162a	4.253	5.562	85.72
Fbxo2	1.587	15.41	0.8384
Usp53	0.04632	7.588	10.82
Emd	0.09848	12.51	7.13
Rnft1	4.038	14.51	0.03348
Lactb2	1.94	6.24	0.004012
Dbx2	5.097	6.915	0.7029
Kcng4	2.745	2.618	0.02083
Aldh1a1	3.106	0.5009	0.09507
Fam181b	1.047	4.208	0.01962
Ppp1r3c	8.222	22.66	0.9263
Rfx4	1.565	0.5484	1.951

Supplementary figure 1. Sequence of mouse CREB and VP16-CREB fusion construct. In yellow is the CREB binding domain (the Q1 domain, in grey, has been eliminated). Primers used for qPCR are labeled in white.

Mouse CREB (Grey: Q1 domain eliminated in VP16-CREB)

ATGACCATGGAATCTGGAGCAGACAACCAGCAGAGTGGAGATGCTGCTGTAACAGAAGCTG
AAAATCAACAAATGACAGTTCAAGCCCAGCCACAGATTGCCACATTAGCCCAGGTATCCAT
GCCAGCAGCTCATGCAACATCATCTGCTCCCACTGTAACCTTAGTGCAGCTGCCCAATGGG
CAGACAGTCCAGGTCCATGGCGTTATCCAGGCGGCCCAGCCATCAGTTATCCAGTCTCCAC
AAGTCCAAACAGTTCAGTCTTCCTGTAAGGACTTAAAAAGACTTTTCTCCGGAACTCAGAT
TTCAACTATTGCAGAAAGTGAAGATTCACAGGAGTCTGTGGATAGTGTAACTGATTCCCAA
AAACGAAGGGAAATCCTTTCAAGGAGGCCTTCCTACAGGAAAATTTTGAATGACTTATCTT
CTGATGCACCAGGGGTGCCAAGGATTGAAGAAGAAAAGTCAGAAGAGGAGACTTCAGCCCC
TGCCATCACCACTGTAACAGTGCCAACCCCCATTTACCAAACTAGCAGTGGGCAGTACATT
GCCATTACCCAGGGAGGAGCAATACAGCTGGCTAACAATGGTACGGATGGGGTACAGGGCC
TGCAGACATTAACCATGACCAATGCAGCTGCCACTCAGCCGGGTACTACCATTCTACAGTA
TGCACAGACCACTGATGGACAGCAGATTCTAGTGCCCAGCAACCAAGTTGTTGTTCAAGCT
GCCTCAGGCGATGTACAAACATACCAGATCCGCACAGCACCCACGAGCACCATTGCCCCTG
GAGTTGTTATGGCGTCCTCCCCAGCACTTCCTACACAGCCTGCTGAAGAAGCAGCACGGAA
GAGAGAGGTCCGTCTAATGAAGAACAGGGAGGCAGCAAGAGAATGTCGTAGAAAGAAGAAA
GAATATGTGAAATGTTTAGAGAACAGAGTGGCAGTGCTTGAAAACCAAAACAAAACATTGA
TTGAGGAGCTAAAAGCACTTAAGGACCTTTACTGCCACAAATCAGATTAA

VP16-CREB fusion construct

EcoRI-VP16-BamHI-CREB(-Q1)-XbaI

GAATTCATGGCGTACAGCCGCGCGCGTACGAAAAACAATTACGGGTCTACCATCGAGGGCC
TGCTCGATCTCCCGGACGACGACGCCCCCGAAGAGGCGGGGCTGGCGGCTCCGCGCCTGTC
CTTTCTCCCCGCGGGACACACGCGCAGACTGTCGACGGCCCCCCCGACCGATGTCAGCCTG
GGGGACGAGCTCCACTTAGACGGCGAGGACGTGGCGATGGCGCATGCCGACGCGCTAGACG
ATTTCGATCTGGACATGTTGGGGGACGGGGATTCCCCGGGTCCGGGATTTACCCCCCACGA
CTCCGCCCCCTACGGCGCTCTGGATATGGCCGACTTCGAGTTTGAGCAGATGTTTACCGAT
GCCCTTGGAATTGACGAGTACGGTggatccTCCTGTAAGGACTTAAAAAGACTTTTCTCCG
GAACTCAGATTTCAACTATTGCAGAAAGTGAAGATTCACAGGAGTCTGTGGATAGTGTAAC
TGATTCCCAAAAACGAAGGGAAATCCTTTCAAGGAGGCCTTCCTACAGGAAAATTTTGAAT
GACTTATCTTCTGATGCACCAGGGGTGCCAAGGATTGAAGAAGAAAAATCAGAAGAAGAGA
CTTCAGCCCCTGCCATCACCACTGTAACAGTGCCAACCCCGATTTACCAAACTAGCAGTGG
GCAGTATATTGCCATTACCCAGGGAGGAGCAATACAGCTGGCTAACAATGGTACCGATGGG
GTACAGGGCCTGCAGACATTAACCATGACCAATGCAGCTGCCACTCAGCCGGGTACTACCA
TTCTACAATATGCACAGACCACTGATGGACAGCAGATTCTAGTGCCCAGCAACCAAGTTGT
TGTTCAAGCTGCCTCTGGTGATGTACAAACATACCAGATTCGCACAGCACCCACTAGCACC
ATTGCCCCTGGAGTTGTTATGGCGTCCTCCCCAGCACTTCCTACACAGCCTGCTGAAGAAG
CAGCACGAAAGAGAGAGGTTCGTCTAATGAAGAACAGGGAAGCAGCAAGAGAATGTCGTAG
AAAGAAGAAAGAATATGTGAAATGTTTAGAGAACAGAGTGGCAGTGCTTGAAAACCAAAAC
AAAACATTGATTGAGGAGCTAAAAGCACTTAAGGACCTTTACTGCCACAAGTCAGATTAAt
ctaga

Suplementary figure 2. Gene ontology of TC-WTC comparison. GO terms for cellular component (CC) are biological process (BP) are shown. Significantly enriched GOs were reduced with ReviGO software to avoid redundancy and allow a better understanding of the output. Size of the bubbles represent the frequency of the term in the rat GOA database (the larger the more general) and colour represent the p-value (the darker the lower). GO terms were grouped according to semantic similarity determined by a 'force-directed' layout algorithm and highly

similar GO terms are linked by edges in the graph, where the line width indicates the degree of similarity.

GO CC TC-WTC

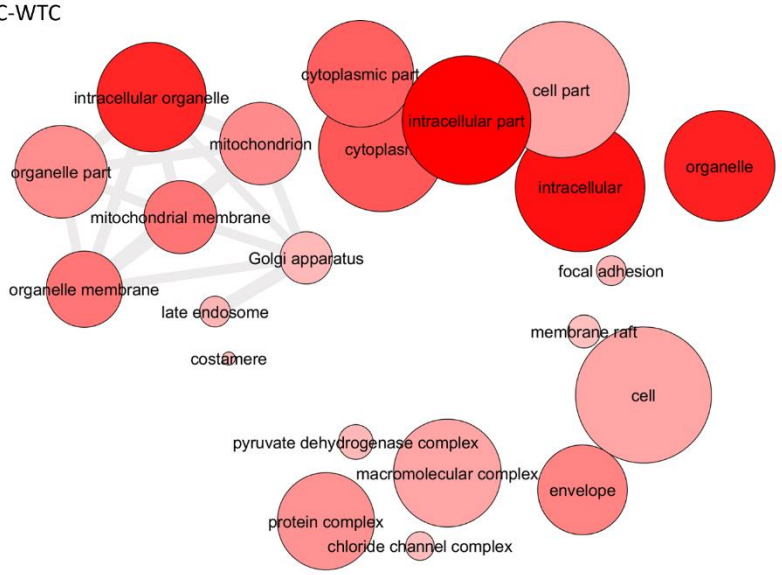

GO BP TC-WTC

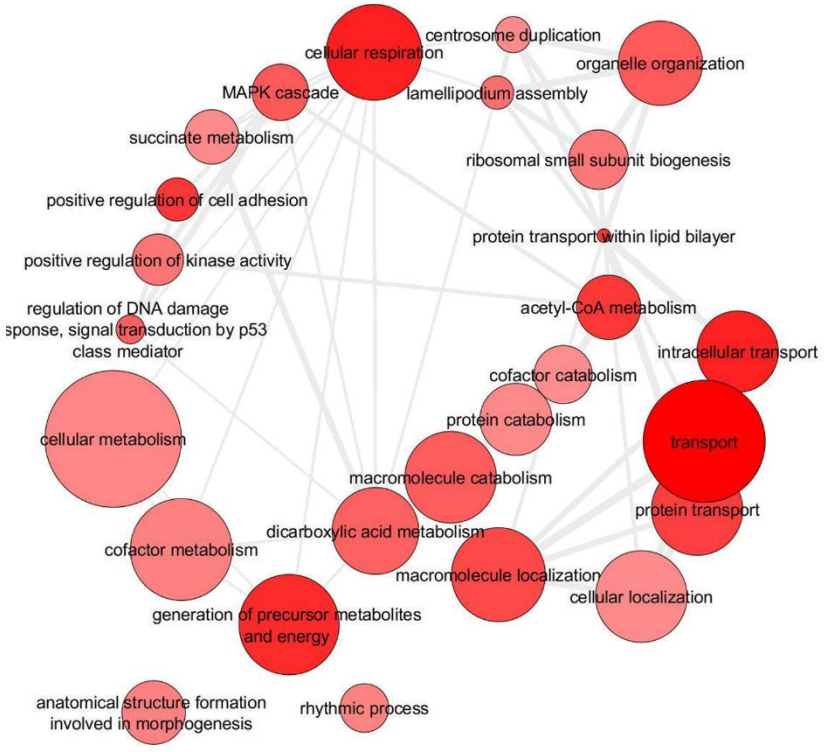

Supplementary Table 1. KEGG pathways differentially expressed in the transcriptome of the TC-

KEGG categories	Pathway term	GSEA mixed	GSEA up	GSEA down	Hyper Geometric	Genes
Energy metabolism	Oxidative phosphorylation	1.58E-20	5.58E-28	1	2.52E-07	*Atp5c,Atp5f1,Atp5g1,Atp6ap1,Cox11,Cox7a2 ,Cox7a2l,Cox7b2,Cox7c,Ndufa10,Ndufa11,Nd ufa6,Ndufa,Ndufb2,Ndufb4,Ndufb5,Ndufb6, Ndufs1,Ndufs2,Ndufs4,Ndufs8,Ndufv2,Ppa1, Ppa2,Sdha,Sdhb,Tcirg1,Uqcr10,Uqcrc1,Uqcrc 2,Uqcrfs1*
	Citrate cycle	1.94E-07	5.23E-07	0.99999	0.00011	*Dld, Sucla2, Pdhb, Idh3a, Sdhb, Pdha1, Sdha, Idh3b, Fh1, Suclg1, Ogdhl, Acly, Dlat.*
Tissue remodeling	Focal adhesion	3.22 E-07	0.99999	1.97E-09	1	*Col2a1, Itgb5, Itgb1, Lamc1, Erbb2, Mapk9, Sos1, Birc2 , Actn4, Mapk8, Igf1, Diap1, Rasgrf1, Tnc, Col4a6, Flna, Myl9, Tln1, Pak1, Akt2, Tnr, Ppp1cb, Pik3cb, Ptk2, Thbs2, Pten, Actn3, Pdgfb, Crk, Map2k1, Pdgfrb, Pik3ca, Col6a6, Fn1, Itga6, Lama5, Kdr, Col1a1, Gsk3b, Rhoa, Pik3cg, Rap1a, Flnb, Ppp1cc, Actn2, Shc1, Mylk2, Parva, Col3a1, Itga7, Src, Col1a2, Rac2.*
	Regulation of actin cytoskeleton	2.59E-06	0.99999	4.54E-06	1	*Itgb5, Itgb1, Fgf12, Pfn1, Nckap1, Wasf2m, Myh9, Sos1, Arhgef7, Actn4, Kras, Fgfr4, Diap1, Gna13, Rras, Myl9, Fgf2, Pak1Nras, Chrm2, Msn, Ppp1cb, Pik3cb, Ptk2, Iqgap1, Arpc1b, Arhgef4, Fgf9, Fgf14, Wasl, Actn3, Pdgfb, Pfn3, Crk, Map2k1, Araf, Arhgef1, Pdgfrb, Fgf22, Pik3ca, Iqgap3, Fgfr2, Diap3, Fn1, Itga6, Rhoa, Pik3cg, Ppcc, Actn2, Mylk2, Bdkrb1, Fgd3, Itga7, Ezr, Rac2.*
	ECM-receptor interaction	0.01503	0.99999	6.32E-09	1	*Col2a1, Itgb5, Itgb1, Dag1, Sdc4, Lamc1, Tnc, Hspg2, Col4a6, Tnr, Thbs2, Hmmr, Col6a6, Fn1, Cd44, Itga6, Lama5, Col1a1, Col3a1, Itga7, Col1a2.*
DNA repair/cell cycle/proliferation	Cell cycle	0.00086	0.99855	0.00144	1	*Cdk4,Orc4l,Cdkn2c,Ccna1,Mcm7,Rbx1,Mcm4, Cul1,Hdac2,Cdc20,Mcm3,Bub1,Cdk7,Orc5l,Cc na2,Crebbp,Tgfb1,Wee1,Plk1,Atm,Pttg1,Skp1 a,Orc3,Tgfb3,Atr, Gsk3b, Cdc14a, Ccne1, E2f5, Ywhag, E2f3.*
Stress response	p53 signaling pathway	0.00014	0.99997	2.16E-05	1	*Cycs, Steap3, Igf1, Cdk4, Siah1a, Pten, Cd82, Atm, Serpine1, Bax, Zmat3, Rchy1, Atr, Sesn3, Ccne1, Serpinb5, Igfbp3.*
	Apoptosis	0.00024	0.95458	0.04542	1	*Cycs, Dffa, Il3ra, Birc2, Irak2, Nfkbia, Akt2, Pik3cb, 1500003O03Rik, Atm, Dffb, Prkar2a, Pik3ca,Prkar1a, Bax, Traf2, Prkar1b, Pik3cg.*
Chemotaxis& inflammation	Chemokine signaling pathway	0.00018	0.99996	3.37E-05	1	*Sos1, Kras, Gm1987, Plcb3, Nfkbib, Nfkbia, Pak1, Akt2, Nras, Prex1, Pik3cb, Ptk2, Cxcr4, Wasl, Pard, Crk, Map2k1, Gnb5, Pik3ca, Cxcl15,Gnb1, Pf4 Gsk3b, Rhoa Pik3cg, Ncf1, Adcy5, Cxcr2, Rap1a, Gnat2, Cxcl1, Ccl17,*
	NOD-like receptor signaling pathway	0.00063	0.99787	0.00212	1	*Mapk9, Birc2, Mapk8, Nfkbib, Nfkbia, Tab3, Il18, Nlrp1a, Naip7, Traf6, Trip6, Cxcl1.*

REFERENCES

Albert-Weissenberger C, Siren AL. 2010. Experimental traumatic brain injury. Exp Transl Stroke Med 2:16.

Almeida AS, Queiroga CSF, Sousa MFQ, Alves PM, Vieira HLA. 2012. Carbon monoxide modulates apoptosis by reinforcing oxidative metabolism in astrocytes: Role of Bcl-2. J. Biol. Chem. 287:10761–10770.

Almolda B, Villacampa N, Manders P, Hidalgo J, Campbell IL, González B, Castellano B. 2014. Effects of astrocyte-targeted production of interleukin-6 in the mouse on the host response to nerve injury. Glia 62:1142–1161.

Barco A, Alarcon JM, Kandel ER. 2002. Expression of constitutively active CREB protein facilitates the late phase of long-term potentiation by enhancing synaptic capture. Cell 108:689–703.

Barco A, Marie H. 2011. Genetic approaches to investigate the role of CREB in neuronal plasticity and memory. Mol. Neurobiol. 44:330–349.

Barco A, Patterson SL, Patterson S, Alarcon JM, Gromova P, Mata-Roig M, Morozov A, Kandel ER. 2005. Gene expression profiling of facilitated L-LTP in VP16-CREB mice reveals that BDNF is critical for the maintenance of LTP and its synaptic capture. Neuron 48:123–37.

Bell KFS, Bent RJ, Meese-Tamuri S, Ali A, Forder JP, Aarts MM. 2013. Calmodulin kinase IV-dependent CREB activation is required for neuroprotection via NMDA receptor-PSD95 disruption. J. Neurochem. 126:274–287.

Benito E, Valor LM, Jimenez-Minchan M, Huber W, Barco A. 2011. cAMP Response Element-Binding Protein Is a Primary Hub of Activity-Driven Neuronal Gene Expression. J. Neurosci. 31:18237–18250.

Burda JE, Sofroniew M V. 2014. Reactive gliosis and the multicellular response to CNS damage and disease. Neuron 81:229–248.

Burnside ER, Bradbury EJ. 2014. Review: Manipulating the extracellular matrix and its role in brain and spinal cord plasticity and repair. Neuropathol. Appl. Neurobiol. 40:26–59.

Bush TG, Puvanachandra N, Horner CH, Polito A, Ostenfeld T, Svendsen CN, Mucke L, Johnson MH, Sofroniew M V. 1999. Leukocyte infiltration, neuronal degeneration, and neurite outgrowth after ablation of scar-forming, reactive astrocytes in adult transgenic mice. Neuron 23:297–308.

Cahoy JD, Emery B, Kaushal A, Foo LC, Zamanian JL, Christopherson KS, Xing Y, Lubischer JL, Krieg P a, Krupenko SA, et al. 2008. A transcriptome database for astrocytes, neurons, and oligodendrocytes: a new resource for understanding brain development and function. J. Neurosci. 28:264–78.

Carriba P, Pardo L, Parra-Damas A, Lichtenstein MP, Saura CA, Pujol A, Masgrau R, Galea E. 2012. ATP and noradrenaline activate CREB in astrocytes via noncanonical Ca2+ and cyclic AMP independent pathways. Glia 60:1330–1344.

Corbin JG, Kelly D, Rath EM, Baerwald KD, Suzuki K, Popko B. 1996. Targeted CNS expression of interferon-gamma in transgenic mice leads to hypomyelination, reactive gliosis, and abnormal cerebellar development. Mol. Cell. Neurosci. 7:354–370.

Dong Y, Nestler EJ. 2014. The neural rejuvenation hypothesis of cocaine addiction. Trends Pharmacol. Sci. 35:374–383.

Faulkner JR, Herrmann JE, Woo MJ, Tansey KE, Doan NB, Sofroniew M V. 2004. Reactive astrocytes protect tissue and preserve function after spinal cord injury. J. Neurosci. 24:2143–2155.

Furman JL, Sama DM, Gant JC, Beckett TL, Murphy MP, Bachstetter AD, Van Eldik LJ, Norris CM. 2012. Targeting astrocytes ameliorates neurologic changes in a mouse model of Alzheimer's disease. J. Neurosci. 32:16129–16140.

Gao Y, Deng K, Hou J, Bryson JB, Barco A, Nikulina E, Spencer T, Mellado W, Kandel ER, Filbin MT. 2004. Activated CREB is sufficient to overcome inhibitors in myelin and promote spinal axon regeneration in vivo. Neuron 44:609–621.

Gautier L, Cope L, Bolstad BM, Irizarry RA. 2004. Affy - Analysis of Affymetrix GeneChip data at the probe level. Bioinformatics 20:307–315.

Giralt M, Penkowa M, Lago N, Molinero A, Hidalgo J. 2002. Metallothionein-1+2 protect the CNS after a focal brain injury. Exp. Neurol. 173:114–128.

Heiman M, Schaefer A, Gong S, Peterson J, Day M, Ramsey E, Suárez-fariñas M, Schwarz C, Stephan D a, James D, et al. 2009. Development of a BACarray translational profiling approach for the molecular characterization of CNS cell types Myriam. Cell 135:738–748.

Kaur H, Prakash A, Medhi B. 2013. Drug therapy in stroke: from preclinical to clinical studies. Pharmacology 92:324–334.

Kim RY, Hoffman AS, Itoh N, Ao Y, Spence R, Sofroniew M V, Voskuhl RR. 2014. Astrocyte CCL2 sustains immune cell infiltration in chronic experimental autoimmune encephalomyelitis. J. Neuroimmunol. 274:53–61.

Kraft AW, Hu X, Yoon H, Yan P, Xiao Q, Wang Y, Gil SC, Brown J, Wilhelmsson U, Restivo JL, et al. 2013. Attenuating astrocyte activation accelerates plaque pathogenesis in APP/PS1 mice. FASEB J. 27:187–198.

Lai TW, Zhang S, Wang YT. 2014. Excitotoxicity and stroke: Identifying novel targets for neuroprotection. Prog. Neurobiol. 115:157–188.

Lattin JE, Schroder K, Su AI, Walker JR, Zhang J, Wiltshire T, Saijo K, Glass CK, Hume DA, Kellie S, et al. 2008. Expression analysis of G Protein-Coupled Receptors in mouse macrophages. Immunome Res. 4:4–5.

Lee Y, Messing A, Su M, Brenner M. 2008. GFAP promoter elements required for region-specific and astrocyte-specific expression. Glia 56:481–493.

Liauw J, Hoang S, Choi M, Eroglu C, Choi M, Sun G, Percy M, Wildman-Tobriner B, Bliss T, Guzman RG, et al. 2008. Thrombospondins 1 and 2 are necessary for synaptic plasticity and functional recovery after stroke. J. Cereb. Blood Flow Metab. 28:1722–1732.

Lichtenstein MP, Madrigal JLM, Pujol A, Galea E. 2012. JNK/ERK/FAK Mediate promigratory actions of basic fibroblast growth factor in astrocytes via CCL2 and COX2. NeuroSignals 20:86–102.

Lin W, Kemper A, McCarthy KD, Pytel P, Wang J-P, Campbell IL, Utset MF, Popko B. 2004. Interferon-gamma induced medulloblastoma in the developing cerebellum. J. Neurosci. 24:10074–10083.

Lioy DT, Garg SK, Monaghan CE, Raber J, Foust KD, Kaspar BK, Hirrlinger PG, Kirchhoff F, Bissonnette JM, Ballas N, et al. 2011. A role for glia in the progression of Rett's syndrome. Nature 475:497–500.

Liu Y, Lü L, Hettinger CL, Dong G, Zhang D, Rezvani K, Wang X, Wang H. 2014. Ubiquilin-1 protects cells from oxidative stress and ischemic stroke caused tissue injury in mice. J. Neurosci. 34:2813–2821.

Ma TC, Barco a., Ratan RR, Willis DE. 2014. cAMP-responsive Element-binding Protein (CREB) and cAMP Co-regulate Activator Protein 1 (AP1)-dependent Regeneration-associated Gene Expression and Neurite Growth. J. Biol. Chem. 289:32914–32925.

Moreno M, Bannerman P, Ma J, Guo F, Miers L, Soulika AM, Pleasure D. 2014. Conditional ablation of astroglial CCL2 suppresses CNS accumulation of M1 macrophages and preserves axons in mice with MOG peptide EAE. J. Neurosci. 34:8175–8185.

Pagliarini DJ, Calvo SE, Chang B, Sheth SA, Vafai SB, Ong SE, Walford GA, Sugiana C, Boneh A, Chen WK, et al. 2008. A Mitochondrial Protein Compendium Elucidates Complex I Disease Biology. Cell 134:112–123.

Park SA, Kim TS, Choi KS, Park HJ, Heo K, Lee BI. 2003. Chronic activation of CREB and p90RSK in human epileptic hippocampus. Exp. Mol. Med. 35:365–370.

Parra-Damas A, Valero J, Chen M, España J, Martín E, Ferrer I, Rodríguez-Alvarez J, Saura C a. 2014. Crtc1 activates a transcriptional program deregulated at early Alzheimer's disease-related stages. J. Neurosci. 34:5776–5787.

Penkowa M, Moos T. 1995. Disruption of the blood-brain interface in neonatal rat neocortex induces a transient expression of metallothionein in reactive astrocytes. Glia 13:217–227.

Pfaffl MW. 2001. A new mathematical model for relative quantification in real-time RT-PCR. Nucleic Acids Res. 29:2003–2007.

Pifarre P, Prado J, Baltrons MA, Giralt M, Gabarro P, Feinstein DL, Hidalgo J, Garcia A. 2011. Sildenafil (Viagra) ameliorates clinical symptoms and neuropathology in a mouse model of multiple sclerosis. Acta Neuropathol. 121:499–508.

Prado J, Pifarré P, Giralt M, Hidalgo J, García A. 2013. Metallothioneins I/II are involved in the neuroprotective effect of sildenafil in focal brain injury. Neurochem. Int. 62:70–78.

Riccio A, Ahn S, Davenport CM, Blendy JA, Ginty DD. 1999. Mediation by a CREB family transcription factor of NGF-dependent survival of sympathetic neurons. Science 286:2358–2361.

Shimohata T, Nakajima T, Yamada M, Uchida C, Onodera O, Naruse S, Kimura T, Koide R, Nozaki K, Sano Y, et al. 2000. Expanded polyglutamine stretches interact with TAFII130, interfering with CREB-dependent transcription. Nat. Genet. 26:29–36.

Silva NA, Sousa N, Reis RL, Salgado AJ. 2014. From basics to clinical: A comprehensive review on spinal cord injury. Prog. Neurobiol. 114:25–57.

Smyth GK. 2005. Limma: linear models fro microarray data. In: Bioinformatics and Computational Biology Solutions using R and Bioconductor. p. 397–420.

Stephan AH, Barres BA, Stevens B. 2012. The Complement System: An Unexpected Role in Synaptic Pruning During Development and Disease. Annu. Rev. Neurosci. 35:369–389.

Sun XL, Hu G. 2010. ATP-sensitive potassium channels: A promising target for protecting neurovascular unit function in stroke. Clin. Exp. Pharmacol. Physiol. 37:243–252.

Takano T, Oberheim NA, Cotrina ML, Nedergaard M. 2009. Astrocytes and ischemic injury. In: Stroke. Vol. 40. p. S8–S12.

Tong X, Ao Y, Faas GC, Nwaobi SE, Xu J, Haustein MD, Anderson M a, Mody I, Olsen ML, Sofroniew M V, et al. 2014. Astrocyte Kir4.1 ion channel deficits contribute to neuronal dysfunction in Huntington's disease model mice. Nat. Neurosci. 17:694–703.

Tymianski M. 2013. Novel approaches to neuroprotection trials in acute ischemic stroke. Stroke. 44:2942–2950.

Valor LM, Jancic D, Lujan R, Barco A. 2010. Ultrastructural and transcriptional profiling of neuropathological misregulation of CREB function. Cell Death Differ. 17:1636–44.

Vandesompele J, De Preter K, Pattyn F, Poppe B, Van Roy N, De Paepe A, Speleman F. 2002. Accurate normalization of real-time quantitative RT-PCR data by geometric averaging of multiple internal control genes. Genome Biol. 3:0034.1–0034.7.

Xiong Y, Mahmood A, Chopp M. 2013. Animal models of traumatic brain injury. Nat. Rev. Neurosci. 14:128–142.

Xu L, Emery JF, Ouyang YB, Voloboueva LA, Giffard RG. 2010. Astrocyte targeted overexpression of Hsp72 or SOD2 reduces neuronal vulnerability to forebrain ischemia. Glia 58:1042–1049.

Xu L, Xiong X, Ouyang Y, Barreto G, Giffard R. 2011. Heat shock protein 72 (Hsp72) improves long term recovery after focal cerebral ischemia in mice. Neurosci. Lett. 488:279–282.

Zamanian JL, Xu L, Foo LC, Nouri N, Zhou L, Giffard RG, Barres BA. 2012. Genomic Analysis of Reactive Astrogliosis. J. Neurosci. 32:6391–6410.

Zambelli F, Pesole G, Pavesi G. 2009. Pscan: Finding over-represented transcription factor binding site motifs in sequences from co-regulated or co-expressed genes. Nucleic Acids Res. 37:247–252.

General Discussion

General discussion.

The transcription factor CREB is essential for the long-term changes in gene expression that underlie synaptic plasticity and memory formation, and plays a critical role in neuroprotective processes following brain damage. The association of CREB to these important functions has allowed multiple studies to characterize the mechanisms of CREB activation, transcriptional induction and gene expression, both in physiological and pathological conditions. However, these studies have focused on neuronal CREB and little effort has been put in the study of astrocytic CREB, despite the fact that astrocytes also have important roles in the aforementioned processes. This thesis contributes to fill the lack of knowledge in the characterization of astrocytic CREB by studying its activation in response to transmitters, its transcriptomic profile under different stimulations and its neuroprotective role in a model of TBI. Our results show novel signalling cascades for CREB activation in astrocytes and depict a central role of this transcription factor in the regulation of many astrocytic functions, such as metabolism, cell communication, signal transduction and modulation of synaptic activity. In addition, we demonstrate the neuroprotective effects of overexpressing a constitutively active form of CREB in astrocytes following TBI, through decrease in inflammation, rescue of bioenergetic failure and protection against axonal degeneration.

CREB signalling pathways in astrocytes

CREB-dependent transcription is induced in neurons in response to signalling cascades triggered by neurotransmitters released during synaptic activity. Meanwhile, astrocytic processes surround the synapsis and express a battery of receptors able to respond to these neurotransmitters. Therefore, it is reasonable to think that synaptic activity can promote the activation of CREB-dependent transcription in astrocytes, but the signalling pathways that trigger this activation are poorly understood. In this thesis, we show that astrocytic CREB activation in response to transmitters ATP and NE does not involve the canonical mediators cAMP, PKA and Ca^{2+}, as it

happens in neurons, but that it is largely dependent on an atypical PKC and ERK 1/2. The activation of CREB via PKC is a common pathway in many cell types and has been confirmed in astrocytes following our work (Corbett et al. 2013), with similar results related to CREB-induced neurotrophin expression. However, no study has reported the participation of an atypical PKC in astrocytic CREB activation, though ceramide stimulation -an atypical PKC activator- has been shown to promote CREB phosphorylation in astrocyte-enriched cultures (Won et al. 2001). Interestingly, a signalling cascade that activates CREB through PKC upon NE stimulation has been reported in brown adipocytes (Thonberg et al. 2002). The authors showed that activation of CREB through NE-binding to α-adrenergic receptors was independent of Ca^{2+} but strongly dependent of PKC and that neither β-adrenergic receptors, nor cAMP were involved in CREB activation, thus pointing to a similar pathway as the one we describe for astrocytes.

On the other side, we and others have shown that the cAMP-mediated CREB activation also takes place in astrocytes, since both the adenylate cyclase activator FSK and the cAMP analogue dbcAMP are able to induce CREB-dependent transcription (Kobierski et al. 1999; Bayatti and Engele 2001). The participation of different signalling pathways in astrocytic CREB activation is no surprise since CREB acts as a central integrator of multiple stimuli in other cell types. However, we observed that the transcriptional programs elicited by CREB activation through distinct signalling cascades – FSK/cAMP and NE/PKC- exhibit strong correlation, thus pointing to a conserved profile of CREB-dependent genes in astrocytes, as opposite to neurons (Ravnskjaer et al. 2007).

Importantly, we studied for the first time the signalling mechanisms involved in the activation of CRTCs in astrocytes and their contribution to CREB-dependent transcription. Contrary to neurons, which express mainly CRTC1 (Kovács et al., 2007), astrocytes express both CRTC1 and CRTC2 isoforms and they seem to contribute equally to CREB-dependent transcription induced by ATP and NE. As it happens with CREB

phosphorylation, CRTCs nuclear translocation does not depend on the canonical mechanism involving Ca^{2+}/CaM and calcineurin but seems to be regulated by PKC and ERK1/2. The fact that the same kinases involved in CREB phosphorylation also promote CRTCs translocation points to a first level of CREB-dependent transcription regulation, which relays on external stimuli. In addition, different dynamics of CRTC1 and 2 according to their permanence in the nucleus suggests a more complex regulation which can involve distinct kinases and phosphatases for each isoform (Takemori et al., 2007; Sasaki et al., 2011; Liu et al., 2012).

Transcriptional programs induced by CREB in astrocytes

CREB is activated in many cell types in response to a wide array of stimuli, and the resulting transcriptional programs vary depending on cell type and context (Cha-Molstad et al. 2004; Lemberger et al. 2008). With the transcriptome analysis of CREB activation, we sought to establish a genetic signature of CREB-dependent transcription in astrocytes, and to address the differences in transcriptional programs resulting from CREB activation through different pathways. Our results, however, show no major differences between FSK and NE stimulation while VP16-CREB overexpression seems to encompass the former treatments. Moreover, given its independence of signalling pathways and its continuous transcriptional activation, VP16-CREB differentially expressed genes should reflect almost the entire CREB-target gene population.

Functional enrichment analysis of upregulated genes in the three conditions shows high alterations in signal transduction through GPCRs and MAPKs, Ca^{2+} and K^{+} homeostasis, neuropeptide expression and oxidative metabolism through either glutamate, GABA or fatty acids. By contrast, downregulated genes are related to cytoskeletal remodelling, cell cycle and extracellular matrix. Interestingly, some of these functional changes also appear in the transcriptome of Gfa2-tTa/TetO-VP16-CREB mice and thus can be, at least in part, associated to astrocytes. Particularly, fatty acid metabolism, which appears in VP16-CREB overexpressing astrocytes in

culture, can be related to the increased oxidative metabolism *in vivo*. This points to a CREB regulation of astrocytic fatty acid metabolism, which provides near 20% of total brain energy (Panov et al. 2014). In addition, downregulated functional categories appear enriched both *in vitro* and *in vivo* and point to a decrease in extracellular matrix components that could underlie the improved axonal regeneration after injury in VP16-CREB mice (Busch and Silver 2007).

Neuroprotection afforded by astrocytic CREB in a TBI model

The clinical challenge in TBI is to prevent the secondary damage that takes place after the insult. This pathophysiological processes include cerebral ischemia, metabolic imbalance, glutamate excitotoxicity and inflammation, which contribute to neuronal death and cognitive impairment (Morganti-Kossmann et al. 2007; Werner and Engelhard 2007). Astrocytes are key players in these processes exerting both protective and detrimental roles. On one hand, they restrict the tissue damage after TBI by forming a glial scar, repairing the damaged BBB or secreting grow factors. However, they also contribute to excitotoxicity by failing in glutamate uptake, impair axonal regeneration and increase inflammation by secreting cytokines that exacerbate leukocyte infiltration from the blood vessels (Sofroniew 2005; Laird et al. 2008). Despite this dual-role, the complete inhibition of astrogliosis has shown negative effects in various models of CNS damage (Bush et al. 1999; Faulkner et al. 2004; Kraft et al. 2013). Therefore, the modulation of astrocyte response emerges as a good target to ameliorate prognosis after TBI.

The neuroprotective role of CREB in pathological processes such as excitotoxicity or ischemic damage, both triggered by brain trauma, has been largely reported (Mabuchi et al. 2001; Hardingham et al. 2002; Kitagawa 2007; Lai et al. 2014). Interestingly, many studies have shown upregulation of CREB in the early stages after injury (Dash et al. 1995; Mabuchi et al. 2001; Hu et al. 2004), which turns into a decrease in the late phases (Atkins et al. 2009; Griesbach et al. 2009). A more detailed observation showed that

neuronal CREB presents this profile while astrocytic CREB remains downregulated immediately after the injury and increases from the first week after trauma (Carbonell and Mandell 2003). In addition, treatments directed to increase CREB or CREB-dependent genes such as *Bdnf* ameliorate cognitive outcome after TBI (Gatson et al. 2012; Titus et al. 2013).

In our model of TBI, we show that the targeted activation of CREB in astrocytes affords protection against the secondary injury induced after the primary insult by decreasing inflammation and neuronal loss, while it rescues the bioenergetic failure by increasing mitochondrial metabolic pathways. First, anti-inflammatory role of astrocytic CREB could relay in the decreased expression of the chemokine *Ccl2/Mcp-1* and the cytokine *Tgfb*, which promote microglial activation and migration to the damaged area, and participate in the recruitment of macrophages from blood vessels (Morganti-Kossmann et al. 2007; Perry 2010). In addition, the decrease in expression of macrophage stimulating factor *Csf1* suggests a decrease in microglial proliferation (De et al. 2014). Second, the increased number of neurons in the lesion border of bitransgenic mice suggests an anti-apoptotic effect that we have also observed *in vitro*, with the increase in genes like *Bcl2* or *Bfar*. Besides, VP16-CREB mice show a general decrease of ECM proteoglycans associated with impairment of axonal regrowth while expression levels of thrombospondin, which has been related to synaptogenesis and is expressed around regenerating axons *in vivo*, is increased (Burnside and Bradbury 2014; Jones and Bouvier 2014). Third, the increased oxidative metabolism suggests a protection of mitochondrial function, which is impaired after TBI (Werner and Engelhard 2007). Metabolic rescue can be ascribed in part to astrocytes through fatty acid oxidation (Panov et al. 2014) or glutamate mobilization, which has been recently proposed as a lactate source for neuronal supply (Dienel and McKenna 2014).

In VP16-CREB mice, the control of the transgene by the GFAP promoter makes its expression starts *after* injury, which is of relevance because it distinguishes from other models that present permanent transgene expression since birth, thus lacking clinical applicability. The high levels of

VP16-CREB mRNA observed 24 h post-injury suggest that its expression begins previously, coinciding with the increase in astrogliosis, which starts 6h post-lesion (Condorelli et al. 1990). Interestingly, the transgenic mice showed increased expression of GFAP at 24h post-lesion which equals to wild-type animals at three days post-lesion, pointing to a role of CREB in the induction of GFAP gene, as reported recently (Zhang et al. 2015). Advanced gliosis in VP16-CREB mice suggests a faster response of these cells to injury and could underlie the neuroprotection achieved, thus supporting the beneficial roles of reactive astrogliosis in CNS injury (Myer et al. 2006; Burda and Sofroniew 2014).

Astrocytic CREB as a potential therapeutic target.

With the characterization of the CREB signalling pathway and transcriptomic profile in astrocytes, we have revealed the multiple roles of this transcription factor and the marked differences in its regulation between astrocytes and neurons. Moreover, we have shown that sustained activation of astrocytic CREB after brain injury can be beneficial to abrogate the pathophysiological events taking place after the primary insult and to aid functional recovery. These arguments allow us to present astrocytic CREB as a potential target for treatment of traumatic brain injury and opens the field to test astrocytic CREB activation in other acute related diseases like stroke or neurodegenerative disorders like Alzheimer's disease or multiple sclerosis, which also feature inflammation and axonal degeneration.

In addition, the participation of an atypical PKC in the activation of astrocytic CREB makes it possible to design specific activators for this pathway. This is of importance given the adverse effects caused by PKA-CREB activators as rolipram in models of TBI or MS (Bielekova et al. 2009; Atkins et al. 2012). Moreover, the neuroprotective and anti-inflammatory actions of astrocytic CREB in cryolesioned mice result from the activation of the transgene *after* the injury, in a time-window that makes possible its translation to clinical treatment. Finally, the multi-modal protective response of astrocytic CREB, acting through different cell players and pathologic

events, addresses the multifactorial nature of TBI and could overcome the failure in clinical translation of actual treatments, which are mainly based in neuroprotection (Xiong et al. 2013).

Study limitations and future directions

The conclusions drawn from this study point to a differential role of astrocytic CREB regarding signalling regulation, transcriptional activation and injury protection. Nevertheless, some limitations need to be addressed in order to validate the results obtained and make them comparable to a physiological situation.

First, the definition of an atypical PKC as the principal kinase that mediates CREB activation upon NE/ATP stimulation is based mainly on the effect of a broad-range PKC inhibitor, as well as on the lack of effect of activators/inhibitors for other PKC isoforms. Thus, alternative approaches will be necessary not only to assess the participation of an atypical PKC but also to identify the concrete isoform. In this direction, the inhibition of astrocytic CREB phosphorylation upon transfection with siRNAs for PKCζ and PKCι –both expressed by astrocytes (Slepko et al. 1999)- should be tested, as well as the increase after stimulation with atypical PKC activators such as ceramide.

Second, the transcriptional profile obtained from microarray data *in vitro* should be verified by qPCR in order to strengthen the conclusions extracted. Moreover, identification of CREB-dependent genes must be validated for CREB occupancy –by chromatin immunoprecipitation- and for transcriptional activation –by qPCR-. Besides, a comparison of array data with transcriptome analysis of VP16-CREB overexpression in neurons (Benito et al. 2011) will establish the different transcriptional programs between both cell types. Similarly, the use of adult astrocyte databases for comparison with our results (Cahoy et al. 2008; Doyle et al. 2008) will provide insight into the pool of genes regulated by astrocytic CREB *in vivo*.

Third, regarding the protective effects of astrocytic CREB activation in TBI, future experiments will be needed to understand the mechanisms of neuroprotection and inflammation decrease. Characterize the activation state of microglia and the nature of infiltrating leukocytes/macrophages will reveal if the actions of astrocytic CREB are more directed to abrogate microglial activation or to decrease infiltration, in which case the status of the Blood-Brain-Barrier should be checked. On the other hand, increased astrocytes proliferation could also underlie neuroprotection and CREB has been traditionally involved in such processes (Mayr and Montminy 2001). In TBI, reactive astrocytes proliferate *in situ* and also from progenitors in the subventricular zone that migrate to the injured area (Robel et al. 2011). In our model, the high expression of GFAP at one day post-lesion could point not only to an increased gliosis but also to higher proliferation that should be addressed by looking for bromo-deoxiuridine (Brdu) staining in the injured brain. Finally, given the detrimental effects produced by sustained activation of neuronal CREB (Valor et al. 2010), a long term analysis would be necessary to assess the consequences of astrocytic CREB over-activation in order to define the limits of a possible chronic treatment.

REFERENCES

Atkins CM, Falo MC, Alonso OF, Bramlett HM, Dietrich WD. 2009. Deficits in ERK and CREB activation in the hippocampus after traumatic brain injury. Neurosci. Lett. 459:52–56.

Atkins CM, Kang Y, Furones C, Truettner JS, Alonso OF, Dietrich WD. 2012. Postinjury treatment with rolipram increases hemorrhage after traumatic brain injury. J. Neurosci. Res. 90:1861–1871.

Bayatti N, Engele J. 2001. Cyclic AMP modulates the response of central nervous system glia to fibroblast growth factor-2 by redirecting signalling pathways. J. Neurochem. 78:972–980.

Benito E, Valor LM, Jimenez-Minchan M, Huber W, Barco A. 2011. cAMP response element-binding protein is a primary hub of activity-driven neuronal gene expression. J. Neurosci. 31:18237–18250.

Bielekova B, Richert N, Howard T, Packer AN, Blevins G, Ohayon J, McFarland HF, Sturzebecher C-S, Martin R. 2009. Treatment with the phosphodiesterase type-4 inhibitor rolipram fails to inhibit blood--brain barrier disruption in multiple sclerosis. Mult. Scler. 15:1206–1214.

Burda JE, Sofroniew M V. 2014. Reactive gliosis and the multicellular response to CNS damage and disease. Neuron 81:229–248.

Burnside ER, Bradbury EJ. 2014. Review: Manipulating the extracellular matrix and its role in brain and spinal cord plasticity and repair. Neuropathol. Appl. Neurobiol. 40:26–59.

Busch S a., Silver J. 2007. The role of extracellular matrix in CNS regeneration. Curr. Opin. Neurobiol. 17:120–127.

Bush TG, Puvanachandra N, Horner CH, Polito A, Ostenfeld T, Svendsen CN, Mucke L, Johnson MH, Sofroniew M V. 1999. Leukocyte infiltration, neuronal degeneration, and neurite outgrowth after ablation of scar-forming, reactive astrocytes in adult transgenic mice. Neuron 23:297–308.

Cahoy JD, Emery B, Kaushal A, Foo LC, Zamanian JL, Christopherson KS, Xing Y, Lubischer JL, Krieg P a, Krupenko SA, et al. 2008. A transcriptome database for astrocytes, neurons, and oligodendrocytes: a new resource for understanding brain development and function. J. Neurosci. 28:264–78.

Carbonell WS, Mandell JW. 2003. Transient neuronal but persistent astroglial activation of ERK/MAP kinase after focal brain injury in mice. J. Neurotrauma 20:327–336.

Condorelli DF, Dell'Albani P, Kaczmarek L, Messina L, Spampinato G, Avola R, Messina A, Giuffrida Stella AM. 1990. Glial fibrillary acidic protein messenger RNA and glutamine synthetase activity after nervous system injury. J. Neurosci. Res. 26:251–257.

Corbett GT, Roy A, Pahan K. 2013. Sodium phenylbutyrate enhances astrocytic neurotrophin synthesis via protein kinase C (PKC)-mediated activation of cAMP-response element-binding protein (CREB): implications for Alzheimer disease therapy. J. Biol. Chem. 288:8299–312.

Cha-Molstad H, Keller DM, Yochum GS, Impey S, Goodman RH. 2004. Cell-type-specific binding of the transcription factor CREB to the cAMP-response element. Proc. Natl. Acad. Sci. 101:13572–13577.

Dash PK, Moore a N, Dixon CE. 1995. Spatial memory deficits, increased phosphorylation of the transcription factor CREB, and induction of the AP-1 complex following experimental brain injury. J. Neurosci. 15:2030–2039.

De I, Nikodemova M, Steffen MD, Sokn E, Maklakova VI, Watters JJ, Collier LS. 2014. CSF1 overexpression has pleiotropic effects on microglia in vivo. Glia 62:1955–1967.

Dienel G a., McKenna MC. 2014. A dogma-breaking concept: glutamate oxidation in astrocytes is the source of lactate during aerobic glycolysis in resting subjects. J. Neurochem. 131:395–398.

Doyle JP, Dougherty JD, Heiman M, Schmidt EF, Stevens TR, Ma G, Bupp S, Shrestha P, Shah RD, Doughty ML, et al. 2008. Application of a Translational Profiling Approach for the Comparative Analysis of CNS Cell Types. Cell 135:749–762.

Faulkner JR, Herrmann JE, Woo MJ, Tansey KE, Doan NB, Sofroniew M V. 2004. Reactive astrocytes protect tissue and preserve function after spinal cord injury. J. Neurosci. 24:2143–2155.

Gatson JW, Liu M-M, Abdelfattah K, Wigginton JG, Smith S, Wolf S, Simpkins JW, Minei JP. 2012. Estrone Is Neuroprotective in Rats after Traumatic Brain Injury. J. Neurotrauma 29:2209–2219.

Griesbach GS, Sutton RL, Hovda DA, Ying Z, Gomez-Pinilla F. 2009. Controlled contusion injury alters molecular systems associated with cognitive performance. J. Neurosci. Res. 87:795–805.

Hardingham GE, Fukunaga Y, Bading H. 2002. Extrasynaptic NMDARs oppose synaptic NMDARs by triggering CREB shut-off and cell death pathways. Nat. Neurosci. 5:405–414.

Hu B, Liu C, Bramlett H, Sick TJ, Alonso OF, Chen S, Dietrich WD. 2004. Changes in trkB-ERK1/2-CREB/Elk-1 pathways in hippocampal mossy fiber organization after traumatic brain injury. J. Cereb. Blood Flow Metab. 24:934–943.

Jones E V., Bouvier DS. 2014. Astrocyte-Secreted Matricellular Proteins in CNS Remodelling during Development and Disease. Neural Plast. 2014:1–12.

Kitagawa K. 2007. CREB and cAMP response element-mediated gene expression in the ischemic brain. FEBS J. 274:3210–3217.

Kobierski LA, Wong AE, Srivastava S, Borsook D, Hyman SE. 1999. Cyclic AMP-dependent activation of the proenkephalin gene requires phosphorylation of CREB at serine-133 and a src-related kinase. J. Neurochem. 73:129–138.

Kraft AW, Hu X, Yoon H, Yan P, Xiao Q, Wang Y, Gil SC, Brown J, Wilhelmsson U, Restivo JL, et al. 2013. Attenuating astrocyte activation accelerates plaque pathogenesis in APP/PS1 mice. FASEB J. 27:187–198.

Lai TW, Zhang S, Wang YT. 2014. Excitotoxicity and stroke: Identifying novel targets for neuroprotection. Prog. Neurobiol. 115:157–188.

Laird MD, Vender JR, Dhandapani KM. 2008. Opposing roles for reactive astrocytes following traumatic brain injury. NeuroSignals 16:154–164.

Lemberger T, Parkitna JR, Chai M, Schütz G, Engblom D. 2008. CREB has a context-dependent role in activity-regulated transcription and maintains neuronal cholesterol homeostasis. FASEB J. 22:2872–2879.

Mabuchi T, Kitagawa K, Kuwabara K, Takasawa K, Ohtsuki T, Xia Z, Storm D, Yanagihara T, Hori M, Matsumoto M. 2001. Phosphorylation of cAMP response element-binding protein in hippocampal neurons as a protective response after exposure to glutamate in vitro and ischemia in vivo. J. Neurosci. 21:9204–9213.

Mayr B, Montminy M. 2001. Transcriptional regulation by the phosphorylation-dependent factor CREB. Nat. Rev. Mol. Cell Biol. 2:599–609.

Morganti-Kossmann MC, Satgunaseelan L, Bye N, Kossmann T. 2007. Modulation of immune response by head injury. Injury 38:1392–1400.

Myer DJ, Gurkoff GG, Lee SM, Hovda DA, Sofroniew M V. 2006. Essential protective roles of reactive astrocytes in traumatic brain injury. Brain 129:2761–2772.

Panov A, Orynbayeva Z, Vavilin V, Lyakhovich V. 2014. Fatty Acids in Energy Metabolism of the Central Nervous System. Biomed Res. Int. 2014:1–22.

Perry VH. 2010. Contribution of systemic inflammation to chronic neurodegeneration. Acta Neuropathol. 120:277–286.

Ravnskjaer K, Kester H, Liu Y, Zhang X, Lee D, Yates JR, Montminy M. 2007. Cooperative interactions between CBP and TORC2 confer selectivity to CREB target gene expression. EMBO J. 26:2880–9.

Robel S, Berninger B, Götz M. 2011. The stem cell potential of glia: lessons from reactive gliosis. Nat. Rev. Neurosci. 12:88–104.

Slepko N, Patrizio M, Levi G. 1999. Expression and translocation of protein kinase C isoforms in rat microglial and astroglial cultures. J. Neurosci. Res. 57:33–38.

Sofroniew M V. 2005. Reactive astrocytes in neural repair and protection. Neuroscientist 11:400–407.

Thonberg H, Fredriksson JM, Nedergaard J, Cannon B. 2002. A novel pathway for adrenergic stimulation of cAMP-response-element-binding protein (CREB) phosphorylation: mediation via alpha1-adrenoceptors and protein kinase C activation. Biochem. J. 364:73–79.

Titus DJ, Sakurai A, Kang Y, Furones C, Jergova S, Santos R, Sick TJ, Atkins CM. 2013. Phosphodiesterase inhibition rescues chronic cognitive deficits induced by traumatic brain injury. Ann. Intern. Med. 158:5216–5226.

Valor LM, Jancic D, Lujan R, Barco A. 2010. Ultrastructural and transcriptional profiling of neuropathological misregulation of CREB function. Cell Death Differ. 17:1636–44.

Werner C, Engelhard K. 2007. Pathophysiology of traumatic brain injury. Br. J. Anaesth. 99:4–9.

Won JS, Choi MR, Suh HW. 2001. Stimulation of astrocyte-enriched culture with C2 ceramide increases proenkephalin mRNA: Involvement of cAMP-response element binding protein and mitogen activated protein kinases. Brain Res. 903:207–215.

Xiong Y, Mahmood A, Chopp M. 2013. Animal models of traumatic brain injury. Nat. Rev. Neurosci. 14:128–142.

Zhang Y, Lv X, Bai Y, Zhu X, Wu X, Chao J, Duan M, Buch S, Chen L, Yao H. 2015. Involvement of sigma-1 receptor in astrocyte activation induced by methamphetamine via up-regulation of its own expression. J. Neuroinflammation 12:1–13.

Conclusions

- The gliotransmitters ATP and NE activate CREB in astrocytes through a Ca^{2+} and PKA independent signalling pathway that involves an atypical PKC and is modulated by ERK 1/2 and CRTC 1/2.

- Transcriptional programs induced by astrocytic CREB are related to oxidative metabolism, ionic homeostasis and intercellular communication, suggesting a regulatory role of CREB in key functions of astrocytes and brain physiology.

- Activation of CREB-dependent transcription in astrocytes with VP16-CREB protects against secondary damage in acute brain injury by increasing neuronal survival and axonal regeneration, decreasing inflammation and rescuing the bioenergetic failure through an increase of mitochondrial metabolic pathways.

Agradecimientos

Durante estos largos meses de encierro me he visualizado muchas veces llegando hasta aquí, pero nunca me lo llegué a creer de verdad. Ahora, cuando me pongo delante del ordenador a escribir estas líneas, siento un profundo alivio, alegría e incertidumbre. Porque el final de la tesis significa para mí el final de muchas cosas pero sobre todo significa el final de una separación forzosa, de un paréntesis que ya duraba demasiado. Meri, ya está, se acaba, se acaba el Skype y los whatsapps de "wenos días menina," se acaban los viajes en solitario y las despedidas entre la multitud de un aeropuerto, se acaba el vernos un fin de semana al mes en el mejor de los casos. Sólo puedo agradecerte la paciencia que has tenido conmigo durante este periodo tan complicado. Gracias por hacerme reír cuando estaba frustrado, por animarme cuando estaba abatido, por enseñarme a creer en mi trabajo y por hacerme desconectar cuando llevaba horas delante del mismo párrafo. Sólo puedo decir que gran parte de esta tesis te la debo así que puedes cobrártela cuando quieras.

Familia, sois el otro pilar que ha aguantado este escrito. Sin este mes de agosto en casa no creo que hubiera sido posible. Mamá, papá, gracias por aguantar mis manías y horarios intempestivos, sin preguntar pero siempre dispuestos a ponérmelo fácil para que sólo tuviera que pensar en escribir. Rafiña, aunque me hubiera gustado hablar más contigo durante este verano, no me hizo falta para darme cuenta de que entendías perfectamente por lo que estaba pasando. Juan, no sé si lo sabes pero eres una de las dos razones por las que me metí en esto de la ciencia -la otra es la abuela Lola-. Espero que te vaya muy bien en tu nuevo periplo por el Cuvi y que encuentres algo que te motive de verdad, porque hay pocas cosas más satisfactorias que ver cumplidos tus objetivos. Ester, no me olvido de ti, en cuanto esto se termine iremos a verte con la furgoneta (aka "Repechitos"), sí, esa que no iba a durar más de un año. Un abrazo fuerte y cuídate mucho, que aún tienes que dar bastante guerra. Tampoco me puedo olvidar de la familia política, Carlos y Ángeles, gracias por cuidarme desde la distancia (y por esas croquetas maravillosas).

Llega el momento de los míticos, fuente inagotable de risotadas, hablar de la vida y aventuras varias. Si es que no hay nada como unos buenos personajes para amenizar la velada. En serio, tengo la tremenda suerte de conservar unos amigos como vosotros desde el instituto, que ya nos ha llovido. Aunque voy menos de lo que me gustaría por Bouzas, siempre que llego se acaba tramando algo. La última, que me pilló en medio de la escritura (e hizo que el mes de julio fuera el menos productivo ever), fue la boda de Prodigio y Ro. Bieeen, por fin pude ir a una boda que no fuese la mía! Espero que el ritmo frenético de Londres os deje algo de espacio para desconectar y disfrutar de la vida. Más míticos, Neguin, grazzie mille por sacarme de casa este verano, cuando ya estaba mareado de tanto escribir. Parreño, gracias por intentar pelearte con la maquetación aunque no llegara a buen puerto. Vaidal, a ver si te prodigas un poco más, que no te veo el pelo, si no me vas a obligar a pillar un avión para Compostela (nada descartable). Burren (ahora más pitillero que nunca), Manki (próximamente en los mejores bares vigueses), Bernabiu (papuchi por partida doble), Friman y Abad (estos no sé realmente si existen), Martiña (no te quejarás de las visitas a Granada), Plumone e Isa (para cuando decís que estará la piscina?), Carmolas (dejó Bouzas huérfana), Carmitas (ahora Urre le hace competencia), y quien me dejo… Ah claro, Milton (el hermoso, aka entrepreneur). Mil gracias a todos por aturar a este personaje, y como siempre digo, a ver cuándo nos marcamos un viaje de mitikez!

A parte de personajes vigueses, también hay algún que otro barcelonés (de facto o adopción) que conforman la llamada ¿pandilla basurilla? De verdad le habéis puesto ese nombre? Se ve que nos puede el bizarrismo. Nurie (sin ti los peces nunca hubieran visto el final de la tesis), Albo (la próxima será la tuya), Jauma (Gaditano y cocinero residente), Diegorl (qué se le habrá perdido en Finland? L'amour c'est claire) gracias por hacer que estos años de rodriguez en Barcelona fueran menos solitarios, gracias por las cenas ¿gourmet? y por los momentos bizarros, como la fiesta 80's en el bingo de Laietana o el estreno mundial de Go Ibiza Go.

Otros compañeros que aparecen aquí por derecho propio son Manel y Ana. Echaré de menos las calçotadas con vosotros, la manufactura de los panellets o esas excursiones con "esmorzar de forquilla" que terminaban sin salir de la masía. Espero que encontréis vuestro espacio en L.A. y que nos volvamos a ver muy pronto.

Vamos ahora con el el Institut de Neurocienciès. En primer lugar no puedo dejar de agradecer a Cris (debes aparecer en todas las tesis, yo que tú iría pidiendo coautoría de los papers) por mil cosas, desde enseñarme cómo se sacan las meninges – y decirme que aquello mejoraría con la práctica cuando, tras 2 horas delante de la lupa, yo lo veía todo negro- hasta tener la paciencia de probar 25 maneras diferentes para que crecieran las malditas hipocampales (que ni siquiera eran para mi tesis). Mar (la técnico de histología más minuciosa que te puedas imaginar), gracias por haberme contagiado el cuidado y cariño que pones en todo tu trabajo, sea una simple tinción de Hematoxilina o la conservación de la muestra más valiosa. Nuria, la verdad que ha sido un lujo trabajar contigo. Me has enseñado un montón de microscopía y siempre tenías un hueco para responder mis dudas (aunque te preguntase 20 veces cual era la apertura numérica del objetivo 40X). No me quiero dejar a Eli y a Susana y tampoco al personal de administración. Sé que vuestro trabajo es difícil y que nosotros lo queremos todo al momento así que gracias por la paciencia. En particular a Enrique, que te llevo mareando todo el doctorado, primero con los pedidos y luego con los congresos, y siempre tienes un momento para explicarme cómo funciona la dichosa burocracia.

Esta tesis no hubiera sido posible sin la dirección de las Dras. Elena Galea y Roser Masgrau. Elena, gracias por confiar en mí para realizar este doctorado, por haberme enseñado que una buena comunicación es tan importante como unos buenos resultados y por haberte preocupado en todo momento de que tuviera un sueldo. Esto último sé que no ha sido fácil y por eso lo quiero poner en valor. Espero haber correspondido con un buen trabajo a la confianza depositada. Roser, gracias por el apoyo que me has dado en estos años, por enseñarme que la precisión bioquímica es muy

importante, y por esforzarte tanto con las correcciones de la tesis (aunque me costase entenderlo al principio).

En estos años que llevo en el astrolab ha pasado mucha gente que me ha ayudado, de una u otra manera, a llegar hasta aquí. Paulina, contigo empezó todo. Gracias por enseñarme a dar mis primeros pasos en el laboratorio y por tener la paciencia que exige el hacer de niñera (esto ahora lo sé por experiencia). Espero que te vaya muy bien por Londres y que seas muy feliz. Mateu, además de la parte científica, te agradezco que me hayas invitado a conocer el "mundillo" del InC en aquellas primeras cenas en las que me sentía como un chaval que se sienta a la mesa con "los mayores". Abel, gracias por entrar con tanta energía y ganas de cambiar cosas, tanto en el tema científico como en el social. Espero que esos Journal club duren mucho tiempo. Raquel y Arantxa, las recién llegadas, tened paciencia con las jefas y mucho ánimo con el doctorado. También quiero agradecer a todos los estudiantes que han ido pasando por el lab: Rubén, Patricia, Elena, Adriá, Roger, Matt, Agus, Paula, Mireia y Marina. Con todos vosotros he aprendido cosas nuevas así que gracias y espero que cumpláis los retos que se os presenten.

Si hay algo que me llevaré siempre del InC es el buen ambiente que hay entre los compañeros, así da gusto trabajar. Ainara y Sergi, este último año se os ha echado de menos mogollón. Pocas cosas mejores hay que te saquen del lab para echar unos pitis y hablar de la vida (y de Terry Pratchett, y del federalisme). La verdad, podría seguir escribiendo sobre las aventuras en furgo por la arrabassada, o el buceo en aguas frías pero prefiero ir a veros y contarlo en directo. Tampoco voy a dejar de dar gracias al resto de compañeros del Institut, con los que he compartido muchos días de curro y alguna que otra noche de juerga: Arnaldo, Lluis, Gerard, Tatiana, Alfredo, Montse, Ana, Dolo, Amaia, Arnau y muchos más que me dejo pero que espero se consideren agradecidos.

Esto se acaba. A todos los que lo habéis hecho posible

Gracias!

Glossary

20-HETE	20-hydroxyeicosatetraenoic acid
AA	Arachidonic acid
AC	Adenylyl cyclase
AD	Alzheimer's disease
AG-1	Angiopoietin-1
AKT	Protein kinase B
ALS	Amyotrophic lateral sclerosis
AMPA	α-amino-3-hydroxy-5-methyl-4-isoxazolepropionic acid
ANP	Atrial natriuretic peptide
aPKC	Atypical PKC
AQP4	Aquaporin 4
ATF-1	Activation transcription factor-1
ATP	Adenosin triphosphate
Aβ	Amyloid β
BBB	Blood Brain Barrier
Bcl-2	B-cell lymphoma 2
BD	Bromodomain
Bdnf	Brain derived neurotrophic factor
bZIP	Basic leucine zipper domain
CA1	Cornus Amonis 1
Calcb	Calcitonin B
CaM	Calmodulin
CaMKII/IV	Ca2+/Calmodulin-dependent kinase II and IV
cAMP	Cyclic adenosine monophosphate
CBF	Cerebral blood flow
CBP/p300	CREB-binding protein
CCL2	Chemokines C– C motif ligand
CDTA	CREB-dependent transcription in astrocytes
CDTN	CREB-dependent transcription in neurons
CLS	Coffin-Lowry syndrome
CN	Calcineurin
CNS	Central nervous system
COX2	Cyclooxygenase 2
CRE	cAMP regulatory element
CREB	c-AMP responsive element binding protein
CREM	cAMP-responsive element modulator

Crhbp	Corticotropin
CRTCs	CREB-regulated transcription coactivators
CsA	Cyclosporine A
CSF	Cerebro-spinal fluid
CSPs	Chondroitin sulphate proteoglycans
Cx43	Connexin 43
CXCL	Chemokines C–X–C motif ligand
Cys	Cysteine
ChIP	Chromatin immunoprecipitation
DAG	Diacylglycerol
DCX	Doublecortin
DG	Hippocampal dental gyrus
DMSO	Dimetyl sulfoxide
dpl	Days post lesion
ECM	Extracellular matrix
EET	Epoxieicosatrienoic acid
ER)	Endoplasmic reticulum
ERK 1/2	Extracellular signal-regulated kinases
FGF	Basic fibroblastic growth factor
FSK	Forskolin
GABAA	γ-aminobutyric acid A
Gad1	Glutamate decarboxylase
GDNF	Glial-derive neurotrophic factor
GFAP	Glial fibrillary acidic protein
GLAST/EAAT1	Glutamate aspartate transporter
GLP-1	Glucagon-like peptide-1
Gls2	Glutaminase 2
GLT-1/EAAT2	Glutamate transporter 1
GLU	Glutamate
GluRs	Ionotropic glutamate receptors
GLUT-1	Glucose transporter 1
Gly	Glycine
GM-CSF	Granulocyte-Macrophage Colony-Stimulating Factor
GO	Gene Ontology
GP	Glial intermediate progenitors
GPCRs	G-protein-coupled receptors
GS	Glutamine synthetase
GSEA	Gene Set Enrichment Analysis
GSH	Glutathione

GSK3β	Glycogen synthase kinase-3β
HAT	Histone acetyltransferase
HD	Huntington's disease
HDAC	Histone deacetylase
HIV-1	Immunodeficiency virus-1
HK	Hexokinase
HMGB1	High mobility group protein B1
Htt	Huntingtin
ICER	Inducible cAMP response element repressor
IEG	Immediate early gene
IFNγ	Interferon γ
IGF-1	Insulin-like growth factor 1
IL-1	Interleukin 1
IL-6)	Interleukin 6
iNOS	NO synthase
IP3	Inositol-1,4,5-trisphosphate
IP3R	IP3 receptor
KID	Kinase-inducible domain
Kir	Inwardly rectified K+ channels
KIX	Kinase-inducible interacting domain
LTP	Long term potentiation
MAPK	Mitogen-activated protein kinase
MAPKAP K2	Mitogen-activated protein kinase-activated protein kinase 2
MCAO	Middle cerebral artery occlusion
Mcl-1	Myeloid cell leukemia 1
MCP-1	Monocyte chemotactic protein-1,
MCT4	Monocarboxilate transporters
MEK	Mitogen-activated protein *kinase kinase*
mGluR	Metabotropic glutamate receptors
MMP-9	Matrix metaloproteinase-9
MRGA1	MAS-related G protein-coupled receptor member A1
MSK1	Mitogen- and stress-activated protein kinase 1
MZ	Marginal zone
NAADP	Nicotinic acid adenine dinucleotide phosphate
NE	Noradrenaline
Nefm	Neurofilament
NFκB	Nuclear factor κ B
NGF	Nerve growth factor

NMDA	N-methyl-D-aspartate
NMDAr	NMDA receptors
NO	Nitric oxide
O-)	Anion superoxide
OB	Olfactory bulb
OXPHOS	Oxidative phosphorylation
P2X	Purinergic receptors family X
P2Y	Purinergic receptors family Y
p38	Mitogen/stress-activated kinase
pCREB	Phosphorylated CREB
PDE4	Phosphodiesterase 4
PGC-1α	Peroxisome proliferator-activated receptor γ co-activator 1 α
PGs	Prostaglandins
PI3K	Phosphatidylinositol 3-kinase
PIP2	Phosphatidylinositol-4,5-bisphosphate
PIP3	Phosphatidylinositol-3, 4, 5-trisphosphate
PKA	Protein kinase A
PKC	Protein kinase C
PKD	Protein kinase D
PKM	Protein kinase M
PLA2	Phospholipase A2
PLCβ	Phospholipase C beta
PLCδ	Phospholipase C delta
PMN	Polymorphonuclear leukocytes
PP1, PP2A	Phosphatases type1 and 2A
Prok2	Prokineticin2
PS	Presenilin
Q1/Q2	Glutamine-rich domains
RG	Radial glia
ROS	Reactive oxygen species
RSK	Ribosomal S kinase
RTS	Rubinstein-Taybi syndrome
SAPK2	Stress-Activated Protein Kinase 2
Ser	Serine
SGZ).	Sub-granular zone
SICs	Slow inward currents
SIK	Salt-inducible kinases
SOD 1/2	Superoxide dismutases

STAT3	Signal transducer and activator of transcription 3
SVZ	Subventricular zone
Syn	Synaptophysin
T	Transgenic
Tac1	Tachykinin1
TAFII130	TBP associated factor 4
TBI	Traumatic brain injury
TBP	TATA box binding protein
TC	Transgenic cryolesioned
TCA	Tricarboxylic acid cycle pathway
TFIID	Basal transcription factor IID
TGFβ	Transforming growth factor β
TLR	Toll-like receptor
TNFα)	Tumour necrosis factor α
TrKs	Tyrosine kinases receptors
TSPs	Thrombospondins
Ucn	Urocortin
VSCC	Voltage-sensitive Ca2+ channels
WT	Wild type
WTC	Wild type cryolesioned